

THE ROLE OF SECA2 PROTEIN EXPORT IN THE VIRULENCE OF MYCOBACTERIUM
TUBERCULOSIS

Katelyn Emily Zulauf

A dissertation submitted to the faculty of the University of North Carolina at Chapel Hill in partial fulfillment of the requirements for the degree of Doctor of Philosophy in the Department of Microbiology and Immunology, School of Medicine.

Chapel Hill
2017

Approved by:

Miriam Braunstein

Thomas Kawula

William Goldman

Peggy Cotter

Rita Tamayo

© 2017
Katelyn Emily Zulauf
ALL RIGHTS RESERVED

ABSTRACT

KATELYN EMILY ZULAUF: The role of SecA2 protein export in the virulence of
Mycobacterium tuberculosis
(Under the direction of Miriam Braunstein)

In order to promote disease, *Mycobacterium tuberculosis* exports proteins outside of the bacterial cell into the host environment where the proteins can interfere with host defense mechanisms such as phagosome maturation. The SecA2 pathway is one system *M. tuberculosis* utilizes to export such proteins. SecA2 is a non-essential specialized SecA ATPase required for exporting a relatively small subset of proteins. The SecA2 pathway, although not essential for growth of *M. tuberculosis* in vitro, is required for virulence of *M. tuberculosis*. The requirement for SecA2 during infection suggests that SecA2 and its exported effectors play important roles in *M. tuberculosis* pathogenesis. Therefore, we set out to both identify *M. tuberculosis* proteins that are exported by the SecA2 pathway and identify functions of SecA2 in *M. tuberculosis* virulence. Using quantitative proteomics, we identified solute binding proteins and Mce proteins as two classes of proteins exported by SecA2 as well additional proteins of unknown function that may account for the role of SecA2 in virulence. We additionally investigated the function of the SecA2 pathway in phagosome maturation arrest which is critical for *M. tuberculosis* replication and pathogenesis, by identifying and investigating proteins exported by the SecA2 pathway that play essential roles in this process. Work presented in this dissertation shows that SecA2 exports two effectors of phagosome maturation arrest: SapM and PknG. We further show that the role of SecA2 in exporting these

effectors contributes to phagosome maturation arrest and growth of *M. tuberculosis* in macrophages. Finally, to further elucidate the functions and mechanisms of the SecA2 export pathway of *M. tuberculosis* beyond phagosome maturation arrest, we utilized genome-wide genetic interaction mapping of *secA2*. Our results expand our understanding of the SecA2 pathway by identifying candidate substrates and components of the export machinery and by revealing roles for SecA2 in *M. tuberculosis* processes involving transporters, phosphate import, copper resistance, peptidoglycan synthesis, and lipid metabolism and homeostasis. Taken together, the findings presented in this dissertation have significantly advanced our understanding of the roles of the SecA2 export pathway in the virulence of *M. tuberculosis*.

TABLE OF CONTENTS

LIST OF TABLES	vi
LIST OF FIGURES	vii
LIST OF ABBREVIATIONS AND SYMBOLS	ix
CHAPTER	
I. Introduction	1
II Label-free quantitative proteomics reveals a role for the <i>Mycobacterium tuberculosis</i> SecA2 pathway in exporting solute binding proteins and Mce transporters to the cell wall	31
III. The SecA2 pathway of <i>Mycobacterium tuberculosis</i> exports effectors that work in concert to arrest phagosome and autophagosome maturation	79
IV. Genome-wide genetic interaction mapping: an approach for understanding the mechanism and function of the SecA2 pathway of <i>Mycobacterium tuberculosis</i>	124
V. Discussion	175

LIST OF TABLES

Table

2.1	Functional categories of proteins showing reduced abundance in the cell wall fraction of the <i>M. tuberculosis</i> <i>secA2</i> mutant versus H37Rv	69
2.2	DosR regulated proteins have altered abundance in the cell wall and cytoplasmic fractions of the <i>M. tuberculosis</i> <i>secA2</i> mutant.....	70
3.1	Plasmids used in this study	117
3.2	Strains used in this study	118
4.1	Significant genetic interactions with <i>secA2</i>	159
4.2	Potential SecA2 substrates	162
4.3	Clusters of genetic interactions with <i>secA2</i>	163
4.4	Primers used in this study.....	166

LIST OF FIGURES

Figure

1.1	Models of SecA1 and SecA2 export in <i>M. tuberculosis</i>	22
1.2	SecA2 export is required for <i>M. tuberculosis</i> virulence.....	23
2.1	Functional categories of cell wall proteins identified by LC MS/MS.....	59
2.2	Percent of functional protein categories showing differences in the cell wall between H37Rv and the <i>secA2</i> mutant.....	60
2.3	Percent of functional protein categories showing differences in the cell wall between H37Rv and the <i>secA2</i> mutant.....	61
2.4	Proteins associations among proteins identified as having differential abundance in the cell wall fractions of H37Rv versus the <i>secA2</i> mutant	62
2.5	Multiple components of Mce1 and Mce4 transporters are reduced in the cell wall of the <i>secA2</i> mutant	63
2.6	Immunoblot validation of protein abundance differences between H37Rv and the <i>secA2</i> mutant.....	64
2.7	Transcript levels for <i>mce</i> genes are unchanged but transcript levels for DosR-regulated genes are higher in the <i>secA2</i> mutant	65
2.8	Relative quantitation of proteins in H37Rv and <i>secA2</i> mutant cytoplasmic fractions	66
2.9	The level of PknG is increased in the cytoplasm and reduced in the cell wall of the <i>secA2</i> mutant.....	67
2.10	A model for SecA2-dependent effects in <i>M. tuberculosis</i>	68
3.1	SapM export is dependent upon the SecA2 pathway.....	107
3.2	SecA2 secretion of SapM is required for EEA1 exclusion from <i>M. tuberculosis</i> containing phagosomes.....	108

3.3	SecA2 secretion of SapM contributes to phagosome maturation arrest and intracellular growth	110
3.4	SecA2 export of PknG contributes to phagosome maturation arrest and growth in macrophages.....	112
3.5	SecA2 export of both SapM and PknG contributes to phagosome maturation arrest and virulence.....	113
3.6	SecA2 is required for <i>M. tuberculosis</i> inhibition of autophagosome maturation.....	115
3.7	SapM and PknG play distinct functions in phagosome maturation arrest but other SecA2 effectors exist	116
4.1	Utilizing TnSeq to identify genetic interactions with <i>secA2</i>	153
4.2	Genetic interactions with <i>secA2</i>	154
4.3	Clusters of alleviating and aggravating interactions with <i>secA2</i>	155
4.4	SecA2 is required for optimal growth on cholesterol.....	156
4.5	SecA2 is required for lysozyme and carbenicillin resistance.....	157
4.6	SecA2 and phosphate import in <i>M. tuberculosis</i>	158
5.1	SecA2 export of LipO contributes to phagosome maturation arrest	191
5.2	SapM is localized to the cytosol of infected macrophages.....	192
5.3	Solute binding proteins and Mce proteins are exported by the SecA2 pathway.....	193

LIST OF ABBREVIATIONS AND SYMBOLS

2D	Two-dimensional
A	alanine
ABC	ATP binding cassette
ADP	adenosine diphosphate
ATP	adenosine triphosphate
BCG	Bacille Calmette-Guerin
CFP	Culture filtrate
CFP	cyan fluorescent protein
cfu	colony forming unit
CW	cell wall fraction
Cyt	cytoplasm
EEA1	Early endosomal antigen 1
ESX	ESAT-6 like secretion system
FDR	false discovery rate
GFP	green fluorescent protein
GTP	guanosine triphosphate
GDP	guanosine diphosphate
H	histadine
H ⁺	hydrogen
HA	hemagglutinin
HOPS	Homotypic fusion and vacuolar sorting
Hr	hour

Hrs	hepatocyte growth factor regulated tyrosine kinase substrate
hyg	hygromycin resistance gene
IFN- γ	Gamma interferon
IL-6	Interleukin-6
kan	kanamycin resistance gene
kDa	kilodalton
L.	Listeria
LAM	Lipoarabinomannan
LC	Liquid chromatography
LC3	microtubule associated proteins 1A/1B light chain 3
LFQ	Label free quantitative
M.	Mycobacterium
ManLAM	Mannose capped lipoarabinomannan
MEM	membrane fraction
mg	milligram
MHC-II	major histocompatibility complex class II
min	minute
ml	milliliter
mM	millimolar
MS	mass spectra
Msmeg	Mycobacterium smegmatis
Mtb	Mycobacterium tuberculosis
Myd88	Myeloid differentiation primary response 88

N-terminal	amino terminal
ng	nanogram
NOS2	nitric oxide synthase 2
Ns	not significant
OD600	optical density at 600 nanometers
ORF	open reading frame
PAGE	polyacrylamide gel electrophoresis
PBS	phosphate buffered saline
PCR	polymerase chain reaction
Phox	phagocytic oxidase
PI(3)P	Phosphatidylinositol-3 phosphate
PI3K	Phosphatidylinositol-3 kinase
PIM	Phosphatidylinositol mannoside
qRT-PCR	quantitative real time PCR
R	arginine
Rab	Ras related protein
RFP	red fluorescent protein
RHOCS	redox homeostatic system
RILP	Rab7 interacting lysosomal protein
RNI	Reactive nitrogen intermediates
ROS	Reactive oxygen species
S.	Streptococcus
SBP	solute-binding protein

SDS	sodium dodecyl sulfate
Sec	secretion
STRING	search tool for the retrieval of interacting genes/proteins
SOL	soluble fraction
T3SS	Type III secretion system
TACO	Tryptophan Aspartate containing Coat protein
Tat	Twin-arginine translocation
TB	Tuberculosis
TLR	Toll-like receptor
TNF- α	Tumor necrosis factor alpha
TR	Texas red
V-ATPase	Vacuolar ATPase
WCL	Whole cell lysate

CHAPTER 1¹

Introduction

Despite the identification of *Mycobacterium tuberculosis* as the etiological agent of the disease tuberculosis over 100 years ago, there remain over 10 million new cases of tuberculosis and 1.8 million deaths attributed to *M. tuberculosis* each year (1). This significant burden of disease makes *M. tuberculosis* the leading infectious killer worldwide. Furthermore, the lack of an efficacious vaccine and the increasing emergence of drug resistant strains has complicated treatment and the elimination of *M. tuberculosis* (2). A better understanding of the mechanisms of *M. tuberculosis* pathogenesis could lead to the identification of novel treatments for *M. tuberculosis*.

M. tuberculosis is spread person to person by aerosols that reach the alveolar spaces of the lung, where the bacterium is phagocytosed by alveolar macrophages. Typically, once taken up by macrophages, the host delivers microbes to membrane bound compartments called phagosomes, and the host mounts multiple anti-microbial defenses against the pathogen (3). In contrast, *M. tuberculosis* blocks these host responses in order to create a hospitable niche for replicating in the phagosomal compartment (4,5). The ability of *M.*

¹Adapted for this dissertation from: Miller BK, Zulauf KE, Braunstein M. 2017. The Secretory Pathways and Exportomes of *Mycobacterium tuberculosis*. *Microbiol Spectr* 5 (2).

tuberculosis to replicate in host cells, specifically macrophages, is critical for virulence. In order to replicate in macrophages, *M. tuberculosis* exports a variety of effector proteins to the host-pathogen interface (6,7). These exported proteins can either be localized to the bacterial surface or fully secreted into the host where they have diverse functions that include limiting damaging host responses to *M. tuberculosis* (e.g. phagosome-lysosome fusion and antigen presentation), resisting immune defense mechanisms (i.e. ROS and RNI), and promoting nutrient uptake (i.e. cholesterol) (7,8). The SecA2-dependent protein export pathway is required for virulence of *M. tuberculosis* and more specifically replication of *M. tuberculosis* in macrophages (9,10). The research described in this thesis is directed at elucidating the mechanisms of SecA2 export that contributes to the success of *M. tuberculosis* as an intracellular pathogen.

Protein export in *M. tuberculosis*

Approximately 20% of all bacterial proteins must be exported beyond the bacterial cytoplasm in order to function (11). Consequently, all bacteria possess protein export pathways that transport proteins beyond the cytoplasmic membrane. These exported proteins may remain in the bacterial cell envelope or be further secreted to the extracellular environment (11). Many exported proteins function in essential physiological processes. Additionally, in bacterial pathogens, including *M. tuberculosis*, many exported proteins have functions in virulence. Consequently, the pathways that export proteins are commonly essential and/or are important for pathogenesis. Across bacteria, including mycobacteria, there are conserved protein export pathways: the general Sec secretion (Sec) and the twin-arginine translocation (Tat) pathways. Both Sec and Tat pathways are essential to the

viability of *M. tuberculosis* and both also contribute to virulence (Rank and Braunstein unpublished, 12-14). In addition to these highly conserved pathways, bacterial pathogens commonly have specialized protein export systems that are important for pathogenesis due to their role in exporting virulence factors. Mycobacteria also have specialized protein export systems: the SecA2 export pathway and five ESX (Type VII) pathways.

Sec (SecA1) protein export pathway

The majority of protein export in bacteria is carried out by the general secretion (Sec) pathway. The Sec pathway is highly conserved and essential in all bacteria (15). The Sec pathway transports proteins from the cytoplasm across the cytoplasmic membrane (Figure 1.1). Sec exported proteins can then remain in the cell envelope or be fully secreted into the extracellular space. Sec exported proteins are transported in an unfolded state through the SecYEG membrane channel. Proteins exported by the Sec export pathway possess an N-terminal signal peptide that directs them to the Sec pathway to be exported (16).

In addition to the SecYEG channel, Sec export requires the essential SecA ATPase that is peripherally associated with SecYEG. SecA is a multifunctional protein that binds to Sec exported proteins in the cytoplasm, targets them to SecYEG, and harnesses energy from repeated rounds of ATP binding and hydrolysis to drive the stepwise export of proteins through the SecYEG channel (17). An unusual feature of mycobacteria is that they possess two SecA proteins (named SecA1 and SecA2) (18). These two SecAs are distinct and have unique functions, with the mycobacterial SecA1 being the essential SecA (described above) that functions in the conserved Sec pathway of mycobacteria to transport the majority of exported proteins.

SecA2 protein export pathway

In contrast to SecA1, the mycobacterial SecA2 is not essential for growth in vitro. SecA2 exports a smaller subset of proteins than SecA1. However, among the proteins exported by SecA2 are proteins with roles in the virulence of the pathogenic mycobacteria *M. tuberculosis* and *M. marinum* in macrophage and animal models of infection (9,10,19-21). As with mycobacteria, in other bacterial pathogens with SecA2 proteins, such as *L. monocytogenes*, *Staphylococcus aureus*, *Streptococcus gordonii*, SecA2 is also nonessential but has a role in virulence (22-24). The mycobacterial SecA2 pathway exports diverse substrates, and studies suggest that SecA2 likely works with the canonical SecYEG channel to export its specific subsets of proteins (Figure 1.1) (19,20,25,26).

Features of SecA2-exported proteins

Studies in *M. tuberculosis*, *M. marinum*, and *M. smegmatis* have identified proteins that are exported in a SecA2-dependent manner (19,20,26). The list of SecA2-dependent proteins includes examples with N-terminal Sec signal peptides as well as proteins lacking recognizable signal peptides (e.g. SodA and PknG). The SecA2-only systems of other pathogens, such as *L. monocytogenes*, are also associated with export of proteins with or without signal peptides (27).

The best studied SecA2-dependent substrates are the *M. smegmatis* lipoproteins Msmeg1704 and Msmeg1712 (26). These proteins are both solute binding proteins (SBPs) that are synthesized as preproteins with Sec signal peptides containing lipobox motifs. SBP lipoproteins are also identified in *M. marinum* as a category of protein exported by the SecA2 pathway (20). The lipidated nature of these proteins does not confer their SecA2-dependency

for export; an amino acid substitution of the invariant cysteine in the lipoboxes of Msmeg1704 and Msmeg1712, which prevents lipid attachment, does not eliminate the requirement for SecA2 in export (28). Although SecA2-dependent substrates containing signal peptides, such as Msmeg1704 and Msmeg1712, require their signal peptide to be exported, their signal peptides do not contain any SecA2 distinguishing features. If their signal peptides are swapped for the signal peptide of a SecA1-dependent substrate, Msmeg1704 and Msmeg1712 retain their SecA2-dependency (28). Thus, the mature domains of these proteins, not signal peptides, impart the requirement for SecA2 in their export.

One possible explanation for the defining feature of the mature domains of SecA2-dependent substrates is a propensity to fold in the cytoplasm prior to export. In support of this idea, when the mature domain of Msmeg1704 is fused to a signal peptide that directs preproteins for export through the twin-arginine translocase (Tat) pathway, Msmeg1704 is no longer exported in a SecA2-dependent manner (28). Instead, when fused to a Tat signal peptide Msmeg1704 is exported by the Tat pathway. The Tat pathway differs from the Sec system in that it requires preproteins to be folded prior to export, unlike Sec export in which preproteins must remain unfolded to be export competent. Thus, the fact that the mature domain of a SecA2 substrate is compatible with export by the Tat pathway suggests that SecA2 dependent substrates can fold in the cytoplasm prior to export and that the role of SecA2 may be to facilitate export of these problematic substrates through the SecYEG channel, which requires proteins to be unfolded. It remains unclear how SecA2 may assist in the export of these substrates. Three nonexclusive possibilities for how SecA2 could be influencing export are either that SecA2 serves a chaperone-like role, is capable of working with a chaperone that keeps preproteins unfolded prior to export, or that SecA2 cooperates

with SecA1 to provide additional energy to translocate challenging substrates through SecYEG.

SecA2-dependent features of the mature domain may also help explain the SecA2-dependence of *M. tuberculosis* proteins lacking signal peptides (e.g. SodA and PknG). There are also SodA proteins lacking signal peptides reported to be exported by the canonical Sec pathway in *Rhizobium leguminosarum* and by the SecA2-only pathway in *L. monocytogenes* (29,30). Further studies of the role of SecA2 in the export of these unconventional proteins is needed because it also remains possible that the effect of SecA2 on exported proteins like SodA is indirect.

Proteins exported by SecA2

As indicated by the virulence defects of *secA2* mutants of *M. tuberculosis* and *M. marinum*, the SecA2-dependent pathway exports proteins with roles in pathogenesis (9,10,19-21). Compared to SecA1 which is responsible for the majority of protein export in the bacterial cell, SecA2 is thought to only export a small number of proteins (likely around 25) (6). Early studies identified a small number of SecA2 exported proteins using comparative two-dimensional gel electrophoresis of cell wall or secreted proteins of *M. smegmatis* and *M. tuberculosis* (19,26). More recent quantitative mass spectrometry analyses of cell envelope fractions of *secA2* mutant *M. marinum* identified additional SecA2 substrates (20). While this mass spectrometry study increased our knowledge of SecA2 exported proteins, further studies are still required to validate the SecA2-dependency of many of the more recently identified proteins as well as to identify SecA2 dependent proteins

in *M. tuberculosis*. Below, we highlight examples of validated SecA2 substrates along with common themes among proteins exported by SecA2.

Solute binding proteins (SBPs)

The best studied SecA2 substrates, the Msmeg1704 and Msmeg1712 lipoproteins of the model organism *M. smegmatis*, represent one class of SecA2 dependent substrates, solute binding proteins (SBPs) (26). SBPs are cell wall localized proteins that deliver solutes to permease components of ATP-binding cassette (ABC) transporters for import using energy from ATP hydrolysis. Although most SBPs in *M. tuberculosis* have not been directly studied and their substrates remain unknown, mycobacterial SBPs are predicted to import a wide range of solutes (from phosphate to sugars) (31). Thus, the role of SecA2 in exporting SBPs could be important for nutrient acquisition and affect the ability of *M. tuberculosis* to thrive and persist in the host.

SodA and KatG

The Fe-superoxide dismutase SodA is another protein identified as being exported in a SecA2-dependent manner (19). The *secA2* mutant of *M. tuberculosis* secretes less SodA protein and exhibits less secreted superoxide dismutase activity than wild type or complemented strains (19,32). As an antioxidant that converts superoxide to hydrogen peroxide and oxygen, secreted SodA could be important for counteracting the macrophage antimicrobial oxidative burst (33). SodA also has cytoplasmic functions and therefore is also localized in the mycobacterial cytoplasm in addition to being secreted (19). SodA is an example of a SecA2-dependent protein lacking a signal peptide. In *L. monocytogenes* a Mn-superoxide dismutase that lacks a signal peptide is also SecA2 dependent (30).

The catalase-peroxidase KatG is another antioxidant reported to be SecA2 dependent for secretion (19). KatG works with SodA to detoxify oxygen radicals by converting damaging hydrogen peroxide to oxygen and water (34). KatG is also able to detoxify the reaction product of superoxide and nitric oxide, peroxynitrite (35). Like SodA, KatG lacks a signal peptide and can be found in the mycobacterial cytoplasm (19). The role of SecA2 in the export of SodA and KatG could translate to a function of the SecA2 pathway in protecting *M. tuberculosis* from the oxidative burst of macrophages.

PknG

The eukaryotic-like serine-threonine kinase PknG is also dependent upon SecA2 for export. In *M. marinum* reduced levels of PknG are detected in the cell envelope of the *secA2* mutant compared to wild type or complemented strains (20). Like SodA and KatG, PknG lacks a signal peptide. Additionally, like SodA and KatG, PknG can be found in both the mycobacterial cytoplasm and its exported location which is consistent with this protein cytoplasmic and exported functions (36,37).

Although PknG is primarily localized in the cell wall and bacterial cytoplasm, PknG has been reported to be fully secreted and has even been identified as reaching the macrophage cytosol (36,38). In the bacterial cytoplasm, PknG regulates glutamate metabolism and redox homeostasis (37,39). PknG is also considered a virulence factor as an *M. tuberculosis pknG* mutant has an in vitro growth defect and is attenuated in mice (36). A hallmark of macrophage infections with *M. tuberculosis* is that the bacterium arrests the normal process of phagosome maturation (4,5). Consequently, *M. tuberculosis* avoids delivery to a mature, fully acidified phagolysosome. Although the mechanistic details remain entirely unknown, PknG plays a role in phagosome maturation arrest. A *pknG* mutant of

BCG fails to block phagosome maturation, and a strain of *M. smegmatis* expressing the BCG *pknG* prevents phagosome maturation unlike wild type *M. smegmatis* (38). This specific role of PknG in phagosome maturation is intriguing because *secA2* mutants of *M. tuberculosis* and *M. marinum* are defective in phagosome maturation arrest (9,20).

Despite the recent expansion in our knowledge of SecA2 substrates, the list of known SecA2 exported proteins likely remains incomplete. Commonly, SecA2 substrates are only partially dependent upon SecA2 for export; residual export of these substrates occurs in *secA2* mutants through yet unidentified mechanisms (19,20,26). Interestingly, *secA2* mutants of other SecA2-only systems also exhibit incomplete export defects (22,27,30,40). The partial dependency of SecA2 substrates creates a unique challenge in identifying substrates and understanding how SecA2 export contributes to *M. tuberculosis* pathogenesis.

SecA2 and virulence of *M. tuberculosis*

In *M. tuberculosis*, SecA2 is not required for growth in vitro, but it is required for virulence (10,19). A *secA2* mutant of *M. tuberculosis* is attenuated in the mouse model of infection. Mice infected with the *secA2* mutant (either by intravenous injection or aerosol) have reduced bacterial burden in initial replication phase of infection, but the *secA2* mutant is able to persist throughout the infection (10,19). Mice infected with the *secA2* mutant also survive significantly longer than mice infected with wild type *M. tuberculosis* (10). The SecA2 pathway is also required for virulence in *M. marinum*, a mycobacterial pathogen of fish and frogs. In both embryonic and adult zebrafish, infection with a *secA2* mutant of *M. marinum* results in reduced bacterial burden and an increased fish survival time (20,21). The

M. marinum secA2 mutant also has a phenotype in the murine tail vein infection model (fewer tail lesions) (21).

Growth in macrophages is vital for *M. tuberculosis* pathogenesis and a *secA2* mutant of *M. tuberculosis* has a significant growth defect in macrophages which fits with the requirement for SecA2 during the replicative phase of murine infection (10). While our understanding of how *M. tuberculosis* survives in macrophages and elicits disease remains incomplete, *M. tuberculosis* is known to limit many anti-microbial activities of macrophages (e.g. phagosome-lysosome fusion, attack by reactive oxygen and nitrogen intermediates (ROI, RNI), apoptosis, inflammatory responses and antigen presentation) (Figure 1.1) (7). Studies of the *M. tuberculosis secA2* mutant in macrophages reveal roles for the SecA2 pathway in these processes (10).

The SecA2 pathway and inhibition of apoptosis

A phenotype exhibited by macrophages infected with the *secA2* mutant is increased apoptosis, which indicates a role for the *M. tuberculosis* SecA2 pathway in blocking macrophage apoptosis (32). Macrophage apoptosis is detrimental to *M. tuberculosis* as subsequent efferocytosis of *M. tuberculosis* infected, apoptotic macrophages will kill the bacteria (41). Apoptosis can also drive establishment of a protective immune response, which is detrimental to the pathogen, by promoting antigen presentation to T cells (32,42). Interestingly, superoxide can be a signal for apoptosis and the pro-apoptotic phenotype of the *secA2* mutant is attributed to the defect in SodA export (9,32). When secretion of SodA is restored in a *secA2* mutant, by overexpressing a version of SodA with a Sec signal peptide fused at its N-terminus (α -SodA), secreted superoxide dismutase activity and anti-apoptotic activity are both restored. However, when tested in macrophages and mice, virulence of the

secA2 mutant expressing α -SodA remains attenuated (9). Thus, on its own, inhibition of apoptosis is insufficient to explain the role of the SecA2 pathway in pathogenesis. However, it is common for bacterial pathogens to have overlapping/redundant virulence mechanisms, which leaves open the possibility of the role of SecA2 in limiting macrophage apoptosis contributing to *M. tuberculosis* pathogenesis.

The SecA2 pathway and immunomodulation

In response to infection with the *secA2* mutant, macrophages produce increased levels of MyD88-dependent RNI and pro-inflammatory cytokines, such as TNF- α and IL-6, in comparison to macrophages infected with wild-type *M. tuberculosis* (10). This altered cytokine profile suggests that the SecA2 pathway has an immunomodulatory effect of inhibiting the innate immune responses of macrophages to *M. tuberculosis* infection. On its own, the altered immune response to the *secA2* mutant is insufficient to explain the attenuated phenotype of the *secA2* mutant in macrophages because the *secA2* mutant remains attenuated in *myd88*^{-/-} macrophages and mice (Sullivan and Braunstein unpublished;9). These results indicate immunomodulation is not the sole function of the SecA2 export pathway; however, it may still be important for pathogenesis given the possibility of redundant immunomodulatory mechanisms. SecA2 substrates may also function in suppressing the adaptive immune response, as the SecA2 pathway additionally impacts the level of IFN- γ -induced MHC II levels during *M. tuberculosis* infection (10). The SecA2 exported proteins that produce immunomodulatory effects are currently unknown.

The SecA2 pathway and reactive radicals

Because SodA and KatG, enzymes important for detoxifying oxygen radicals, are secreted in a SecA2-dependent manner, an additional function of the SecA2 pathway could

be to protect against the damaging reactive oxygen radicals produced by infected macrophages (10). The SecA2 pathway also limits production of RNI produced by macrophages (mentioned above) (43). Both ROI and RNI are important for controlling microbial growth in macrophages. However, when *phox*^{-/-} macrophages, which fail to undergo an oxidative burst, or *NOS2*^{-/-} macrophages, which fail to produce RNI, are infected with the *secA2* mutant, the mutant remains attenuated for intracellular growth (9). While these results indicate that protection from reactive radicals is not the sole function of the SecA2 pathway in pathogenesis, due to the potential for redundant mechanisms that protect against reactive radicals in *M. tuberculosis*, this role for SecA2 could still also contribute to virulence.

The SecA2 pathway and phagosome maturation arrest

Following phagocytosis by macrophages, *M. tuberculosis* replicates intracellularly. Typically, once phagocytosed, microbes are delivered to phagosomes that subsequently mature, acidify, and fuse with a lysosome resulting in destruction of the microbe. In contrast, *M. tuberculosis* arrests this process at an early stage, and *M. tuberculosis* avoids delivery to acidified phagolysosomes (5). One of the most striking phenotypes exhibited by *M. tuberculosis* and *M. marinum* *secA2* mutants in macrophages is that a *secA2* mutant fails to arrest phagosome maturation, which results in the mutant residing in a more mature, acidic phagosome (9,20). When phagosome acidification is chemically inhibited, the *M. tuberculosis* *secA2* mutant grows comparably to wild-type, indicating SecA2 inhibition of phagosome maturation is required for intracellular growth in macrophages (20).

In summary, SecA2 affects several diverse host immune pathways highlighting the importance of the SecA2 pathway and its exported proteins in mycobacterial infection. While

the role of the SecA2 pathway in phagosome maturation arrest is proven to be critical for *M. tuberculosis* virulence, additional effects of SecA2 export on macrophages may also be significant. The significance of these other SecA2 effects may be masked by redundant virulence mechanisms as *M. tuberculosis* has additional, and likely SecA2-independent, apoptotic inhibitory factors, ROI resistance mechanisms and immunomodulatory factors. More research is needed to understand all of the distinct roles SecA2 substrates play in promoting pathogenesis.

Phagosome maturation arrest by *M. tuberculosis*

To avoid trafficking to the antimicrobial environment of acidified phagolysosomes, *M. tuberculosis* blocks the normal series of phagosome maturation events that occurs following phagocytosis (5). As a result, *M. tuberculosis* resides in phagosomes that resemble early endosomes. In addition to creating a hospitable environment for bacterial replication, preventing maturation of the phagosome also reduces antigen presentation and thus has implications in inhibiting a successful adaptive immune response by the host (44). Although the ability of *M. tuberculosis* to arrest phagosome maturation and replicate in macrophages is established as critical for virulence, the mechanisms and host-pathogen interactions that block phagosome maturation remain to be clarified (9). Phagosome maturation is complex and involves many host pathways. The mechanisms of *M. tuberculosis* phagosome maturation arrest appear equally complex (4). Therefore *M. tuberculosis* targets multiple steps of phagosome maturation and in many cases, there are redundant mechanisms targeting a single step.

Typically when microbes are taken up into phagosomes, the phagosomes progress through a series of maturation stages in which the phagosomes sequentially acquire host proteins culminating in the fusion of the phagosome with the proteolytic degradative lysosome. First the phagosomes accumulate the GTPase Rab5 and the lipid phosphatidylinositol-3-phosphate (PI3P) (45). Rab5 and PI3P in turn recruit host proteins including early endosome antigen 1 (EEA1) and hepatocyte growth factor-regulated tyrosine kinase substrate (Hrs) that drive further maturation events of the phagosome (46). EEA1 promotes fusion events between phagosomes and endosomes in the cell (47). Hrs also promotes fusion of the phagosome with endosome compartments. Hrs additionally contributes to the fusion of the phagosome with late, more mature endosomes and lysosomes (48). As phagosomes mature, Rab5 is exchanged for the GTPase Rab7 through mechanisms that are not well understood (45). The host exchange factor Mon1/Ccz1 is reported to mediate exchange of Rab5 and Rab7 but it is not known what other host proteins contribute to this important process (49). Rab7 in turn recruits many proteins that promote fusion of phagosomes with lysosomes. In addition to Rab proteins, phagosomes acquire the Vacuolar H⁺ ATPase (V-ATPase) as they mature. V-ATPase is a multi-subunit proton pump that acidifies the phagosome (50).

As mentioned above, *M. tuberculosis* is able to block the maturation of the phagosomes and resides in a compartment that resembles early endosomes (5). The early endosome-like *M. tuberculosis* phagosome is characterized by the retention of Rab5 on the phagosomal membrane (51). The high levels of Rab5 in conjunction with high levels of the transferrin receptor on *M. tuberculosis* phagosomes indicate that the *M. tuberculosis* phagosome, despite being arrested, interacts and fuses with other early endosomes in the

macrophage (52,53). In fact, *M. tuberculosis* phagosomes also contain high levels of Rab14, which is thought to promote fusion with early endosomes. It remains unknown how *M. tuberculosis* retains these host factors on the phagosome (54). *M. tuberculosis* phagosomes also contain high levels of the actin binding Coronin 1-A (TACO) (55). The *M. tuberculosis* exported effector LpdC has been shown to promote this Coronin-1A accumulation on phagosomes. Notably, Coronin-1A activates the host phosphatase calcineurin, which acts to inhibit phagosome-lysosome fusion through unknown mechanisms (55).

In addition to retaining host markers of early endosomes, *M. tuberculosis* phagosomes actively subvert subsequent phagosome maturation events. PI3P is a vital host factor that drives maturation of the phagosomal compartment (56). By inhibiting PI3P production as well as dephosphorylating PI3P, *M. tuberculosis* prevents the recruitment of PI3P binding proteins to the phagosome (57,58). PI3P binding proteins such as EEA1 and Hrs drive downstream maturation events of the phagosome (discussed above). Vps34 is the host phosphoinositide-3 kinase (PI3K) that phosphorylates phosphatidylinositol (PI) to generate PI3P on the phagosomal membrane (59). A cell-envelope glycolipid of *M. tuberculosis*, Mannosylated Lipoarabinomannan (ManLAM), alters calcium concentrations in the macrophage, which prevents recruitment of Vps34 to the phagosome (60). However, ManLAM is not the only *M. tuberculosis* effector impacting PI3P levels on phagosomes. *M. tuberculosis* also secretes the phosphatase SapM, which dephosphorylates PI3P(58). In addition to preventing recruitment of Hrs through reducing PI3P levels on the phagosome, *M. tuberculosis* also exports the EsxH protein, which directly interacts with and inhibits Hrs activity by preventing binding of Hrs with other host proteins that promote fusion of the phagosome with the lysosome (61). The existence of multiple *M. tuberculosis* mechanisms to

limit PI3P levels and PI3P binding protein functions exemplifies the complexity and redundancy of *M. tuberculosis* effectors of phagosome maturation arrest.

Another step in phagosome maturation targeted by *M. tuberculosis* is the exchange of the early endosome marker Rab5 for Rab7, which promotes fusion with late endosomes and lysosomes. The prevention of Rab7 recruitment to the phagosome is a requisite step in phagosome maturation arrest by *M. tuberculosis* (51). The specific mechanism of Rab7 inhibition by *M. tuberculosis* is not well understood. PI3P promotes the exchange of Rab5 for Rab7 so *M. tuberculosis* may inhibit Rab7 through dephosphorylation of PI3P (56). Additionally, the host exchange factor Mon1/Ccz1 functions in the exchange of Rab5 and Rab7 (49). However, it is not known if *M. tuberculosis* affects this host factor. In addition to inhibiting Rab7 recruitment, *M. tuberculosis* also inactivates Rab7. Rab proteins are GTPases that are functionally active when bound to GTP. *M. tuberculosis* secretes Ndk which dephosphorylates GTP in Rab7 producing GDP thereby blocking Rab7 activity (62).

M. tuberculosis also inhibits recruitment of Rab20 to phagosomes. Although not much is known about Rab20 and its recruitment to phagosomes, it is known that Rab20 mediates phagosomal spaciousness (63). Through inhibiting Rab20, *M. tuberculosis* maintains a phagosomal membrane that is tightly associated with the mycobacterial cell wall (63). The connection between phagosomal spaciousness and phagosome maturation arrest by *M. tuberculosis* is intriguing and highlights the importance of mycobacterial cell wall associated proteins and lipids in the process of phagosome maturation arrest. The ability of *M. tuberculosis* to inhibit Rab20 recruitment depends upon the Esx-1 secretion system (63). It is unknown if Esx-1 exports a protein that interferes with Rab20 localization or if the

phagosome membrane perturbations caused by the Esx-1 exported effector ESAT 6 result in this exclusion of Rab20 (discussed below).

Yet another step in phagosome maturation blocked by *M. tuberculosis* is phagosomal acidification. *M. tuberculosis* phagosomes only acidify slightly to a pH of 6.5. The failure of *M. tuberculosis* phagosomes to fully acidify has been attributed to the ability of *M. tuberculosis* to prevent phagosome recruitment and assembly of V-ATPase, a multi-subunit proton pump that acidifies the phagosome (64). *M. tuberculosis* has multiple mechanisms of inhibiting V-ATPase recruitment. *M. tuberculosis* induces the host cytokine inducible SH2 containing protein, CISH, which leads to ubiquitination and subsequent degradation of the catalytic subunit of V-ATPase (65). The *M. tuberculosis* effector that induces this degradation pathway remains unknown. Additionally, *M. tuberculosis* secretes a phosphatase PtpA which binds directly to the H subunit of the V-ATPase preventing assembly of the proton pump on the phagosome (66). PtpA has an additional role in phagosome maturation arrest in dephosphorylating the host protein VPS33B, which blocks fusion of the phagosome with lysosomes (67).

In addition to the specific effectors of phagosome maturation arrest discussed above, there are other phagosome maturation arrest effectors of unknown function (ie PknG) (38). Additionally, several putative effectors have been identified in transposon mutagenesis screens, although these effectors have yet to be validated as functioning in phagosome maturation arrest (68-70). Furthermore, the interplay between effectors remains to be determined, and it remains unclear if all the effectors of phagosome maturation arrest have been identified at this point. The gaps in our understanding are partly due to redundancy among effectors and the potential for effectors to be multi-functional proteins that act in

additional aspects of *M. tuberculosis* pathogenesis or physiology beyond phagosome maturation arrest.

As effectors need to reach their host target, they must either be localized to the mycobacterial cell wall or be fully secreted into the host; therefore, the export systems responsible for localizing effectors are also required for phagosome maturation arrest. As mentioned above, the SecA2 dependent protein export system is required for phagosome maturation arrest by *M. tuberculosis* indicating proteins exported by SecA2 contribute to phagosome maturation arrest (9). SecA2 is required for the inhibition of Rab7, V-ATPase, and phagosome acidification (9). It is not known what proteins are exported by SecA2 that contribute to inhibition of these host factors. In addition to SecA2, the specialized Esx-1 and Esx-3 secretion systems have also been demonstrated to function in phagosome maturation arrest by *M. tuberculosis* (61,71). Esx-3 is responsible for exporting EsxH (discussed above) (61). As the host target of some effectors are localized beyond the phagosomes some effectors of phagosome maturation arrest need to cross the phagosomal membrane into the macrophage cytosol in order to function. Esx1 secretes the ESAT-6 protein, which permeabilizes the phagosomal membrane and allow cytoplasmic access to at least some *M. tuberculosis* molecules (72).

In addition to residing in phagosomes, intracellular *M. tuberculosis* can also localize to double membrane bound compartments known as autophagosomes. Autophagosomes progress through similar maturation stages as phagosomes, ultimately fusing with lysosomes to form degradative autophagolysosomes (73). As with phagosomes, *M. tuberculosis* is able to arrest autophagosome maturation and prevent fusion with lysosomes (74,75). However, unlike the process of phagosome maturation arrest, there has been very little study of *M.*

tuberculosis mechanisms and effectors of autophagosome maturation arrest. Additionally, it is not clear how many host factors are shared between phagosome and autophagosome maturation.

Summary

Our understanding of the multiple roles played by the SecA2 export pathway and its substrates in the virulence of *M. tuberculosis* remain limited. Further complicating our understanding of the role of SecA2 in *M. tuberculosis* virulence is the fact that we likely have not identified all proteins exported by the SecA2 pathway and all functions of the SecA2 pathway during infection. The goal of my thesis research was to fill in these gaps in our understanding of the SecA2 export pathway.

Chapter 2 describes the use of a semi-quantitative comparative mass spectrometry approach to identify new examples of proteins that are exported to the cell wall of *M. tuberculosis* by the SecA2 pathway. We identify two classes of SecA2 exported proteins in *M. tuberculosis*: solute binding proteins of ABC transporters as well as Mce lipid transporters. We additionally identify the kinase PknG with functions in phagosome maturation arrest as exported by the SecA2 pathway of *M. tuberculosis*. In addition to identifying previously unknown SecA2 exported proteins, we also reveal altered transcriptional regulation in the *secA2* mutant of *M. tuberculosis* that indicates that the *secA2* mutant may be under more innate stress or be more prone to stress.

Chapter 3 demonstrates how SecA2 export of two effectors contributes to both phagosome and autophagosome maturation arrest by *M. tuberculosis*. We identify the phosphatase SapM as a SecA2 exported protein that contributes to phagosome maturation

arrest. Using an approach of restoring export of effectors to the *secA2* mutant, we reveal that SecA2 export of SapM and another SecA2 exported protein PknG contribute to multiple stages of phagosome maturation arrest and growth of *M. tuberculosis* in macrophages. We additionally reveal a previously unknown role for SecA2, SapM, and PknG in autophagosome maturation arrest by *M. tuberculosis*.

Chapter 4 describes the use of genome-wide genetic interaction mapping to further elucidate the functions and mechanisms of the SecA2 export pathway of *M. tuberculosis*. Genetic interaction mapping involves identifying mutations that result in altered fitness when combined with the absence of *secA2*. We identify alleviating and aggravating interactions with *secA2* in a murine model of *M. tuberculosis* infection. Alleviating interactions represent genes in the same pathway as SecA2 and they could encode for components of the SecA2 export machinery or SecA2 exported proteins. Aggravating interactions represent genes in a separate pathway that have redundant functions as SecA2 (and SecA2 exported effectors) and could indicate currently unknown functions of the SecA2 pathway in virulence. Our results expand our understanding of the SecA2 pathway by identifying putative substrates and components of the export machinery and by revealing roles for SecA2 in *M. tuberculosis* transporters, phosphate import, copper resistance, peptidoglycan synthesis, and lipid metabolism and homeostasis.

Together, these studies reinforce the importance of the SecA2 pathway to the pathogenesis of *M. tuberculosis*, and they expand our knowledge of proteins exported by the pathway and the mechanisms used by *M. tuberculosis* to arrest phagosome and

autophagosome maturation. Our identification of genetic interactions with *secA2* leads to new hypotheses of SecA2 functions and the identification of proteins exported by the SecA2 pathway that warrant further investigation in the future.

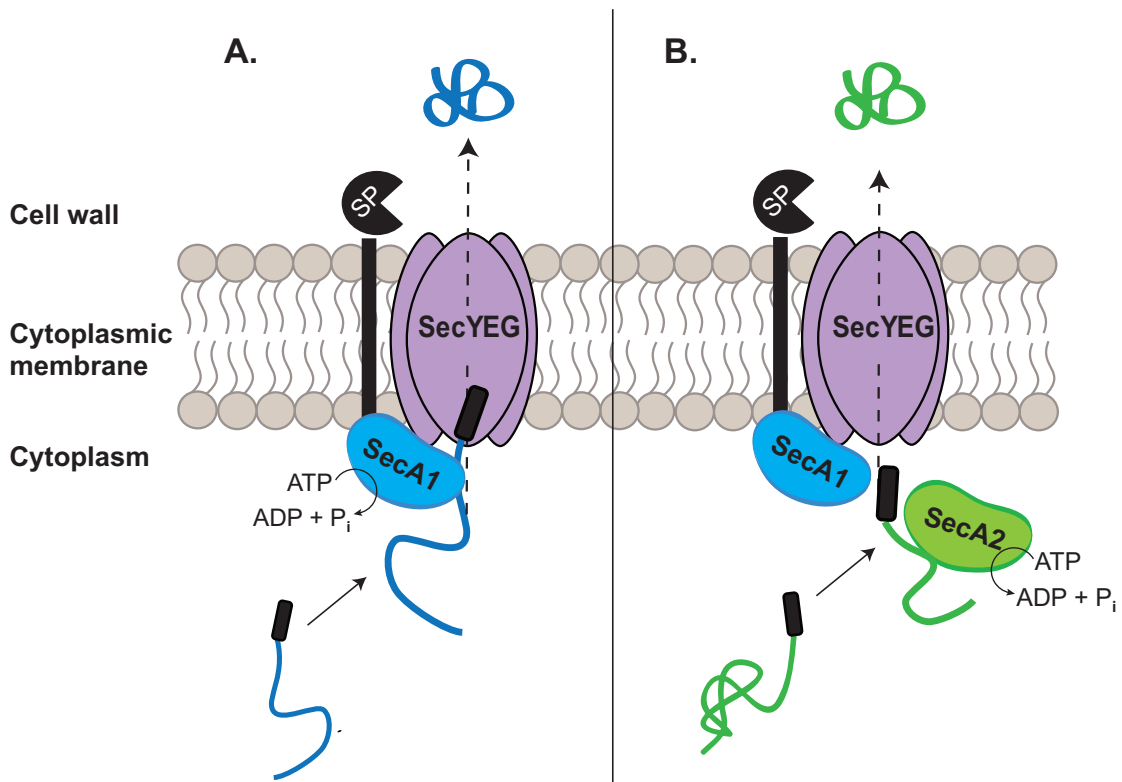


Figure 1.1 Models of SecA1 and SecA2 export in *M. tuberculosis*.

(A) SecA1 uses ATP hydrolysis to export preproteins through the SecYEG channel in an unfolded, export competent state. Sec signal peptides (black rectangle) target preproteins (blue ribbon) for export through SecYEG and are then cleaved by a signal peptidase (SP). (B) SecA2 also uses the SecYEG channel and possibly SecA1 to export its own subset of preproteins (green ribbon). The signal peptide (black rectangle) is indistinguishable from canonical Sec signal peptides. Instead, the mature domain's propensity for cytoplasmic folding is predicted to confer specificity for SecA2.

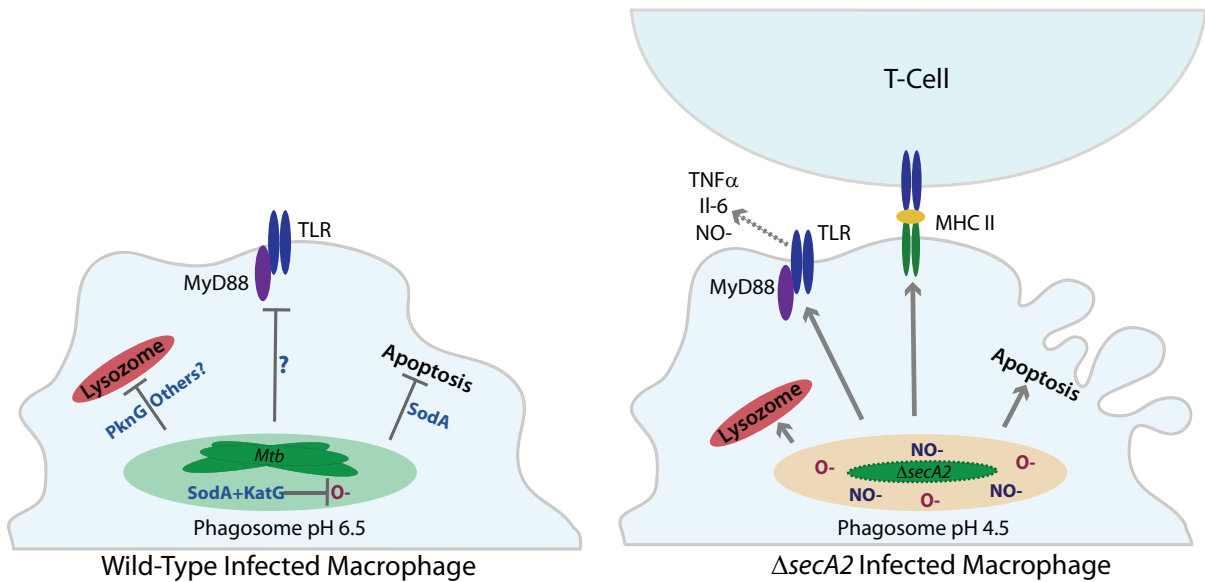


Figure 1.2 SecA2 export is required for *M. tuberculosis* virulence.

The SecA2 pathway combats multiple host immune mechanisms of macrophages. SecA2 export of PknG in addition to other unknown effectors prevents phagosome acidification and fusion with degradative lysosomes. Export of SodA and KatG by SecA2 combats harmful reactive oxygen radicals and limits apoptosis. SecA2 also inhibits signaling through MyD88 by unknown mechanisms, resulting in lower levels of pro-inflammatory cytokines Il-6 and TNF- α along with nitric oxide. Additionally, SecA2 reduces IFN- γ induced MHC II levels, which could impact antigen presentation to CD4⁺ T-cells.

REFERENCES

1. World Health Organization. Global tuberculosis report 2016. World Health Organization; 2016.
2. Smith T, Wolff KA, Nguyen L. Molecular Biology of Drug Resistance in *Mycobacterium tuberculosis*. In: Pathogenesis of *Mycobacterium tuberculosis* and its Interaction with the Host Organism. Berlin, Heidelberg: Springer Berlin Heidelberg; 2012. pp. 53–80. (Current Topics in Microbiology and Immunology; vol. 374).
3. Flannagan RS, Cosío G, Grinstein S. Antimicrobial mechanisms of phagocytes and bacterial evasion strategies. *Nature Reviews Microbiology*. Nature Publishing Group; 2009 May;7(5):355–66.
4. Hussain Bhat K, Mukhopadhyay S. Macrophage takeover and the host-bacilli interplay during tuberculosis. *Future Microbiol*. Future Medicine Ltd London, UK; 2015;10(5):853–72.
5. Armstrong JA, Hart PD. Response of cultured macrophages to *Mycobacterium tuberculosis*, with observations on fusion of lysosomes with phagosomes. *The Journal of Experimental Medicine*. The Rockefeller University Press; 1971 Sep 1;134(3 Pt 1):713–40.
6. Miller BK, Zulauf KE, Braunstein M. The Sec Pathways and Exportomes of *Mycobacterium tuberculosis*. *Microbiol Spectr*. American Society of Microbiology; 2017 Apr;5(2).
7. Awuh JA, Flo TH. Molecular basis of mycobacterial survival in macrophages. *Cell Mol Life Sci*. Springer International Publishing; 2017 May;74(9):1625–48.
8. Hilbi H, Haas A. Secretive bacterial pathogens and the secretory pathway. *Traffic*. 2012 Sep;13(9):1187–97.
9. Sullivan JT, Young EF, McCann JR, Braunstein M. The *Mycobacterium tuberculosis* SecA2 system subverts phagosome maturation to promote growth in macrophages. *Infect Immun*. 2012 Mar;80(3):996–1006.
10. Kurtz S, McKinnon KP, Runge MS, Ting JP-Y, Braunstein M. The SecA2 secretion factor of *Mycobacterium tuberculosis* promotes growth in macrophages and inhibits the host immune response. *Infect Immun*. 2006 Dec;74(12):6855–64.
11. Schneider G. How many potentially secreted proteins are contained in a bacterial genome? *Gene*. 1999 Sep;237(1):113–21.
12. Sassetti CM, Boyd DH, Rubin EJ. Genes required for mycobacterial growth defined by high density mutagenesis. *Mol Microbiol*. Blackwell Science Ltd; 2003 Mar 25;48(1):77–84.

13. Saint-Joanis B, Demangel C, Jackson M, Brodin P, Marsollier L, Boshoff H, et al. Inactivation of Rv2525c, a Substrate of the Twin Arginine Translocation (Tat) System of *Mycobacterium tuberculosis*, Increases β -Lactam Susceptibility and Virulence. *J Bacteriol.* 2006 Sep 4;188(18):6669–79.
14. McDonough JA, Hacker KE, Flores AR, Pavelka MS, Braunstein M. The Twin-Arginine Translocation Pathway of *Mycobacterium smegmatis* Is Functional and Required for the Export of Mycobacterial β -Lactamases. *J Bacteriol.* 2005 Nov 2;187(22):7667–79.
15. Vrontou E, Economou A. Structure and function of SecA, the preprotein translocase nanomotor. *Biochimica et Biophysica Acta (BBA) - Molecular Cell Research.* 2004 Nov;1694(1-3):67–80.
16. Heijne von G. The signal peptide. *The Journal of Membrane Biology.* Springer-Verlag; 1990 May;115(3):195–201.
17. Economou A, Wickner W. SecA promotes preprotein translocation by undergoing ATP-driven cycles of membrane insertion and deinsertion. *Cell.* 1994 Sep;78(5):835–43.
18. Braunstein M, Brown AM, Kurtz S, Jacobs WR. Two nonredundant SecA homologues function in mycobacteria. *J Bacteriol.* 2001 Dec;183(24):6979–90.
19. Braunstein M, Espinosa BJ, Chan J, Belisle JT, Jacobs WR. SecA2 functions in the secretion of superoxide dismutase A and in the virulence of *Mycobacterium tuberculosis*. *Mol Microbiol.* 2003 Apr;48(2):453–64.
20. van der Woude AD, Stoop EJM, Stiess M, Wang S, Ummels R, van Stempvoort G, et al. Analysis of SecA2-dependent substrates in *Mycobacterium marinum* identifies protein kinase G (PknG) as a virulence effector. *Cell Microbiol.* 2014 Feb;16(2):280–95.
21. Watkins BY, Joshi SA, Ball DA, Leggett H, Park S, Kim J, et al. *Mycobacterium marinum* SecA2 promotes stable granulomas and induces tumor necrosis factor alpha in vivo. *Infect Immun.* 2012 Oct;80(10):3512–20.
22. Lenz LL, Mohammadi S, Geissler A, Portnoy DA. SecA2-dependent secretion of autolytic enzymes promotes *Listeria monocytogenes* pathogenesis. *Proc Natl Acad Sci USA.* 2003 Oct 14;100(21):12432–7.
23. Siboo IR, Chambers HF, Sullam PM. Role of SraP, a Serine-Rich Surface Protein of *Staphylococcus aureus*, in Binding to Human Platelets. *Infect Immun.* 2005 Mar 21;73(4):2273–80.
24. Bensing BA, Sullam PM. An accessory sec locus of *Streptococcus gordonii* is required for export of the surface protein GspB and for normal levels of binding to human platelets. *Mol Microbiol.* Blackwell Science Ltd; 2002 May 9;44(4):1081–94.

25. Ligon LS, Rigel NW, Romanchuk A, Jones CD, Braunstein M. Suppressor analysis reveals a role for SecY in the SecA2-dependent protein export pathway of Mycobacteria. *J Bacteriol.* 2013 Oct;195(19):4456–65.
26. Gibbons HS, Wolschendorf F, Abshire M, Niederweis M, Braunstein M. Identification of two Mycobacterium smegmatis lipoproteins exported by a SecA2-dependent pathway. *J Bacteriol.* 2007 Jul;189(14):5090–100.
27. Renier S, Chambon C, Viala D, Chagnot C, Hébraud M, Desvaux M. Exoproteomic analysis of the SecA2-dependent secretion in Listeria monocytogenes EGD-e. *J Proteomics.* 2013 Mar 27;80:183–95.
28. Feltcher ME, Gibbons HS, Ligon LS, Braunstein M. Protein export by the mycobacterial SecA2 system is determined by the preprotein mature domain. *J Bacteriol.* 2013 Feb;195(4):672–81.
29. Krehenbrink M, Edwards A, Downie JA. The superoxide dismutase SodA is targeted to the periplasm in a SecA-dependent manner by a novel mechanism. *Mol Microbiol.* Blackwell Publishing Ltd; 2011 Oct;82(1):164–79.
30. Archambaud C, Nahori M-A, Pizarro-Cerda J, Cossart P, Dussurget O. Control of Listeria superoxide dismutase by phosphorylation. *J Biol Chem.* 2006 Oct 20;281(42):31812–22.
31. Braibant M, Gilot P, Content J. The ATP binding cassette (ABC) transport systems of Mycobacterium tuberculosis. *FEMS Microbiol Rev.* 2000 Oct;24(4):449–67.
32. Hinchey J, Lee S, Jeon BY, Basaraba RJ, Venkataswamy MM, Chen B, et al. Enhanced priming of adaptive immunity by a proapoptotic mutant of Mycobacterium tuberculosis. *J Clin Invest.* American Society for Clinical Investigation; 2007 Aug;117(8):2279–88.
33. De Groote MA, Ochsner UA, Shiloh MU, Nathan C, McCord JM, Dinauer MC, et al. Periplasmic superoxide dismutase protects Salmonella from products of phagocyte NADPH-oxidase and nitric oxide synthase. *Proc Natl Acad Sci USA.* National Academy of Sciences; 1997 Dec 9;94(25):13997–4001.
34. Heym B, Zhang Y, Poulet S, Young D, Cole ST. Characterization of the katG gene encoding a catalase-peroxidase required for the isoniazid susceptibility of Mycobacterium tuberculosis. *J Bacteriol.* American Society for Microbiology (ASM); 1993 Jul;175(13):4255–9.
35. Wengenack NL, Jensen MP, Rusnak F, Stern MK. Mycobacterium tuberculosis KatG is a peroxynitritase. *Biochem Biophys Res Commun.* 1999 Mar 24;256(3):485–7.
36. Cowley S, Ko M, Pick N, Chow R, Downing KJ, Gordhan BG, et al. The Mycobacterium tuberculosis protein serine/threonine kinase PknG is linked to cellular glutamate/glutamine levels and is important for growth in vivo. *Mol Microbiol.*

Blackwell Science Ltd; 2004 Jun;52(6):1691–702.

37. O'Hare HM, Durán R, Cerveñansky C, Bellinzoni M, Wehenkel AM, Pritsch O, et al. Regulation of glutamate metabolism by protein kinases in mycobacteria. *Mol Microbiol.* Blackwell Publishing Ltd; 2008 Dec;70(6):1408–23.
38. Walburger A, Koul A, Ferrari G, Nguyen L, Prescianotto-Baschong C, Huygen K, et al. Protein kinase G from pathogenic mycobacteria promotes survival within macrophages. *Science.* 2004 Jun 18;304(5678):1800–4.
39. Wolff KA, la Peña de AH, Nguyen HT, Pham TH, Amzel LM, Gabelli SB, et al. A redox regulatory system critical for mycobacterial survival in macrophages and biofilm development. Boshoff HI, editor. *PLoS Pathog.* 2015 Apr;11(4):e1004839.
40. Nguyen-Mau S-M, Oh S-Y, Kern VJ, Missiakas DM, Schneewind O. Secretion genes as determinants of *Bacillus anthracis* chain length. *J Bacteriol.* 2012 Aug;194(15):3841–50.
41. Martin CJ, Booty MG, Rosebrock TR, Nunes-Alves C, Desjardins DM, Keren I, et al. Efferocytosis is an innate antibacterial mechanism. *Cell Host & Microbe.* 2012 Sep 13;12(3):289–300.
42. Schaible UE, Winau F, Sieling PA, Fischer K, Collins HL, Hagens K, et al. Apoptosis facilitates antigen presentation to T lymphocytes through MHC-I and CD1 in tuberculosis. *Nat Med.* Nature Publishing Group; 2003 Aug;9(8):1039–46.
43. Nathan C, Shiloh MU. Reactive oxygen and nitrogen intermediates in the relationship between mammalian hosts and microbial pathogens. *Proc Natl Acad Sci USA.* National Academy of Sciences; 2000 Aug 1;97(16):8841–8.
44. Portal-Celhay C, Tufariello JM, Srivastava S, Zahra A, Klevorn T, Grace PS, et al. *Mycobacterium tuberculosis* EsxH inhibits ESCRT-dependent CD4(+) T-cell activation. *Nat Microbiol.* Nature Publishing Group; 2016 Dec 5;2(2):16232.
45. Vieira OV, Bucci C, Harrison RE, Trimble WS, Lanzetti L, Gruenberg J, et al. Modulation of Rab5 and Rab7 recruitment to phagosomes by phosphatidylinositol 3-kinase. *Mol Cell Biol.* American Society for Microbiology (ASM); 2003 Apr;23(7):2501–14.
46. Lawe DC, Chawla A, Merithew E, Dumas J, Carrington W, Fogarty K, et al. Sequential roles for phosphatidylinositol 3-phosphate and Rab5 in tethering and fusion of early endosomes via their interaction with EEA1. *J Biol Chem.* 2002 Mar 8;277(10):8611–7.
47. Simonsen A, Lippé R, Christoforidis S, Gaullier JM, Brech A, Callaghan J, et al. EEA1 links PI(3)K function to Rab5 regulation of endosome fusion. *Nature.* 1998 Jul 30;394(6692):494–8.

48. Sun W, Yan Q, Vida TA, Bean AJ. Hrs regulates early endosome fusion by inhibiting formation of an endosomal SNARE complex. *J Cell Biol.* 2003 Jul 7;162(1):125–37.
49. Yasuda S, Morishita S, Fujita A, Nanao T, Wada N, Waguri S, et al. Mon1-Ccz1 activates Rab7 only on late endosomes and dissociates from the lysosome in mammalian cells. *J Cell Sci.* 2016 Jan 15;129(2):329–40.
50. Cotter K, Stransky L, McGuire C, Forgac M. Recent Insights into the Structure, Regulation, and Function of the V-ATPases. *Trends Biochem Sci.* 2015 Oct;40(10):611–22.
51. Via LE, Deretic D, Ulmer RJ, Hibler NS, Huber LA, Deretic V. Arrest of mycobacterial phagosome maturation is caused by a block in vesicle fusion between stages controlled by rab5 and rab7. *J Biol Chem.* 1997 May 16;272(20):13326–31.
52. Olakanmi O, Schlesinger LS, Ahmed A, Britigan BE. Intraphagosomal Mycobacterium tuberculosis acquires iron from both extracellular transferrin and intracellular iron pools. Impact of interferon-gamma and hemochromatosis. *J Biol Chem.* 2002 Dec 20;277(51):49727–34.
53. Rybin V, Ullrich O, Rubino M, Alexandrov K, Simon I, Seabra MC, et al. GTPase activity of Rab5 acts as a timer for endocytic membrane fusion. *Nature.* 1996 Sep 19;383(6597):266–9.
54. Kyei GB, Vergne I, Chua J, Roberts E, Harris J, Junutula JR, et al. Rab14 is critical for maintenance of Mycobacterium tuberculosis phagosome maturation arrest. *EMBO J.* EMBO Press; 2006 Nov 15;25(22):5250–9.
55. Deghmane A-E, Soualhine H, Soulhine H, Bach H, Sendide K, Itoh S, et al. Lipoamide dehydrogenase mediates retention of coronin-1 on BCG vacuoles, leading to arrest in phagosome maturation. *J Cell Sci.* 2007 Aug 15;120(Pt 16):2796–806.
56. Jeschke A, Haas A. Deciphering the roles of phosphoinositide lipids in phagolysosome biogenesis. *Commun Integr Biol.* Taylor & Francis; 2016 May;9(3):e1174798.
57. Purdy GE, Owens RM, Bennett L, Russell DG, Butcher BA. Kinetics of phosphatidylinositol-3-phosphate acquisition differ between IgG bead-containing phagosomes and Mycobacterium tuberculosis-containing phagosomes. *Cell Microbiol.* Blackwell Science Ltd; 2005 Nov;7(11):1627–34.
58. Vergne I, Chua J, Lee H-H, Lucas M, Belisle J, Deretic V. Mechanism of phagolysosome biogenesis block by viable Mycobacterium tuberculosis. *Proc Natl Acad Sci USA.* 2005 Mar 15;102(11):4033–8.
59. Jaber N, Zong W-X. Class III PI3K Vps34: essential roles in autophagy, endocytosis, and heart and liver function. *Ann N Y Acad Sci.* 2013 Mar;1280(1):48–51.
60. Fratti RA, Chua J, Vergne I, Deretic V. Mycobacterium tuberculosis glycosylated

phosphatidylinositol causes phagosome maturation arrest. *Proc Natl Acad Sci USA*. 2003 Apr 29;100(9):5437–42.

61. Mehra A, Zahra A, Thompson V, Sirisaengtaksin N, Wells A, Porto M, et al. Mycobacterium tuberculosis type VII secreted effector EsxH targets host ESCRT to impair trafficking. Sassetti CM, editor. *PLoS Pathog*. 2013 Oct;9(10):e1003734.
62. Sun J, Wang X, Lau A, Liao T-YA, Bucci C, Hmama Z. Mycobacterial nucleoside diphosphate kinase blocks phagosome maturation in murine RAW 264.7 macrophages. Tyagi AK, editor. *PLoS ONE*. Public Library of Science; 2010 Jan 19;5(1):e8769.
63. Schnettger L, Rodgers A, Repnik U, Lai RP, Pei G, Verdoes M, et al. A Rab20-Dependent Membrane Trafficking Pathway Controls M. tuberculosis Replication by Regulating Phagosome Spaciousness and Integrity. *Cell Host & Microbe*. 2017 May 10;21(5):619–628.e5.
64. Sturgill-Koszycki S, Schlesinger PH, Chakraborty P, Haddix PL, Collins HL, Fok AK, et al. Lack of acidification in Mycobacterium phagosomes produced by exclusion of the vesicular proton-ATPase. *Science*. 1994 Feb 4;263(5147):678–81.
65. Queval CJ, Song O-R, Carralot J-P, Saliou J-M, Bongiovanni A, Deloison G, et al. Mycobacterium tuberculosis Controls Phagosomal Acidification by Targeting CISH-Mediated Signaling. *Cell Rep*. 2017 Sep 26;20(13):3188–98.
66. Wong D, Bach H, Sun J, Hmama Z, Av-Gay Y. Mycobacterium tuberculosis protein tyrosine phosphatase (PtpA) excludes host vacuolar-H⁺-ATPase to inhibit phagosome acidification. *Proc Natl Acad Sci USA*. 2011 Nov 29;108(48):19371–6.
67. Bach H, Papavinasasundaram KG, Wong D, Hmama Z, Av-Gay Y. Mycobacterium tuberculosis Virulence Is Mediated by PtpA Dephosphorylation of Human Vacuolar Protein Sorting 33B. *Cell Host & Microbe*. 2008 May;3(5):316–22.
68. Brodin P, Poquet Y, Levillain F, Peguillet I, Larrouy-Maumus G, Gilleron M, et al. High content phenotypic cell-based visual screen identifies Mycobacterium tuberculosis acyltrehalose-containing glycolipids involved in phagosome remodeling. Deretic V, editor. *PLoS Pathog*. 2010 Sep 9;6(9):e1001100.
69. Stewart GR, Patel J, Robertson BD, Rae A, Young DB. Mycobacterial mutants with defective control of phagosomal acidification. *PLoS Pathog*. Public Library of Science; 2005 Nov;1(3):269–78.
70. Pethe K, Swenson DL, Alonso S, Anderson J, Wang C, Russell DG. Isolation of Mycobacterium tuberculosis mutants defective in the arrest of phagosome maturation. *Proc Natl Acad Sci USA*. 2004 Sep 14;101(37):13642–7.
71. MacGurn JA, Cox JS. A Genetic Screen for Mycobacterium tuberculosis Mutants Defective for Phagosome Maturation Arrest Identifies Components of the ESX-1

Secretion System. *Infect Immun.* 2007 May 18;75(6):2668–78.

72. de Jonge MI, Pehau-Arnaudet G, Fretz MM, Romain F, Bottai D, Brodin P, et al. ESAT-6 from *Mycobacterium tuberculosis* Dissociates from Its Putative Chaperone CFP-10 under Acidic Conditions and Exhibits Membrane-Lysing Activity. *J Bacteriol.* 2007 Aug 1;189(16):6028–34.
73. He C, Klionsky DJ. Regulation mechanisms and signaling pathways of autophagy. *Annu Rev Genet. Annual Reviews*; 2009;43(1):67–93.
74. Chandra P, Ghanwat S, Matta SK, Yadav SS, Mehta M, Siddiqui Z, et al. *Mycobacterium tuberculosis* Inhibits RAB7 Recruitment to Selectively Modulate Autophagy Flux in Macrophages. *Sci Rep. Nature Publishing Group*; 2015 Nov 6;5(1):16320.
75. Romagnoli A, Etna MP, Giacomini E, Pardini M, Remoli ME, Corazzari M, et al. ESX-1 dependent impairment of autophagic flux by *Mycobacterium tuberculosis* in human dendritic cells. *Autophagy. Taylor & Francis*; 2012 Sep;8(9):1357–70.

CHAPTER 2¹

Label-free quantitative proteomics reveals a role for the *Mycobacterium tuberculosis* SecA2 pathway in exporting solute binding proteins and Mce transporters to the cell wall

INTRODUCTION

Mycobacterium tuberculosis, the etiological agent of tuberculosis, remains a severe health concern, infecting an estimated one-third of the global population and causing an approximated 1.3 million deaths annually (1). Following inhalation into the lung, *M. tuberculosis* bacilli are engulfed by macrophages, which fail to destroy the pathogen and instead provide a niche for *M. tuberculosis* replication (2). *M. tuberculosis* proteins that are exported from the cytoplasm to the bacterial cell wall or into the host environment are ideally positioned for host-pathogen interactions or physiologic processes important to infection,

¹ Adapted for this dissertation from: Feltcher ME*, Gunawardena HP*, **Zulauf KE***, Malik S, Griffin JE, Sasseti CM, Chen X, Braunstein M. Label-free quantitative proteomics reveals a role for the *Mycobacterium tuberculosis* SecA2 pathway in exporting solute binding proteins and Mce transporters to the cell wall. *Mol Cell Proteomics*. 2015 Mar 26. pii: mcp.M114.044685. PubMed PMID: 25813378. *contributed equally

such as nutrient uptake and cell wall biogenesis (3). *M. tuberculosis* has several systems for exporting proteins to extracytoplasmic locations, one of which is the SecA2-dependent protein export pathway (4). In *M. tuberculosis*, SecA2 is required for virulence in both mice and macrophage models of infection, making the identification of SecA2-dependent exported proteins important for understanding *M. tuberculosis* pathogenesis (5-7).

Mycobacteria, including *M. tuberculosis*, are among a select group of bacteria that have two non-redundant SecA ATPases, known as SecA1 and SecA2 (8). SecA1 is the housekeeping SecA, conserved throughout bacteria, and a central component of the essential general secretion (Sec) pathway. SecA1 powers translocation of unfolded proteins across a cytoplasmic membrane channel comprised of SecYEG proteins. Proteins exported by SecA1/SecYEG possess N-terminal Sec signal peptides that are cleaved following export to liberate the mature protein. In bacteria with two SecA proteins, SecA2 is generally nonessential but required for export of a limited set of proteins and, in the case of bacterial pathogens, SecA2 often contributes to virulence (8, 9). Bacterial SecA2 systems fall into two main groups based on the membrane channel they work with and the types of substrates they transport. One type of system, called a SecA2-SecY2 system, utilizes an accessory SecY2 channel protein and appears to be dedicated to exporting a single glycosylated protein (10-13). The other type of system, which is the case in mycobacteria, does not include an accessory SecY and the repertoire of exported proteins is more diverse (5, 14-17). In these SecA2-only or multi-substrate SecA2 systems, SecA2 appears to work with the SecYEG channel for protein translocation (9, 17-20). Studies conducted in mycobacteria suggest that the proteins exported by its SecA2-only pathway have a tendency to fold in the cytoplasm prior to export, which distinguishes them from proteins that remain unfolded and are

exclusively exported by SecA1. This folding feature of SecA2-exported proteins may dictate the need for SecA2 in their export (21).

In mycobacteria, and more specifically *M. tuberculosis*, the number of known SecA2-dependent proteins remains small. In the non-pathogenic *Mycobacterium smegmatis*, there are two cell wall proteins that are well-established as being exported via the SecA2 pathway: Ms1704 and Ms1712 (15, 20, 21). Both of these proteins are lipoproteins with Sec signal peptides and members of the solute-binding protein (SBP) family (15). SBPs are cell wall proteins that work with membrane localized ABC transporters to import solutes into the bacterial cytoplasm. Like all mycobacteria, *Mycobacterium marinum*, a pathogen of fish and frogs, also has a SecA2-only system (16, 22). As many as 40 *M. marinum* proteins are predicted by proteomics to be SecA2-dependent (16). The most striking finding of this *M. marinum* study is that PknG, a protein associated with virulence and lacking a Sec signal peptide, is reduced in abundance in a cell envelope fraction of a *M. marinum secA2* mutant compared to wild type (16, 23, 24). There are no direct orthologs of Ms1704 and Ms1712 in *M. tuberculosis* and the mode of PknG export by *M. tuberculosis* has not been established. Past efforts to identify SecA2-dependent proteins in *M. tuberculosis* are limited to comparative two-dimensional gel electrophoresis (2D-GE) of fully secreted proteins. With this approach, superoxide dismutase SodA (5) was identified as a protein requiring SecA2 for its secretion. Like PknG, SodA lacks a predicted Sec signal peptide. However, because inadequate SodA secretion is insufficient to explain the virulence defect of a *M. tuberculosis secA2* mutant (7), there must exist additional *M. tuberculosis* SecA2-dependent proteins. Here, we set out to identify *M. tuberculosis* proteins dependent on SecA2 for their export by

comparing the cell wall and cytoplasmic proteomes of *M. tuberculosis* wild type and a *secA2* mutant using label-free quantitative (LFQ) shotgun proteomics.

Our LFQ analysis revealed reduced cell wall levels of almost all of the predicted *M. tuberculosis* SBPs in the *secA2* mutant versus wild type, suggesting a broad role for SecA2 in the export of this family of proteins. Further, multiple protein components of Mce1 and Mce4 transporters were reduced in the *secA2* mutant cell wall, suggesting a dependence on SecA2 for cell wall localization of these transport systems. Our proteomics approach also revealed an unexpected role for SecA2 in the DosR-regulated stress response of *M. tuberculosis*, with higher abundance of many cytoplasmic DosR-dependent proteins detected in the *secA2* mutant compared to wild type. Finally, we obtained data consistent with *M. tuberculosis* PknG being exported by the SecA2 pathway. By expanding our knowledge of the types of proteins exported by the mycobacterial SecA2 system, this study helps our effort to understand the mechanism of this specialized protein export pathway. At the same time, the SecA2-dependent proteins identified in this work provide valuable insight into potential role(s) of the SecA2 pathway in *M. tuberculosis* virulence and physiology.

MATERIALS AND METHODS

***M. tuberculosis* strains and plasmids used in this study.**

The following *M. tuberculosis* strains were used in this study: H37Rv (wild type), mc²3112 (*secA2*) and a complemented strain MBTB476 (mc²3112, pSM15) (5). Plasmid pSM15 is a derivative of pMV306.kan that carries the *M. tuberculosis secA2* gene under the

control of the *hsp60* promoter. In experiments involving the complemented strain, H37Rv and *secA2* strains carried the empty pMV261.kan plasmid to allow all strains to be grown in the presence of kanamycin.

Growth conditions.

M. tuberculosis strains were first grown at 37°C in Middlebrook 7H9 medium (Difco) supplemented with 0.5% glycerol, 1X ADS [0.5% bovine serum albumin, 0.2% glucose, 0.85% NaCl], 0.05% Tyloxapol (Sigma), and 20 μ g/ml kanamycin, if necessary. After reaching an OD₆₀₀ of 2, cells were centrifuged and twice washed in modified 7H9 media: Middlebrook 7H9 supplemented with 0.1% glycerol, 1 mM propionic acid (Sigma), 0.5% bovine serum albumin, 0.1% Tyloxapol, pH adjusted to 6.5 and buffered with 100 mM 2-(4-morpholino)-ethane sulfonic acid. This modified 7H9 media was used in all subsequent steps of preparing samples and was designed to reflect features of the host environment encountered by *M. tuberculosis*. During infection, *M. tuberculosis* is exposed to a mildly acidic pH of 6.5 in a macrophage (25) and utilizes fatty acids as a carbon source (26-28). Washed cells were used to inoculate modified 7H9 medium at an OD₆₀₀ of 0.08. Upon reaching an OD₆₀₀ of 1.0, the cells were pelleted, washed with 1X phosphate-buffered saline (PBS) and sterilized by gamma-irradiation in a JL Shephard Mark I 137Cs irradiator (Dept. of Radiobiology, University of North Carolina at Chapel Hill) prior to removal from BSL-3 containment. In some experiments, a 40 ml volume of cells in modified 7H9 medium (OD₆₀₀ of 0.8-1.0) was transferred to a 50 ml conical tube and let stand at 37°C for 2 or 24 hours as a strategy to induce the DosR-dependent regulon (29).

Preparation of subcellular fractions.

Subcellular fractions were isolated as previously described (30). Briefly, irradiated cells suspended in 1X PBS containing protease inhibitors were lysed by passage through a French pressure cell. Unlysed cells were removed by centrifugation at 3,000 x g to generate clarified whole cell lysates (WCLs), which were then spun at 27,000 x g for 30 minutes to pellet the cell wall fraction. The supernatant was then spun at 100,000 x g for 2 hours to separate the cytoplasmic membrane fraction and collect the soluble cytoplasm-containing fraction. Protein concentrations were determined by Bicinchoninic acid assay (Pierce).

SDS-PAGE separation and in-gel trypsin digestion of proteins.

Cell wall proteins (34 µg) and cytoplasmic proteins (91 µg) from three biological replicates each of H37Rv and the *secA2* mutant were separated on individual lanes of a precast 12% SDS-PAGE gel. Protein bands were visualized by Coomassie Blue R-250 staining (Bio-Rad, Hercules, CA) and each lane was cut into 32 gel slices for cell wall samples and 10 gel slices for cytoplasmic samples. In-gel trypsin digestion was performed, as previously described (31), with each gel slice being processed individually in a single well of a 96-well polypropylene plate. Peptides were stored at -80°C until lyophilized.

Liquid chromatography and tandem mass spectrometry analysis.

Peptides were desalted using PepClean C18 spin columns (Pierce, Rockford, IL) and re-suspended in an aqueous solution of 0.1% formic acid. Samples were analyzed by reversed phase LC-MS/MS using a 2D-nanoLC ultra system (Eksigent Inc, Dublin, CA)

coupled to an LTQ-Orbitrap XL system with ETD (Thermo Scientific, San Jose, CA). The Eksigent system was configured to trap and elute peptides in 1D mode of operation via a sandwiched injection of ~ 250 fmol of sample. The trapping was performed on a 3 cm long 100 μm i.d. C18 column while elution was performed on a 15 cm long 75 μm i.d., 5 μm , 300Å particle; ProteoPep II integraFrit C18 column (New Objective Inc, Woburn, MA). Analytical separation of tryptic peptides was achieved with a linear gradient of 2-40% over 120 min at a 200 nL/min flow rate, where buffer A is aqueous solution of 0.1% formic acid and buffer B is a solution of acetonitrile in 0.1% formic acid. Mass spectrometric data acquisition was performed in a data dependent manner. A full scan mass analysis on an LTQ-Orbitrap (externally calibrated to a mass accuracy of < 1 ppm, and resolution of 60 000 at 400 Th) was followed by intensity dependent MS/MS of the 10 most abundant peptide ions. The dynamic exclusion time window was set to 60 s. with monoisotopic precursor ion selection (MIPS) and charge state screening enabled for charges $\geq +2$ for triggering data dependent MS/MS scans.

Peptide and protein identification.

Mass spectra were processed, and peptide identification was performed using Mascot ver. 2.3 (Matrix Science Inc.) implemented on Proteome Discoverer ver. 1.3 (Thermo-Fisher Scientific). All searches were performed against the National Center for Biotechnology (NCBI) *M. tuberculosis* H37Rv protein sequence database (RefSeq NC_000962 uid 57777, 3906 protein entries). Peptides were identified using a target-decoy approach with a peptide false discovery rate (FDR) of 1% (32, 33). A precursor ion mass tolerance of 200 p.p.m. and a product ion mass tolerance of 0.5 Da (34) were used during the search to increase search

space and reduce false positive identifications with a maximum of two missed trypsin cleavage sites and oxidation of methionine residues as dynamic modification.

Peptide validation and spectral count-based label-free quantitation (LFQ).

Peptide and protein validation and label-free spectral count-based quantitation was performed using ProteoIQ: ver 2.3.02 (PREMIER Biosoft international, Palo Alto, CA). Mascot search engine results against forward and decoy *M. tuberculosis* databases were obtained for all RAW data. Both forward and decoy search results were imported as DAT files into ProteoIQ to assess FDR. A peptide FDR of 1% and protein FDR of 5% were used to filter valid spectra. Peptide assignment to proteins was achieved by considering Occam's Razor principle that takes into account the presence of protein groups and penalizes proteins containing peptides identified in multiple proteins. The PROVALT algorithm in ProteoIQ was used to determine ion score thresholds and protein FDR (33). Mascot protein identifications were also subjected to probability-based confidence measurements using an independent implementation of the statistical models commonly known as peptide and protein Prophet deployed in ProteoIQ (35, 36). All protein hits were filtered with peptide Prophet using a minimum probability threshold of 0.5. Evaluation of sensitivity and error rates in this filtered data set for the cell wall proteome demonstrated a sensitivity of 95% with a 4.8% error rate while the filtered data for the cytoplasm had 90% sensitivity with a 6.2% error rate. From a total of 2194 proteins detected in the cell wall and 2226 detected in cytoplasmic samples the data was filtered for proteins identified by a minimum of 2 peptides resulting in 1729 cell wall and 1810 cytoplasmic proteins identified, reported and used in all further analysis in this study.

Relative protein quantitation was performed using spectral count-based LFQ. For each biological sample, data from the individual gel slices were combined. Statistical analysis was performed on all proteins identified with average spectral counts of ≥ 4 among the three replicates of at least one strain. The spectral count data was normalized by total spectral counts in each sample, using ProteoIQ, to adjust for differences in overall protein levels between samples. The normalized spectral count data was then used to calculate a ratio of the average spectral counts obtained for each strain *secA2*/H37Rv. Proteins were considered to have a significant difference in abundance if there was a difference of 2-fold or greater in average spectral counts between strains and a p value ≤ 0.01 using an unpaired two-tailed Student's t-test. Multiple hypothesis testing was also applied to the data by computing q values using QVALUE software (<http://genomics.princeton.edu/storeylab/qvalue/>). The q values for quantitated proteins are reported on the data tables. The q value is an estimate of the minimum FDR for proteins judged to be significantly changed at a given p value (in our case $p \leq 0.01$) (37).

Immunoblotting.

Equal protein content for whole cell lysates, cell wall or cytoplasmic fractions from H37Rv, *secA2* mutant, and the complemented strain were separated by SDS-PAGE and then transferred to nitrocellulose membranes. After blocking for 1 hour at room temperature, proteins were detected using the following antibodies: anti-Mce1A at 1:10,000, anti-Mce1C at 1:5,000, anti-Mce1F at 1:10,000, anti-LprK at 1:5,000, anti-19kD at 1:20,000 (provided by Douglas Young, Imperial College, United Kingdom), anti-PhoS1 at 1:20,000 (IT23, NIH Biodefense and Emerging Infections Research Resources Repository, NIAID), anti-PknG at

1:5,000 (provided by Yossef Av-Gay, University of British Columbia, Canada) and anti-HspX at 1:1000 (IT20, NIH Biodefense and Emerging Infections Research Resources Repository, NIAID). Anti-mouse and anti-rabbit IgG conjugated horseradish peroxidase (Bio-Rad) secondary antibodies were used and signal was detected using Western Lightning Chemiluminescent detection reagent (Perkin-Elmer).

Anti-Mce antibody production.

Anti-peptide antibodies for Mce1A, 1C, 1F, and LprK were generated in rabbits using peptides conjugated to keyhole limpet hemocyanin by Open Biosystems (Huntsville, AL). The peptides used were the following: GRVDTISEVTRDGESA (Mce1A), DLLVDRKEDLAETLTILGR (Mce1C), SAVYSPASGELVGPDGVKY (Mce1F), and DPSPVPLKDGDTIPLKRS (LprK). Immunoaffinity chromatography was used for antibody purification.

Bioinformatic analysis.

Sec signal peptides were predicted using Signal P 4.01 and default options for Gram positive bacteria (38). Tat signal peptide predictions were compiled using TatP 1.03, TATFIND v1.44, and TigrFAM5 (39-42). Transmembrane predictions were made using TMHMM 2.06 (43). Mycobacterial lipoproteins were predicted using the list compiled by Sutcliffe and Harrington (44). Protein associations were predicted using the Search Tool for the Retrieval of Interacting Genes/Proteins (STRING) (version 9.1) set for a medium confidence level (0.4) (45).

Quantitative Real-Time PCR.

Triplicate cultures were grown in modified 7H9 medium to an OD₆₀₀ of 1.0 and pelleted by centrifugation at 3,000 rpm for 10 min. Bacteria were lysed in 1 ml 3:1 chloroform-methanol, then vortexed with 5 ml TRIzol (Invitrogen) and incubated for 10 min at room temperature. Phases were separated by centrifugation at 3,000 rpm for 15 min at 4°C, and RNA was precipitated from the upper phase using 1X volume of isopropanol. RNA was pelleted by centrifugation at 12,000 rpm for 30 min at 4°C, washed twice with cold 70% ethanol, and resuspended in RNase-free water. RNA samples were treated with DNase (Promega) and then column purified (Zymo RNA clean and concentrator kit). Following RNA isolation, cDNA was synthesized with random primers using the iScript cDNA Synthesis Kit (BioRad). Real-time PCR was completed using 25ng of cDNA template in triplicate technical replicates using the SensiMix SYBR and fluorescein kit (Bioline). Transcripts were normalized to the housekeeping gene *sigA* (46).

RESULTS

Proteomic analysis of differentially abundant proteins in the cell wall of H37Rv (wild type) versus *secA2* mutant *M. tuberculosis*.

Triplicate cultures of *M. tuberculosis* H37Rv (wild type) and *secA2* mutant were grown to mid-log phase, at which time cells were sterilized by gamma irradiation and lysed with a French pressure cell to generate whole cell lysates (WCL). WCLs were then subjected to differential ultracentrifugation to generate cell wall fractions. Immunoblot analysis of the cell wall fractions demonstrated the presence of the 19 kD lipoprotein but not the cytoplasmic SigA and MtrA proteins, as expected (data not shown).

Since cell wall proteins often exhibit solubility problems, we combined SDS-solubilization and SDS-PAGE separation of cell wall fractions with LC-MS/MS to analyze the cell wall proteomes, as previously described (30). For each biological replicate, cell wall proteins were collected from an entire lane of an SDS-PAGE gel in 32 slices of equal size. Tryptic peptides from each slice were analyzed separately by LC-MS/MS. In total, we identified 1729 proteins with a minimum of two unique peptides among the cell wall fractions of H37Rv (wild type) and the *secA2* mutant. These cell wall-associated proteins fall into diverse functional categories (Figure 2.1). The largest functional groups of proteins identified are predicted to be involved in cell wall processes, intermediary metabolism/respiration, or are conserved hypothetical proteins (47). This distribution of cell wall-associated proteins among functional groups is similar to what is seen in other *M. tuberculosis* cell wall proteome studies (48, 49).

Of these 1729 proteins identified, 501 are predicted to be fully exported across or inserted into the cytoplasmic membrane due to the presence of a predicted Sec or Tat signal peptide (183 proteins) and/or a transmembrane domain (405 proteins). Additionally, 67 proteins were predicted to be lipoproteins, representing 70% of the lipoproteins predicted in the H37Rv genome (44), which is consistent with the role of lipidation in anchoring proteins to the bacterial cell envelope (50). The identification of proteins lacking a predicted signal peptide or transmembrane domain in the cell wall fraction was not surprising as past proteomic studies of mycobacterial membrane and cell wall fractions identify a similar percentage of proteins lacking export signals (31, 48, 49, 51, 52). Some of these proteins

may be unconventional exported proteins lacking recognizable signals for export. However, due to the high sensitivity of mass spectrometry, cytoplasmic and cytoplasmic membrane contaminants can also be identified in the cell wall fraction.

Using spectral counting, we compared the composition and relative levels of proteins in the *secA2* mutant to H37Rv cell wall fractions. Spectral counting is based on the observation that the total number of MS/MS spectra assigned to a protein correlates with the abundance of that protein (53). In order to avoid low abundance proteins that fall outside of the linear dynamic range of spectral counting, we limited our analysis to the 1,318 proteins identified by a minimum of 2 peptides with an average of ≥ 4 spectral counts (53) among the replicates of at least one of the strains (H37Rv or *secA2* mutant). When the spectral count data for each replicate was compared, a good correlation was revealed between biological replicates (Pearson's correlation coefficient of $r > 0.92$). Following normalization by total spectral counts for each protein, spectral count ratios ($\log_2(\text{secA2}/\text{H37Rv})$) were calculated for 1,300 proteins that were detected in both strains. For 18 proteins with average of ≥ 4 spectral counts, spectral count ratios could not be calculated because these proteins were only identified in one of the two strains: 4 proteins were exclusively identified in H37Rv (unidentified in the mutant) and 14 proteins were only identified in the *secA2* mutant. Proteins exclusively identified in one of the strains are most likely present in the other strain, but at levels that fall below our limit of detection. For the 1,300 proteins with spectral count ratios calculated, significant differences in protein levels between the two strains were determined by a Student's t-test ($p < 0.01$) and by having a difference of 2-fold or greater between strains (\log_2 spectral count ratio of ± 1.0). To visualize the distribution of spectral count ratios for the cell wall proteins, a volcano plot of the \log_2 ratio of *secA2* /H37Rv versus

$-\log p$ value was generated (Figure 2.2). The majority of proteins were present at similar levels in the two strains. Of note, the SecA1 ATPase was detected at equivalent levels in the *secA2* mutant and H37Rv (Figure 2.2), which reinforces past conclusions that the absence of SecA2 does not alter the level of SecA1 (54). Among the proteins exhibiting significant differences (>2 -fold difference, $p < 0.01$), there were 33 proteins with significantly decreased levels in the cell wall fraction of the *secA2* mutant versus H37Rv and 33 proteins with significantly increased levels in the *secA2* mutant cell wall fraction relative to H37Rv. Proteins chosen for independent validation in this study are labeled on the volcano plot.

From the spectral counting analysis, we expected to detect protein abundance differences resulting from SecA2-dependent export defects as well as regulatory consequences of the absence of SecA2. Altogether, there were 37 proteins whose level was either reduced or unidentified in the *secA2* cell wall when compared to H37Rv. Of these proteins, which represent candidates for being exported by the SecA2 pathway, 46% possess a predicted Sec or Tat signal peptide or putative transmembrane domain, with 4 of these proteins being predicted lipoproteins. Conversely, there were 47 proteins either increased or uniquely identified in the *secA2* mutant compared to H37Rv. In this latter collection of proteins, there were a smaller percentage of predicted exported proteins (28%) and only 1 predicted lipoprotein. This latter group of proteins seems likely to include more examples of contaminating cytoplasmic proteins.

Protein families and networks exhibiting differences in the *secA2* mutant versus H37Rv.

To identify functional categories and protein families that are SecA2-dependent we plotted the percentage of proteins in a given functional group, as defined by Tuberculist (47),

that exhibited differential levels between the *secA2* mutant and H37Rv (Figure 2.3).

However, none of these broad functional categories revealed a strong association with SecA2-dependent proteins (Figure 2.3).

Solute Binding Proteins (SBPs).

Due to the precedent of two *M. smegmatis* SBPs being SecA2-dependent exported proteins (15), we inspected the spectral counting data for the 15 SBPs we identified in the cell wall fraction (18 SBPs are predicted to exist in *M. tuberculosis*) (44, 55). This analysis revealed a trend in SBPs being reduced in the cell wall of the *secA2* mutant when compared to H37Rv (Figure 2.3; Table 2.1). There were 4 SBPs significantly reduced (≥ 2 -fold decreased, $p < 0.01$) in the *secA2* mutant cell wall compared to H37Rv. Furthermore, there were an additional 9 SBPs reduced in the *secA2* mutant cell wall, although the reduction relative to H37Rv did not always reach 2-fold or achieve statistical significance. All of these SBPs are predicted lipoproteins, which is consistent with their localization to the cell wall. Altogether, 13 of the 15 SBPs we identified were reduced to some degree in the *secA2* mutant cell wall.

Mce Proteins.

As an alternate approach to find functional categories or networks influenced by SecA2, we entered the SecA2-dependent proteins showing significant differences between strains (≥ 2 -fold difference, $p < 0.01$, or unidentified) into the Search Tool for the Retrieval of Interacting Genes (STRING) database of known and predicted protein associations (45). For clarity, Figure 2.4 only shows portions of the STRING analysis. Among the proteins reduced/unidentified in the cell wall of the *secA2* mutant versus H37Rv, there was a cluster of members of two of the four Mce transporter systems (Mce1 and Mce4) (Figure 2.4A).

When the percentage of all Mce transporter components showing differential abundance in the *secA2* mutant versus H37Rv was plotted, the reduction in Mce protein family members in the *secA2* cell wall was evident (Figure 2.3).

Mce transporters are multi-protein complexes localized to the cell envelope (56, 57) that are proposed to function in lipid uptake by mycobacteria. Mce transporters are encoded by 8-12 gene operons. Each system contains *yrbE* genes encoding putative membrane-spanning proteins, five *mce* genes encoding proteins with potential signal peptides or N-terminal transmembrane domains and one *lpr* gene encoding a lipoprotein (Figure 2.5). Most Mce systems also have genes that encode Mce-associated proteins (*mas*) possessing transmembrane domains. Of the 9 proteins encoded by the *mce4* locus, 6 proteins were significantly reduced in the *secA2* mutant cell wall (≥ 2 -fold, $p < 0.01$) (Figure 2.5, Table 2.1). Mce4F and Mas4B were also reduced in the $\Delta secA2$ mutant, although the differences did not meet one or both of our cutoffs. Among the 12 components of the Mce1 system, 6 proteins were significantly reduced in the *secA2* mutant cell wall ($p < 0.01$); however, only 2 of them (Mce1A and Mce1F) were reduced by ≥ 2 -fold. The Mce-associated ATPase MceG (Mkl) was also significantly reduced in the $\Delta secA2$ mutant by 1.8-fold.

DosR-regulated proteins.

Among the proteins that were increased in the *secA2* mutant relative to H37Rv, the STRING database identified a cluster of proteins that are members of the DosR regulon (58) (Figures 2.3 and 2.4B). Of the 21 DosR-regulated proteins we identified, 13 were increased (≥ 2 -fold, $p < 0.01$) or exclusively identified in the *secA2* cell wall. The mostly cytoplasmic proteins within the DosR regulon are under the transcriptional control of the DosR/S/T two component regulatory system. One of the proteins significantly increased in the *secA2*

mutant was the DosR response regulator, which is known to autoregulate itself at the transcriptional level (59). The remaining 8 DosR-regulated proteins we identified in the cell wall followed the same trend of being increased in the *secA2* mutant, although their differences failed to meet our significance and/or 2-fold cut-offs (Figure 2.3, Table 2.2).

Validation of cell wall protein differences.

To validate the spectral counting identifications of the above families and networks of differentially abundant proteins, we performed immunoblot analysis on sets of newly prepared cell wall samples that included a complemented strain, which represents the *secA2* mutant carrying a plasmid expressing wild type *secA2*. Using antibodies to PhoS1, we monitored the abundance of this representative SBP in the cell wall fractions of H37Rv, *secA2*, and the complemented strain (Figure 2.6A). As predicted by the spectral counting analysis, PhoS1 was partially reduced in the *secA2* mutant cell wall. Importantly, the level of PhoS1 in the cell wall was restored in the complemented strain. PhoS1 levels in whole cell lysates were the same between strains (Figure 2.6B) indicating that the reduced amount of PhoS1 in the *secA2* cell wall is not due to an effect on total PhoS1 levels. Rather, these results support PhoS1 being dependent on SecA2 for export to the cell wall. Using a series of antibodies to Mce1 components (Mce1A, Mce1C, Mce1F, LprK) we similarly assessed the levels of Mce1 proteins in the cell wall. The levels of all four of these proteins were reduced in the cell wall of the *secA2* mutant when compared to H37Rv and the complemented strain (Figure 2.6A). In this case, lower levels of the Mce proteins were also observed in whole cell lysates of the *secA2* mutant (Figure 2.6B). Immunoblot analysis of

cell wall fractions was also performed with anti-19kDa lipoprotein antibodies. As predicted by the spectral counting data of cell wall fractions, the amount of the 19kDa lipoprotein was the same in the cell wall of all three strains.

We attempted immunoblot analysis with antibodies to HspX, as a representative DosR-regulated protein; however, the amount of HspX in the cell wall was below the level of detection. Therefore, in order to test the effect of SecA2 on HspX, we prepared samples from cultures that were left standing in 50 ml conical tubes for 2 or 24 hours to induce DosR-dependent *hspX* expression (29). In these induced samples, HspX was detected in the cell wall and was present at higher levels in the *secA2* mutant (Figure 2.6C). Higher levels of HspX were also observed in the whole cell lysate as well as in the cytoplasm of the *secA2* mutant indicating an overall increase in HspX levels in the *secA2* mutant.

Transcriptional effects do not account for the reduced cell wall localization of Mce proteins but can account for DosR-regulated effects.

Genes in the *mce1* and *mce4* loci (Figure 2.5) are organized in operons (61), which raises the possibility of a transcriptional effect accounting for the reduced levels of multiple Mce components that we observed in whole cell lysates and cell wall fractions of the *secA2* mutant. To address the possibility of their being a transcriptional effect, we performed quantitative real time PCR (qRT-PCR) on RNA prepared from H37Rv, *secA2*, and complemented strains using primers for *mce1A*, *mce1F*, *mce4A* and *mce4F*. Transcript levels were normalized to the housekeeping control *sigA* (46). For all four genes, there was no significant difference in transcript levels between H37Rv and the *secA2* mutant (Figure 2.7A). This result argues against a transcriptional effect on *mce* loci. Rather, it supports the

alternate explanation for the immunoblot data, which is that there is a Mce export defect in the *secA2* mutant and subsequent degradation of unexported Mce transporter components. In multiple experiments, the complemented strain showed a significantly lower level of *mce1A*, *mce1F*, *mce4F* transcript than either H37Rv or *secA2*. The explanation for this effect is not clear, although it could reflect feedback regulation of *mce* expression in the presence of higher than normal SecA2 levels resulting from the complementation construct.

The DosR-regulated proteins identified as more abundant in the *secA2* mutant are all under transcriptional control of the DosR/S/T system. To test if SecA2 affects transcription of DosR-regulated genes we measured *hspX* transcript levels in H37Rv, *secA2*, and complemented strains. RNA was prepared from uninduced samples and standing cultures that sat for 2 or 24 hours to induce the DosR-regulon. In all conditions (+/- induction), the level of *hspX* transcript was higher in *secA2* versus H37Rv or the complemented strain (Figure 2.7B). We also found that the level of *dosR* transcript was higher in the *secA2* mutant, although the difference was only statistically significant after 2 hr induction. Interestingly, in both the *hspX* and *dosR* transcript analyses the difference between H37Rv and *secA2* samples was most pronounced at 2 hrs and waned at 24 hours. Overall, these results indicate that the higher abundance of DosR-regulated proteins in the *secA2* mutant can be attributed to increased transcription.

Proteomic analysis of differentially abundant proteins in the cytoplasm of H37Rv versus the *secA2* mutant.

Our detection of upregulated cytoplasmic members of the DosR regulon in the *secA2* mutant was fortuitous: a likely consequence of these proteins being highly expressed

contaminants of cell wall fractions. To more directly test for cytoplasmic effects in the *secA2* mutant, we performed LFQ analysis on cytoplasmic fractions prepared from triplicate H37Rv and *secA2* mutant cultures. A total of 1,810 proteins were identified by a minimum of 2 peptides among the cytoplasmic fractions of H37Rv and the *secA2* mutant. As expected, proteins identified in the cytoplasmic fraction fall into diverse functional categories (Figure 2.8A). As with the cell wall proteome, intermediary metabolism/respiration and conserved hypothetical proteins were among the largest functional groups of proteins identified in the cytoplasmic proteome. However, a much smaller percentage of proteins with predicted functions in cell wall processes were identified in the cytoplasm versus the cell wall (9.7% vs 22.7%), as expected.

Spectral count ratios were calculated for the 1,266 proteins in the cytoplasmic fraction having average spectral counts ≥ 4 across the biological replicates of at least one of the strains. Once again, there was strong correlation between the spectral count data of replicates (Pearson's correlation coefficient of $r > 0.99$ between replicate cytoplasmic fractions). A volcano plot of the \log_2 ratio of *secA2*/H37Rv shows the distribution of spectral count ratios (Figure 2.8B). Among the proteins exhibiting significant differences (≥ 2 -fold, $p < 0.01$) between strains, there were 17 proteins with higher levels in the *secA2* mutant and 1 protein with reduced levels of protein in the mutant. There were an additional 3 proteins with ≥ 4 average spectral counts that could not be quantitated because they were undetected in one of the two strains: 2 proteins were exclusively identified in *secA2* mutant samples and SecA2 was the only protein exclusively identified in H37Rv. Of the proteins that were significantly increased or only identified in the *secA2* mutant, 68% of them were DosR-regulated proteins (13 of 19 proteins) (Table 2.2). As seen in the cell wall fractions, the other DosR-regulated

proteins identified followed the same trend of being upregulated in the *secA2* mutant although the differences failed to meet our significance cut-offs. STRING analysis performed on proteins showing significant differences between strains (≥ 2 -fold difference, $p < 0.01$, or unidentified) identified no pathways, besides the DosR regulon, as being altered in the *secA2* mutant.

PknG levels are increased in the cytoplasm of the *M. tuberculosis secA2* mutant.

Among the small number of non DosR-regulated proteins detected at significantly higher levels in the cytoplasm of the *secA2* mutant was the virulence factor PknG (6.1 fold increased, $p = 0.009$), which is reported to be SecA2-dependent in *M. marinum* (16). In some cases, when a protein is not being properly exported it will accumulate in the cytoplasm (15). Therefore, to follow up on this result, we performed immunoblot analysis with anti-PknG antibodies on fractions prepared from H37Rv, *secA2* mutant, and the complemented strain. While PknG levels in the whole cell lysate were the same between the strains, the immunoblot confirmed a higher amount of PknG was present in the cytoplasmic fraction of the *secA2* mutant (Figure 2.9). Further, immunoblotting revealed less PknG in the cell wall fraction of the *secA2* mutant when compared to H37Rv and the complemented strain. Therefore, although PknG did not meet our criteria of a significant difference in the LFQ analysis of the cell wall, our combined results from LFQ analysis of the cytoplasmic samples and immunoblot analysis are consistent with PknG being exported by the SecA2 pathway of *M. tuberculosis*, as reported to be the case for *M. marinum* (16).

DISCUSSION

Despite progress in understanding the mycobacterial SecA2 system, the identity of the proteins exported by the SecA2 pathway, most specifically of *M. tuberculosis*, has remained a critical unknown. Here, we took an unbiased proteomic approach using LFQ analysis with spectral counting to discover new proteins exported by the SecA2 pathway of *M. tuberculosis*. Using a cutoff of a ≥ 2 -fold difference and $p < 0.01$ we substantially increased the list of mycobacterial proteins observed to be affected by deletion of *secA2* (5, 15, 16). We mined this dataset to identify probable SecA2-dependent exported substrates and differences reflective of physiological effects of the SecA2 export pathway (Figure 2.10). As with all proteomic studies of this sort, generating a comprehensive list of biologically significant differences is a challenge. Some differences and their significance will not be detected, as appears to have occurred for PknG in the cell wall analysis. Possible reasons for this occurring include quantitative measurement bias from missing data, incomplete sampling due to dynamic range issues, or matrix interference. At the same time, it is critical that differences detected in discovery experiments be validated with independently prepared samples, as performed for several proteins in this study.

Differences in protein families and networks in the *secA2* mutant.

A striking observation from this study was the lower level of nearly all signal peptide-containing SBP lipoproteins identified (13 of 15) in the *secA2* mutant versus H37Rv cell wall. Although the best-studied mycobacterial SecA2 substrates are *M. smegmatis* SBPs (15, 20, 21), this is the first demonstration of SecA2-dependent SBP export in *M. tuberculosis*.

The reduction in SBP localization to the *M. tuberculosis secA2* cell wall was not complete (i.e. residual export occurred in the absence of SecA2). However, partial export defects were also seen with other proteins identified in this study and in past studies of SecA2-dependent proteins of *M. tuberculosis*, *M. smegmatis*, and *M. marinum* (5, 15, 16). Our data argues for a general property of SBPs that imparts a requirement for SecA2 in their export. In support of this idea, three SBPs are among the proteins reduced in a proteomic study of the *M. marinum* cell envelope of a *secA2* mutant (16). An association of SBPs with SecA2-dependent export may also exist outside of mycobacteria. The *Listeria monocytogenes* SecA2-only system is reported to export 3 SBPs to the cell surface (14), although there are conflicting reports about the SecA2-dependent nature of some of these substrates (62, 63).

An interesting observation is that 4 of the 13 SBPs reduced in the *M. tuberculosis secA2* mutant have predicted or proven Tat signal peptides (Table 2.1) (39). The twin-arginine translocation (Tat) pathway operates independently and quite differently from the Sec pathway. The most notable feature of the Tat pathway is that it exports folded proteins across the cytoplasmic membrane (64). There are also examples of SBPs with Tat signal peptides in other bacteria, which suggests that cytoplasmic folding may be a common property of the SBP protein family (65, 66). A propensity for SecA2 exported proteins to fold in the cytoplasm is consistent with current models proposing a role for SecA2 in facilitating the export of such problematic proteins through the SecYEG channel that is built to accommodate proteins in an unfolded state (Figure 2.10) (19, 21). These findings raise the possibility of at least some SBPs being compatible with Tat or SecA2 pathways, and for the

Tat pathway being responsible for the residual export of SBPs that occurs in the absence of SecA2. It is important to note that only a subset of Tat substrates were SecA2-dependent in our study, ruling out a more general role for SecA2 in Tat export.

A new finding of this study was the effect of SecA2 on Mce1 and Mce4 transport systems. Since Mce2 or Mce3 proteins were not identified by an average of ≥ 4 spectral counts, we do not know if other *M. tuberculosis* Mce systems depend on SecA2. However, reduced levels of LprM (Mce3E) as well as Mce4D were observed in the proteomic study of the *M. marinum* *secA2* mutant cell envelope suggesting export of other Mce systems may also depend on SecA2 (16). With qRT-PCR, we ruled out transcriptional effects being the cause of reduced Mce levels. The large number of exported Mce components reduced in the *secA2* mutant could reflect a role for SecA2 in exporting numerous Mce transporter components. However it is also possible that SecA2 exports one or a small number of Mce components and that a defect in localizing a single Mce protein in the *secA2* mutant destabilizes the entire complex. Along these lines, we identified reduced MceG levels in the *secA2* mutant versus H37Rv. MceG is a predicted Mce-associated cytoplasmic ATPase and previous studies show MceG stability is influenced by the presence of Mce transporters (67). Mce systems are proposed to import lipids in a manner analogous to solute import by ABC transporters (68, 69). Furthermore, Mce and Lpr proteins have been considered functionally similar to the SBPs of ABC transporters (68, 69), making our identification of both SBPs and Mce proteins as SecA2-dependent an interesting similarity.

Our studies of cell wall and cytoplasmic fractions revealed increased induction of the DosR regulon in the *secA2* mutant (58, 70). Although first identified as a coordinated response to hypoxia, a condition associated with *M. tuberculosis* latency, the DosR regulon is

now appreciated as being induced by a number of stresses (29, 70-75). Standing cultures of *M. tuberculosis* are reportedly able to induce expression of DosR-regulated proteins, presumably due to hypoxic conditions for the settled bacteria (29). Our storage of cell pellets prior to irradiation and fractionation likely provided a DosR-inducing signal, revealing an unanticipated SecA2-dependent effect on this regulatory response. Using qRT-PCR, we showed increased transcription of DosR-regulated genes occurs in the *secA2* mutant. Interestingly, with both *hspX* and *dosR* transcripts the fold difference observed in the *secA2* mutant was greater at earlier time points and less dramatic at 24 hrs post-induction. Together, our results demonstrate increased transcription and possibly accelerated induction of the DosR regulon in the *secA2* mutant. The *secA2* mutant may be altered in a way that allows it to recognize or respond more quickly to DosR inducing stimuli. Alternatively, the absence of SecA2 could produce an underlying level of stress that primes the mutant for DosR induction, although our LFQ analysis of cytoplasmic fractions did not reveal other stress pathways being upregulated in the *secA2* mutant. Our discovery of enhanced DosR responses could be useful for efforts to develop the *M. tuberculosis secA2* mutant into a live attenuated vaccine (76, 77). Because of the desire for a tuberculosis vaccine to work with latent *M. tuberculosis* infections, a vaccine with improved ability to elicit immune responses to latency associated antigens, such as DosR-regulated proteins, would be advantageous (78).

SecA2-dependent proteins with functions in virulence.

SecA2 is required for growth and survival of *M. tuberculosis* in macrophages and mice (5-7). Although many differences detected by LFQ analysis remain to be validated, the

results presented serve to expand the list of candidates to consider as SecA2-dependent effectors and help to develop new hypotheses for how SecA2 contributes to the pathogenesis of *M. tuberculosis*.

One way the SecA2 pathway functions in *M. tuberculosis* virulence is by enabling the bacterium to arrest phagosome maturation and avoid acidified phagolysosomes in macrophages (7). We identified two proteins that may help explain the role of *M. tuberculosis* SecA2 in arresting phagosome maturation. A predicted esterase LipO was significantly reduced in the *secA2* mutant cell wall in comparison to H37Rv (6.9 fold reduced, $p=0.005$). A *lipO* (*rv1426c*) mutant is defective in phagosome maturation arrest, indicating a potential role for LipO as an effector of this process (79). LipO has a predicted Sec signal peptide to account for its export to the cell wall. While further studies are needed, our results raise the possibility of SecA2 localizing LipO to the cell wall and, thereby, enabling LipO to carry out a role in phagosome maturation arrest. An additional candidate for a being a SecA2 exported effector of phagosome maturation arrest is the protein kinase PknG, which is also implicated in phagosome maturation arrest (23). SecA2-dependent export of PknG likely contributes to phagosome maturation arrest, but there are probably additional SecA2-dependent effectors involved. This likelihood is supported by an experiment performed with the *M. marinum* *secA2* mutant that shows restoration of PknG export in a *secA2* mutant rescues some, but not all, phagosome maturation arrest in macrophages (16). Like the SecA2-dependent secreted SodA protein, PknG lacks an export signal. Thus, our results in support of PknG being exported by the SecA2 pathway of *M. tuberculosis* are also important in reinforcing earlier observations that SecA2-dependent substrates of mycobacteria include examples with and without signal peptides (5, 15, 16).

A role of SecA2 in exporting SBPs and Mce transporters may additionally contribute to *M. tuberculosis* virulence. Although most SBPs have yet to be investigated in terms of function, a wide range of solutes are predicted to be imported by these proteins. Collectively, the role of SecA2 in proper localization of SBPs could have a significant impact on nutrient acquisition or signaling during *M. tuberculosis* infection. Mce1 and Mce4 transporters are more firmly established as having roles in *M. tuberculosis* virulence. Although there is one conflicting report, multiple studies show Mce1 (like SecA2) is important for growth in macrophages and during the early phase of murine infection (5-7, 67, 80-83). The specific function of Mce1 during infection is not clear, but a potential role of Mce1 in importing free mycolic acids was recently proposed (57, 84). Mce4 is the best studied Mce transporter, with a demonstrated role in cholesterol import (85, 86) and a role in virulence (85, 87). Thus, another way that the SecA2 pathway may contribute to *M. tuberculosis* infection could be through its role in SBP and Mce transporter localization.

Conclusion.

Using a large-scale LFQ proteomic approach, we generated a list of candidates for cell wall proteins exported by the SecA2 pathway of *M. tuberculosis*. Our results are significant in highlighting SBPs as a family of SecA2-exported proteins and reinforcing prior observations that mycobacterial proteins exported in a SecA2-dependent fashion include examples with and without Sec signal peptides. At the same time, our results revealed unexpected contributions of SecA2 to Mce transport and DosR regulation. The proteins

identified in this report represent a valuable resource for understanding the mechanism of SecA2-dependent export and contributions of this pathway to *M. tuberculosis* virulence and biology.

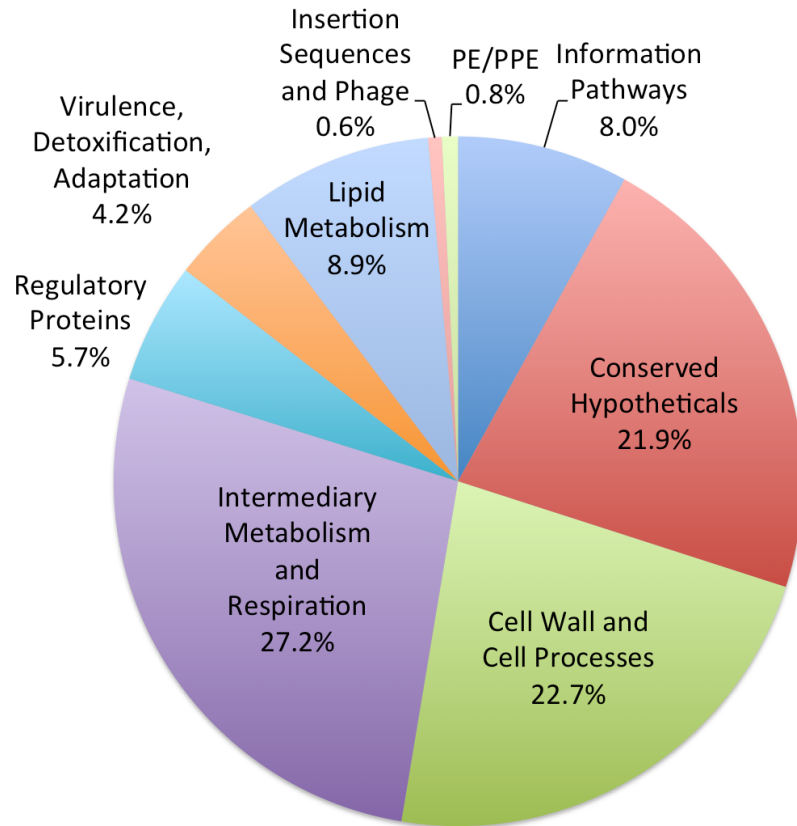


Figure 2.1: Functional categories of cell wall proteins identified by LC-MS/MS. The 1,729 cell wall-associated proteins identified by LC-MS/MS by a minimum of two peptides were assigned to functional categories according to Tuberculist (47).

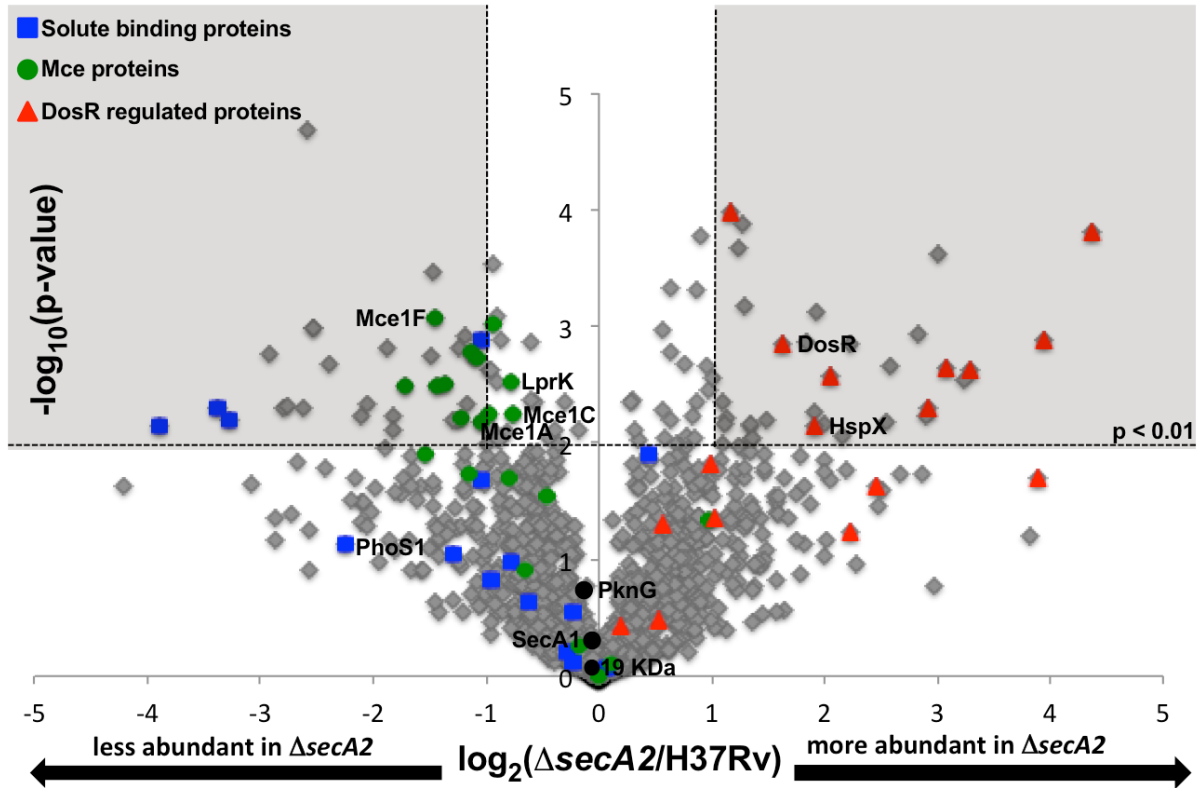


Figure 2.2: Relative quantitation of proteins in H37Rv and $\Delta secA2$ mutant cell wall-fractions. Ratios for the 1,300 proteins having average spectral counts of ≥ 4 in H37Rv and/or $\Delta secA2$ are shown plotted by $\log_2(\Delta secA2/H37Rv)$ and $-\log_{10}(p\text{-value})$. The shaded area of the graph indicates proteins showing 2-fold differences, $p < 0.01$. Solute binding proteins (green circles), Mce transporter proteins (blue squares) and DosR-regulated proteins (red triangles) are marked on the plot, and proteins later validated are identified. In addition, SecA1, is identified on the plot as a protein expected to be present in similar amounts between strains (54).

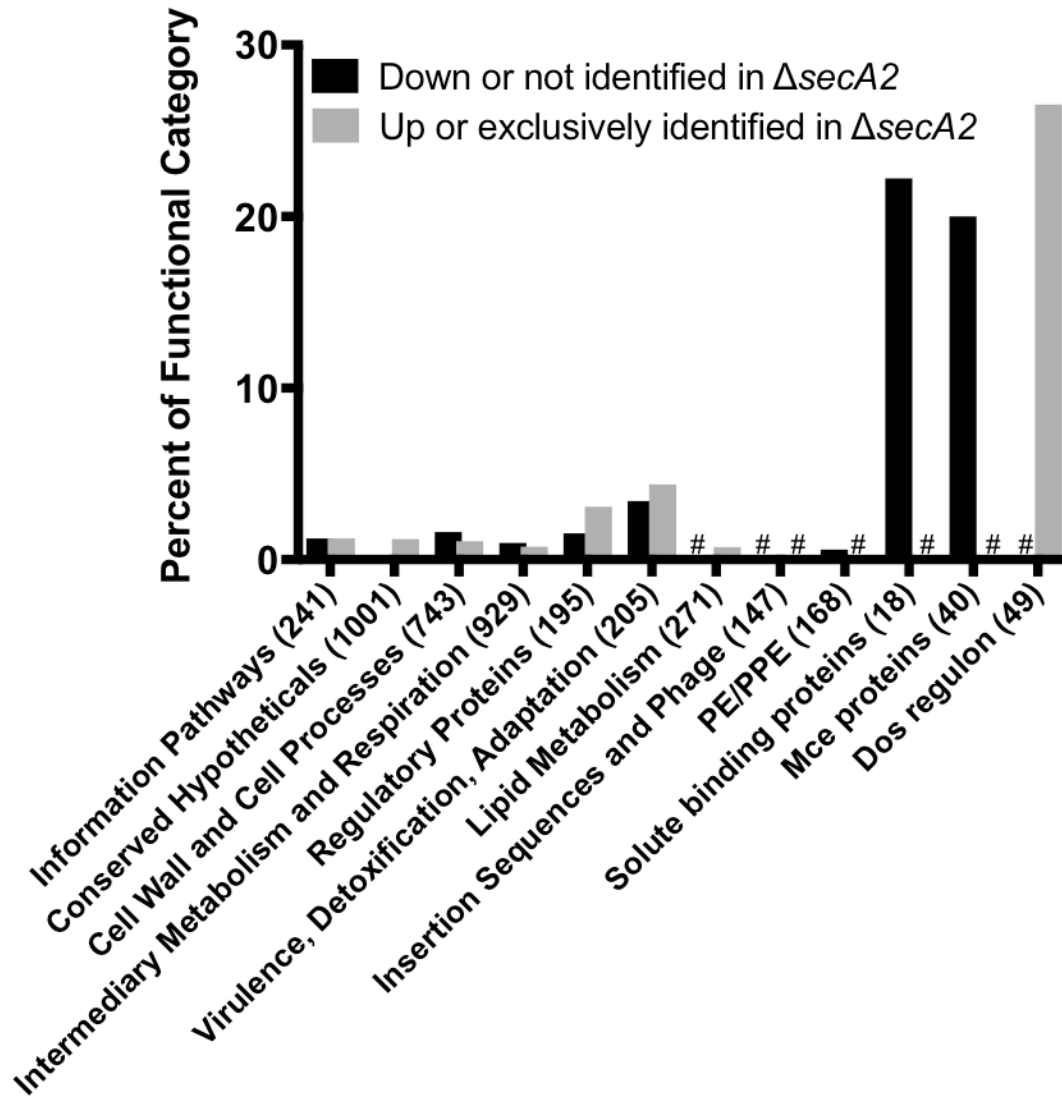
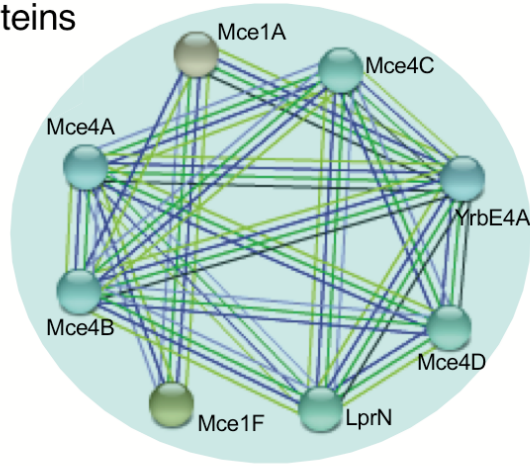


Figure 2.3: Percent of functional protein categories showing differences in the cell wall between H37Rv and the $\Delta secA2$ mutant. Shown is the percent of proteins in a given functional category showing SecA2-dependence, defined as ≥ 2 -fold difference, $p < 0.01$ between H37Rv and $\Delta secA2$ or exclusively identified in one of the two strains. With the exception of SBPs (44, 55), Mce transporters (representing Mce1-4 systems) (68), and DosR-regulated proteins (58), functional groups were predicted by Tuberculist (47). The total number of proteins in each functional category is denoted in parentheses. # indicates no proteins in that category.

A. Mce proteins



B. DosR regulated proteins

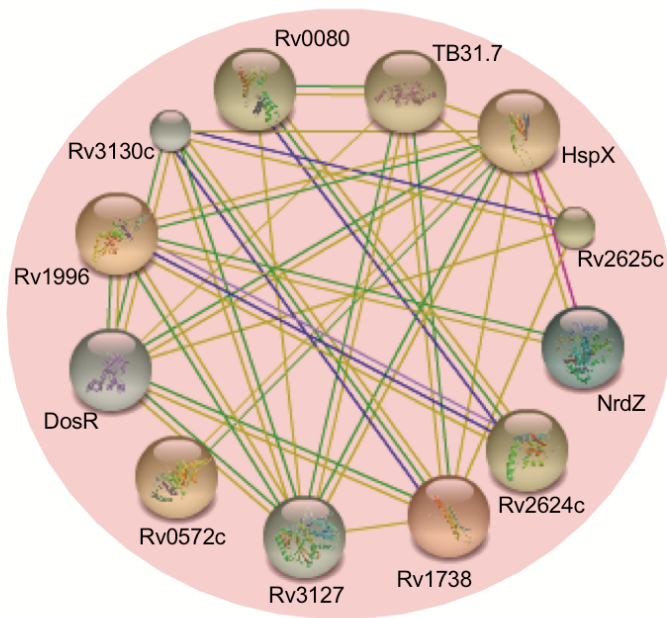


Figure 2.4: Protein associations among proteins identified as having differential abundance in the cell wall fractions of H37Rv versus the $\Delta secA2$ mutant. (A) Proteins that were less abundant (≤ 2 -fold, $p < 0.01$) or not identified in the $\Delta secA2$ mutant and (B) proteins that were more abundant (≥ 2 -fold, $p < 0.01$) or exclusively identified in the $\Delta secA2$ mutant were examined for protein associations. A portion of the protein associations predicted using the Search Tool for the Retrieval of Interacting Genes/Proteins (STRING) v9.1 using medium confidence are shown (45). Each line represents a different association between proteins.

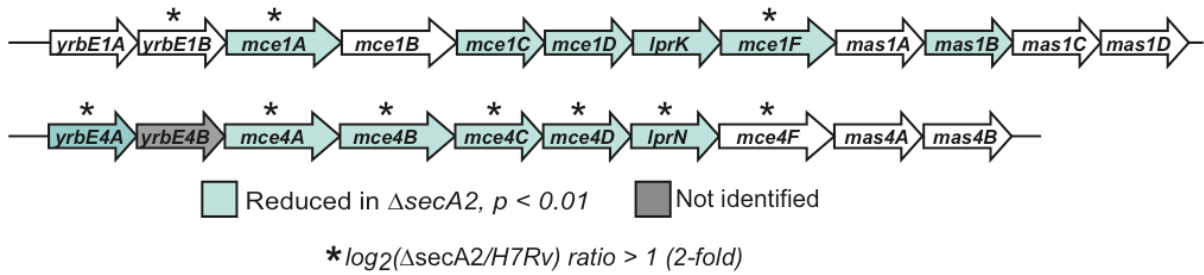


Figure 2.5: Multiple components of Mce1 and Mce4 transporters are reduced in the cell wall of the $\Delta secA2$ mutant. The *M. tuberculosis* H37Rv genome contains four *mce* loci encoding putative lipid transporters. The genomic regions encoding Mce1 and Mce4 transporter components are shown with Open Reading Frames (ORF) colored for significant differences between strains of $p < 0.01$, as observed by spectral counting. An asterisk above the ORF indicates a difference of at least 2-fold.

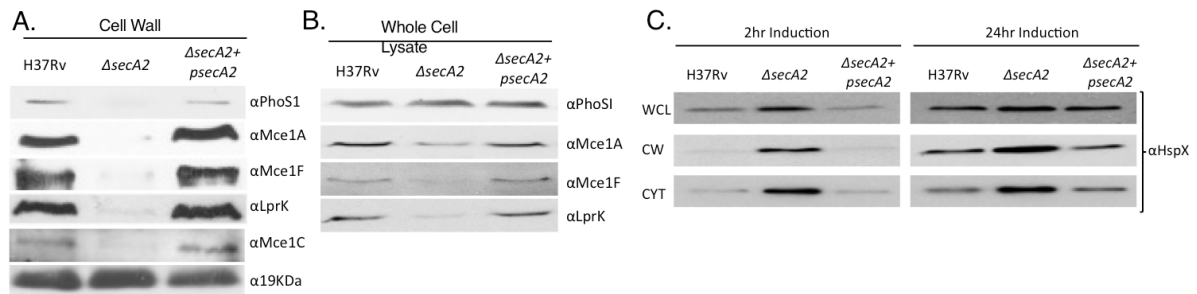


Figure 2.6: Immunoblot validation of protein abundance differences between H37Rv and the $\Delta secA2$ mutant. (A) Equalized cell wall fractions of H37Rv, $\Delta secA2$, and complemented ($\Delta secA2+psecA2$) strains were analyzed by immunoblot using anti-PhoS1, anti-Mce1A, anti-Mce1C, anti-Mce1F, anti-LprK, and anti-19KDa antibodies to monitor differences in protein levels. The 19kDa lipoprotein was used as a control for a protein present in equal amounts across the strains. (B) Equalized whole cell lysates of H37Rv, $\Delta secA2$, and complemented ($\Delta secA2+psecA2$) strains were analyzed by immunoblot using anti-PhoS1, anti-Mce1A, anti-Mce1F, and anti-LprK antibodies. (C) H37Rv, $\Delta secA2$, and $\Delta secA2+psecA2$ samples in which the DosR regulon was induced for 2 or 24 hours were analyzed. Whole cell lysate (WCL), cell wall (CW) and cytoplasmic (CYT) fractions were equalized for protein content and analyzed by immunoblot using anti-HspX antibodies. For all data shown, a representative experiment is presented of a minimum of three that were performed.

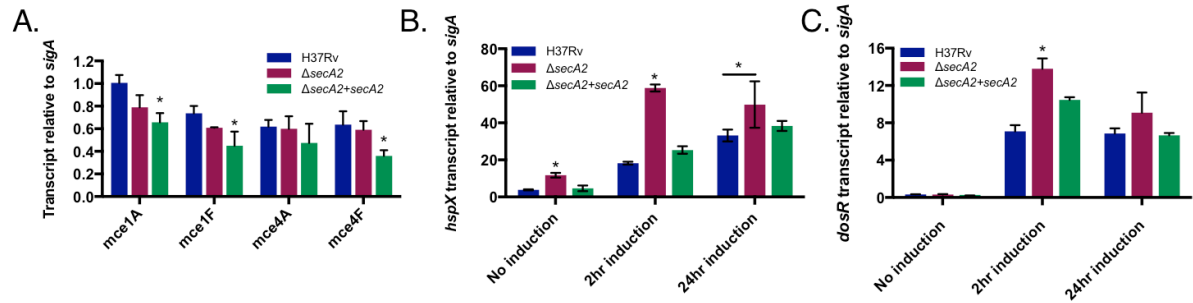


Figure 2.7: Transcript levels for *mce* genes are unchanged but transcript levels for DosR-regulated genes are higher in the $\Delta secA2$ mutant. (A) RNA was isolated from H37Rv, $\Delta secA2$, and complemented ($\Delta secA2+psecA2$) strains. *mce* transcript levels were measured by quantitative RT-PCR and normalized to the level of *sigA* transcript. Data shown is for the mean of three biological replicates. (* $p < 0.05$ by ANOVA) (B and C) RNA was isolated from H37Rv, $\Delta secA2$, and complemented ($\Delta secA2+psecA2$) stains in which the DosR regulon was not intentionally induced or was induced for 2 or 24 hours. (B) *hspX* transcript levels and (C) *dosR* transcript levels were measured by quantitative RT-PCR and normalized to *sigA* transcript. Data represents the means of three biological replicates. (* $p < 0.05$ by ANOVA)

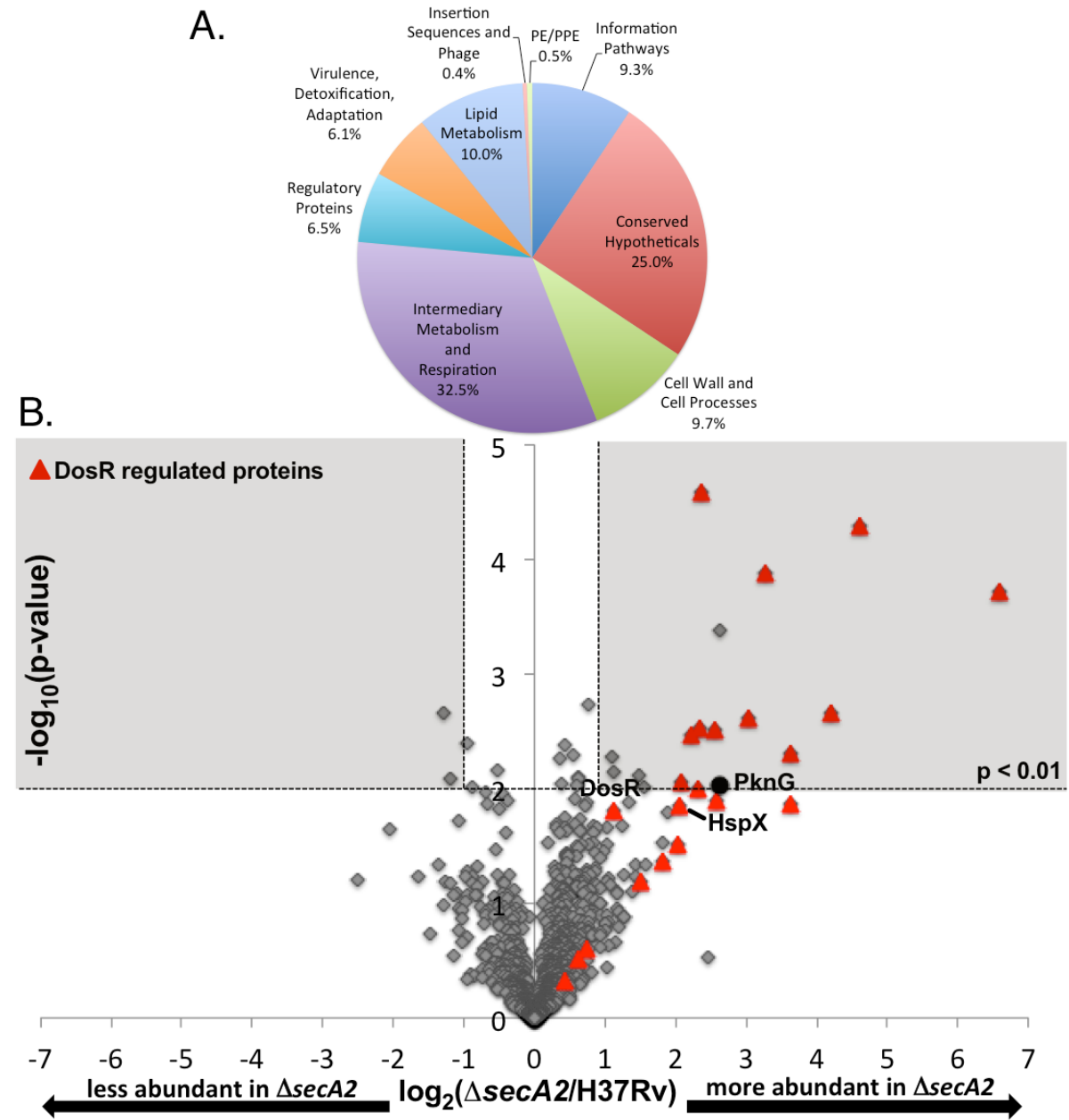


Figure 2.8: Relative quantitation of proteins in H37Rv and ΔsecA2 mutant cytoplasmic fractions. (A) The 1,810 cytoplasmic proteins identified by LC-MS/MS by a minimum of two peptides were assigned to functional categories according to Tuberculist (47). (B) Ratios for the 1,266 proteins identified by an average ≥ 4 spectral counts in H37Rv and/or ΔsecA2 are shown plotted by $\log_2(\Delta\text{secA2}/\text{H37Rv})$ and $-\log_{10}(\text{p-value})$. The shaded area of the graph indicates proteins showing 2-fold differences, $p < 0.01$. DosR-regulated proteins (red triangles) and PknG (black circle) are marked on the plot.

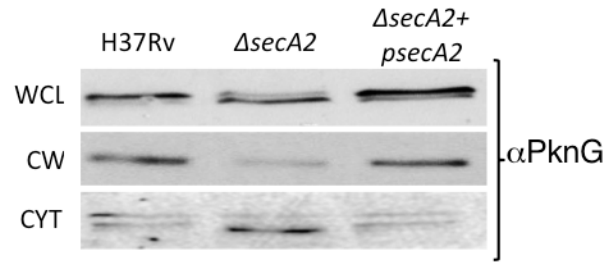


Figure 2.9: The level of PknG is increased in the cytoplasm and reduced in the cell wall of the $\Delta secA2$ mutant. Equalized fractions of H37Rv, $\Delta secA2$, and complemented ($\Delta secA2+psecA2$) strains were analyzed by immunoblot using anti-PknG antibodies. PknG levels in whole cell lysate (WCL), cell wall (CW) and cytoplasmic (CYT) fractions are shown. Shown is a representative of three experiments.

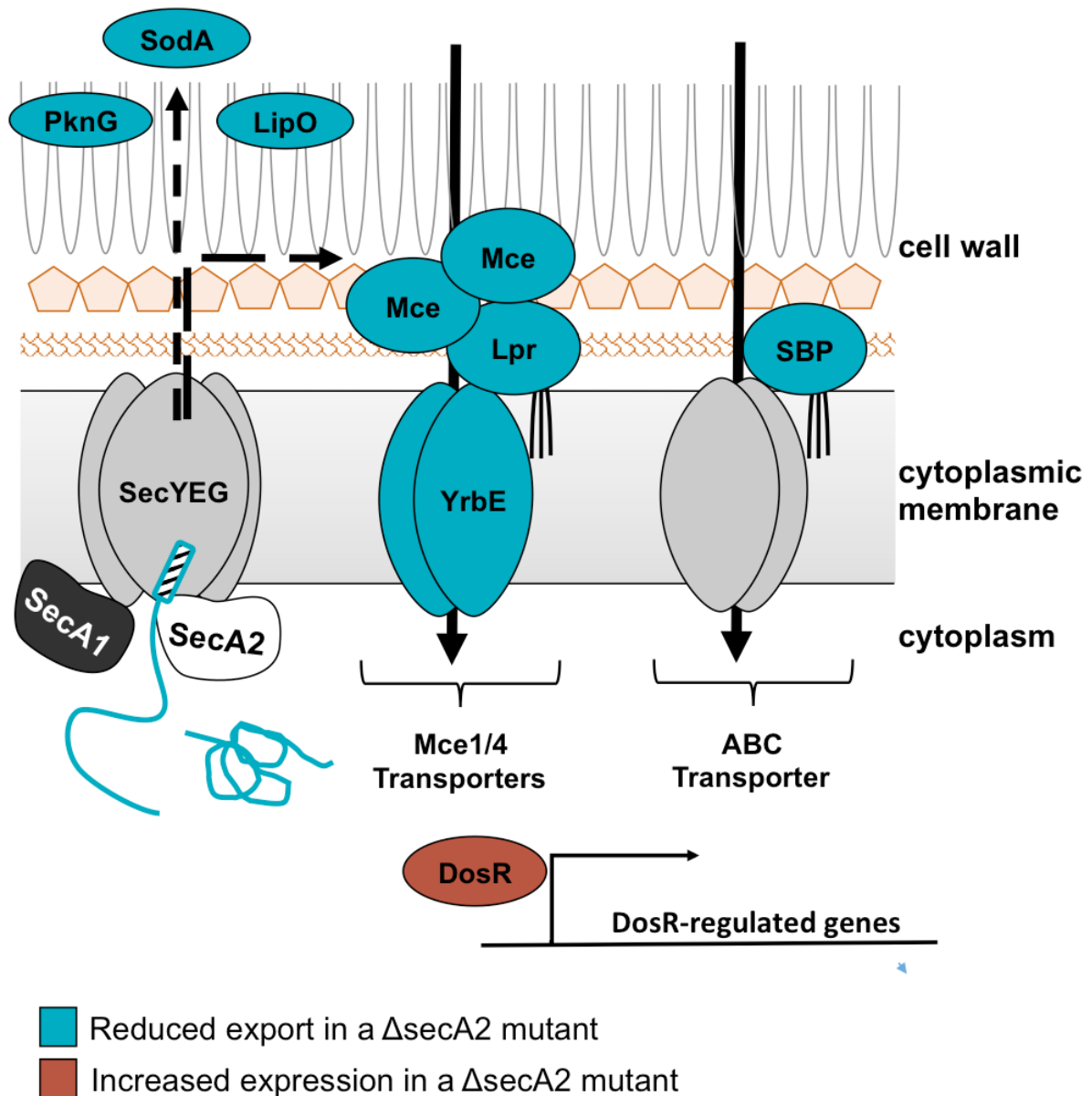


Figure 2.10: A model for SecA2-dependent effects in *M. tuberculosis*. In the current model for SecA2-dependent protein export, the SecA2 ATPase promotes the export of select proteins across the cytoplasmic membrane through the SecYEG channel, possibly with the help of SecA1 (8, 19, 20). Proteins identified as being exported by the SecA2 pathway include examples with signal peptides (hatched rectangle) (i.e. SBPs) and examples lacking signal peptides (i.e. PknG). The SecA2-dependent proteins identified in this study are shown in the model with proteins identified as reduced in the *secA2* mutant colored blue (i.e. PknG, SBPs, LipO, Mce, Lpr) and proteins identified as increased in the $\Delta secA2$ mutant colored red (i.e. DosR-regulated proteins).

Table 2.1: Functional categories of proteins showing reduced abundance in the cell wall fraction of the *M. tuberculosis* $\Delta secA2$ mutant versus H37Rv

Sequence ID	Rv number	Gene name	Description	Total Peptides	Total Spectra	p value	q value	log2 ($\Delta secA2/H37Rv$)	Sec signal peptide	Tat signal peptide	Transmembrane domain	Lipoprotein
SOLUTE BINDING PROTEINS												
NP_216916.1	Rv2400c	subI	sulfate binding lipoprotein	3	15	0.007	0.060	-3.888				X
NP_218183.1	Rv3666c	dppA	peptide binding lipoprotein	8	32	0.005	0.055	-3.381			X	X
NP_214925.1	Rv0411c	glnH	glutamine binding lipoprotein	6	35	0.006	0.058	-3.270	X	X		X
NP_215796.1	Rv1280c	oppA	peptide binding lipoprotein	17	120	0.001	0.035	-1.051		X	X	X
YP_177705.1	Rv0265c	fecB2	iron (III) dicitratebinding lipoprotein	7	68	0.020	0.088	-1.037		X		X
NP_216557.1	Rv2041c		sugar binding lipoprotein	6	27	0.073	0.151	-2.256	X	X		X
YP_177770.1	Rv0934	phoS1	phosphate binding lipoprotein	13	765	0.090	0.172	-1.286	X			X
NP_217101.1	Rv2585c		peptide binding lipoprotein	12	70	0.150	0.234	-0.961	X			X
NP_217560.1	Rv3044	fecB	iron (III) dicitrate binding lipoprotein	10	121	0.104	0.190	-0.786	X			X
YP_177769.1	Rv0932c	pstS2	phosphate binding lipoprotein	11	147	0.232	0.299	-0.613	X			X
NP_218276.1	Rv3759c	proX	glycine/betaine/L-proline binding lipoprotein	6	37	0.628	0.516	-0.275	X			X
NP_215760.1	Rv1244	lpqZ	glycine/betaine binding lipoprotein	5	28	0.745	0.563	-0.231	X			X
NP_215751.1	Rv1235	lpqY	sugar binding lipoprotein	15	132	0.285	0.333	-0.224	X			X
NP_215682.1	Rv1166	lpqW	peptidebinding lipoprotein	12	109	0.861	0.603	0.062	X			X
YP_177768.1	Rv0928	pstS3	phosphate binding lipoprotein	7	49	0.013	0.078	0.443	X			X
MCE1												
NP_214681.1	Rv0167	yrbE1A	integral membrane protein YRBE1A	4	77	0.121	0.205	-0.662			X	
NP_214682.1	Rv0168	yrbE1B	integral membrane protein YRBE1B	3	23	0.019	0.086	-1.158			X	
YP_177701.1	Rv0169	mce1A	MCE-family protein MCE1A	18	431	0.007	0.058	-1.042			X	
NP_214684.1	Rv0170	mce1B	MCE-family protein MCE1B	19	667	0.020	0.088	-0.802			X	
NP_214685.1	Rv0171	mce1C	MCE-family protein MCE1C	31	774	0.006	0.058	-0.967	X		X	
NP_214686.1	Rv0172	mce1D	MCE-family protein MCE1D	19	638	0.001	0.035	-0.931			X	
NP_214687.1	Rv0173	lprK	MCE-family lipoprotein LprK	23	594	0.006	0.058	-0.770			X	X
NP_214688.1	Rv0174	mce1F	MCE-family protein MCE1F	19	837	0.002	0.036	-1.134			X	
NP_214689.1	Rv0175	mas1A	mce associated membrane protein	6	96	0.045	0.127	0.965			X	
NP_214690.1	Rv0176	mas1B	mce associated transmembrane protein	6	159	0.003	0.044	-0.772			X	
NP_214691.1	Rv0177	mas1C	MCE associated protein	10	135	0.543	0.479	-0.179			X	
NP_214692.1	Rv0178	mas1D	mce associated membrane protein	14	280	0.792	0.581	0.114			X	
MCE 4												
NP_218009.1	Rv3492c	mas4B	Mce associated protein	5	94	0.028	0.100	-0.469	X		X	
NP_218010.1	Rv3493c	mas4A	Mce associated alanine and valine rich protein	8	109	0.984	0.636	-0.007			X	
NP_218011.1	Rv3494c	mce4F	MCE-family protein MCE4F	9	85	0.013	0.078	-1.535			X	
NP_218012.1	Rv3495c	lprN	MCE-family lipoprotein LprN	14	153	0.003	0.046	-1.435				X
NP_218013.1	Rv3496c	mce4D	MCE-family protein MCE4D	12	102	0.003	0.046	-1.722			X	
NP_218014.1	Rv3497c	mce4C	MCE-family protein MCE4C	19	234	0.001	0.035	-1.458			X	
NP_218015.1	Rv3498c	mce4B	MCE-family protein MCE4B	14	123	0.006	0.058	-1.229	X		X	
YP_177977.1	Rv3499c	mce4A	MCE-family protein MCE4A	12	105	0.002	0.036	-1.071	X		X	
NP_218018.1	Rv3501c	yrbE4A	integral membrane protein YrbE4a	5	62	0.003	0.045	-1.370			X	

Shaded areas of the table indicate proteins that satisfied our criterion of having >2-fold difference in abundance between the $\Delta secA2$ mutant and H37Rv and $p < 0.01$ or were exclusively identified in one of the strains.

Table 2.2: DosR regulated proteins have altered abundance in the cell wall and cytoplasmic fractions of the *M. tuberculosis* $\Delta secA2$ mutant

Sequence ID	Rv number	Gene name	Description	Cell Wall					Cytoplasm				
				Total Peptides	Total Spectra	log2 ($\Delta secA2/H37Rv$)	p value	q value	Total Peptides	Total Spectra	log2 ($\Delta secA2/H37Rv$)	p value	q value
NP_214594.1	Rv0080		hypothetical protein Rv0080	4	34	1.9151	0.0073	0.0606	-	-	-	-	-
NP_215084.1	Rv0570	nrzD	ribonucleoside-diphosphate reductase large subunit NrdZ	8	31	3.0784	0.0022	0.0385	-	-	-	-	-
NP_215086.1	Rv0572c		hypothetical protein Rv0572c	4	12	$\Delta secA2$ only	-	-	-	-	-	-	-
NP_216254.1	Rv1738		hypothetical protein Rv1738	3	30	3.2958	0.0023	0.0385	5	56	2.3085	0.0101	0.3424
NP_216512.1	Rv1996		hypothetical protein Rv1996	6	52	1.1671	0.0001	0.0175	10	66	2.0856	0.0089	0.3424
NP_216547.1	Rv2031c	hspX	heat shock protein hspX	8	173	2.0492	0.0026	0.0418	16	233	2.0544	0.0141	0.3646
NP_217139.1	Rv2623	TB31.7	hypothetical protein Rv2623	6	38	4.3776	0.0002	0.0175	20	294	2.5884	0.0125	0.3646
NP_217140.1	Rv2624c		hypothetical protein Rv2624c	4	18	$\Delta secA2$ only	-	-	5	15	$\Delta secA2$ only	-	-
NP_217141.1	Rv2625c		hypothetical protein Rv2625c	5	41	$\Delta secA2$ only	-	-	-	-	-	-	-
NP_217143.1	Rv2627c		hypothetical protein Rv2627c	8	55	3.9478	0.0013	0.0347	-	-	-	-	-
NP_217643.1	Rv3127		hypothetical protein Rv3127	6	22	$\Delta secA2$ only	-	-	14	103	6.5866	0.0002	0.0551
NP_217646.1	Rv3130c	tgs1	triacylglycerol synthase	13	86	2.9266	0.0049	0.0554	-	-	-	-	-
NP_217649.1	Rv3133c	dosR/devR	two component transcriptional regulatory protein DevR	3	22	1.6321	0.0014	0.0347	13	228	1.1133	0.0157	0.3896
NP_214593.1	Rv0079		hypothetical protein Rv0079	4	55	2.2214	0.0582	0.1400	-	-	-	-	-
NP_214595.1	Rv0081		transcriptional regulatory protein	-	-	-	-	-	5	39	0.4374	0.4681	0.8975
NP_215083.1	Rv0569		hypothetical protein Rv0569	-	-	-	-	-	4	65	2.5575	0.0031	0.2815
NP_216252.1	Rv1736c	narX	nitrate reductase NarX	6	99	1.0219	0.0436	0.1261	-	-	-	-	-
NP_216328.1	Rv1812c		dehydrogenase	6	47	0.1962	0.3793	0.3885	4	25	0.7515	0.2483	0.8020
NP_216519.1	Rv2003c		hypothetical protein Rv2003c	-	-	-	-	-	7	14	3.6192	0.0138	0.3646
NP_216520.1	Rv2004c		hypothetical protein Rv2004c	-	-	-	-	-	4	19	2.3486	0.0030	0.2815
NP_216521.1	Rv2005c		hypothetical protein Rv2005c	8	108	0.9888	0.0153	0.0843	15	111	2.0395	0.0309	0.4987
YP_177855.1	Rv2006	otsB1	trehalose-6-phosphate phosphatase	-	-	-	-	-	9	26	6.6305	0.0012	0.8306
NP_216523.1	Rv2007c	fdxA	ferredoxin FDxA	-	-	-	-	-	1	20	1.5136	0.0641	0.6161
NP_216544.1	Rv2028c		hypothetical protein Rv2028c	-	-	-	-	-	5	22	3.2650	0.0001	0.0509
NP_216546.1	Rv2030c		hypothetical protein Rv2030c	18	58	3.8953	0.0199	0.0878	16	70	3.6237	0.0049	0.2815
NP_216548.1	Rv2032	acg	hypothetical protein Rv2032	-	-	-	-	-	21	191	3.0202	0.0024	0.2815
NP_217142.1	Rv2626c		hypothetical protein Rv2626c	-	-	-	-	-	7	59	2.2287	0.0034	0.2815
NP_217145.1	Rv2629		hypothetical protein Rv2629	-	-	-	-	-	14	153	2.3547	0.0003	0.0299
NP_217647.1	Rv3131		hypothetical protein Rv3131	-	-	-	-	-	15	81	4.6169	0.0001	0.0299
NP_217648.1	Rv3132c	dosS/devS	two component sensor histidine kinase DEVS	16	150	0.5352	0.3297	0.3614	8	28	1.8222	0.0424	0.5412
NP_217650.1	Rv3134c		hypothetical protein Rv3134c	7	35	2.4513	0.0230	0.0917	7	40	4.1997	0.0022	0.2676
NP_218358.1	Rv3841	bfrB	bacterioferritin BfrB	6	108	0.5677	0.0501	0.1314	-	-	-	-	-

Shaded areas of the table indicate proteins that satisfied our criterion of having >2-fold difference in abundance between the $\Delta secA2$ mutant and H37Rv and $p < 0.01$ or were exclusively identified in one of the strains.

REFERENCES

1. WorldHealthOrganization (2012) Global tuberculosis report 2012.
2. Russell, D. G. (2008) *Mycobacterium tuberculosis*: life and death in the phagosome. In: Kaufmann, S. H., and Rubin, E. J., eds. *Handbook of Tuberculosis: Molecular Biology and Biochemistry*, pp. 307-322, Wiley-VCH
3. Hilbi, H., and Haas, A. (2012) Secretive bacterial pathogens and the secretory pathway. *Traffic* 13, 1187-1197
4. Ligon, L. S., Hayden, J. D., and Braunstein, M. (2012) The ins and outs of *Mycobacterium tuberculosis* protein export. *Tuberculosis (Edinb)* 92, 121-132
5. Braunstein, M., Espinosa, B., Chan, J., Belisle, J. T., and Jacobs, W. R. J. (2003) SecA2 functions in the secretion of superoxide dismutase A and in the virulence of *Mycobacterium tuberculosis*. *Molecular Microbiology* 48, 453-464
6. Kurtz, S., McKinnon, K. P., Runge, M. S., Ting, J. P., and Braunstein, M. (2006) The SecA2 secretion factor of *Mycobacterium tuberculosis* promotes growth in macrophages and inhibits the host immune response. *Infect Immun*
7. Sullivan, J. T., Young, E. F., McCann, J. R., and Braunstein, M. (2012) The *Mycobacterium tuberculosis* SecA2 system subverts phagosome maturation to promote growth in macrophages. *Infect Immun* 80, 996-1006
8. Feltcher, M. E., and Braunstein, M. (2012) Emerging themes in SecA2-mediated protein export. *Nat Rev Microbiol* 10, 779-789
9. Bensing, B. A., Seepersaud, R., Yen, Y. T., and Sullam, P. M. (2014) Selective transport by SecA2: an expanding family of customized motor proteins. *Biochim Biophys Acta* 1843, 1674-1686
10. Bensing, B. A., and Sullam, P. M. (2002) An accessory sec locus of *Streptococcus gordonii* is required for export of the surface protein GspB and for normal levels of binding to human platelets. *Mol Microbiol* 44, 1081-1094
11. Siboo, I. R., Chaffin, D. O., Rubens, C. E., and Sullam, P. M. (2008) Characterization of the accessory Sec system of *Staphylococcus aureus*. *J Bacteriol* 190, 6188-6196
12. Chen, Q., Wu, H., and Fives-Taylor, P. M. (2004) Investigating the role of secA2 in secretion and glycosylation of a fimbrial adhesin in *Streptococcus parasanguis* FW213. *Mol Microbiol* 53, 843-856

13. Mistou, M. Y., Dramsi, S., Brega, S., Poyart, C., and Trieu-Cuot, P. (2009) Molecular dissection of the secA2 locus of group B Streptococcus reveals that glycosylation of the Srr1 LPXTG protein is required for full virulence. *J Bacteriol* 191, 4195-4206
14. Lenz, L. L., Mohammadi, S., Geissler, A., and Portnoy, D. A. (2003) SecA2-dependent secretion of autolytic enzymes promotes *Listeria monocytogenes* pathogenesis. *Proc Natl Acad Sci U S A* 100, 12432-12437
15. Gibbons, H. S., Wolschendorf, F., Abshire, M., Niederweis, M., and Braunstein, M. (2007) Identification of two *Mycobacterium smegmatis* lipoproteins exported by a SecA2-dependent pathway. *J Bacteriol* 189, 5090-5100
16. van der Woude, A. D., Stoop, E. J., Stuess, M., Wang, S., Ummels, R., van Stempvoort, G., Piersma, S. R., Cascioferro, A., Jimenez, C. R., Houben, E. N., Luirink, J., Pieters, J., van der Sar, A. M., and Bitter, W. (2014) Analysis of SecA2-dependent substrates in *Mycobacterium marinum* identifies protein kinase G (PknG) as a virulence effector. *Cell Microbiol* 16, 280-295
17. Fagan, R. P., and Fairweather, N. F. (2011) *Clostridium difficile* has two parallel and essential Sec secretion systems. *J Biol Chem* 286, 27483-27493
18. Rigel, N. W., and Braunstein, M. (2008) A new twist on an old pathway--accessory Sec systems. *Mol Microbiol* 69, 291-302
19. Ligon, L. S., Rigel, N. W., Romanchuk, A., Jones, C. D., and Braunstein, M. (2013) Suppressor analysis reveals a role for SecY in the SecA2-dependent protein export pathway of *Mycobacteria*. *J Bacteriol* 195, 4456-4465
20. Rigel, N. W., Gibbons, H. S., McCann, J. R., McDonough, J. A., Kurtz, S., and Braunstein, M. (2009) The Accessory SecA2 System of *Mycobacteria* Requires ATP Binding and the Canonical SecA1. *J Biol Chem* 284, 9927-9936
21. Feltcher, M. E., Gibbons, H. S., Ligon, L. S., and Braunstein, M. (2013) Protein export by the mycobacterial SecA2 system is determined by the preprotein mature domain. *J Bacteriol* 195, 672-681
22. Watkins, B. Y., Joshi, S. A., Ball, D. A., Leggett, H., Park, S., Kim, J., Austin, C. D., Paler-Martinez, A., Xu, M., Downing, K. H., and Brown, E. J. (2012) *Mycobacterium marinum* SecA2 promotes stable granulomas and induces tumor necrosis factor alpha in vivo. *Infect Immun* 80, 3512-3520
23. Walburger, A., Koul, A., Ferrari, G., Nguyen, L., Prescianotto-Baschong, C., Huygen, K., Klebl, B., Thompson, C., Bacher, G., and Pieters, J. (2004) Protein kinase G from pathogenic mycobacteria promotes survival within macrophages. *Science* 304, 1800-1804

24. Cowley, S., Ko, M., Pick, N., Chow, R., Downing, K. J., Gordhan, B. G., Betts, J. C., Mizrahi, V., Smith, D. A., Stokes, R. W., and Av-Gay, Y. (2004) The Mycobacterium tuberculosis protein serine/threonine kinase PknG is linked to cellular glutamate/glutamine levels and is important for growth in vivo. *Mol Microbiol* 52, 1691-1702
25. Rohde, K. H., Abramovitch, R. B., and Russell, D. G. (2007) Mycobacterium tuberculosis invasion of macrophages: linking bacterial gene expression to environmental cues. *Cell Host Microbe* 2, 352-364
26. Schnappinger, D., Ehrt, S., Voskuil, M. I., Liu, Y., Mangan, J. A., Monahan, I. M., Dolganov, G., Efron, B., Butcher, P. D., Nathan, C., and Schoolnik, G. K. (2003) Transcriptional Adaptation of Mycobacterium tuberculosis within Macrophages: Insights into the Phagosomal Environment. *J Exp Med* 198, 693-704
27. McKinney, J. D., Honer zu Bentrup, K., Munoz-Elias, E. J., Miczak, A., Chen, B., Chan, W. T., Swenson, D., Sacchettini, J. C., Jacobs, W. R., Jr., and Russell, D. G. (2000) Persistence of Mycobacterium tuberculosis in macrophages and mice requires the glyoxylate shunt enzyme isocitrate lyase. *Nature* 406, 735-738
28. Marrero, J., Rhee, K. Y., Schnappinger, D., Pethe, K., and Ehrt, S. (2010) Gluconeogenic carbon flow of tricarboxylic acid cycle intermediates is critical for Mycobacterium tuberculosis to establish and maintain infection. *Proc Natl Acad Sci U S A* 107, 9819-9824
29. Kendall, S. L., Movahedzadeh, F., Rison, S. C., Wernisch, L., Parish, T., Duncan, K., Betts, J. C., and Stoker, N. G. (2004) The Mycobacterium tuberculosis dosRS two-component system is induced by multiple stresses. *Tuberculosis (Edinb)* 84, 247-255
30. Gu, S., Chen, J., Dobos, K. M., Bradbury, E. M., Belisle, J. T., and Chen, X. (2003) Comprehensive Proteomic Profiling of the Membrane Constituents of a Mycobacterium tuberculosis Strain. *Molecular & cellular proteomics : MCP* 2, 1284-1296
31. Gunawardena, H. P., Felcher, M. E., Wrobel, J. A., Gu, S., Braunstein, M., and Chen, X. (2013) Comparison of the membrane proteome of virulent Mycobacterium tuberculosis and the attenuated Mycobacterium bovis BCG vaccine strain by label-free quantitative proteomics. *J Proteome Res* 12, 5463-5474
32. Elias, J. E., and Gygi, S. P. (2007) Target-decoy search strategy for increased confidence in large-scale protein identifications by mass spectrometry. *Nature methods* 4, 207-214
33. Weatherly, D. B., Atwood, J. A., 3rd, Minning, T. A., Cavola, C., Tarleton, R. L., and Orlando, R. (2005) A Heuristic method for assigning a false-discovery rate for protein

- identifications from Mascot database search results. *Molecular & cellular proteomics* : MCP 4, 762-772
34. Hsieh, E. J., Hoopmann, M. R., MacLean, B., and MacCoss, M. J. (2010) Comparison of database search strategies for high precursor mass accuracy MS/MS data. *J Proteome Res* 9, 1138-1143
 35. Keller, A., Nesvizhskii, A. I., Kolker, E., and Aebersold, R. (2002) Empirical statistical model to estimate the accuracy of peptide identifications made by MS/MS and database search. *Analytical chemistry* 74, 5383-5392
 36. Nesvizhskii, A. I., Keller, A., Kolker, E., and Aebersold, R. (2003) A statistical model for identifying proteins by tandem mass spectrometry. *Analytical chemistry* 75, 4646-4658
 37. Storey, J. D., and Tibshirani, R. (2003) Statistical significance for genomewide studies. *Proc Natl Acad Sci U S A* 100, 9440-9445
 38. Petersen, T. N., Brunak, S., von Heijne, G., and Nielsen, H. (2011) SignalP 4.0: discriminating signal peptides from transmembrane regions. *Nature methods* 8, 785-786
 39. McDonough, J. A., McCann, J. R., Tekippe, E. M., Silverman, J. S., Rigel, N. W., and Braunstein, M. (2008) Identification of functional Tat signal sequences in *Mycobacterium tuberculosis* proteins. *J Bacteriol* 190, 6428-6438
 40. Bendtsen, J. D., Nielsen, H., Widdick, D., Palmer, T., and Brunak, S. (2005) Prediction of twin-arginine signal peptides. *BMC Bioinformatics* 6, 167
 41. Rose, R. W., Bruser, T., Kissinger, J. C., and Pohlschroder, M. (2002) Adaptation of protein secretion to extremely high-salt conditions by extensive use of the twin-arginine translocation pathway. *Mol Microbiol* 45, 943-950
 42. Selengut, J. D., Haft, D. H., Davidsen, T., Ganapathy, A., Gwinn-Giglio, M., Nelson, W. C., Richter, A. R., and White, O. (2007) TIGRFAMs and Genome Properties: tools for the assignment of molecular function and biological process in prokaryotic genomes. *Nucleic Acids Res* 35, D260-264
 43. Krogh, A., Larsson, B., von Heijne, G., and Sonnhammer, E. L. (2001) Predicting transmembrane protein topology with a hidden Markov model: application to complete genomes. *J Mol Biol* 305, 567-580
 44. Sutcliffe, I. C., and Harrington, D. J. (2004) Lipoproteins of *Mycobacterium tuberculosis*: an abundant and functionally diverse class of cell envelope components. *FEMS Microbiol Rev* 28, 645-659

45. Franceschini, A., Szklarczyk, D., Frankild, S., Kuhn, M., Simonovic, M., Roth, A., Lin, J., Minguez, P., Bork, P., von Mering, C., and Jensen, L. J. (2013) STRING v9.1: protein-protein interaction networks, with increased coverage and integration. *Nucleic Acids Res* 41, D808-815
46. Manganelli, R., Dubnau, E., Tyagi, S., Kramer, F. R., and Smith, I. (1999) Differential expression of 10 sigma factor genes in *Mycobacterium tuberculosis*. *Mol Microbiol* 31, 715-724
47. Lew, J. M., Kapopoulou, A., Jones, L. M., and Cole, S. T. (2011) TubercuList--10 years after. *Tuberculosis (Edinb)* 91, 1-7
48. Mawuenyega, K. G., Forst, C. V., Dobos, K. M., Belisle, J. T., Chen, J., Bradbury, E. M., Bradbury, A. R., and Chen, X. (2005) Mycobacterium tuberculosis functional network analysis by global subcellular protein profiling. *Mol Biol Cell* 16, 396-404
49. Wolfe, L. M., Mahaffey, S. B., Kruh, N. A., and Dobos, K. M. (2010) Proteomic definition of the cell wall of Mycobacterium tuberculosis. *J Proteome Res* 9, 5816-5826
50. Hutchings, M. I., Palmer, T., Harrington, D. J., and Sutcliffe, I. C. (2009) Lipoprotein biogenesis in Gram-positive bacteria: knowing when to hold 'em, knowing when to fold 'em. *Trends Microbiol* 17, 13-21
51. Malen, H., De Souza, G. A., Pathak, S., Softeland, T., and Wiker, H. G. (2011) Comparison of membrane proteins of Mycobacterium tuberculosis H37Rv and H37Ra strains. *BMC Microbiol* 11, 18
52. He, Z., and De Buck, J. (2010) Cell wall proteome analysis of Mycobacterium smegmatis strain MC2 155. *BMC Microbiol* 10, 121
53. Liu, H., Sadygov, R. G., and Yates, J. R., 3rd (2004) A model for random sampling and estimation of relative protein abundance in shotgun proteomics. *Analytical chemistry* 76, 4193-4201
54. Hou, J. M., D'Lima, N. G., Rigel, N. W., Gibbons, H. S., McCann, J. R., Braunstein, M., and Teschke, C. M. (2008) ATPase activity of Mycobacterium tuberculosis SecA1 and SecA2 proteins and its importance for SecA2 function in macrophages. *J Bacteriol* 190, 4880-4887
55. Braibant, M., Gilot, P., and Content, J. (2000) The ATP binding cassette (ABC) transport systems of Mycobacterium tuberculosis. *FEMS Microbiol Rev* 24, 449-467
56. Chitale, S., Ehrt, S., Kawamura, I., Fujimura, T., Shimono, N., Anand, N., Lu, S., Cohen-Gould, L., and Riley, L. W. (2001) Recombinant Mycobacterium tuberculosis protein associated with mammalian cell entry. *Cell Microbiol* 3, 247-254

57. Forrellad, M. A., McNeil, M., Santangelo Mde, L., Blanco, F. C., Garcia, E., Klepp, L. I., Huff, J., Niederweis, M., Jackson, M., and Bigi, F. (2014) Role of the Mce1 transporter in the lipid homeostasis of *Mycobacterium tuberculosis*. *Tuberculosis (Edinb)* 94, 170-177
58. Park, H. D., Guinn, K. M., Harrell, M. I., Liao, R., Voskuil, M. I., Tompa, M., Schoolnik, G. K., and Sherman, D. R. (2003) Rv3133c/dosR is a transcription factor that mediates the hypoxic response of *Mycobacterium tuberculosis*. *Mol Microbiol* 48, 833-843
59. Bagchi, G., Chauhan, S., Sharma, D., and Tyagi, J. S. (2005) Transcription and autoregulation of the Rv3134c-devR-devS operon of *Mycobacterium tuberculosis*. *Microbiology* 151, 4045-4053
60. Boon, C., Li, R., Qi, R., and Dick, T. (2001) Proteins of *Mycobacterium bovis* BCG induced in the Wayne dormancy model. *J Bacteriol* 183, 2672-2676
61. Kumar, A., Bose, M., and Brahmachari, V. (2003) Analysis of expression profile of mammalian cell entry (mce) operons of *Mycobacterium tuberculosis*. *Infect Immun* 71, 6083-6087
62. Halbedel, S., Hahn, B., Daniel, R. A., and Flieger, A. (2012) DivIVA affects secretion of virulence-related autolysins in *Listeria monocytogenes*. *Mol Microbiol* 83, 821-839
63. Renier, S., Chambon, C., Viala, D., Chagnot, C., Hebraud, M., and Desvaux, M. (2013) Exoproteomic analysis of the SecA2-dependent secretion in *Listeria monocytogenes* EGD-e. *Journal of proteomics* 80C, 183-195
64. Palmer, T., and Berks, B. C. (2012) The twin-arginine translocation (Tat) protein export pathway. *Nat Rev Microbiol* 10, 483-496
65. Shruthi, H., Babu, M. M., and Sankaran, K. (2010) TAT-pathway-dependent lipoproteins as a niche-based adaptation in prokaryotes. *Journal of molecular evolution* 70, 359-370
66. Chater, K. F., Biro, S., Lee, K. J., Palmer, T., and Schrempf, H. (2010) The complex extracellular biology of *Streptomyces*. *FEMS Microbiol Rev* 34, 171-198
67. Joshi, S. M., Pandey, A. K., Capite, N., Fortune, S. M., Rubin, E. J., and Sasseti, C. M. (2006) Characterization of mycobacterial virulence genes through genetic interaction mapping. *Proc Natl Acad Sci U S A* 103, 11760-11765
68. Casali, N., and Riley, L. W. (2007) A phylogenomic analysis of the Actinomycetales mce operons. *BMC Genomics* 8, 60

69. Kumar, A., Chandolia, A., Chaudhry, U., Brahmachari, V., and Bose, M. (2005) Comparison of mammalian cell entry operons of mycobacteria: in silico analysis and expression profiling. *FEMS immunology and medical microbiology* 43, 185-195
70. Sherman, D. R., Voskuil, M., Schnappinger, D., Liao, R., Harrell, M. I., and Schoolnik, G. K. (2001) Regulation of the Mycobacterium tuberculosis hypoxic response gene encoding alpha -crystallin. *Proc Natl Acad Sci U S A* 98, 7534-7539
71. Boon, C., and Dick, T. (2012) How Mycobacterium tuberculosis goes to sleep: the dormancy survival regulator DosR a decade later. *Future Microbiol* 7, 513-518
72. Shiloh, M. U., Manzanillo, P., and Cox, J. S. (2008) Mycobacterium tuberculosis senses host-derived carbon monoxide during macrophage infection. *Cell Host Microbe* 3, 323-330
73. Kumar, A., Deshane, J. S., Crossman, D. K., Bolisetty, S., Yan, B. S., Kramnik, I., Agarwal, A., and Steyn, A. J. (2008) Heme oxygenase-1-derived carbon monoxide induces the Mycobacterium tuberculosis dormancy regulon. *J Biol Chem* 283, 18032-18039
74. Voskuil, M. I., Schnappinger, D., Visconti, K. C., Harrell, M. I., Dolganov, G. M., Sherman, D. R., and Schoolnik, G. K. (2003) Inhibition of respiration by nitric oxide induces a Mycobacterium tuberculosis dormancy program. *J Exp Med* 198, 705-713
75. Kumar, A., Toledo, J. C., Patel, R. P., Lancaster, J. R., Jr., and Steyn, A. J. (2007) Mycobacterium tuberculosis DosS is a redox sensor and DosT is a hypoxia sensor. *Proc Natl Acad Sci U S A* 104, 11568-11573
76. Hinchey, J., Lee, S., Jeon, B. Y., Basaraba, R. J., Venkataswamy, M. M., Chen, B., Chan, J., Braunstein, M., Orme, I. M., Derrick, S. C., Morris, S. L., Jacobs, W. R., Jr., and Porcelli, S. A. (2007) Enhanced priming of adaptive immunity by a proapoptotic mutant of Mycobacterium tuberculosis. *The Journal of clinical investigation* 117, 2279-2288
77. Hinchey, J., Jeon, B. Y., Alley, H., Chen, B., Goldberg, M., Derrick, S., Morris, S., Jacobs, W. R., Jr., Porcelli, S. A., and Lee, S. (2011) Lysine auxotrophy combined with deletion of the SecA2 gene results in a safe and highly immunogenic candidate live attenuated vaccine for tuberculosis. *PLoS One* 6, e15857
78. Geluk, A., van Meijgaarden, K. E., Joosten, S. A., Commandeur, S., and Ottenhoff, T. H. (2014) Innovative Strategies to Identify M. tuberculosis Antigens and Epitopes Using Genome-Wide Analyses. *Frontiers in immunology* 5, 256

79. Pethe, K., Swenson, D. L., Alonso, S., Anderson, J., Wang, C., and Russell, D. G. (2004) Isolation of Mycobacterium tuberculosis mutants defective in the arrest of phagosome maturation. *Proc Natl Acad Sci U S A* 101, 13642-13647
80. McCann, J. R., McDonough, J. A., Sullivan, J. T., Feltcher, M. E., and Braunstein, M. (2011) Genome-wide identification of Mycobacterium tuberculosis exported proteins with roles in intracellular growth. *J Bacteriol* 193, 854-861
81. Rengarajan, J., Bloom, B. R., and Rubin, E. J. (2005) Genome-wide requirements for Mycobacterium tuberculosis adaptation and survival in macrophages. *Proc Natl Acad Sci U S A* 102, 8327-8332
82. Gioffre, A., Infante, E., Aguilar, D., Santangelo, M. P., Klepp, L., Amadio, A., Meikle, V., Etchechoury, I., Romano, M. I., Cataldi, A., Hernandez, R. P., and Bigi, F. (2005) Mutation in mce operons attenuates Mycobacterium tuberculosis virulence. *Microbes Infect* 7, 325-334
83. Shimono, N., Morici, L., Casali, N., Cantrell, S., Sidders, B., Ehrt, S., and Riley, L. W. (2003) Hypervirulent mutant of Mycobacterium tuberculosis resulting from disruption of the mce1 operon. *Proc Natl Acad Sci U S A* 100, 15918-15923
84. Cantrell, S. A., Leavell, M. D., Marjanovic, O., Iavarone, A. T., Leary, J. A., and Riley, L. W. (2013) Free mycolic acid accumulation in the cell wall of the mce1 operon mutant strain of Mycobacterium tuberculosis. *Journal of microbiology* 51, 619-626
85. Pandey, A. K., and Sasseti, C. M. (2008) Mycobacterial persistence requires the utilization of host cholesterol. *Proc Natl Acad Sci U S A* 105, 4376-4380
86. Klepp, L. I., Forrellad, M. A., Osella, A. V., Blanco, F. C., Stella, E. J., Bianco, M. V., Santangelo Mde, L., Sasseti, C., Jackson, M., Cataldi, A. A., Bigi, F., and Morbidoni, H. R. (2012) Impact of the deletion of the six mce operons in Mycobacterium smegmatis. *Microbes Infect* 14, 590-599
87. Senaratne, R. H., Sidders, B., Sequeira, P., Saunders, G., Dunphy, K., Marjanovic, O., Reader, J. R., Lima, P., Chan, S., Kendall, S., McFadden, J., and Riley, L. W. (2008) Mycobacterium tuberculosis strains disrupted in mce3 and mce4 operons are attenuated in mice. *Journal of medical microbiology* 57, 164-170

CHAPTER 3¹

The SecA2 pathway of *Mycobacterium tuberculosis* exports effectors that work in concert to arrest phagosome and autophagosome maturation

INTRODUCTION

In 2015, 1.8 million deaths were attributed to infection with *Mycobacterium tuberculosis*, the causative agent of tuberculosis (1). *M. tuberculosis* is an intracellular pathogen that subverts multiple antimicrobial mechanisms of the host in order to survive and replicate in macrophages (2). To avoid trafficking to the antimicrobial environment of acidified phagolysosomes, *M. tuberculosis* blocks the normal series of phagosome maturation events that occurs following phagocytosis (2,3). As a result, *M. tuberculosis* resides in phagosomes that resemble early endosomes in retaining Rab5 on their surface, avoiding host factors that drive downstream maturation events (e.g. phosphatidylinositol-3-phosphate [PI3P], Rab7, and the vacuolar-H⁺-ATPase [V-ATPase]) and failing to fuse with lysosomes (4-7). Notably, the ability of *M. tuberculosis* to prevent phagosome recruitment and assembly

¹ Contributing authors: Jonathan Tabb Sullivan and Miriam Braunstein (Department of Microbiology and Immunology, School of Medicine, The University of North Carolina at Chapel Hill, Chapel Hill, NC)

of V-ATPase, the proton pump that acidifies the phagosome, helps explain the failure of *M. tuberculosis* phagosomes to fully acidify (4).

Phagosome maturation is a complex multi-step process and there are multiple *M. tuberculosis* protein and lipid effectors that are thought to play a role in arresting phagosome maturation (8). However, the specific function(s) of effectors and the interplay between effectors remains to be determined. It also remains unclear if all the effectors of this process are known. The gaps in our understanding are partly due to redundancy among effectors and the potential for effectors to have functions in other aspects of *M. tuberculosis* pathogenesis or physiology beyond phagosome maturation arrest (9-15). These features of effectors make it difficult to study the contribution of individual effectors to phagosome maturation arrest using loss of function mutants.

In addition to residing in phagosomes, intracellular *M. tuberculosis* can also localize to double membrane bound compartments known as autophagosomes. Autophagosomes progress through similar maturation stages as phagosomes and culminate in fusion with lysosomes to form degradative autophagolysosomes (16). As with phagosomes, *M. tuberculosis* is able to arrest autophagosome maturation and prevent fusion with lysosomes (17,18). However, unlike the process of phagosome maturation arrest, there has been very little study of *M. tuberculosis* mechanisms and effectors of autophagosome maturation arrest.

Most of the reported effectors of *M. tuberculosis* phagosome maturation arrest are either exported to the bacterial cell wall or fully secreted (19). In *M. tuberculosis*, the SecA2 protein export pathway is required for phagosome maturation arrest, which indicates that this pathway exports effectors required to inhibit phagosome maturation (20). Unlike the paralogous SecA1 ATPase, which is responsible for the bulk of housekeeping export and is

essential for bacterial viability, SecA2 is a non-essential specialized SecA ATPase required for exporting a relatively small subset of proteins (21-24). Although not required for growth *in vitro*, SecA2 is required for *M. tuberculosis* replication in macrophages and mice (22,25). Unlike wild type *M. tuberculosis*, during macrophage infection, a *secA2* mutant of *M. tuberculosis* is delivered to acidified mature phagosomes (20). The failure of the *secA2* mutant to arrest phagosome maturation was previously shown to be responsible for its intracellular growth defect (20).

We hypothesized that the role of the SecA2 pathway in phagosome maturation arrest is to export multiple effectors of the process. Here, we identify SapM, a secreted phosphatase previously reported to function in phagosome maturation arrest, as being exported by the *M. tuberculosis* SecA2 pathway (7,26). We further show that the SecA2 dependent export of this protein contributes to both phagosome maturation arrest and intracellular growth of *M. tuberculosis*. By identifying a histidine residue that is essential for SapM phosphatase activity, we confirm that the phosphatase activity of SapM is required for its function. Along with SapM, our data indicates the existence of other SecA2-dependent effectors of phagosome maturation arrest and we identify the *M. tuberculosis* eukaryotic-like serine/threonine protein kinase PknG as one of these additional factors. By restoring export of SapM and PknG individually and in combination to the *secA2* mutant, we provide unique insight into specific steps in phagosome maturation arrest that are impacted by one or both of these effectors, as well as extend our understanding of the role of SecA2, SapM, and PknG to *M. tuberculosis* inhibition of autophagosome maturation. These studies additionally reveal the value of using the *secA2* mutant as a novel platform to study functions of effectors in phagosome maturation arrest.

RESULTS

The SapM phosphatase is secreted by the SecA2 pathway.

With the goal of understanding the contribution of SecA2 to phagosome maturation arrest by *M. tuberculosis*, we tested the possibility that the SapM phosphatase, which is a known effector of phagosome maturation arrest, is exported by the SecA2 pathway (26). Immunoblot analysis with SapM antisera was performed on *M. tuberculosis* culture supernatants. Compared to the parental *M. tuberculosis* strain, H37Rv, and a complemented strain, the *M. tuberculosis secA2* mutant had significantly reduced levels of secreted SapM, although a low residual level of SapM secretion was always observed in the mutant (Figure 3.1A). The amount of SapM in whole cell lysates was also reduced, albeit more modestly (Figure 3.1B). These reduced levels of SapM were not due to transcriptional effects in the *secA2* mutant, as shown by qRT-PCR measurements of *sapM* transcript in the *secA2* mutant compared to H37Rv (data not shown). Thus, the lower levels of secreted and cellular SapM in the *secA2* mutant are the likely consequence of a SapM export defect.

We also examined the contribution of SecA2 to SapM export by quantifying phosphatase activity in culture supernatants using p-nitrophenyl phosphate (pNPP) as a substrate. There was significantly less phosphatase activity in culture supernatants of the *secA2* mutant when compared to H37Rv or the complemented strain (Figure 3.1C). Importantly, in the presence of sodium molybdate, a known inhibitor of SapM, the secreted phosphatase activity of the *secA2* mutant was equivalent to that of H37Rv and complemented strains which is consistent with a SapM secretion defect (data not shown)(27). Together, the immunoblot and activity data provide the first evidence of SapM being secreted by the SecA2 pathway.

SapM secretion by the SecA2 pathway limits EEA1 localization to phagosomes.

SapM was previously shown to dephosphorylate PI3P, which should limit recruitment of PI3P binding proteins, such as EEA1, that promote downstream phagosome maturation events (7,28,29). Consequently, we hypothesized that SapM secretion by the SecA2 pathway contributes to phagosome maturation arrest by enabling *M. tuberculosis* to avoid EEA1 localization to phagosomes. As a first step to test this possibility, murine bone marrow derived macrophages were infected with the *secA2* mutant, H37Rv or the complemented strain and EEA1 localization to *M. tuberculosis*-containing phagosomes was determined using the endogenous auto-fluorescent signal of *M. tuberculosis* and immunostaining with anti-EEA1 antibodies. Compared to phagosomes containing H37Rv or the complemented strain, which avoid EEA1 localization, phagosomes containing the *secA2* mutant exhibited significantly higher EEA1 co-localization at both 1hr and 24hrs post infection (Figure 3.1D-E, data not shown).

We next set out to determine if the failure of the *secA2* mutant to prevent EEA1 recruitment to phagosomes is due to the SapM secretion defect of the mutant. For this purpose, we built a strain of the *secA2* mutant with the amount of secreted SapM restored to wild type levels. If SapM is the only SecA2-dependent effector preventing EEA1 recruitment, then restoring SapM secretion to wild type levels in the *secA2* mutant background should rescue this step of phagosome maturation arrest. However, if additional SecA2-dependent effectors exist with roles in this step of phagosome maturation arrest, their export will remain compromised and the EEA1 defect will persist. To restore the level of SapM secretion, we introduced a plasmid that overexpressed SapM in the *secA2* mutant background (*secA2*+SapM). In this *secA2* mutant strain, the level of secreted SapM was

restored, even surpassing the level seen with H37Rv (Figure 3.2A). While the mechanism of restored secretion is not clear, we suspect the overexpressed SapM is exported by an alternate pathway, as some SapM is observed in culture supernatants of the *secA2* mutant (Figure 3.1A). Importantly, the overexpressed SapM was functional as demonstrated by the increased secreted phosphatase activity of the *secA2*+SapM strain (Figure 3.2B).

Using this *secA2*+SapM strain, we tested how restored SapM secretion affects EEA1 recruitment to *secA2* mutant containing phagosomes. Restored SapM secretion in the *secA2* mutant fully rescued the *secA2* mutant defect in preventing EEA1 (Figure 3.2F, data not shown) (*i.e.* the percent EEA1+ *M. tuberculosis* containing phagosomes was equivalent between *secA2*+SapM and H37Rv). This result indicates that the defect in SapM secretion of the *secA2* mutant accounts for the failure to exclude EEA1 from phagosomes. In other words, SecA2 secretion of SapM is required for *M. tuberculosis* to prevent EEA1 recruitment to phagosomes. The effect of overexpressing SapM was specific to the *secA2* mutant, as SapM overexpression in H37Rv did not further reduce EEA1 recruitment (Figure 3.2F, data not shown).

SapM phosphatase activity prevents phagosomal EEA1 localization.

Past studies lead to a model of SapM functioning to block phagosome maturation by dephosphorylating PI3P (7). However, there is no direct evidence that the role of SapM in phagosome maturation arrest is through its phosphatase activity. By overexpressing a SapM variant lacking phosphatase activity in the *secA2* mutant we were able to directly test the significance of SapM phosphatase activity. Since catalytic residues and the active site of SapM are unknown, to create a phosphatase defective SapM, we substituted an alanine for

histidine 204, which aligns with a catalytically important residue in fungal acid phosphatases (Figure 3.2C) (30). When plasmids overexpressing SapM or SapM^{H204A} were introduced in the *secA2* mutant, the level of secreted SapM was comparable, as measured by immunoblot (Figure 3.2D). However, unlike overexpressed wild-type SapM, when SapM^{H204A} was overexpressed there was no increase in secreted phosphatase activity, indicating H204 is essential for SapM phosphatase activity (Figure 3.2E). Using SapM^{H204A}, we then tested the importance of phosphatase activity to the role of SapM in preventing EEA1 recruitment to *M. tuberculosis* containing phagosomes. Unlike overexpressed SapM (*secA2*+SapM), SapM^{H204A} (*secA2*+SapM^{H204A}) was unable to rescue the defect of the *secA2* mutant in preventing EEA1 recruitment (Figure 3.2G, data not shown). This result proves that the phosphatase activity of SapM is essential for SapM to exclude EEA1 from *M. tuberculosis* containing phagosomes.

SapM affects multiple steps of phagosome maturation and is not the only SecA2-dependent effector of phagosome maturation arrest.

During the normal process of phagosome maturation, Rab5 is recruited to early phagosomes and is then exchanged for Rab7 as phagosomes mature. However, phagosome maturation arrest caused by *M. tuberculosis* results in Rab5 retention and the exclusion of Rab7 from phagosomes (5). As PI3P, a substrate of SapM, contributes to the exchange of Rab5 for Rab7, we examined the association of Rab5 and Rab7 on *M. tuberculosis* containing phagosomes (31). Using immunofluorescence microscopy, we measured percent co-localization of Rab5 and Rab7 with *secA2* mutant containing phagosomes. In contrast to H37Rv-containing phagosomes, *secA2* mutant-containing phagosomes retained less Rab5 and recruited more Rab7, confirming the *secA2* mutant is defective for phagosome

maturation arrest (Figure 3.3A-B). Taking advantage of the *secA2*+SapM strain, we tested if SapM additionally impacts Rab5-Rab7 exchange. When secreted SapM was restored to the *secA2* mutant, a partial, but significant, rescue of *M. tuberculosis* inhibition of Rab5-Rab7 exchange on phagosomes was observed (i.e. restoring secreted SapM significantly increased Rab5 retention and reduced Rab7 recruitment) (Figure 3.3A-B). Furthermore, as shown with the phosphatase defective SapM^{H204A}, the phosphatase activity of SapM is required for its function in inhibiting Rab5-Rab7 exchange (Figure 3.3C-D). However, because the *secA2*+SapM strain did not restore the block in Rab5-Rab7 exchange to levels seen with H37Rv infected macrophages, this data argues for the existence of additional *M. tuberculosis* effectors exported by the SecA2 pathway impacting this step of phagosome maturation. It is noteworthy that the effect of the *secA2*+SapM strain on Rab5 retention and Rab7 exclusion waned as infection progressed (1 hr versus 24 hrs post infection) (Figure 3.3A-B).

Avoiding phagosome acidification is another feature of *M. tuberculosis* phagosome maturation arrest that is impaired in *secA2* mutant containing phagosomes (20). Using LysoTracker, an acidotropic dye that accumulates in acidified compartments, we examined if restoring secreted SapM to the *secA2* mutant rescues the ability of the mutant to avoid acidified phagosomes. The *secA2*+SapM strain was associated with a significant reduction in the percent LysoTracker co-localization (acidification) when compared to the *secA2* mutant, indicating that SapM secretion by the SecA2 pathway contributes to *M. tuberculosis* inhibition of phagosome acidification (Figure 3.3E, data not shown). However, the percentage of LysoTracker co-localization observed for the *secA2*+SapM strain was still significantly higher than that observed for H37Rv-containing phagosomes. This partial rescue reinforces the above conclusion that SapM is not the only SecA2-dependent effector

of phagosome maturation arrest. The phosphatase activity of SapM is also required to prevent phagosome acidification as shown with SapM^{H204A} (Figure 3.3F, data not shown). We next examined the effect of restoring secreted SapM to the *secA2* mutant on the ability to inhibit V-ATPase, the proton pump that acidifies the phagosome (4). We previously showed that V-ATPase is excluded from *M. tuberculosis* containing phagosomes but has a significantly higher association with *secA2* mutant-containing phagosomes (20). In stark contrast to the effect restoring SapM secretion to the *secA2* mutant had on phagosome acidification, no effect was observed on V-ATPase recruitment (Figure 3.3G, data not shown). These results are significant in revealing a role of SapM in preventing phagosome acidification that is independent from inhibiting recruitment of V-ATPase to phagosomes.

SapM contributes to the role of SecA2 in promoting *M. tuberculosis* intracellular growth.

Having previously linked the failure of the *secA2* mutant to arrest phagosome maturation with the intracellular growth defect of the mutant, we tested the effect of restoring secreted SapM to the *secA2* mutant on growth in macrophages. Intracellular growth was monitored over time by plating macrophage lysates for viable bacilli. As shown previously, intracellular growth of the *secA2* mutant was significantly attenuated compared to H37Rv (Figure 3.3H). When secreted SapM was added back to the *secA2* mutant, intracellular growth of the mutant significantly improved (Figure 3.3H). However, intracellular growth of the *secA2*+SapM strain was not restored to the level exhibited by H37Rv, which reinforces the above conclusions that additional SecA2 exported effectors must exist. Notably, there was no effect on intracellular growth with SapM overexpression in H37Rv.

SecA2 export of PknG contributes to phagosome maturation arrest and growth in macrophages.

Recent studies identified the PknG kinase, a protein with functions in *M. tuberculosis* physiology as well as phagosome maturation arrest, as being exported by the SecA2 pathway to the cell wall of *M. tuberculosis* and *Mycobacterium marinum* (11,23,32,33). To elucidate the role of SecA2 export of PknG in phagosome maturation arrest, we took the same approach as used with SapM of testing the effect of restoring PknG export to the *secA2* mutant. By overexpressing *pknG* in the *secA2* mutant (*secA2*+PknG) we were able to restore export of PknG to greater than wild type levels (Figure 3.4A).

In contrast to the full rescue in EEA1 inhibition observed with SapM restoration in the *secA2* mutant, restoring PknG export to the *secA2* mutant had no effect on EEA1 (Figure 3.4B, data not shown). However, restoring the levels of exported PknG to the *secA2* mutant significantly increased the ability of the *secA2* mutant to retain Rab5 and exclude Rab7 on phagosomes (Figure 3.4 C-D). This result reveals a role for PknG in preventing Rab5-Rab7 exchange that has not been described previously. However, like the *secA2*+SapM strain, the *secA2*+PknG strain was not as effective as H37Rv in inhibiting Rab5-Rab7 exchange, indicating it is not the only SecA2 exported effector involved in inhibiting this step of phagosome maturation. Intriguingly, unlike SapM, the effect seen with PknG restoration was consistent at both 1hr and 24hrs post infection (Figure 3.4 C-D).

When we examined phagosome acidification using LysoTracker, restored PknG export in the *secA2* mutant partially rescued the ability of the mutant to inhibit phagosome acidification (Figure 3.4E, data not shown). However, as with restoring SapM secretion, V-

ATPase recruitment was unaffected by restoring export of PknG in the *secA2* mutant (Figure 3.4F, data not shown).

Finally, we tested the effect of restored levels of exported PknG on intracellular growth of the *secA2* mutant. The *secA2*+PknG strain grew significantly better than the *secA2* mutant in macrophages, indicating SecA2 export of PknG contributes to intracellular growth of *M. tuberculosis* but, again, additional SecA2 exported proteins are also required, as growth was not restored to the levels seen with H37Rv (Figure 3.4G).

When added back simultaneously, SapM and PknG have a combined effect on phagosome maturation arrest and intracellular growth.

We next tested the effect of restoring export of SapM and PknG in combination to determine if these effectors have cumulative effects and if together they are sufficient to fully rescue the defects of a *secA2* mutant. We simultaneously overexpressed *sapM* and *pknG* to restore export of both effectors in the *secA2* mutant (*secA2*+SapM+PknG). As expected, the *secA2*+SapM+PknG strain fully inhibited EEA1 recruitment, like the *secA2*+SapM strain (Figure 3.2F, 3.5A, data not shown). When we examined Rab5 and Rab7 localization on phagosomes, simultaneous restoration of exported SapM and PknG to the *secA2* mutant inhibited Rab5-Rab7 exchange significantly more than restoration of either effector individually (Figure 3.5 B-C). In fact, when compared to H37Rv at 1hr post infection, full rescue of the Rab5-Rab7 exchange inhibition was observed for the *secA2*+SapM+PknG strain. However, at 24hrs post infection the effect waned, which is reminiscent of what was observed with the *secA2*+SapM strain (Figure 3.3 A-B).

In regards to phagosome acidification, the *secA2*+SapM+PknG strain had a greater

effect on inhibiting phagosome acidification (LysoTracker) than observed with restoration of either effector individually (Figure 3.5D, data not shown). However, phagosome acidification was still not inhibited to wild-type levels by the *secA2*+SapM+PknG strain (Figure 3.5D, data not shown). Furthermore, even when export of both effectors was restored, there was no rescue of the ability to exclude V-ATPase from the phagosome (Figure 3.5F, data not shown).

Finally, we tested the effect of restoring export of both effectors on growth of the *secA2* mutant in macrophages. The *secA2*+SapM+PknG strain grew significantly better than the *secA2* mutant with each effector restored individually (Figure 3.5F, data not shown). However, as seen with phagosome maturation arrest, the *secA2*+SapM+PknG strain was not fully rescued in its ability to grow intracellularly (Figure 3.5F, data not shown).

Thus, the *secA2*+SapM+PknG strain revealed a cumulative effect of adding back exported SapM and PknG on Rab5-Rab7 exchange, acidification and intracellular growth. However, in nearly all cases adding back these two effectors was insufficient to restore phenotypes to the level seen with H37Rv, which indicates the existence of even more SecA2-dependent effectors of phagosome maturation arrest.

The SecA2 pathway is required to inhibit autophagosome maturation (flux).

In addition to phagosome maturation arrest, *M. tuberculosis* inhibits the maturation of autophagosomes to autophagolysosomes which is sometimes referred to as autophagy flux (17,18). To determine if the SecA2 pathway is additionally required for autophagosome maturation arrest, we used LC3-II, the lipid modified form of LC3 that is associated with autophagosomes, to monitor autophagy in H37Rv and *secA2* mutant infected RAW 264.7

macrophages (34). Lower levels of LC3-II were observed in *secA2* mutant infected macrophages when compared to H37Rv infected macrophages (Figure 3.6A). The lower LC3-II levels were not due to a reduced bacterial burden in *secA2* mutant infected RAW cells as there was no difference in intracellular burden of H37Rv or the *secA2* mutant at these time points (data not shown). The lower levels of LC3-II in *secA2* mutant infected macrophages could indicate a defect of the *secA2* mutant in arresting autophagosome maturation such that there are more mature autophagosomes resulting in more LC3-II degradation. To test this possibility *M. tuberculosis* infected cells were treated with Bafilomycin A1, which blocks autophagosome acidification, maturation and the associated degradation of LC3-II. With Bafilomycin A1 treatment, the levels of LC3-II were comparable in *secA2* mutant and H37Rv infected macrophages. This result is consistent with the *secA2* mutant being defective in the ability to arrest autophagosome maturation (Figure 3.6A).

To further examine the requirement for the SecA2 pathway in autophagosome maturation arrest we utilized RAW 264.7 macrophages expressing a dual RFP::GFP::LC3 fusion protein (RAW-Difluo mLC3 cells). While RFP is resistant to the acidic environment of the autophagolysosome, GFP is acid sensitive and the signal is quenched in autophagolysosomes. By quantifying the number of RFP+ and GFP+/- autophagosomes, this cell line can report on autophagosome maturation. When we infected cells expressing RFP::GFP::LC3 with the *secA2* mutant, H37Rv or the complemented strain, there was no difference in the percent of *M. tuberculosis* that co-localized with all LC3+ compartments (RFP+, GFP+/-) (Figure 3.6B, data not shown). However, when we specifically examined the association of *M. tuberculosis* with mature autophagosomes by quantifying the percentage of *M. tuberculosis* that localize to autophagolysosomes (RFP+, GFP-), we found a significantly

higher association of the *secA2* mutant with autophagolysosomes than either H37Rv or the complemented strain. Together, the LC3-II immunoblots and the RFP::GFP::LC3 reporter indicate an additional role of the SecA2 pathway in autophagosome maturation arrest (Figure 3.6C, data not shown).

SecA2 export of SapM and PknG contributes to inhibition of autophagosome maturation (flux).

Using the *secA2* mutant strains with restored export of SapM and/or PknG, we next set out to determine if SecA2 export of SapM and PknG contributes to the function of SecA2 in autophagosome maturation arrest. Restored export of either SapM or PknG reduced localization of the *secA2* mutant in autophagolysosomes indicating both SapM and PknG contribute to *M. tuberculosis* inhibition of autophagosome maturation (Figure 3.6D, data not shown). Notably, restored SapM secretion resulted in a more significant reduction in *secA2* localization to autophagolysosomes than PknG (Figure 3.6D, data not shown). Simultaneous restoration of SapM and PknG export was more effective than restoration of either effector individually (Figure 3.6D, data not shown). In fact, when compared to H37Rv, full rescue of autophagosome maturation arrest was observed for the *secA2*+SapM+PknG strain (Figure 3.6D, data not shown).

A benefit of utilizing the RFP::GFP::LC3 expressing cell line is the ability to simultaneously examine autophagosome and phagosome maturation in the same cells. In order to monitor phagosome maturation, we quantified co-localization of LC3 negative (LC3-) *M. tuberculosis* with LysoTracker. In LC3- phagosomes, the *secA2* mutant localized more frequently to mature LysoTracker positive phagosomes than H37Rv (Figure 3.6E, data

not shown). Moreover, the *secA2*+SapM and *secA2*+PknG strains exhibited significantly reduced localization to mature LC3- phagosomes when compared to the *secA2* mutant (Figure 3.6E, data not shown). Interestingly unlike with autophagosome maturation arrest, the effect on phagosome maturation of adding back exported SapM to the *secA2* mutant was significantly less than that of PknG (Figure 3.6E, data not shown). The *secA2*+SapM+PknG strain exhibited even greater rescue of phagosome maturation arrest than observed with restoration of either effector individually (Figure 3.6E, data not shown). However, in contrast to autophagosome maturation, the *secA2*+SapM+PknG strain was not fully rescued in its ability to arrest phagosome maturation (Figure 3.6E, data not shown). The function of SapM in both autophagosome and phagosome maturation arrest depends on SapM phosphatase activity, as shown by the *secA2*+SapM^{H204A} strain remaining defective in both processes (data not shown). Together, these results demonstrate that both phagosome and autophagosome maturation arrest depend on the SecA2 pathway, SapM, and PknG. However, these experiments also reveal differences in the contribution individual effectors make to each process and expose the existence of additional SecA2-dependent effectors required for phagosome maturation arrest but not necessarily for autophagosome maturation arrest.

DISCUSSION

Phagosome maturation arrest by *M. tuberculosis* is complex and much remains to be learned about the effectors involved in the process and how they work together. We showed previously that the SecA2 pathway is required for *M. tuberculosis* to inhibit phagosome maturation; however, the SecA2-dependent effectors of phagosome maturation arrest

remained unknown (20). Here, we identified two SecA2 exported effectors of *M. tuberculosis* phagosome maturation arrest as the phosphatase SapM and the kinase PknG. Then, using a strategy of adding back export of SapM and PknG to the *secA2* mutant, we not only established the significance of the role of the SecA2 pathway in exporting these proteins but we identified steps in phagosome maturation that are impacted by these factors individually and in combination. Moreover, we revealed that the SecA2 pathway, SapM, and PknG also function in inhibiting autophagosome maturation.

Prior to this study, SapM was not known to be secreted by the SecA2 export pathway. By testing the requirement for SecA2 in the export of a set of known effectors of phagosome maturation arrest (SapM, LpdC, Ndk) we identified SapM as a SecA2-exported protein (13,35). The SecA2 pathway did not contribute to LpdC or Ndk secretion, and these effectors were not studied further (data not shown). PknG was identified as being exported by the SecA2 pathways of *M. tuberculosis* and *M. marinum* in recent proteomic studies (23,32). While SapM and PknG are both known to function in phagosome maturation arrest and there are reports of *M. tuberculosis* mutants lacking these effectors having defects in phagosome maturation arrest, our understanding of their roles in inhibiting specific steps of phagosome maturation is far from complete (7,10,11,26).

We established the significance of SecA2 export of SapM and PknG to phagosome maturation arrest and intracellular growth, using the strategy of adding back export of these proteins to the *secA2* mutant. To create the necessary strains, we reasoned that overexpressing SecA2-dependent proteins in the *secA2* mutant could boost their export through the alternate mechanism, possibly the SecA1-dependent pathway, that accounts for the residual export in the *secA2* mutant of SapM, PknG and all SecA2 exported proteins

identified to date (22,23,32,36). Using overexpression, we achieved our goal of producing a *secA2* mutant strain that has at least as much exported SapM and/or PknG as detected in the wild type H37Rv strain. Notably, even when overexpressed, the *secA2* mutant exported less SapM and PknG than the corresponding H37Rv overexpression strain, confirming the dependency of these effectors on SecA2 for export. The effects of SapM and/or PknG overexpression were specific to the *secA2* mutant and specific to the overexpressed proteins. H37Rv was unaffected by increased levels of these proteins and equivalent levels of overexpressed SapM^{H204A} in the *secA2* mutant had no effects. We also repeated the experiments using a single-copy vector with reduced, though still higher than wild-type levels, of secreted SapM and saw comparable restoration of phagosome maturation arrest and intracellular growth (data not shown).

The *secA2* mutant strains with restored levels of exported SapM and/or PknG proved to be powerful tools for investigating steps in phagosome maturation affected by these effectors (Figure 3.7). Past studies demonstrate purified SapM can dephosphorylate PI3P *in vitro* (7). This data led to a model for secreted SapM dephosphorylating PI3P and inhibiting recruitment of PI3P binding proteins, such as EEA1 to the phagosome to arrest phagosome maturation. However, critical details of this model have not been confirmed, including an effect of SapM on EEA1 and proof that SapM functions as a phosphatase to arrest phagosome maturation. Thus, our demonstration that restored levels of exported wild type SapM, but not the phosphatase defective SapM^{H204A}, inhibits EEA1 localization to phagosomes provides important validation of the model. Adding back wild type SapM also partially restored inhibition of Rab5-Rab7 exchange and this again depends on SapM phosphatase activity. This effect of SapM on Rab5-Rab7 exchange was not previously noted,

but it is consistent with the known function of PI3P in Rab5-Rab7 exchange and is intriguing given a report of SapM binding to Rab7 (31,37,38). The SapM effect on Rab5-Rab7 exchange was reproducibly more extreme at 1hr versus 24hrs post infection (Figure 3.3 A-B). The temporal nature of effector functions revealed by this data reveals another layer of complexity to phagosome maturation arrest by *M. tuberculosis*.

The strategy of overexpressing PknG to restore exported levels to the *secA2* mutant was used previously in *M. marinum* (32). Similar to what we observed, adding back exported PknG to the *secA2* mutant of *M. marinum* results in a partial restoration of phagosome maturation arrest. However, in the *M. marinum* study, the effect of PknG was only assessed on co-localization with the late lysosomal-associated membrane protein (LAMP1)(32). Since the function(s) of PknG that impact phagosome maturation is unknown, we took advantage of the *secA2*+PknG strain and examined effects on earlier steps of phagosome maturation. PknG had no effect on EEA1 recruitment to phagosomes, but it did partially restore inhibition of Rab5-Rab7 exchange, revealing for the first time a function of PknG in inhibiting Rab5-Rab7 exchange (Figure 3.7). Interestingly, when exported SapM and PknG were added back simultaneously, a combined effect was observed that resulted in complete inhibition of Rab5-Rab7 exchange at 1hr post infection but waned as infection progressed. Thus, multiple SecA2-dependent effectors act on the same step of phagosome maturation and the combinatorial effects of these effectors suggests SapM and PknG work through different but complementary mechanisms.

Studies of PknG function in phagosome maturation arrest are complicated by the fact that, in addition to being exported, PknG is in the bacterial cytoplasm where it functions in glutamate metabolism, regulation of the TCA cycle, and in a redox homeostatic system

(RHOCS) that contributes to resistance to oxidative stress (9,10,33,39). Because *M. tuberculosis* mutants with RHOCS defects are delivered to mature phagosomes and have intracellular growth defects, it raised the possibility that the redox function of PknG explains its role in phagosome maturation arrest (10). However, this does not appear to be the case as the *secA2* mutant does not exhibit a RHOCS defect, as assessed by sensitivity to redox stress, and overexpression of PknG did not increase resistance of the mutant to redox stress (data not shown). Going forward the *secA2* mutant, in conjunction with the *secA2*+PknG strain, may be an ideal platform to further study the function(s) and target(s) of PknG in phagosome maturation arrest.

We also observed partial effects of SapM and PknG on phagosome acidification. Surprisingly, adding back these effectors inhibited phagosome acidification, but had no effect on preventing V-ATPase localization to *M. tuberculosis* phagosomes. The ability of *M. tuberculosis* to exclude V-ATPase from the phagosome is generally assumed to account for the block acidification of *M. tuberculosis* phagosomes (4). Our demonstration that SapM and PknG inhibit acidification without blocking recruitment of the V-ATPase indicates the existence of another mechanism for *M. tuberculosis* to prevent phagosome acidification. At the same time, because adding back SapM and PknG failed to rescue the mutant defect in excluding V-ATPase from the phagosome, there is at least one additional SecA2-dependent effector involved in this step of phagosome maturation arrest. PtpA, which binds subunit H of V-ATPase and thereby excludes the proton pump from phagosomes, is a candidate for this missing SecA2-exported effector (15). Unfortunately, our inability to detect secreted PtpA in *M. tuberculosis* cultures prevented us from determining if PtpA is secreted by the SecA2 pathway.

Compared to phagosome maturation arrest, even less is known about autophagosome maturation arrest by *M. tuberculosis*. Using the RFP::GFP::LC3 reporter, we were able to reveal a role for SecA2 export in the maturation arrest of both LC3- phagosomes and LC3+ autophagosomes. It is important to note in this study, we are unable to distinguish between autophagosomes and other LC3+ compartments, including LC3 associated phagosomes (LAP) so we cannot exclude a function for SecA2 in those processes. Using the *secA2*+SapM+PknG strain we were able to demonstrate a function for both SapM and PknG in autophagosome maturation arrest by *M. tuberculosis*. Our data confirms a recent study using *sapM* transfected cells that suggests a role for SapM in autophagosome maturation arrest but this is the first evidence indicating a function for PknG in this process (37).

Intriguingly, the SecA2 exported effectors do not affect both autophagosome and phagosome maturation equally. SapM seems to have more of an effect on autophagosomes while PknG is more impactful on altering phagosomes. Further, while simultaneous restoration of both effectors was able to fully rescue the defect of the *secA2* mutant in autophagosome maturation, it was not sufficient to rescue the defect in phagosome maturation. Our results highlight the overlap in *M. tuberculosis* factors involved in phagosome and autophagosome maturation but at the same time reveal differences in specificity of *M. tuberculosis* effectors for both processes.

When we investigated the effect of SecA2 export of SapM and PknG on *M. tuberculosis* growth in macrophages, we found adding back either effector individually improved intracellular growth of the *secA2* mutant while restoring export of both effectors simultaneously resulted in a further improvement. This correlation between rescue of phagosome maturation arrest with the rescue of intracellular growth reinforces prior studies

which indicate that the role of SecA2 in inhibiting *M. tuberculosis* delivery to mature phagosomes is required for intracellular growth (20). Furthermore, the effect of SecA2, SapM and PknG on phagosome maturation arrest will likely extend beyond promoting replication in macrophages. By arresting phagosome maturation, *M. tuberculosis* also limits the presentation of antigenic peptides to the immune system, which contributes to suboptimal adaptive immune responses to *M. tuberculosis* (40).

In summary, our studies demonstrate that multiple effectors require the SecA2 pathway for their export and function in phagosome maturation arrest and they provide unique insight into how *M. tuberculosis* effectors work in concert to inhibit phagosome and autophagosome maturation. Through our studies, we revealed the advantages of using of the *secA2* mutant as a platform to study the function of effectors individually or in combination. This approach provides an alternative to studying effectors through deletion analysis, which can be problematic for effectors that share redundant functions or for effectors that have additional unrelated functions in *M. tuberculosis* (such as PknG). The use of the *secA2* mutant also provides insight on the effectors that are exported in a SecA2-independent manner (i.e. unchanged in the *secA2* mutant). These effectors although still exported and functional in the mutant are still not sufficient to arrest phagosome maturation. In this study, we discovered new layers of complexity in how *M. tuberculosis* arrests phagosome maturation (multiple means of inhibiting acidification, temporal effects), uncovered distinct and cumulative effects of a pair of effectors, and revealed a broad role of the SecA2 pathway in phagosome and autophagosome maturation arrest that involves SapM, PknG and additional effectors that await identification.

Materials and Methods:

Ethics Statement

This study included the use of mice and followed recommendations in the Guide for the Care and Use of Laboratory Animals of the National Institutes of Health. The protocol was approved by the International Animal Care and Use Committee at the University of North Carolina at Chapel Hill (protocol: 15-018.0).

Strains and Media Conditions

In this study we used the *Mycobacterium tuberculosis* wild type strain H37Rv, and the $\Delta secA2$ mutant (mc²3112) generated in the H37Rv background (22). The plasmids and strains over-expressing *sapM* and/or *pknG* constructed for this study are listed in Table 3.1 and Table 3.2 respectively.

M. tuberculosis strains were cultured in either liquid Middlebrook 7H9(BD) or on solid Middlebrook 7H10(BD) or 7H11 (Sigma) media supplemented with 0.05% Tween 80, 0.5% glycerol, 1x albumin dextrose saline (ADS) and kanamycin (20 μ g/ml) or hygromycin (50 μ g/ml) when appropriate. Sauton media was used for preparation of culture supernatants containing 30mM DL-asparagine, 7mM sodium citrate, 3mM potassium phosphate dibasic, 4mM magnesium sulfate, 0.2mM ferric ammonium citrate and 4.8% glycerol adjusted to a pH of 7.4. For cell wall isolation, we utilized a modified Middlebrook 7H9 based media containing 0.1% glycerol, 1mM propionic acid, 0.1% tyloxapol, 0.1M MES (buffer), 0.5% BSA, and adjusted to a pH of 6.5 (23).

SapM Site-directed Mutagenesis

The Histidine at position 204 of SapM was changed to an Alanine using site directed mutagenesis to generate SapM^{H204A}. The *sapM* expression plasmid pJTS130 was used as a template. Primer sequences are as follows: 5'-cgatcgagccgctcggccatgctcgttgctgg-3' and 5'-ccgacaacgacatggccgacggctcgatcg-3'. Dpn1 (NEB) was added to degrade the methylated template. Mutation was confirmed by sequencing.

Culture Supernatant isolation

For culture supernatant isolation, cultures were first grown to log-phase in Middlebrook 7H9 with 0.05% tyloxapol. Cultures were then washed in Sauton media and grown in Sauton media with 0.05% tyloxapol for 5 days after which cultures were washed again to remove detergent and sub-cultured into 100ml Sauton media (no detergent) at a starting OD600 of 0.25 for 2 days. Then the entire 100 ml culture was centrifuged at 3500 rpm and supernatants were collected and double filtered with a 0.2µm filter to remove cells. Culture supernatants were concentrated 100-fold using a 15 ml capacity 10,000 MW cut off centrifugal filter (Millipore). For Immunoblots, proteins were isolated by precipitation using 10% trichloroacetic acid overnight. To confirm that the supernatants were free of cytosolic contamination due to cell lysis, samples were examined by Immunoblot for absence of the cytoplasmic mycobacterial proteins SigA, GroEL, and SecA1.

Cell wall isolation

For cell wall isolation, *M. tuberculosis* was first grown in 7H9 0.05% Tyloxapol to mid-log phase and then sub-cultured into the modified 7H9 media at a starting OD600 of 0.125. Cultures were harvested when they reached an OD600 of 1.0 and were then sterilized by gamma-irradiation in a JL Shephard Mark I 137Cs irradiator (Dept. of Radiobiology,

University of North Carolina at Chapel Hill) prior to removal from BSL-3 containment.

Subcellular fractions were isolated as previously described (41). Briefly, irradiated cells were suspended in 1X PBS containing protease inhibitors and lysed by passage four times through a French pressure cell. Unlysed cells were removed by centrifugation at 3500 rpm to generate clarified whole cell lysates (WCLs), which were then spun at 25,000 rpm for 30 minutes to pellet the cell wall fraction.

Immunoblots

Protein concentrations were determined by Bicinchoninic acid assay (Pierce). Equal protein for whole cell lysates, cell wall fractions, or concentrated culture supernatants was run on a SDS-PAGE gel, and then transferred to nitrocellulose membranes. After transfer, the membranes were blocked for one hour and then probed with primary antibodies. Antibodies to *M. tuberculosis* proteins were kind gifts of Vojo Deretic, University of New Mexico (SapM), Zakaria Hmama, University of British Columbia (LpdC and NdkA), Yossef Av-Gay, University of British Columbia (PknG) and Douglas Young, Imperial College (19kDa). LC3 and Actin antibodies were acquired from Cell Signaling Technologies. Antibodies were used at the following dilutions (SapM 1:5,000, LpdC 1:2,000, NdkA 1:2,000, PknG 1:5,000, 19kDa 1:20,000, LC3 1:500, and Actin 1:1000) Secondary antibodies were conjugated to horseradish peroxidase (BioRad) and signal was detected using chemiluminescence (Western Lighting Perkin Elmer).

Phosphatase activity assay

SapM phosphatase activity was assayed as described previously(27). The phosphatase activity of 5 µg of culture supernatants was assessed for triplicate samples. Each reaction contained 0.1mM Tris base pH 6.8 and 50mM p-nitrophenyl phosphate (pNPP)(New

England Biolabs) with either 2 mM sodium tartrate to inhibit background phosphatase activity or 1 mM sodium molybdate to inhibit SapM activity. Samples were incubated at 37°C and the absorbance at 405nm was measured every minute for two hours. We then calculated the rate of pNPP conversion and normalized the data to H37Rv.

Quantitative Real-Time PCR.

Triplicate *M. tuberculosis* cultures were grown in modified 7H9 medium to an OD₆₀₀ of 1.0 and pelleted by centrifugation at 3,000 rpm for 10 min. Bacteria were lysed in 1 ml 3:1 chloroform-methanol, then vortexed with 5 ml TRIzol (Invitrogen) and incubated for 10 min at room temperature. Phases were separated by centrifugation at 3,000 rpm for 15 min at 4°C, and RNA was precipitated from the upper phase using 1X volume of isopropanol. RNA was pelleted by centrifugation at 12,000 rpm for 30 min at 4°C, washed twice with cold 70% ethanol, and resuspended in RNase-free water. RNA samples were treated with DNase (Promega) and then column purified (Zymo RNA clean and concentrator kit). Following RNA isolation, cDNA was synthesized with random primers using the iScript cDNA Synthesis Kit (BioRad). Real-time PCR was completed using 25ng of cDNA template in triplicate technical replicates using the SensiMix SYBR and fluorescein kit (Bioline). Transcripts were normalized to the housekeeping gene *sigA*. Primer sequences are for *sapM* (ATCGTTGCTGGCCTCATGG and AGGGAGCCGACTTGTTACC) and *sigA* (GAGATCGGCCAGGTCTACGGCGTG and CTGACATGGGGGCCCGCTACGTTG).

Macrophage Infections

For bone marrow-derived macrophages (BMDM), femurs were isolated from C57/Bl6 (Jackson Labs) mice and flushed with complete DMEM (DMEM [Sigma] supplemented with 10% Heat inactivated fetal bovine serum [FBS] 5mM non-essential

amino acids and 5mM L-glutamine). Bone marrow cells were washed, re-suspended and plated in complete DMEM containing 20% L-929 cell conditioned media (LCM). After six days, the cells were lifted off the plates using cold 5mM EDTA in PBS. Macrophages were seeded at 2×10^5 macrophages/well in complete DMEM containing 20% LCM using either eight-well chambered slides to monitor growth of *M. tuberculosis* or chambered cover slips for microscopy experiments. After resting 24 hours the macrophages were infected with *M. tuberculosis* grown to log-phase, and washed twice with PBS containing 0.05% Tween 80 and diluted in warm complete DMEM. BMDM were infected at an MOI of 1.0 for four hours. Infected macrophages were then washed three times with pre-warmed complete DMEM to remove extracellular bacteria. Macrophages were lysed using 0.1% Triton X-100 at various time points and lysates were plated for cfu determination or slides were fixed in 4% paraformaldehyde (PFA) for immunofluorescence staining.

RAW 264.7 cells were cultured in DMEM supplemented with 10% FBS. Cells were seeded at 1×10^6 macrophages/well (6-well plate) or 1×10^5 macrophages/well (8-well chamber slide). For immunoblots, RAW cells were infected at an MOI of 10 for 3 hrs and washed three times with pre-warmed DMEM to remove extracellular bacteria. Bafilomycin A1 (Sigma) was utilized at a concentration of 10nM and maintained throughout the course of the experiment. Cells were lysed using RIPA buffer (50mM Tris-HCL pH 7.4, 1% NP-40, 0.25% Sodium deoxycholate, 150mM NaCl, and protease inhibitors). For cfu determination RAW cells were infected at an MOI of 1 for 4 hrs and washed three times with pre-warmed DMEM to remove extracellular bacteria. Cells were lysed using 0.1% Triton X-100 at various time points and lysates were plated for cfu determination.

RAW-Difluo mLC3 Cells expressing RFP::GFP::LC3 (InvivoGen) were cultured in DMEM supplemented with 10% FBS and zeocin. Cells were seeded at 1×10^5 macrophages/well without zeocin and infected at an MOI of 1 for 4 hrs and washed three times with pre-warmed DMEM to remove extracellular bacteria. At 1hr or 24hrs post infection cells were fixed in 4% PFA.

LysoTracker staining and Immunofluorescent Microscopy

For LysoTracker staining, media on *M. tuberculosis* infected BMDM was replaced with prewarmed DMEM containing 100nM LysoTracker Red DND99 (Invitrogen) for BMDM and 100nM LysoTracker Deep Red (Invitrogen) for RAW 264.7 cells and incubated for one hour. After which, media was removed and the slides fixed in 4% PFA.

For immunofluorescence, media was removed from *M. tuberculosis* infected macrophages and the slides were submerged in 4% PFA. The fixed slides were submerged in PBS to remove residual PFA and then cells were permeabilized with 0.1% Triton-X 100 in PBS for 5 minutes at room temperature, washed in PBS and blocked in PBS containing 10% donkey serum. Antibodies to mammalian markers (Rab5, Rab7 and V-ATPase B1/B2) and Texas Red conjugated donkey anti-rabbit secondary antibodies were acquired from Santa Cruz Biotechnology. Antibodies to EEA1 were acquired from Abcam. Primary antibodies were used at a 1:50 dilution in PBS with 3% serum and incubated overnight at 4°C. After which slides were washed in PBS, and secondary antibodies conjugated to TR fluorophores were used at 1:100 dilution in PBS with 3% serum and incubated at room temperature for one hour. Slides were washed to remove the secondary antibody and Fluormount-G (Southern Biotech) was added to each well to protect the fluorescent signal. As controls we included unstained cells as well as stained uninfected cells with the antibodies listed above.

Widefield fluorescence microscopy was performed using an Olympus IX-81 controlled by the Volocity software package. All images were taken using a 60X oil-immersion objective. Mycobacterial autofluorescence was visualized using a CFP filter cube (Semroc) with an excitation band of 426-450nm and emission band of 467-600nm (20). A minimum of eight fields per well were captured and a minimum of 250 bacteria per well were scored for phagosomal markers. For each experimental group four replicate wells were analyzed per experiment.

Oxidative Stress Resistance

To assess sensitivity to oxidative stress *M. tuberculosis* cultures were exposed to 5mM H₂O₂ in 7H9+ADS 0.05% Tween 80 for 24 and 48 hours. Survival was assessed by plating for viable CFU. Cultures without H₂O₂ were included as controls. Strains tested in this manner include H37Rv and the *secA2* mutant with and without PknG overexpression. A *pstA1::tn* mutant (generous gift of Jyothi Rengarajan, Emory University) which is extremely sensitive to oxidative stress was included as a control (42,43).

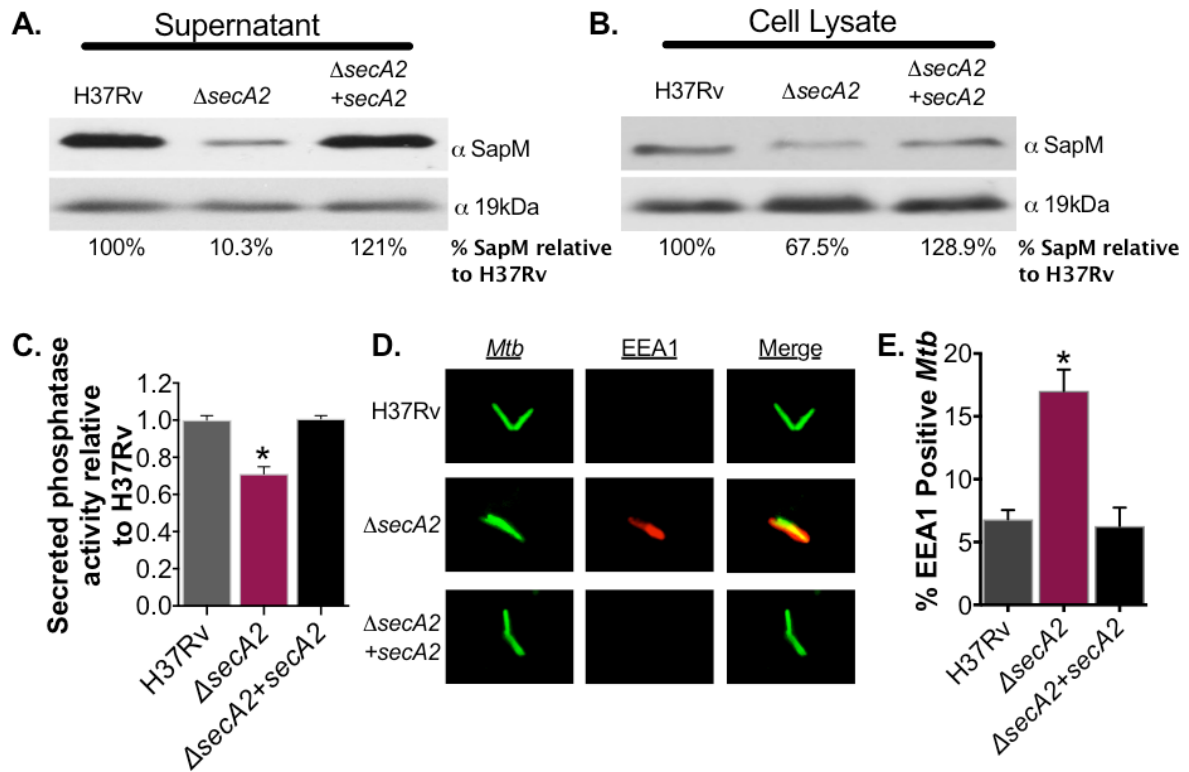


Figure 3.1: SapM export is dependent upon the SecA2 pathway.

(A) Equal protein from culture supernatants or (B) cell lysates from the wild-type strain H37Rv, the *secA2* mutant and the complemented strain were examined for levels of SapM or the SecA2 independent loading control 19kDa by Immunoblot. Densitometry was used to quantify SapM levels relative to H37Rv (ImageJ) (C) Phosphatase activity in triplicate culture supernatant samples was examined by quantifying cleavage of pNPP. Rates of pNPP cleavage were normalized to H37Rv. (D) Quadruplicate wells of murine bone marrow derived macrophages were infected and EEA1 recruitment to phagosomes was assessed by Immunofluorescence. Representative images of EEA1 stained *M. tuberculosis* infected macrophages are shown. (E) The percentage of *M. tuberculosis* containing phagosomes that co-localized with EEA1 at 1hr post infection was determined. * $p < 0.01$ ANOVA Holm-Sidak post Hoc test. Data represents at least two independent experiments.

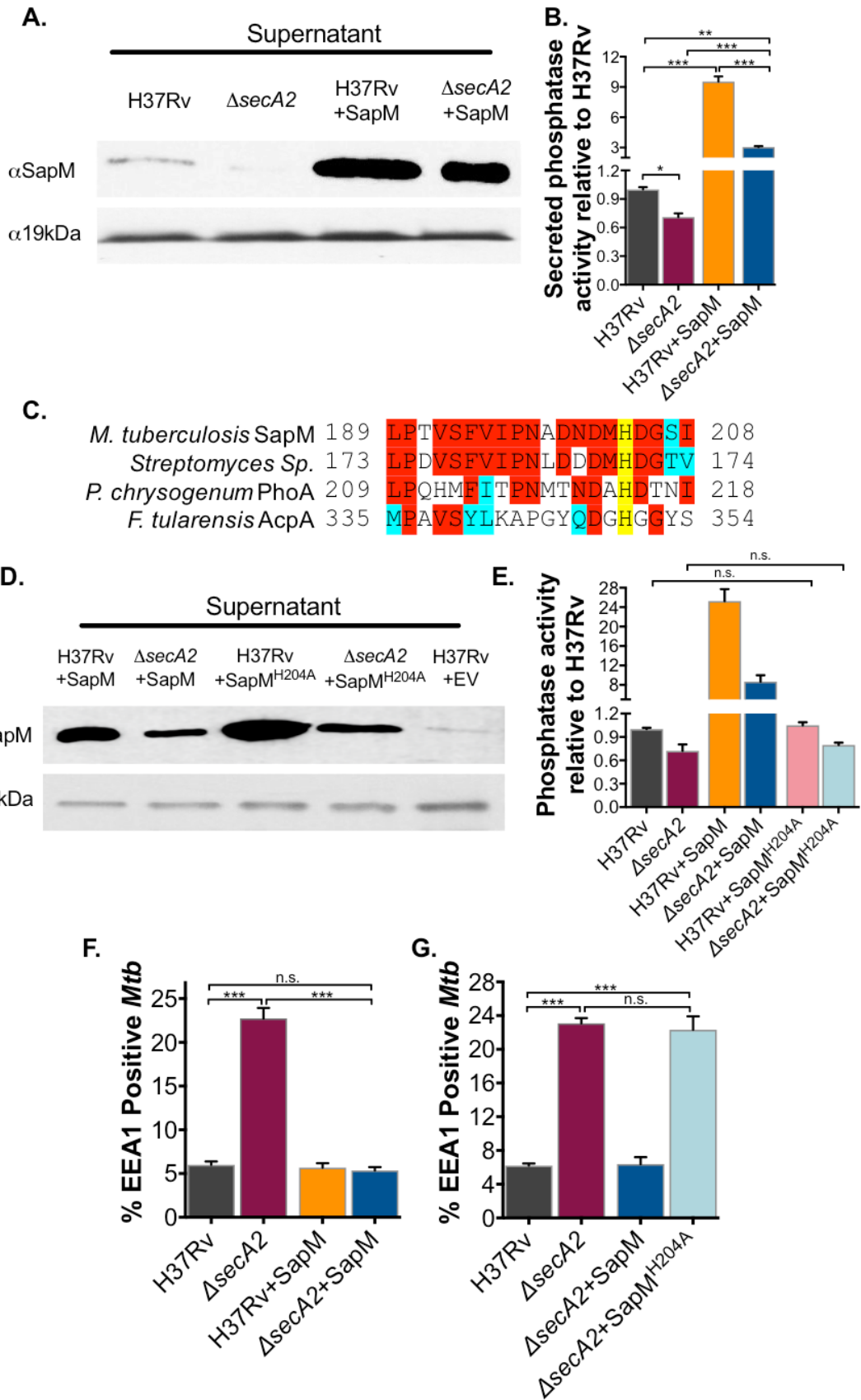


Figure 3.2: SecA2 secretion of SapM is required for EEA1 exclusion from *M. tuberculosis* containing phagosomes

(A) Equal protein from culture supernatants isolated from the H37Rv, the *secA2* mutant and the SapM overexpression strains was examined for levels of SapM or the SecA2 independent loading control 19kDa by Immunoblot. (B) Phosphatase activity of triplicate culture supernatant samples was examined by quantifying cleavage of pNPP. Rates of pNPP cleavage were normalized to H37Rv. (C) The potential active site of SapM was aligned to the amino acid sequence of an acid phosphatase from *Streptomyces sp.* (WP_063837857.1), PhoA from *Penicillium chrysogenum* and AcpA from *Francisella tularensis*. Identical residues are shaded red and similar residues are shaded blue. The conserved active Histidine is highlighted in yellow. (D) Equal protein from culture supernatants isolated from H37Rv and the *secA2* mutant overexpressing wild-type SapM as well as from H37Rv and the *secA2* mutant overexpressing SapM^{H204A} was examined for levels of SapM or the SecA2 independent loading control 19kDa by Immunoblot. (E) Phosphatase activity of triplicate culture supernatant samples was examined by quantifying cleavage of pNPP. Rates of pNPP cleavage were normalized to H37Rv. (F and G) The percentage of *M. tuberculosis* containing phagosomes that contain EEA1 was assessed in quadruplicate wells of *M. tuberculosis* infected BMDM by Immunofluorescence at 1hr post-infection. *p<0.05 **p<0.001 ***p<0.0001 ANOVA Holm-Sidak post Hoc test. Data represents at least two independent experiments.

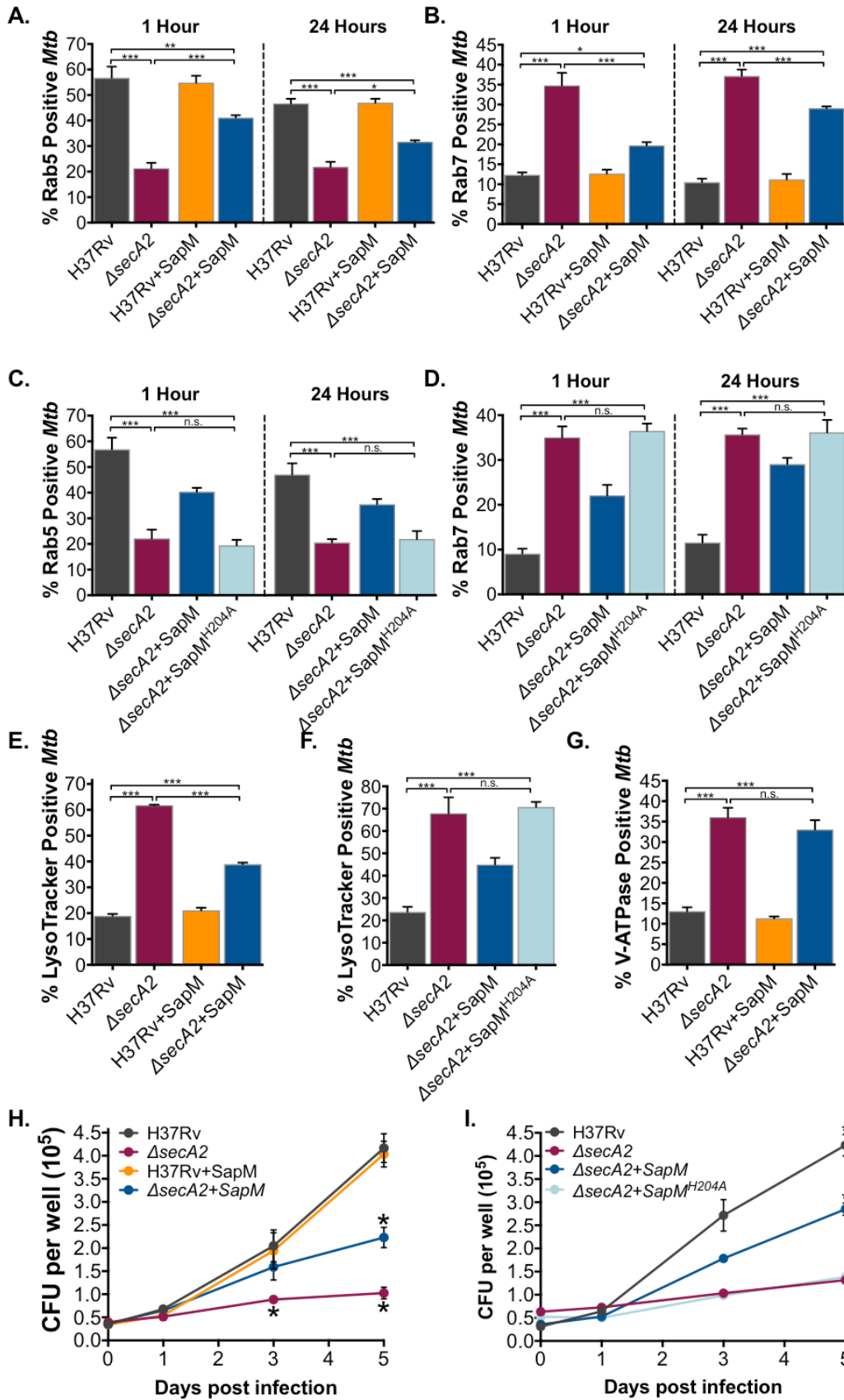


Figure 3.3: SecA2 secretion of SapM contributes to phagosome maturation arrest and intracellular growth

The percentage of *M. tuberculosis* containing phagosomes that contain (A, C) Rab5 and (B,D) Rab7 was assessed in quadruplicate wells of *M. tuberculosis* infected BMDM by Immunofluorescence at both 1hr and 24hrs post-infection. (E,F) The percentage of *M. tuberculosis* phagosomes that were acidified was determined using LysoTracker staining of quadruplicate wells of infected cells at 1hr post infection. (G) The percentage of *M. tuberculosis* containing phagosomes that contain V-ATPase was assessed in quadruplicate wells of *M. tuberculosis* infected BMDM by Immunofluorescence at 1hr post infection. (H,I) Triplicate wells of BMDM were infected at an MOI of 1 and CFU burden was assessed over the course of a 5 day infection. * $p < 0.05$ ** $p < 0.001$ *** $p < 0.0001$ ANOVA Holm-Sidak post Hoc test. Data represents at least two independent experiments.

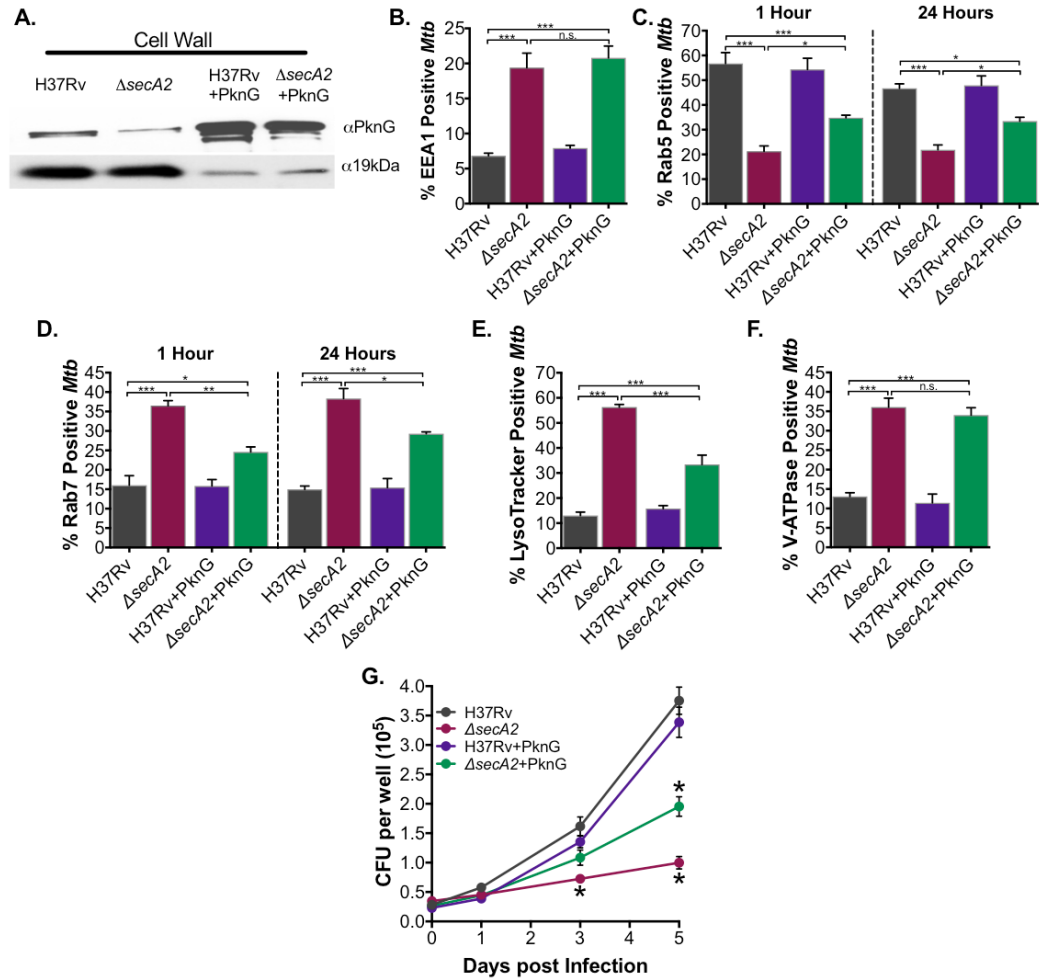


Figure 3.4: SecA2 export of PknG contributes to phagosome maturation arrest and growth in macrophages.

(A) Cell wall fractions were isolated from *M. tuberculosis* strains and levels of PknG and the SecA2 independent loading control 19kDa were assessed by Immunoblot. 10x protein was loaded for H37Rv and *secA2* mutant than the corresponding *pknG* overexpression strains. (B) The percentage of *M. tuberculosis* containing phagosomes that contain EEA1 was assessed in quadruplicate wells of *M. tuberculosis* infected BMDM by Immunofluorescence at 1hr post-infection. The percentage of *M. tuberculosis* containing phagosomes that contain (C) Rab5 and (D) Rab7 was assessed in quadruplicate wells of *M. tuberculosis* infected BMDM by Immunofluorescence at both 1hr and 24hrs post-infection. (E) The percentage of *M. tuberculosis* phagosomes that were acidified was determined using LysoTracker staining of quadruplicate wells of infected cells at 1hr post infection. (F) The percentage of *M. tuberculosis* containing phagosomes that contain V-ATPase was assessed in quadruplicate wells of *M. tuberculosis* infected BMDM by Immunofluorescence at 1hr post-infection. (G) Triplicate wells of BMDM were infected at an MOI of 1 and CFU burden was assessed over the course of a 5 day infection. * $p < 0.05$ ** $p < 0.001$ *** $p < 0.0001$ ANOVA Holm-Sidak post Hoc test. Data represents at least two independent experiments.

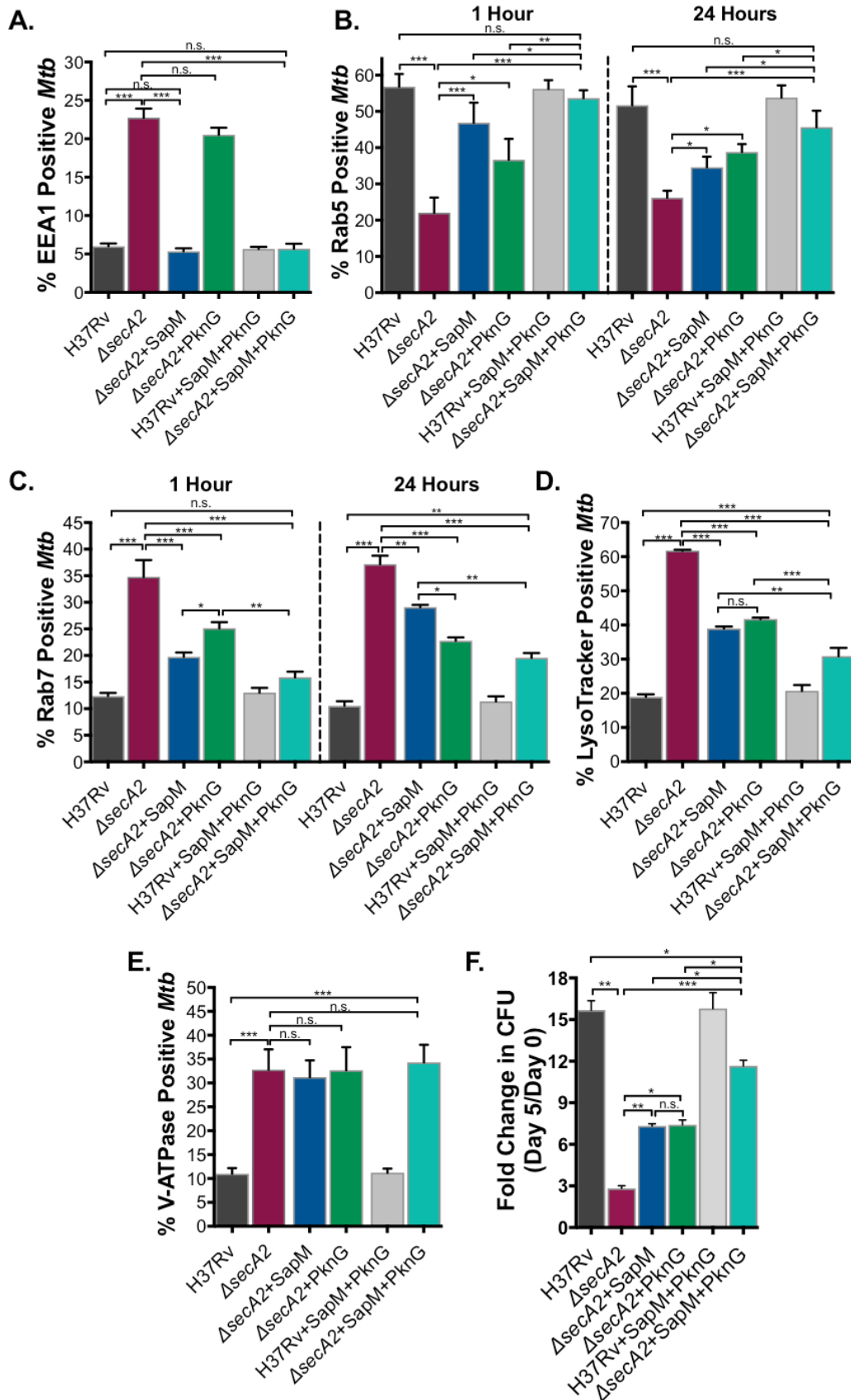


Figure 3.5: SecA2 export of both SapM and PknG contributes to phagosome maturation arrest and virulence.

(A) The percentage of *M. tuberculosis* containing phagosomes that contain EEA1 was assessed in quadruplicate wells of *M. tuberculosis* infected BMDM by Immunofluorescence at 1hr post-infection. The percentage of *M. tuberculosis* containing phagosomes that contain (B) Rab5 and (C) Rab7 was assessed in quadruplicate wells of *M. tuberculosis* infected BMDM by Immunofluorescence at both 1hr and 24hrs post-infection. (D) The percentage of *M. tuberculosis* phagosomes that were acidified was determined using LysoTracker staining of quadruplicate wells of infected cells at 1hr post-infection. (E) The percentage of *M. tuberculosis* containing phagosomes that contain V-ATPase was assessed in quadruplicate wells of *M. tuberculosis* infected BMDM by Immunofluorescence at 1hr post-infection. (F) Triplicate wells of BMDM were infected at an MOI of 1 and CFU burden was assessed over the course of a 5 day infection. The fold change in CFU over the course of the 5 day macrophage infection for each *M. tuberculosis* strain was calculated. * $p < 0.05$ ** $p < 0.001$ *** $p < 0.0001$ ANOVA Holm-Sidak post Hoc test. Data represents at least two independent experiments.

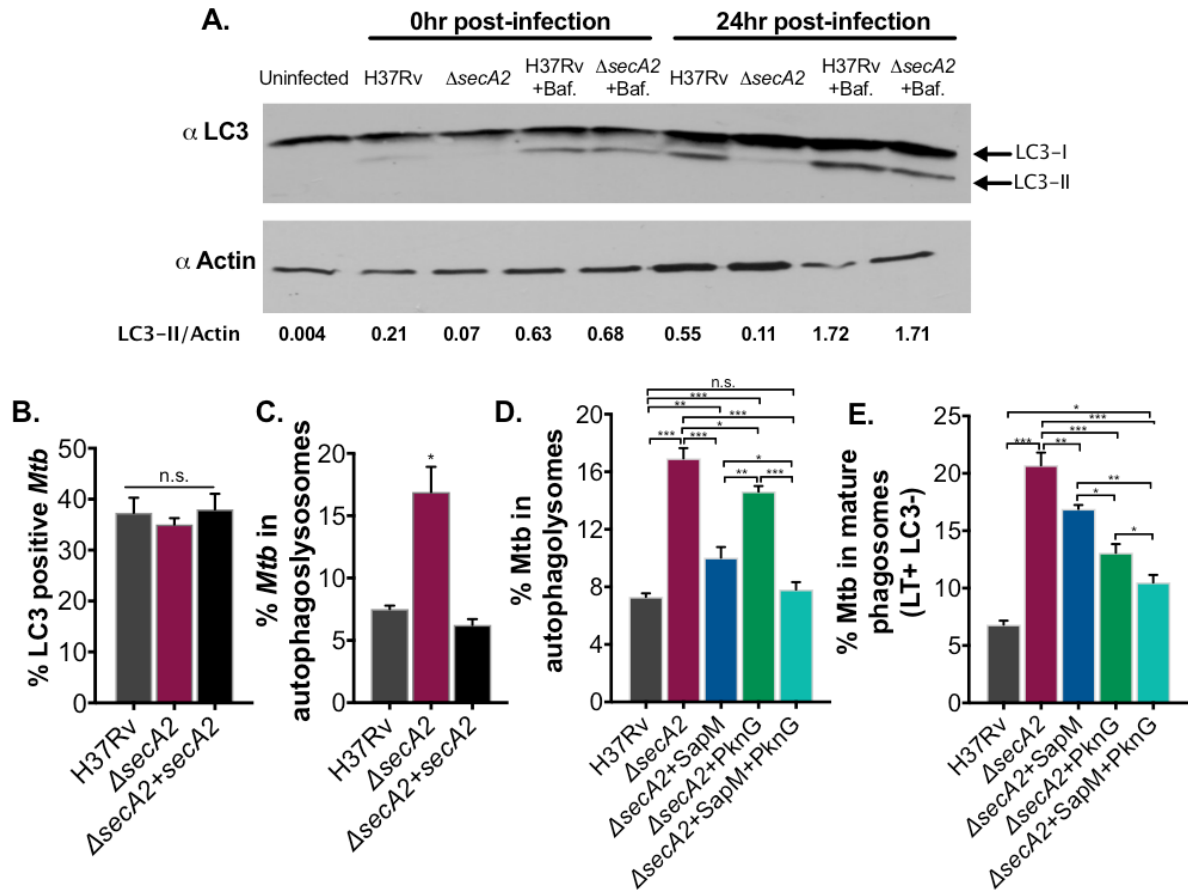


Figure 3.6: SecA2 is required for *M. tuberculosis* inhibition of autophagosome maturation.

(A) RAW 264.7 cells were infected with H37Rv and the *secA2* mutant at an MOI of 10 and lysed either immediately after infection or 24hrs post-infection. One set of infected cells was treated with 100nm Bafilomycin A1 (Baf). Cell lysates were examined for levels of LC3 or the loading control Actin. Densitometry was used to quantify LC3-II relative to Actin (ImageJ). Values are the average of duplicate experiments. Quadruplicate wells of RAW-Difluo mLC3 cells were infected with H37Rv, the *secA2* mutant and the complemented strain at an MOI of 1. (B) The percentage of LC3+ *M. tuberculosis* (RFP+) was assessed at 1hr post infection. (C) The percentage of *M. tuberculosis* that was localized in an autophagolysosome (RFP+GFP-) was assessed at 1hr post infection. Quadruplicate wells of RAW-Difluo mLC3 cells were infected with H37Rv and the *secA2* mutant SapM and/or PknG restoration strains at an MOI of 1. (D) The percentage of *M. tuberculosis* that was localized in an autophagolysosome (RFP+GFP-) was assessed at 1hr post infection. (E) The percentage of *M. tuberculosis* phagosomes that were acidified was determined using LysoTracker (LT) staining of quadruplicate wells of infected cells at 1hr post-infection. Mature phagosomes were identified by lack of LC3 (LC3-) and presence of LT staining (LT+RFP-). *p<0.05 **p<0.001 ***p<0.0001 ANOVA Holm-Sidak post Hoc test. Data represents at least two

independent experiments.

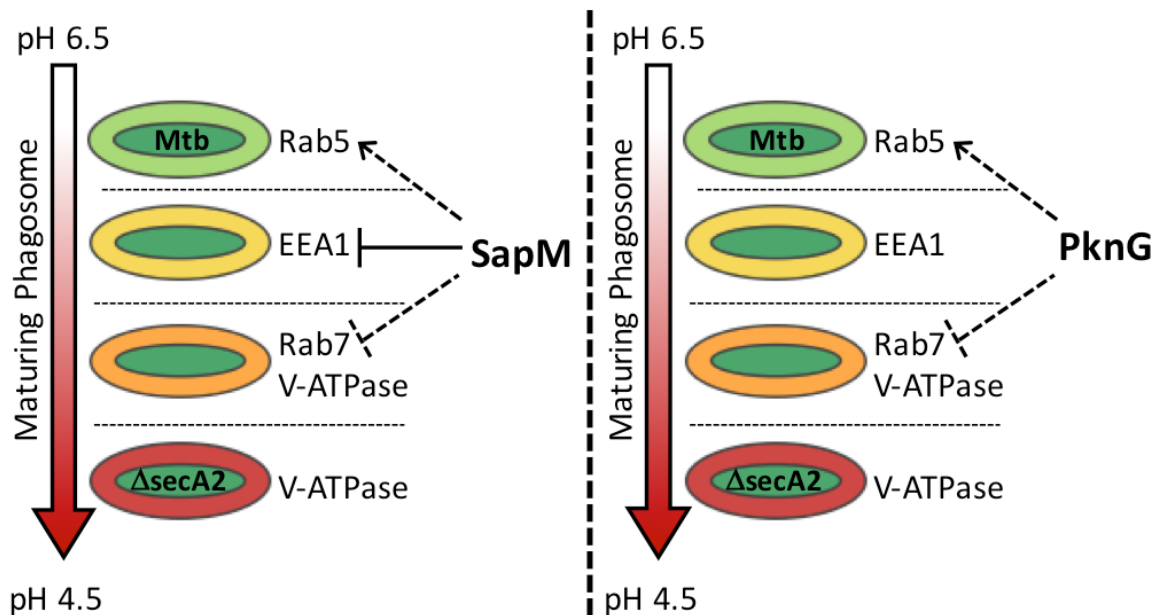


Figure 3.7: SapM and PknG play distinct functions in phagosome maturation arrest but other SecA2 effectors exist.

SecA2 export of SapM inhibits EEA1 recruitment to *M. tuberculosis* phagosomes and also contributes to the retention of Rab5 and the exclusion of Rab7 from *M. tuberculosis* phagosomes. In addition to SapM, SecA2 exports PknG which also contributes to the retention of Rab5 and exclusion of Rab7 from phagosomes. However, SecA2 must also export at least one additional effector of phagosome maturation arrest that inhibits Rab5-Rab7 exchange and prevents assembly of V-ATPase on phagosomes.

Table 3.1: Plasmids used in this study

Plasmid	Description	Reference
pSM15	Single-copy KanR Hsp60 driven <i>secA2</i>	[24]
pJTS130	Multi-copy KanR Hsp60 driven <i>sapM</i>	This study
pKZ136	Multi-copy KanR Hsp60 driven <i>sapM</i> ^{H204A}	This study
pKZ133	Multi-copy HygR Hsp60 <i>sapM</i>	This study
pKZ121	Single copy KanR Acetemide inducible <i>pknG</i> (used without induction) based on pMK4 (generous gift of Y. Av Gay)	This study and [33]
pMV206	Multi-copy HygR empty vector control	[44]
pMV261	Multi-copy KanR empty vector control	[44]
pMV306	Single-copy KanR empty vector control	[44]

Table 3.2: Strains used in this study

Strain Name	Strain background	Plasmids	Overexpression	Resistance Marker(s)
MBTB438	H37Rv	pMV261	N/A	Kanamycin
MBTB443	<i>secA2</i>	pMV261	N/A	Kanamycin
MBTB476 [23]	<i>secA2</i>	pSM15	<i>secA2</i>	Kanamycin
MBTB434	H37Rv	pJTS130	<i>sapM</i>	Kanamycin
MBTB435	<i>secA2</i>	pJTS130	<i>sapM</i>	Kanamycin
MBTB683	H37Rv	pKZ136	<i>sapM</i> ^{H204A}	Kanamycin
MBTB684	<i>secA2</i>	pKZ136	<i>sapM</i> ^{H204A}	Kanamycin
MBTB615	H37Rv	pKZ121	<i>pknG</i>	Kanamycin
MBTB616	<i>secA2</i>	pKZ121	<i>pknG</i>	Kanamycin
MBTB666	H37Rv	pKZ133	<i>sapM</i>	Kanamycin
		pMV306		Hygromycin
MBTM667	<i>secA2</i>	pKZ133	<i>sapM</i>	Kanamycin
		pMV306		Hygromycin
MBTB650	H37Rv	pKZ121	<i>pknG</i>	Kanamycin
		pMV206		Hygromycin
MBTB651	<i>secA2</i>	pKZ121	<i>pknG</i>	Kanamycin
		pMV206		Hygromycin
MBTB664	H37Rv	pMV206	N/A	Kanamycin
		pMV306		Hygromycin
MBTB665	<i>secA2</i>	pMV206	N/A	Kanamycin
		pMV306		Hygromycin
MBTB652	H37Rv	pKZ121,	<i>sapM</i>	Kanamycin
		pKZ133	<i>pknG</i>	Hygromycin
MBTB653	<i>secA2</i>	pKZ121,	<i>sapM</i>	Kanamycin
		pKZ133	<i>pknG</i>	Hygromycin
[42]	<i>pstA1::tn</i>	N/A	N/A	Kanamycin

REFERENCES

1. World Health Organization. Global tuberculosis report 2016. World Health Organization; 2016.
2. Awuh JA, Flo TH. Molecular basis of mycobacterial survival in macrophages. *Cell Mol Life Sci*. Springer International Publishing; 2017 May;74(9):1625–48.
3. Armstrong JA, Hart PD. Response of cultured macrophages to *Mycobacterium tuberculosis*, with observations on fusion of lysosomes with phagosomes. *The Journal of Experimental Medicine*. The Rockefeller University Press; 1971 Sep 1;134(3 Pt 1):713–40.
4. Sturgill-Koszycki S, Schlesinger PH, Chakraborty P, Haddix PL, Collins HL, Fok AK, et al. Lack of acidification in *Mycobacterium* phagosomes produced by exclusion of the vesicular proton-ATPase. *Science*. 1994 Feb 4;263(5147):678–81.
5. Via LE, Deretic D, Ulmer RJ, Hibler NS, Huber LA, Deretic V. Arrest of mycobacterial phagosome maturation is caused by a block in vesicle fusion between stages controlled by rab5 and rab7. *J Biol Chem*. 1997 May 16;272(20):13326–31.
6. Vergne I, Chua J, Deretic V. *Mycobacterium tuberculosis* phagosome maturation arrest: selective targeting of PI3P-dependent membrane trafficking. *Traffic*. 2003 Sep;4(9):600–6.
7. Vergne I, Chua J, Lee H-H, Lucas M, Belisle J, Deretic V. Mechanism of phagolysosome biogenesis block by viable *Mycobacterium tuberculosis*. *Proc Natl Acad Sci USA*. 2005 Mar 15;102(11):4033–8.
8. Hussain Bhat K, Mukhopadhyay S. Macrophage takeover and the host-bacilli interplay during tuberculosis. *Future Microbiol*. Future Medicine Ltd London, UK; 2015;10(5):853–72.
9. Rieck B, Degiacomi G, Zimmermann M, Cascioferro A, Boldrin F, Lazar-Adler NR, et al. PknG senses amino acid availability to control metabolism and virulence of *Mycobacterium tuberculosis*. Boshoff HI, editor. *PLoS Pathog*. 2017 May;13(5):e1006399.
10. Wolff KA, la Peña de AH, Nguyen HT, Pham TH, Amzel LM, Gabelli SB, et al. A redox regulatory system critical for mycobacterial survival in macrophages and biofilm development. Boshoff HI, editor. *PLoS Pathog*. 2015 Apr;11(4):e1004839.
11. Walburger A, Koul A, Ferrari G, Nguyen L, Prescianotto-Baschong C, Huygen K, et

- al. Protein kinase G from pathogenic mycobacteria promotes survival within macrophages. *Science*. 2004 Jun 18;304(5678):1800–4.
12. Mishra S, Jakkala K, Srinivasan R, Arumugam M, Ranjeri R, Gupta P, et al. NDK Interacts with FtsZ and Converts GDP to GTP to Trigger FtsZ Polymerisation--A Novel Role for NDK. Scheffers D-J, editor. *PLoS ONE*. 2015;10(12):e0143677.
 13. Sun J, Wang X, Lau A, Liao T-YA, Bucci C, Hmama Z. Mycobacterial nucleoside diphosphate kinase blocks phagosome maturation in murine RAW 264.7 macrophages. Tyagi AK, editor. *PLoS ONE*. Public Library of Science; 2010 Jan 19;5(1):e8769.
 14. Bach H, Papavinasasundaram KG, Wong D, Hmama Z, Av-Gay Y. Mycobacterium tuberculosis Virulence Is Mediated by PtpA Dephosphorylation of Human Vacuolar Protein Sorting 33B. *Cell Host & Microbe*. 2008 May;3(5):316–22.
 15. Wong D, Bach H, Sun J, Hmama Z, Av-Gay Y. Mycobacterium tuberculosis protein tyrosine phosphatase (PtpA) excludes host vacuolar-H⁺-ATPase to inhibit phagosome acidification. *Proc Natl Acad Sci USA*. 2011 Nov 29;108(48):19371–6.
 16. He C, Klionsky DJ. Regulation mechanisms and signaling pathways of autophagy. *Annu Rev Genet*. Annual Reviews; 2009;43(1):67–93.
 17. Chandra P, Ghanwat S, Matta SK, Yadav SS, Mehta M, Siddiqui Z, et al. Mycobacterium tuberculosis Inhibits RAB7 Recruitment to Selectively Modulate Autophagy Flux in Macrophages. *Sci Rep*. Nature Publishing Group; 2015 Nov 6;5(1):16320.
 18. Romagnoli A, Etna MP, Giacomini E, Pardini M, Remoli ME, Corazzari M, et al. ESX-1 dependent impairment of autophagic flux by Mycobacterium tuberculosis in human dendritic cells. *Autophagy*. Taylor & Francis; 2012 Sep;8(9):1357–70.
 19. Poirier V, Av-Gay Y. Mycobacterium tuberculosis modulators of the macrophage's cellular events. *Microbes Infect*. 2012 Nov;14(13):1211–9.
 20. Sullivan JT, Young EF, McCann JR, Braunstein M. The Mycobacterium tuberculosis SecA2 system subverts phagosome maturation to promote growth in macrophages. *Infect Immun*. 2012 Mar;80(3):996–1006.
 21. Braunstein M, Brown AM, Kurtz S, Jacobs WR. Two nonredundant SecA homologues function in mycobacteria. *J Bacteriol*. 2001 Dec;183(24):6979–90.
 22. Braunstein M, Espinosa BJ, Chan J, Belisle JT, Jacobs WR. SecA2 functions in the

secretion of superoxide dismutase A and in the virulence of *Mycobacterium tuberculosis*. *Mol Microbiol*. 2003 Apr;48(2):453–64.

23. Feltcher ME, Gunawardena HP, Zulauf KE, Malik S, Griffin JE, Sassetti CM, et al. Label-free Quantitative Proteomics Reveals a Role for the *Mycobacterium tuberculosis* SecA2 Pathway in Exporting Solute Binding Proteins and Mce Transporters to the Cell Wall. *Mol Cell Proteomics*. 2015 Jun;14(6):1501–16.
24. Miller BK, Zulauf KE, Braunstein M. The Sec Pathways and Exportomes of *Mycobacterium tuberculosis*. *Microbiol Spectr*. American Society of Microbiology; 2017 Apr;5(2).
25. Kurtz S, McKinnon KP, Runge MS, Ting JP-Y, Braunstein M. The SecA2 secretion factor of *Mycobacterium tuberculosis* promotes growth in macrophages and inhibits the host immune response. *Infect Immun*. 2006 Dec;74(12):6855–64.
26. Puri RV, Reddy PV, Tyagi AK. Secreted acid phosphatase (SapM) of *Mycobacterium tuberculosis* is indispensable for arresting phagosomal maturation and growth of the pathogen in guinea pig tissues. Neyrolles O, editor. *PLoS ONE*. Public Library of Science; 2013;8(7):e70514.
27. Saleh MT, Belisle JT. Secretion of an acid phosphatase (SapM) by *Mycobacterium tuberculosis* that is similar to eukaryotic acid phosphatases. *J Bacteriol*. American Society for Microbiology (ASM); 2000 Dec;182(23):6850–3.
28. Lawe DC, Chawla A, Merithew E, Dumas J, Carrington W, Fogarty K, et al. Sequential roles for phosphatidylinositol 3-phosphate and Rab5 in tethering and fusion of early endosomes via their interaction with EEA1. *J Biol Chem*. 2002 Mar 8;277(10):8611–7.
29. Jeschke A, Haas A. Deciphering the roles of phosphoinositide lipids in phagolysosome biogenesis. *Commun Integr Biol*. Taylor & Francis; 2016 May;9(3):e1174798.
30. Wong D, Chao JD, Av-Gay Y. *Mycobacterium tuberculosis*-secreted phosphatases: from pathogenesis to targets for TB drug development. *Trends Microbiol*. 2013 Feb;21(2):100–9.
31. Vieira OV, Bucci C, Harrison RE, Trimble WS, Lanzetti L, Gruenberg J, et al. Modulation of Rab5 and Rab7 recruitment to phagosomes by phosphatidylinositol 3-kinase. *Mol Cell Biol*. American Society for Microbiology (ASM); 2003 Apr;23(7):2501–14.
32. van der Woude AD, Stoop EJM, Stuess M, Wang S, Ummels R, van Stempvoort G, et

- al. Analysis of SecA2-dependent substrates in *Mycobacterium marinum* identifies protein kinase G (PknG) as a virulence effector. *Cell Microbiol.* 2014 Feb;16(2):280–95.
33. Cowley S, Ko M, Pick N, Chow R, Downing KJ, Gordhan BG, et al. The *Mycobacterium tuberculosis* protein serine/threonine kinase PknG is linked to cellular glutamate/glutamine levels and is important for growth in vivo. *Mol Microbiol.* Blackwell Science Ltd; 2004 Jun;52(6):1691–702.
 34. Kabeya Y, Mizushima N, Ueno T, Yamamoto A, Kirisako T, Noda T, et al. LC3, a mammalian homologue of yeast Apg8p, is localized in autophagosome membranes after processing. *EMBO J.* EMBO Press; 2000 Nov 1;19(21):5720–8.
 35. Deghmane A-E, Soualhine H, Soulhine H, Bach H, Sendide K, Itoh S, et al. Lipoamide dehydrogenase mediates retention of coronin-1 on BCG vacuoles, leading to arrest in phagosome maturation. *J Cell Sci.* 2007 Aug 15;120(Pt 16):2796–806.
 36. Gibbons HS, Wolschendorf F, Abshire M, Niederweis M, Braunstein M. Identification of two *Mycobacterium smegmatis* lipoproteins exported by a SecA2-dependent pathway. *J Bacteriol.* 2007 Jul;189(14):5090–100.
 37. Hu D, Wang W, Zhao R, Xu X, Xing Y, Ni S, et al. [SapM-induced fusion blocking of autophagosome-lysosome is depended on interaction with Rab7]. *Xi Bao Yu Fen Zi Mian Yi Xue Za Zhi.* 2016 Sep;32(9):1178–82.
 38. Poteryaev D, Datta S, Ackema K, Zerial M, Spang A. Identification of the switch in early-to-late endosome transition. *Cell.* 2010 Apr 30;141(3):497–508.
 39. Mueller P, Pieters J. Identification of mycobacterial GarA as a substrate of protein kinase G from *M. tuberculosis* using a KESTREL-based proteome wide approach. *J Microbiol Methods.* 2017 May;136:34–9.
 40. Portal-Celhay C, Tufariello JM, Srivastava S, Zahra A, Klevorn T, Grace PS, et al. *Mycobacterium tuberculosis* EsxH inhibits ESCRT-dependent CD4(+) T-cell activation. *Nat Microbiol.* Nature Publishing Group; 2016 Dec 5;2(2):16232.
 41. Gu S, Chen J, Dobos KM, Bradbury EM, Belisle JT, Chen X. Comprehensive proteomic profiling of the membrane constituents of a *Mycobacterium tuberculosis* strain. *Mol Cell Proteomics.* 2003 Dec;2(12):1284–96.
 42. Rengarajan J, Bloom BR, Rubin EJ. Genome-wide requirements for *Mycobacterium tuberculosis* adaptation and survival in macrophages. *Proc Natl Acad Sci USA.* 2005 Jun 7;102(23):8327–32.

43. Tischler AD, Leistikow RL, Kirksey MA, Voskuil MI, McKinney JD. Mycobacterium tuberculosis requires phosphate-responsive gene regulation to resist host immunity. *Infect Immun. American Society for Microbiology*; 2013 Jan;81(1):317–28.

CHAPTER 4¹

Genome-wide genetic interaction mapping: an approach for understanding the mechanism and functions of the SecA2 pathway of *Mycobacterium tuberculosis*

INTRODUCTION

Mycobacterium tuberculosis, the etiological agent of the disease tuberculosis, infects an estimated 10.4 million people each year and is responsible for approximately 1.8 million deaths (1). The ability of *M. tuberculosis* to replicate in host cells, specifically macrophages, is critical for the virulence of this important human pathogen (2). In order to replicate in macrophages, *M. tuberculosis* exports a variety of effector proteins either to the bacterial surface or into the host (3). These exported proteins have diverse roles in infection including inhibiting immune defense mechanisms and promoting nutrient uptake (3).

¹ Contributing authors: Laura Rank, Brittany Miller and Miriam Braunstein (Department of Microbiology and Immunology, School of Medicine, The University of North Carolina at Chapel Hill, Chapel Hill, NC) Michael DeJesus and Thomas Ioerger (Department of Computer Science and Engineering, Texas A&M University, College Station TX)

The SecA2 pathway is one system *M. tuberculosis* utilizes to export proteins to the extra-cytoplasmic environment (4). Unlike the SecA1 ATPase, which is responsible for the bulk of housekeeping export and is essential for bacterial viability, SecA2 is a non-essential specialized SecA ATPase required for exporting a relatively small subset of proteins (5,6). Although not essential for growth of *M. tuberculosis* in vitro, the SecA2 pathway is required for *M. tuberculosis* virulence in both murine and macrophage models of infection (6-8). The requirement for SecA2 during infection indicates that SecA2 and its exported proteins play important roles in *M. tuberculosis* pathogenesis.

SecA2 is required for growth in macrophages and past studies demonstrate roles of the SecA2 pathway in limiting many anti-microbial activities of macrophages (e.g. phagosome-lysosome fusion, attack by reactive oxygen and nitrogen intermediates (ROI, RNI), apoptosis, inflammatory responses and antigen presentation) (7,8). In addition to evading these host immune responses, the SecA2 pathway may also contribute to nutrient import during infection through its role exporting solute binding proteins of multiple ABC transporters as well as components of the Mce lipid transporters (9).

While the aforementioned activities that depend on SecA2 have been identified, their significance to pathogenesis has often been difficult to prove. When the defects in apoptosis, reactive oxygen and nitrogen intermediates, and pro-inflammatory cytokine signaling are corrected individually in the *secA2* mutant background, the *secA2* mutant remains attenuated indicating that none of these virulence properties of the SecA2 pathway are sufficient on their own to explain the role of SecA2 in pathogenesis (7,8). However, like other bacterial pathogens, *M. tuberculosis* has redundant virulence mechanisms, which may mask the significance of the individual SecA2 effects in these experiments (2). For example, there are

many *M. tuberculosis* proteins reported to limit apoptosis, cytokine production, and antigen presentation, not all of which depend on SecA2 (NuoG, PknE, EsxH, etc.) (2,10,11).

Similarly, there are multiple mechanisms that *M. tuberculosis* utilizes to protect against reactive oxygen and nitrogen intermediates (SseA, RenU, MefH, etc.) (2,12-14).

Additionally, it is likely that there are yet to be discovered functions of the SecA2 pathway. Currently there are 12 validated SecA2-exported proteins in *M. tuberculosis*, and approximately 20 additional proteins identified by proteomics as SecA2-dependent that remain to be validated (6,9). However, all approaches conducted so far to identify SecA2 exported proteins are limited by their use of *in vitro* growth conditions. As a result, any proteins exclusively exported during infection were overlooked. Additionally, technical limitations of previous approaches may have missed identifying proteins that are exported in low abundance (i.e. below the limit of detection). Thus, while examples of SecA2-exported proteins help predict functions of the SecA2 pathway in pathogenesis, it is likely that not all SecA2 substrates are known. Additionally, the majority of studies examining the role of the SecA2 export pathway in pathogenesis have been conducted in the macrophage model of *M. tuberculosis* infection (7,8). When compared to the complexity of a whole animal infection, the macrophage model is a simplified system that may be unable to reveal all functions of the SecA2 pathway in *M. tuberculosis* pathogenesis.

Along with gaps in our understanding of the significance of the SecA2 pathway and SecA2 exported proteins to pathogenesis, gaps remain in our understanding of the mechanism of SecA2 protein export. Current models predict that SecA2 works with the canonical SecYEG channel to export its substrates but it is not known if other proteins are required or contribute to SecA2 protein export (15). Recently, our lab identified a putative

chaperone, SatS, that aids in the export of some SecA2 dependent proteins (Miller and Braunstein, unpublished). As SatS does not affect all SecA2 exported proteins, additional unidentified chaperones or other components of the SecA2 export machinery may exist.

In order to fill in the gaps in our understanding of SecA2 protein export, we utilized genome-wide genetic interaction mapping to further elucidate the functions and mechanisms of the SecA2 export pathway of *M. tuberculosis*. Genetic interaction mapping identifies mutations that result in altered fitness when combined with a mutation in a gene of interest, in our case *secA2*. Genetic interaction mapping is a powerful approach for identifying other members of a pathway, as well as redundant pathways or factors. The approach we took was to use saturating transposon mutagenesis and compare survival during murine infection of individual transposon mutants in a wild-type *M. tuberculosis* H37Rv background to survival of the same mutants in the *secA2* mutant background. There are two forms of genetic interactions: aggravating and alleviating interactions. Aggravating interactions are defined by a mutation that has a significantly more severe (i.e. attenuating) phenotype in the *secA2* mutant background versus the H37Rv strain. Aggravating interactions will include mutations in genes in pathways that have redundant functions as SecA2 (and SecA2 exported effectors); these interactions could reveal functions of the SecA2 pathway in virulence. Alleviating interactions are defined by a mutation that has a significantly less attenuating effect in the *secA2* mutant background as compared to H37Rv. Alleviating interactions will include genes in the same pathway as SecA2 (e.g. components of the SecA2 export machinery) or in pathways in which SecA2 exported proteins act. Suppressors, mutations that reduce or compensate for the *secA2* virulence defects, will also be included among alleviating interactions. Using genetic interaction mapping, we identified 27 aggravating and

35 alleviating interactions with *secA2*. Our results expand our understanding of the SecA2 pathway by revealing roles for SecA2 in *M. tuberculosis* transporters, phosphate import, copper resistance, peptidoglycan synthesis, and lipid metabolism and homeostasis.

RESULTS AND DISCUSSION

We utilized genetic interaction mapping to further understand the mechanism and contribution of SecA2 to *M. tuberculosis* pathogenesis in a murine model of infection. We used transposon mutagenesis and high-throughput sequencing to define genetic interactions with *secA2* on a genome-wide scale. First, transposon (Tn) mutant libraries were generated in both *secA2* mutant and wild-type H37Rv strain backgrounds. Second, mice were infected with the Tn mutant libraries. Third, survival of individual transposon mutants following infection was assessed by analyzing recovered bacteria from infected mice using high-throughput sequencing. Fourth, statistical comparison of the transposon insertion profiles of the wild-type and *secA2* mutant libraries recovered from mice was used to identify alleviating and aggravating genetic interactions with *secA2*.

Identification of genetic interactions with *secA2*

Step1: To generate *secA2* mutant and H37Rv Tn mutant libraries, we utilized a temperature sensitive mycobacteriophage system to deliver a Mariner transposon which inserts at TA sites throughout the genome. Each library contained approximately 2×10^5 transposon mutants resulting in a Tn insertion density of approximately 60% for

H37Rv and 50% for the *secA2* mutant as determined by high-throughput sequencing. This insertional density is sufficient for subsequent genetic interaction studies (16).

Step 2: To identify the mutants with altered fitness in the *secA2* background, representing genetic interactions with *secA2 in vivo*, we first infected C57Bl6 mice with either the H37Rv or the *secA2* mutant Tn library via tail vein injection containing $2-3 \times 10^6$ cfu (colony forming units). As the *secA2* mutant is attenuated by approximately 10-fold during the growth in vivo phase of infection in mice, fewer cfu are recovered from each mouse infected with the *secA2* mutant Tn library compared to the H37Rv Tn library (6). This disparity in cfu burden results in an unequal total Tn insertion density in the recovered bacteria from each strain, which complicates subsequent statistical analysis. Therefore, to account for the virulence defect of the *secA2* mutant and start the analysis with an equal number of recovered cfu, we infected 7 times more mice with the *secA2* mutant Tn library (49 mice) versus the H37Rv Tn library (7). To confirm mice were successfully infected with both libraries, two mice infected with each library were sacrificed at Day 1 post infection and bacterial burden of lungs, liver and spleens was determined by plating for cfu (Figure 4.1 B). Mice infected with both libraries had approximately the same bacterial burden at Day 1 post infection and had the correct proportion of the inoculum seeding each organ (5% lung, 20% spleen, 75% liver) (17).

Step 3: We let the infection progress for 18 days. This time point allowed us to focus on the early replication stage rather than the persistence stage of infection. *M. tuberculosis* replicates *in vivo* until an effective T-cell (TH1) cell mediated immune response is established at 21 days post-infection, after which time *M. tuberculosis* persists in the host at the same level of cfu throughout the remainder of the infection (18). At 18 days post-

infection, spleens were removed from infected mice and plated for viable cfu. As mentioned above spleens and not lungs, the natural site of *M. tuberculosis* infection, were used as there is better seeding of the spleen compared to the lung (2×10^5 vs 4×10^4 cfu per organ). Better bacterial seeding means more individual transposon mutants will be analyzed which minimizes bottleneck effects that would result in less robust data for statistical analysis. As expected, from past murine infections with the *M. tuberculosis secA2* mutant, at 18 days post infection significantly fewer cfu were recovered from individual mice infected with the *secA2* Tn library compared to mice infected with the H37Rv Tn library reflecting the virulence defect of the *secA2* mutant (Figure 4.1C) (6). However as more mice were infected with the *secA2* Tn library, total cfu recovered from all infected mice were equivalent between the two strains (approximately 2×10^7 cfu).

After 3 weeks of growth, the cfu recovered from spleen homogenates of each library were scraped from the agar plates into 3 independent pools, generating triplicate samples for sequencing (Figure 4.1A). Genomic DNA was isolated, sheared and an adaptor for sequencing was ligated to the DNA fragments. Then, using primers that correspond to the transposon and the ligated adaptor sequence, the transposon insertion sites were amplified by PCR. High-throughput sequencing was then used to identify and quantify Tn insertion sites. The representation of individual Tn mutants in mice at 18 days was quantified by sequencing read count using Transit (77). The Tn insertion density recovered from mice for the H37Rv library was 39% and 46% for the *secA2* mutant which is acceptable for genetic interaction analysis (14,19-22).

Step 4: Data were normalized by total read-count for each replicate sample and a beta-geometric correction was performed to adjust for any disparity between replicate

samples and strains (23). Individual mutants with altered fitness representing genetic interactions with *secA2* were identified in the triplicate samples using a permutation test and p-values were adjusted for multiple-comparisons using Benjamin-Hochberg (16,77). A genetic interaction with *secA2* was defined as a 2-fold or greater difference in survival when compared to the same mutation in the H37Rv background (\log_2 read-count ratio [*secA2*/H37Rv] of ± 1) and an adjusted p-value < 0.05 (Figure 4.2A). Using this approach, we identified a total of 62 genetic interactions with *secA2* (Table 4.1). Mutations that resulted in more severe attenuation in the *secA2* mutant background than the H37Rv background were classified as aggravating interactions (\log_2 read-count ratio (*secA2*/H37Rv) < 1 indicating less cfu recovered in the *secA2* mutant background than H37Rv background) (Figure 4.1B). Whereas mutations that resulted in more severe attenuation in the H37Rv background than the *secA2* mutant background were classified as alleviating interactions (\log_2 read-count ratio (*secA2*/H37Rv) > 1 indicating more cfu was recovered in the *secA2* mutant background than H37Rv background) (Figure 4.1B). We identified a total of 27 aggravating and 35 alleviating interactions with *secA2* (Table 4.1). This number of genetic interactions ($\sim 1.5\%$ of the genome) is similar to the number identified in other genome wide genetic interaction screens in *M. tuberculosis* and other bacteria (Figure 4.2B) (14,19-22). Additionally, the fold difference of the genetic interactions (\log_2 read-count ratio (*secA2*/H37Rv)) identified in this study is also comparable to genetic interactions identified in other studies (14,19-22).

Genetic interactions with *secA2* are enriched for genes encoding exported proteins

Both alleviating and aggravating interaction categories are enriched for exported proteins. Compared to the 25% of the *M. tuberculosis* genome that is predicted to be exported, 43% of alleviating and 48% of aggravating genetic interactions are predicted to encode for exported proteins (Figure 4.2 E-F) (24). As SecA2 functions to export proteins, this result was not surprising and is consistent with the application of this approach to identify genetic interactions with an export system.

One of the largest functional categories representing alleviating interactions corresponds to genes that function in *M. tuberculosis* cell wall and cell processes (29%) (Figure 4.2C). This functional category also represents over half of all identified aggravating interactions with *secA2* (52%) (Figure 4.2 D). As only 19% of the *M. tuberculosis* genome falls into the cell wall and cell processes functional category, this finding suggests SecA2 contributes to formation/maintenance of the mycobacterial cell wall (25). The large number of genetic interactions involving the mycobacterial cell wall could be due to the fact that several proteins in *M. tuberculosis* depend upon the SecA2 export pathway for export to the cell wall (9). This result suggests a role for SecA2 in *M. tuberculosis* cell wall maintenance that was not appreciated before.

Genetic interactions with *secA2* identify putative components of SecA2 export machinery

As SecA2 export is abolished in the *secA2* mutant, mutations in genes corresponding to other components of the SecA2 export pathway should fall in the category of alleviating

interactions as their absence will not significantly attenuate the *secA2* mutant further. One of the most significant alleviating interactions with *secA2* was *satS*. Mutations in *satS* is 8.5-fold less attenuated in the *secA2* mutant background when compared to the H37Rv background (adjusted p-value <0.0001). The identification of this alleviating interaction is very exciting because SatS contributes to the export of a subset of SecA2 substrates (Miller and Braunstein unpublished). In fact, unpublished data indicates that SatS is a chaperone for the SecA2 export system. Thus, the identification of *satS* as an alleviating interaction validates the genetic interaction approach as a method to identify components of the SecA2 export machinery.

As SatS appears to function with only a subset of SecA2 exported proteins, additional SecA2 chaperones may exist for other SecA2 substrates. The hypothetical protein Rv1691 is a candidate for such a chaperone. A mutation in *rv1691* alleviates the *secA2* mutant to a similar degree as a *satS* mutation, which is consistent with Rv1691 being in the same pathway as SecA2. An *rv1691* mutant is 8.8-fold less attenuated in *secA2* mutant background compared to H37Rv (adjusted p-value 0.01). Although Rv1691 is not predicted to be essential for *M. tuberculosis* virulence by TnSeq, in those studies *rv1691* mutants were at very low abundance therefore a requirement for Rv1691 in vivo may have been missed (26). Rv1691 contains tetratricopeptide repeat (TPR) domains. TPR domains consist of a series of 34 amino acid repeat sequences and are classically protein binding domains (27,28). Interestingly TPR domains are common in chaperones of type III secretion systems, therefore Rv1691 may be an unidentified chaperone for the SecA2 export pathway (29). An alternative possibility is that a *rv1691* mutation may act as a suppressor and relieve the *secA2*

mutant virulence phenotype and further study is required to understand the interaction between Rv1691 and SecA2.

The most extreme interaction with *secA2* is the alleviating interaction with *hab* (*rv3078*). A *hab* mutant in the *secA2* background is ~100-fold less attenuated than a mutant in the H37Rv background (adjusted p-value <0.0001). Although Hab is not predicted to have a role in virulence by TnSeq, expression of *hab* is induced in vivo (26,30). Hab is predicted to function in nitrobenzene metabolism and detoxify hydroxylamino products (31). Intriguingly, Hab possesses a predicted wnt binding domain which targets proteins for secretion in mammalian cells suggesting Hab may assist in protein export via the SecA2 pathway (32). The identification of *hab* as an alleviating interaction with *secA2* suggests that Hab may function in the same pathway as SecA2 and thus may represent a novel component of the SecA2 export machinery. As like with *rv1691*, an alternative possibility is that a *hab* mutation may act as a suppressor and relieve the *secA2* mutant virulence phenotype and further study is required to distinguish between these possibilities.

Genetic interactions with *secA2* identify SecA2 substrates

Along with components of the SecA2 export machinery, proteins exported by SecA2 can also be alleviating interactions; as they depend upon SecA2 for export, these proteins are in the same pathway as SecA2. One significant alleviating interaction with *secA2* is *sapM*. A *sapM* mutant is 2.4-fold less attenuated in the *secA2* mutant background than in the H37Rv background (adjusted p-value 0.02). SapM is a phosphatase that is exported by the SecA2 pathway (Zulauf and Braunstein unpublished). SecA2 export of SapM contributes to both

phagosome maturation arrest by *M. tuberculosis* and growth of *M. tuberculosis* in macrophages (Zulauf and Braunstein unpublished). Specifically, SapM dephosphorylates PI3P on phagosomal membranes, which prevents recruitment of PI3P binding proteins (EEA1) and subsequent phagosome maturation steps (33). As SapM export is already significantly reduced in the *secA2* mutant, a Tn mutation in *sapM* would have less of an effect in the *secA2* mutant background compared to the effect of this mutation in the H37Rv strain background that is competent for SapM export. The identification of SapM validates the use of genetic interaction mapping to reveal SecA2 exported effectors that contribute to virulence of *M. tuberculosis*.

There are also four alleviating interactions with *secA2* that map to putative SecA2 exported proteins (Rv3803, Rv0875c, LppS, and Rv0265c). These four proteins were identified by quantitative proteomics as reduced in the cell wall of the *secA2* mutant but have yet to be validated as SecA2 substrates by Immunoblot; however, their identification as alleviating interactions strengthens the likelihood that these proteins depend on SecA2 for export and indicates that these proteins may have functions in virulence therefore these proteins warrant further study (9).

The list of alleviating genetic interactions also has the potential to contain SecA2-dependent effectors that have not previously been discovered. To identify potential SecA2 substrates, we searched for genes interacting with *secA2* that encode for proteins with a predicted export signal. We loosened the statistical requirements to a p-value <0.05 for this analysis as residual export of SecA2 substrates occurs in the absence of *secA2* which may affect their identification in this study (9,36). On the list of alleviating interactions, there are 27 genes encoding proteins with a predicted Sec or Tat export signal sequence (34,35).

SecA2 has been shown to export proteins containing either signal sequence (Table 4.2) (9,36). Further studies are warranted to determine if these are SecA2-exported proteins. As SecA2 is also associated with the export of select proteins lacking conventional export signals (i.e. SodA and PknG) in *M. tuberculosis* and other bacterial species, alleviating interactions in proteins lacking a classical signal sequence could also represent new SecA2 substrates (6,9).

Genetic interactions with *secA2* highlight functions of the SecA2 export pathway

When multiple genetic interactions have related functions, it strengthens the argument for the SecA2 pathway functioning in that process. Therefore, we mined the data set and grouped significant genetic interactions into clusters corresponding to similar gene functions. In order to appreciate clusters associated with the SecA2 pathway, we loosened the statistical requirements and included interactions with an adjusted p-value <0.1 in this analysis. Over 50 of the identified aggravating and alleviating interactions can be grouped into 8 main clusters (Figure 4.3). While not always the case, we often found aggravating and alleviating interactions in the same cluster. While alleviating interactions can represent genes in the same pathways as SecA2 or SecA2 exported proteins, alleviating interactions can also reflect suppressor mutations that reduce or compensate for the *secA2* virulence defects. Aggravating interactions are in a parallel or redundant pathway as *secA2*. Identification of both alleviating and aggravating interactions in the same cluster indicates a significant role for the SecA2 pathway in that process as it supports the existence of both a function for SecA2 as well as the existence of redundant virulence mechanisms.

Phagosome maturation arrest

A cluster of five alleviating interactions with connections to phagosome maturation arrest were identified, including SapM, the effector of phagosome maturation arrest discussed above (33,37-40). Given the established role of SecA2 in phagosome maturation arrest, the identification of alleviating mutations in genes linked to phagosome maturation arrest help validate the genetic interaction approach. As for SapM, the other alleviating interactions could represent phagosome maturation arrest effectors that are exported by SecA2. However, unlike SapM, these other proteins lack recognizable export signals. Another possibility is that these mutations act as suppressors and ameliorate the virulence defect of the *secA2* mutant. For instance, the alleviating interactor *rv2506* encodes a predicted transcriptional repressor (37,41). Thus, transposon insertions in *rv2506* could upregulate proteins involved in phagosome maturation arrest that compensate for the *secA2* mutant defect in phagosome maturation arrest. Further supporting this hypothesis is the identification of one gene *rv0575*, that is predicted to be repressed by Rv2506 as an aggravating interaction with *secA2*. However the interaction between *rv0576* and *secA2* does not meet the statistical cutoffs used in this study (41). A mutation in *rv0576* attenuated the *secA2* mutant 2.8-fold more than H37Rv (adjusted p-value 0.2). Unfortunately, nothing is known about the function of Rv0576.

Cholesterol and Lipid Transport/ Homeostasis

A cluster of 15 genetic interactions suggests roles for SecA2 in host cholesterol or *M. tuberculosis* lipid transport/homeostasis. Cholesterol is utilized by *M. tuberculosis* during infection and five genetic interactions with the *secA2* mutation are associated with

cholesterol metabolism (20). Both aggravating and alleviating interactions in genes associated with cholesterol utilization were identified, which supports an important function of the SecA2 pathway in cholesterol utilization by *M. tuberculosis*. Aggravating Tn insertions mapped to the oxygenase *kshA* and glutamate dehydrogenase *gdh* genes while alleviating insertions mapped to cholesterol oxidase *cyp142*, enoyl-coA hydratase *echA19*, and acyl-coA dehydrogenase *fadE25* genes. All five of these cholesterol metabolism genes are predicted to be required for growth of *M. tuberculosis* on cholesterol by TnSeq analysis (20). All the interacting proteins in this cholesterol metabolism cluster are predicted to function in the bacterial cytoplasm and are, therefore, unlikely to be SecA2 exported effectors. However, their identification as genetic interactions support previous findings concerning functions of SecA2 export in cholesterol utilization.

One class of SecA2 exported proteins are Mce transporters. Mce transporters are multi-component lipid transporters of which *M. tuberculosis* has four. Prior mass spectrometry studies indicate that the Mce4 cholesterol importer depends upon the SecA2 pathway for export (9). Although no *mce4* genes were identified as genetic interactors with *secA2* this may reflect the fact that Mce4 is important for the later persistence stage of infection in the murine model as opposed to the earlier growth in vivo phase of infection (18 days) that was the focus of our search for genetic interactions (42,43). The identification of genetic interactions related to cholesterol during the in vivo growth stage of infection may suggest that SecA2 has a second connection to cholesterol in addition to Mce4. Further research is required to fully understand the connection(s) between SecA2 and cholesterol.

To directly examine the importance of the SecA2 pathway to cholesterol use by *M. tuberculosis*, we examined growth of the *secA2* mutant in media containing cholesterol as the

sole carbon source. The *secA2* mutant was significantly attenuated for growth on cholesterol when compared to H37Rv and this phenotype could be complemented (Figure 4.4). An *mce4* mutant which is known to be required for growth on cholesterol was included as a control. Importantly the *secA2* mutant grew comparably to H37Rv in media containing glycerol (43). In summary, this result indicates SecA2 is required for optimal growth on cholesterol and validates the findings of the genetic interaction study.

In addition to the five cholesterol related genes, our study revealed 10 genetic interactions involving genes with roles in synthesis or transport of *M. tuberculosis* cell envelope lipids. An alleviating interaction was identified in *rv1506c*, which is required for synthesis of 2,3-diacyltrehaloses (DAT) lipids in the cell envelope and is also in the cluster of genes with functions in *M. tuberculosis* phagosome maturation arrest (39). Additionally, an alleviating interaction was identified in *ppm1*, which modifies lipoarabinomannan (LAM), a lipid in the mycobacterial cell envelope with functions in pathogenesis that include anti-inflammatory, anti-apoptotic, and anti-phagosome maturation properties (44,45). As SecA2 has been shown to contribute to all of the aforementioned virulence mechanisms, it is possible that Rv1506c and Ppm1 act in the same pathways as SecA2 exported effectors. An additional genetic interaction with *secA2* in this cluster is the aggravating interaction with *drrB* which encodes a component of the ABC transporter responsible for exporting phthiocerol dimycocerosates (PDIM) (46). PDIM is a cell envelope lipid that contributes to many virulence properties including macrophage invasion, masking of immune stimulating pathogen associated molecular patterns (PAMPS), resistance to reactive nitrogen intermediates (RNI), phagosomal escape and induction of necrosis (45,47). As the SecA2 pathway limits production of RNI produced by macrophages and suppresses the host immune

response to *M. tuberculosis*, PDIM and SecA2 exported effectors likely function in parallel virulence pathways (7). In summary, our studies suggest a role for the SecA2 pathway in *M. tuberculosis* utilization of cholesterol as well as lipid transport and homeostasis.

Peptidoglycan

Another cluster of genetic interactions with *secA2* contains genes with roles in peptidoglycan synthesis. We identified alleviating interactions in a gene encoding an amidase Rv3717. Rv3717 binds peptidoglycan fragments and is predicted to function in peptidoglycan recycling (48). Rv3717 contains a predicted Sec signal sequence and may be an unidentified SecA2 substrate (35). Further, Rv3717 is previously predicted to have a role in *M. tuberculosis* virulence based on TraSH and TnSeq studies (26,49). An additional alleviating interaction in this category is *glnA2*, which encodes a protein that catalyzes synthesis of D-glutamine and isoglutamine which are important precursors for peptidoglycan synthesis (50). As GlnA2 is not predicted to be exported, GlnA2 is unlikely to be a SecA2 substrate but instead is in the same pathway as SecA2 dependent effectors. Further supporting a function of SecA2 in mycobacterial peptidoglycan homeostasis are the aggravating interactions with *ripC* and *rv1566c*, which encode for additional peptidoglycan amidases (51,52). The fact that amidases involved in peptidoglycan synthesis were identified as both the alleviating and aggravating interaction categories could indicate that SecA2 exports the alleviating amidase Rv3717 and the other two amidases possess redundant functions with Rv3717. Interestingly, although proteomics studies have not identified any mycobacterial amidases as exported by SecA2, amidases are a category of SecA2 dependent proteins in *Listeria monocytogenes* (53).

Together, these genetic interactions suggest a function of SecA2 in peptidoglycan synthesis or homeostasis. As peptidoglycan defects can lead to lysozyme sensitivity, we assessed the sensitivity of the *secA2* mutant to lysozyme (54). The *secA2* mutant was significantly more sensitive than H37Rv to lysozyme, which is consistent with the *secA2* mutant having a defect in peptidoglycan synthesis, assembly, or homeostasis. As a parallel approach, we examined the sensitivity of the *secA2* mutant to carbenicillin, a B-lactam antibiotic that inhibits peptidoglycan synthesis. The *secA2* mutant had a significantly reduced MIC₉₅ to carbenicillin when compared to H37Rv. The increased sensitivity of the *secA2* mutant to carbenicillin was not due to reduced B-lactamase export in this strain (data not show). This increased sensitivity to carbenicillin of the *secA2* mutant further supports the role of SecA2 in peptidoglycan synthesis and validates the approach of genetic interaction mapping to identify previously unknown functions of the SecA2 pathway in *M. tuberculosis*.

Transporters

SecA2 was previously shown to play a prominent role in the export of solute binding proteins (9). Solute binding proteins work with ABC transporters to import various substrates into the bacterial cell. Of the 62 genetic interactions identified for *secA2*, nine correspond to components of ABC transporters. However, along with interactions involving ABC transporter, eight additional interactions mapped to other types of transporters. The ion transporters *chaA*, which encodes a predicted Ca²⁺ H⁺ antiporter, and *mgtE*, which encodes a Mg²⁺ transporter, are alleviating interactions with *secA2*. Additionally, two genes encoding integral membrane components of an anion transporter, *rv3679* and *rv3680*, are aggravating interactions with *secA2*. The interaction between ion transporters and *secA2* suggests that SecA2 may be important for maintaining appropriate membrane potential in the

mycobacterial cell (55). Additionally, genetic interactions with *secA2* were also identified in components of a predicted efflux pumps (Rv0876 and Rv1458c). In summary, this genetic interaction study revealed a broad role for the SecA2 export pathway in mycobacteria transporters that goes beyond ABC transporters.

Although genetic interactions were identified in many types of transporters that import/export a wide variety of substrates, 6 of the 17 transporter interactions involved phosphate uptake. *M. tuberculosis* has two ABC transporters that import phosphate: the PstA2 system comprised of PstA2, PstC1, and PhoS1(also called PstS1) and the PstA1 system comprised of PstA1, PstC2 and PstS3 (Figure 4.6) (56,57). Interestingly, components of the PstA2 system were identified as alleviating interactions while components of the PstA1 system were identified as aggravating interactions. Because PhoS1, the solute binding protein of the PstA2 transporter, is exported by the SecA2 pathway, it is not surprising to discover mutations in genes encoding other components of the PstA2 transporter as alleviating interactions with the *secA2* mutation (9). Due to the PhoS1 export defect of the *secA2* mutant, the PstA2 system is presumably nonfunctional in the *secA2* mutant and additional mutations in this transporter are, therefore, expected to be alleviating interactions. On the other hand, our discovery of genes encoding components of the PstA1 system as being aggravating interactions suggests the PstA1 transporter is in a parallel redundant pathway of phosphate acquisition to the SecA2-dependent PstA2 pathway. If one phosphate import system (PstA2) is defective in the *secA2* mutant, the other system (PstA1) may become more important to bacterial fitness. These interactions highlight the important contribution of the SecA2 export pathway to phosphate acquisition by *M. tuberculosis* during host infection.

We additionally identified ATPase components of the phosphate transporters, *pstB* and *phoT*, as genetic interactors with *secA2*. While *pstB* is a significant alleviating interaction, *phoT* is a significant aggravating interaction with *secA2*. This result is intriguing as it is not currently known which ATPase works with each phosphate transporter or, alternatively, if the ATPases are promiscuous and can function with either transporter (57). As components of the PstA2 system are alleviating while components of the PstA1 system are aggravating, our data suggests that the alleviating *pstB* functions with the PstA2 transporter while the aggravating *phoT* functions with the PstA1 transporter. Additional experiments are required to validate this finding.

Further examination of our genetic interaction data revealed signs of altered gene regulation in the *secA2* mutant that is indicative of a defect in phosphate import. Mutations in *regX3* and *esxA5* were identified as alleviating interactions with *secA2*. Under low phosphate conditions the *regX3* regulon is induced, which includes genes involved in Esx5 secretion and components of the SecA2 independent PstA1 phosphate transporter (58-60). RegX3 via Esx5 induction induces cell membrane permeability (58). Increased membrane permeability may be detrimental to the survival of the *secA2* mutant *in vivo* as the *secA2* mutant encounters several stressors in the host (7). The *secA2* mutant may also have an altered cell wall that increases sensitivity to membrane permeability. Thus, the elimination of the RegX3-Esx5 signaling cascade likely restores the integrity of the *M. tuberculosis* cell membrane and increases resistance to anti-microbial host responses. It is also possible that the RegX3-Esx5 signaling cascade is more highly induced in the *secA2* mutant than H37Rv. As PhoS1 is dependent on SecA2 for export there is likely less phosphate import in the *secA2* mutant (9). As low phosphate activates the RegX3-Esx5 pathway, this would lead to

increased expression of RegX3-Esx5 in the *secA2* mutant and subsequently increased membrane permeability which may be detrimental in vivo (58). However, this model remains to be tested.

Stress Response

The *secA2* mutant induces a pro-inflammatory response in the host and the *secA2* mutant is trafficked to an acidic degradative phagolysosome (7,8). Therefore, the *secA2* mutant encounters many stresses during infection including acid stress, hypoxia, and reactive oxygen and nitrogen species. Even absent exposure to these host factors there is indication that the *secA2* mutant is innately under stress or could be more sensitive to stresses. The DosR regulon is induced more quickly and to a higher degree in the *secA2* mutant when compared to H37Rv (9). Although first identified as a coordinated response to hypoxia, the DosR regulon is now appreciated as being induced by a number of stresses including nitric oxide stress (61,62). An additional reason the *secA2* mutant may be more sensitive to stress is the altered cell wall of the mutant due to differences in peptidoglycan and lipid content (discussed above).

Our genetic interaction data further highlights the stress the *secA2* mutant experiences during infection, as 8 stress related genes represent another cluster of genetic interactions with *secA2*. Three of the alleviating interactions in this category are repressors of stress response pathways (BlaR, HspR, OprA) (63-65). These alleviating interactions may reflect suppression of *secA2* mutant stress-related phenotypes. In the absence of these repressors, the stress response pathways are constitutively active, boosting the resistance of the *secA2* mutant to stressors encountered in the host. One such regulator, OprA, is involved in

resistance to osmotic stress indicating that the *secA2* mutant may experience osmotic stress in the host (63). The osmotic stress may be due to function of the SecA2 pathway in exporting ABC transporter components as altered solute import/export may affect the osmotic state of the bacterial cell. A further indication that the *secA2* mutant undergoes stress in the host is the identification of *relA* as an aggravating interaction. RelA mediates the stringent response and downregulates translation in response to stress (66,67). Thus, RelA may be needed to protect the *secA2* mutant from stress encountered in the host and loss of RelA worsens the *secA2* mutant phenotype.

Copper

A cluster of genetic interactions related to copper revealed a previously unknown role for the SecA2 pathway in resistance to high levels of copper. Copper toxicity is one anti-microbial defense mechanism of macrophages. *M. tuberculosis* has multiple mechanisms to detoxify copper (68). Many of these mechanisms are regulated by the transcriptional repressor RicR (69,70). Mutations in the *ricR* gene are alleviating interactions with *secA2* suggesting that induction of this copper resistance regulon suppresses the virulence defect of the *secA2* mutant *in vivo*. This result could indicate either that the SecA2 pathway exports effectors that block or detoxify the copper influx into phagosomes such that the *secA2* mutant resides in a higher copper environment than H37Rv or that the *secA2* mutant is more sensitive to high levels of copper. Supporting the possibility of the *secA2* mutant being localized to a higher-copper environment in macrophages is the identification of *rv2199c* as an alleviating interaction. Transcription of *rv2199c* is suppressed by high copper levels, therefore *rv2199c* may be downregulated by high copper levels encountered by the *secA2* mutant and loss of *rv2199c* would not attenuate a *secA2* mutant further (69). Although not

meeting statistical cutoffs used in the cluster analysis, mutations in the multicopper oxidase *mmcO* are also alleviating interactions with *secA2* (*mmcO* mutants are 2.3 fold less attenuated in the *secA2* background compared to H37Rv, p-value 0.05). MmcO is exported to the *M. tuberculosis* cell envelope making it a putative SecA2 substrate (71). MmcO is required for *M. tuberculosis* copper resistance and functions by oxidizing and detoxifying copper (71). If the *secA2* mutant has a defect in MmcO export, then it would be expected that the *secA2* mutant would be in a high copper environment which would explain the genetic interactions with both *ricR* and *rv2199c*. However, the SecA2 dependency of MmcO remains to be tested directly. Cumulatively, our data suggest a previously unknown function for the SecA2 pathway in combatting the anti-microbial copper response of the host.

Esx Protein Export

An unexpected discovery was a cluster of interactions between Esx systems and SecA2. Although we identified four genetic interactions associated with specialized Esx export pathways, the majority of Esx secretion system components and exported effectors did not interact with *secA2*. The genetic interactions between these two classes of specialized export systems suggest that these systems may have similar functions in virulence and the identification of EspK which is involved in phagosome maturation arrest supports this (39). As Esx systems are composed of multiple subunits, the identification of so few Esx components does not support Esx and SecA2 being truly interacting pathways (72). Further study is required to investigate the potential connection between these export systems.

SUMMARY

Using genetic interaction mapping we identified a total of 62 genetic interactions with *secA2* composed of 27 alleviating and 35 aggravating interactions. Alleviating interactions represent genes in the same pathway as SecA2 and could represent SecA2 substrates or components of the SecA2 export machinery. Alleviating interactions could also reflect mutations that suppress *secA2* mutant virulence phenotypes. On the other hand, aggravating interactions represent genes in a parallel pathway as *secA2* and have the potential to reveal new functions of the SecA2 pathway in pathogenesis of *M. tuberculosis*.

As not all SecA2 exported proteins have been identified to date, genetic interaction mapping provides an alternative approach for identification of SecA2 substrates. Genetic interaction mapping takes into account the importance of the function of the protein in pathogenesis and it thereby provides a powerful alternative for identifying SecA2 exported effectors that contribute to virulence of *M. tuberculosis* (possibilities listed in Table 4.2). The identification of *satS* and *sapM* as alleviating interactions provides important validation of this approach to identify both components of SecA2 export machinery and SecA2 exported effectors. However, genetic interaction mapping is a predictive tool; thus, all findings will need to be validated. Nonetheless, our results lead to several new hypotheses for how SecA2 contributes to the pathogenesis of *M. tuberculosis* (i.e. peptidoglycan synthesis, phosphate import, resistance to copper in the host).

Although many important discoveries of *M. tuberculosis* pathogenesis and SecA2 export have been identified and studied using the macrophage model, *M. tuberculosis* infection in a whole animal model is much more complex. Multiple immune cell types, in

addition to macrophages, affect the progression of *M. tuberculosis* disease (73). This approach not only revealed previously unknown functions for SecA2 export in *M. tuberculosis* pathogenesis, the study also validated prior research identifying the role SecA2 in phagosome maturation arrest as a vital virulence function of the export system.

As the focus of this genetic interaction study was mapping interactions with *secA2* *in vivo*, this study does not take into account *in vitro* phenotypes. Some of the Tn mutants identified as genetic interactors *in vivo* may additionally affect the fitness of the *secA2* mutant in *in vitro* growth conditions. For example, the role of the SecA2 pathway in peptidoglycan synthesis may represent a more general function of SecA2 export and not be specific to the host environment. As the Tn libraries generated to infect mice were propagated under *in vitro* conditions, Tn insertions in these samples can be similarly evaluated to map *in vitro* genetic interactions with *secA2*.

In total, we identified roles for the SecA2 pathway in *M. tuberculosis* transporter function, cholesterol and lipid metabolism, peptidoglycan synthesis, copper resistance, and *M. tuberculosis* stress response. We also identified new potential components of the SecA2 export machinery as well as previously unidentified candidate SecA2 exported effectors that play important roles in virulence. Our study speaks to the power of genetic interaction studies and the application of these studies to elucidate the function and components of bacterial protein export systems.

MATERIALS AND METHODS

Strains and Media Conditions

In this study, we used the *Mycobacterium tuberculosis* wild type strain H37Rv, and the *secA2* mutant (mc²3112) generated in the H37Rv background(6). *M. tuberculosis* strains were cultured in either liquid Middlebrook 7H9(BD) or on solid Middlebrook 7H10(BD) or 7H11 (Sigma) media supplemented with 0.05% Tween 80, 0.5% glycerol, 1x albumin dextrose saline (ADS) and kanamycin (20µg/ml) when appropriate.

Tn library generation

M. tuberculosis transposon mutant libraries were constructed in H37Rv and *secA2* strains by *HimarI* mutagenesis using the MycoMarT7 temperature sensitive phage as previously described(74,75). *M. tuberculosis* cultures grown to an OD of 1.0 were incubated at an MOI of 10 with the MycoMarT7 phage at 39°C overnight. Ten replicate transductions were completed for each strain to generate comprehensive Tn libraries in each strain background comprised of approximately 2×10^5 mutants each. The following day cells were washed and plated to recover the Tn mutants. Three weeks after plating the Tn libraries were pooled and sequenced to ensure adequate insertion density. Although, the *secA2* mutant has a higher level of intrinsic level of kanamycin resistance approximately the same number of Tn mutants were recovered from the *secA2* mutant library.

Murine infection

As previously described, 8-week-old female C57Bl/6 were intravenously infected with 3×10^6 *M. tuberculosis* from either the H37Rv Tn library or the *secA2* Tn library(6). A total of nine mice were infected with the H37Rv Tn library and 51 mice were infected with

the *secA2* Tn library. One day post-infection two mice from each group were sacrificed to determine bacterial seeding. Consistent with previous studies, approximately 20% of the inoculum seeded the spleen, 75% seeded the liver and 5% seeded the lungs(17). At 18 days post infection mice were sacrificed and spleens were harvested, homogenized and plated onto 7H10 agar to isolate surviving bacteria. After 3 weeks of growth, colonies were scraped from the agar plates and pooled into three independent groups for each mutant library to generate triplicate samples.

Genomic DNA isolation and sample preparation for sequencing

The triplicate library samples for each strain were resuspended in TE and an equal volume of 2:1 chloroform-methanol was added and incubated at room temperature for 5 minutes. Samples were centrifuged and supernatant discarded. The pellets were dried and then subsequently resuspended in 100ug/ml lysozyme in TE and incubated at 37 overnight. The next day SDS and proteinase K were added to the samples for a final concentration of 1% and 10ug/ml respectively. Samples were incubated at 50°C for 3 hours. Samples were then incubated with phenol-chloroform-isoamyl alcohol (25:24:1) and centrifuged to isolate the aqueous phase. Two subsequent chloroform extractions were performed and DNA was precipitated with 0.3M sodium acetate and 10% isopropanol and dissolved in TE.

Genomic DNA was sheared by nebulization at 45psi for 3 minutes in TE containing 53% Glycerol, 37mM Tris-HCl, and 5.5mM EDTA. Sheared DNA was isolated using a Quiagen PCR purification kit. A blunting kit (NEB) was utilized to repair the DNA ends and fragments were A-tailed. Adaptors generated from primers Adaptor 1.1 and 1.2 were ligated to the DNA fragments (Table 4.4)(76). Fragments containing transposon insertions were

amplified using a mixture of primers recognizing the transposon sequence (sol-mar, sol-mar 1b, sol-mar 4b, sol-mar 5b) and an adaptor primer containing sequences unique for each replicate library (Table 4.4). Fragments of 200-400bp were isolated from each sample by gel purification and sequenced using an Illumina HiSeq platform.

Sequencing data analysis and identification of genetic interactions

The sequence data were processed using the TPP tool included with TRANSIT(77). Reads were mapped to the genome using the Burroughs-Wheeler Aligner. The set of reads with a prefix matching the end of the *HimarI* transposon were mapped to the corresponding TA site in the genome (stripping off the transposon prefix). The read counts were reduced to template counts by discarding duplicates with the same barcode. The final template counts were normalized across all the data sets using Trimmed Total Reads (TTR) normalization. TTR normalizes data sets so that they have the same mean template count, while ignoring (“trimming”) the top and bottom 5% of read counts to reduce the influence of outliers. To reduce the number of false positives a beta-geometric correction was performed. A Benjamini-Hochberg correction was applied to account for multiple tests and adjusted p-values are provided.

Growth on cholesterol

A cholesterol stock solution was prepared as previously described by solubilizing cholesterol in ethanol and tyloxapol(78). 7H9 media containing 0.025% Tyloxapol and 1X albumin saline (ADS lacking glucose) (7AS) was supplemented with either 6% glycerol or 0.5 mM cholesterol. 10^4 cfu of *M. tuberculosis* strains were aliquoted into 96 well plates containing the 7AS media with either glycerol or cholesterol and plates incubated shaking at 37°C for

seven days. Resazurin (Sigma) was added to a final concentration 0.0125 mg/ml. Resazurin conversion was assessed after five days using fluorescence and was monitored by a Tecan Infinite 200 Pro at $h\nu=544$ nm excitation and $h\nu=590$ nm emission.

Lysozyme Sensitivity

10^5 cfu of *M. tuberculosis* strains were aliquoted into 96 well plates containing 7AGT with or without 0.4mg/ml lysozyme. Plates were incubated shaking at 37°C for 24 hours. Resazurin (Sigma) was added to a final concentration 0.0125 mg/ml and fluorescence was assessed 48 hours after resazurin addition.

Carbenicillin Resistance

10^5 cfu of *M. tuberculosis* strains were aliquoted into 96 well plates containing 7AGT with varying concentrations of carbenicillin (0-2mg/ml). Plates were incubated shaking at 37°C for four days. Resazurin (Sigma) was added to a final concentration 0.0125 mg/ml and fluorescence was assessed three days after resazurin addition. The concentration of carbenicillin that inhibited resazurin conversion by 95% as compared to untreated controls was defined as the MIC 95.

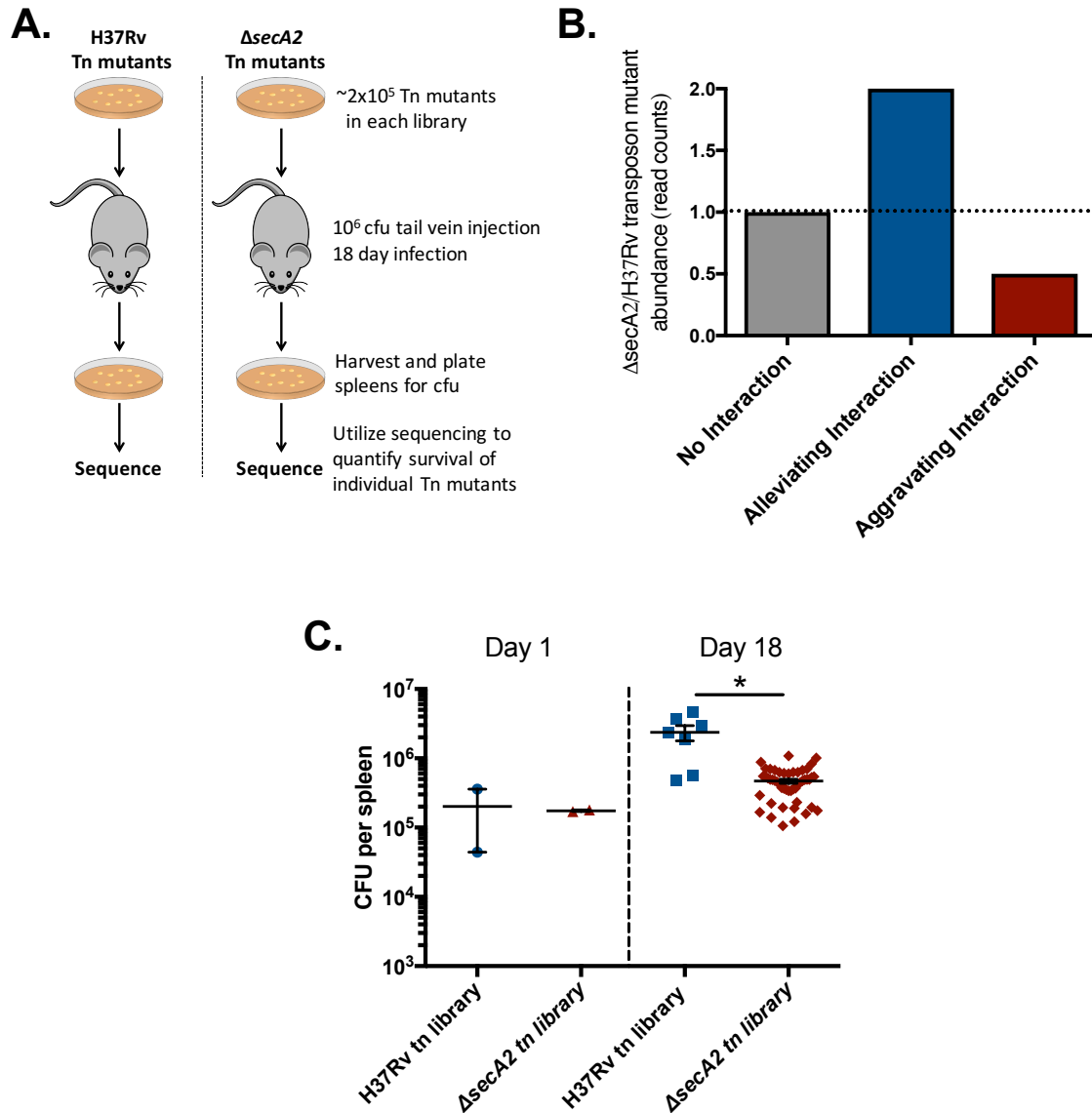


Figure 4.1: Utilizing TnSeq to identify genetic interactions with *secA2*

(A) Overview of experimental approach. Transposon mutagenesis was utilized to generate mutant libraries in both the wild-type H37Rv and *secA2* mutant strain backgrounds. Mice were infected with 10^6 cfu for 18 days and then spleens were harvested and plated for CFU. CFU recovered from the mice were analyzed by high-throughput sequencing to identify individual Tn mutants that had altered survival in each strain background. (B) Survival of individual Tn mutants during the murine infection was quantified by total read counts. Tn mutants that had equivalent read counts (equal CFU) in each strain background represent genes that had no interaction with *secA2*. Tn mutants that had more reads (increased survival or cfu) in the *secA2* mutant background are alleviating genetic interactions with *secA2*. Tn mutants that had less reads (reduced survival or CFU) in the *secA2* mutant background are aggravating genetic interactions with *secA2*. (C) Mice infected with H37Rv and *secA2* Tn mutant libraries were sacrificed at either 1 day or 18 days post infection. Spleens were isolated and homogenized. Spleen homogenates were plated for viable CFU. * $p < 0.01$.

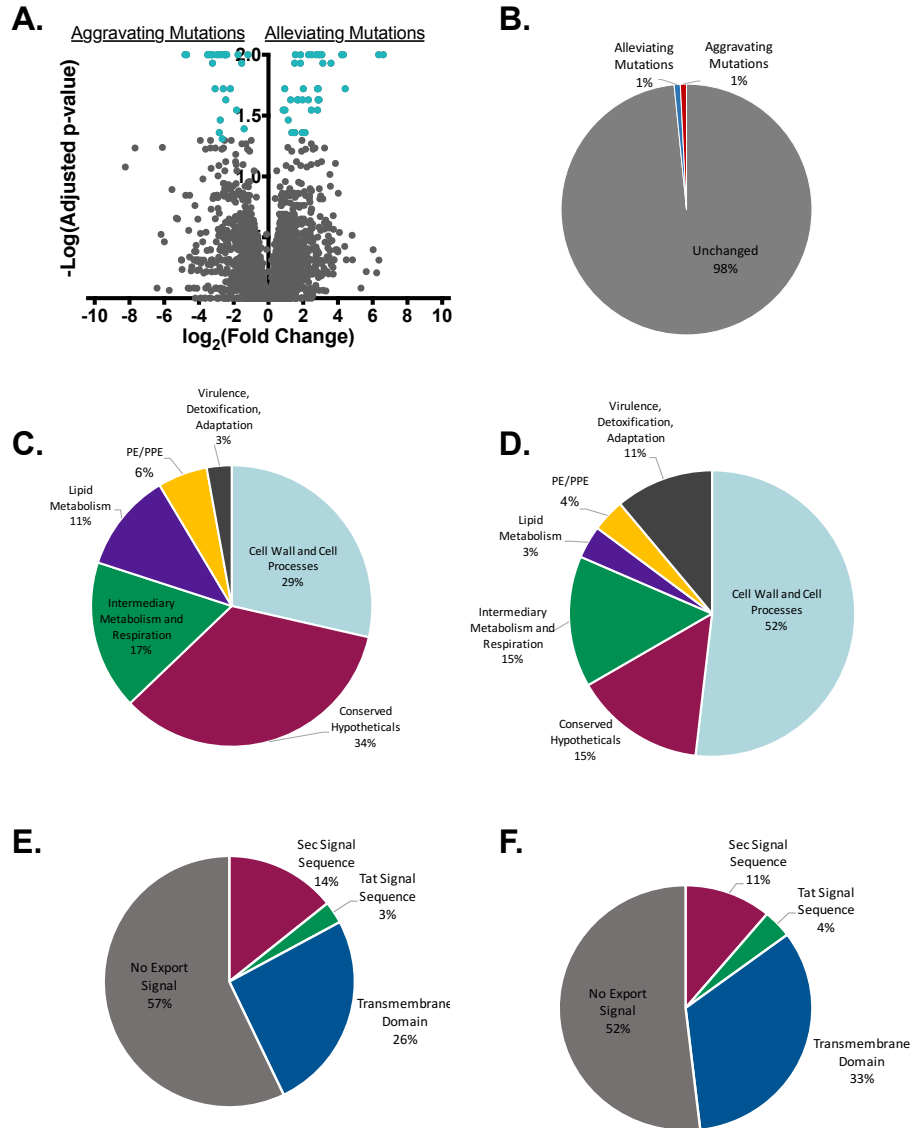


Figure 4.2: Genetic interactions with *secA2*

(A) Individual Tn mutants identified by sequencing are shown plotted by \log_2 (Fold Change: *secA2*/H37Rv) and $-\log_{10}(p\text{-value})$. Blue points represent mutations that had an adjusted p -value < 0.05 and a Fold change larger than 2 and are classified as genetic interactions with *secA2* whereas grey points represent mutations that had no interaction with *secA2*. (B) The percentage of genes that have significant interactions with *secA2* are shown. (C) The significant alleviating interactions with *secA2* were assigned to functional categories by Tuberculist. (D) The significant aggravating interactions with *secA2* were assigned to functional categories by Tuberculist. (E) The percentage of significant alleviating interactions with *secA2* that encode for proteins with predicted export signals are shown. (F) The percentage of significant aggravating interactions with *secA2* that encode for proteins with predicted export signals are shown.

Esx Secretion:

eccA5
eccB4
espK (esx1)
PPE20 (esx3)

Phagosome maturation arrest:

sapM
rv1506c
espK
rv2506

Stress related:

blaR
hspR
oprA
rv2034
rpfC
relA
rpfB
rv3134c

Cholesterol:

echA19
cyp142
fadE25
KshA
Gdh

Mtb lipids

rv1506c
ppm1
impA
glpK
rv1565c
mmaA4
drrB
rv2252
rv2956
rv3779

Peptidoglycan:

rv3717
glnA2
rv1566c
ripC
uspA

Transporters:

pstB
pstA2
rv1458c
chaA
mgtE
rv0488
pstC2
pstS3
pstA1
phoT
rv3679
rv3680
mam1C
uspA
drrB
rv0876

Copper:

ricR
rv2199c
rv0850
rv3851

Figure 4.3: Clusters of alleviating and aggravating interactions with *secA2*

Genes that significantly interacted with *secA2* are grouped into clusters based on predicted function. Significant alleviating interactions are in blue whereas significant aggravating interactions are in red. To be included in this analysis there must have been at least a 2-fold difference in survival between the H37Rv and *secA2* mutant libraries and the interaction had to have an adjusted p-value that is less than 0.1.

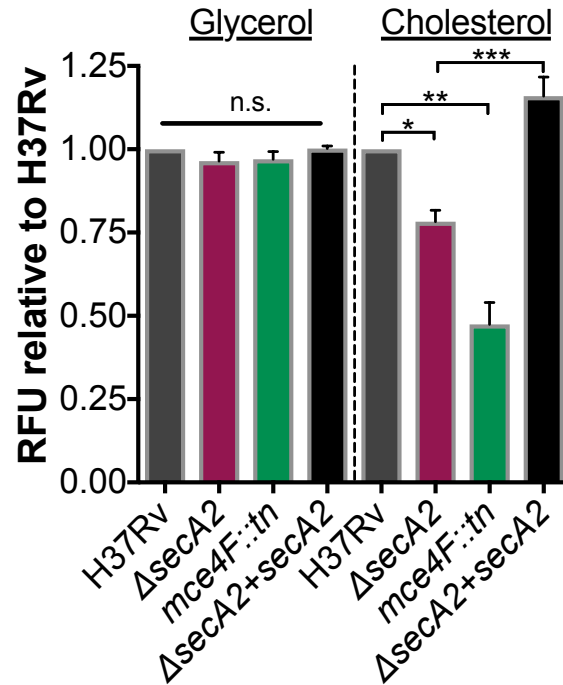


Figure 4.4: SecA2 is required for optimal growth on cholesterol

10^4 cfu of indicated *Mtb* strains were grown in 7H9 media with either glycerol or cholesterol as the sole carbon source. Metabolic activity as monitored by resazurin conversion over time was used to monitor growth in either carbon source. Plotted is the average RFU of five independent experiments relative to H37Rv five day after resazurin addition. * $p < 0.01$, ** $p < 0.001$, *** $p < 0.0001$

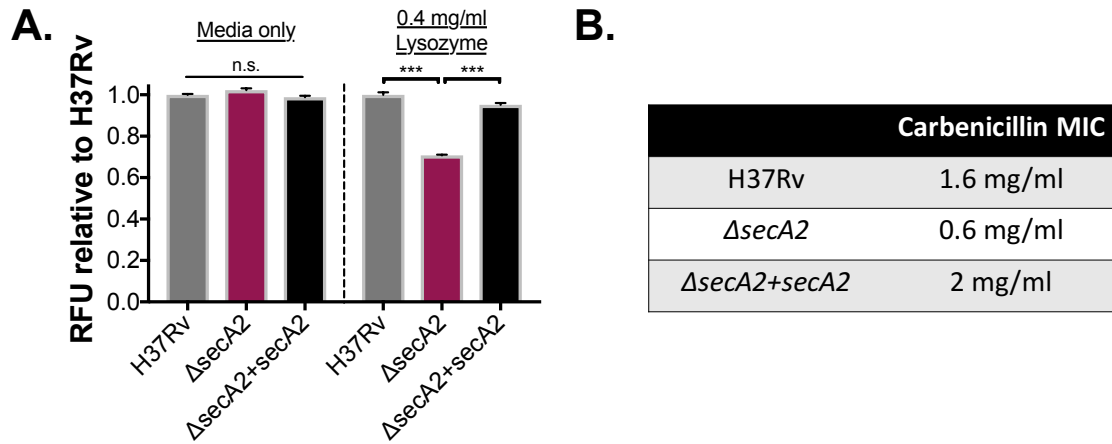


Figure 4.5: SecA2 is required for lysozyme and carbenicillin resistance

(A) 10^5 cfu of indicated *Mtb* strains were grown in 7AGT with or without 0.4mg/ml lysozyme for 24 hours. Metabolic activity as monitored by resazurin conversion over time was used to monitor growth in either condition. Plotted is the average RFU of four replicate wells relative to H37Rv three day after resazurin addition. *** $p < 0.0001$ (B) Shown is the MIC 95 for the indicated *Mtb* strains. The MIC was determined by incubating 10^5 cfu with a range of concentrations of carbenicillin (0-2mg/ml). Metabolic activity as monitored by resazurin conversion over time was used to monitor survival.

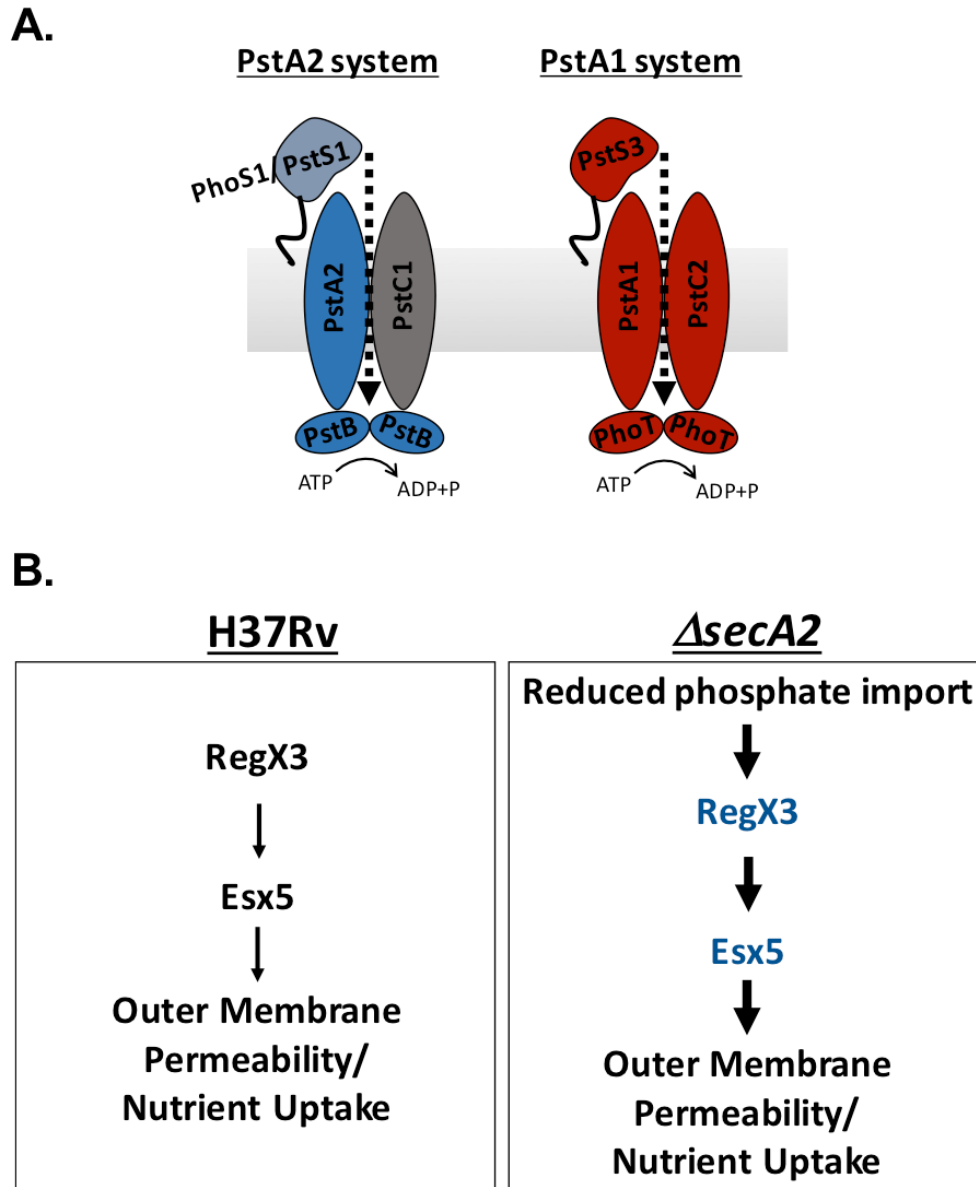


Figure 4.6: SecA2 and phosphate import in *M. tuberculosis*

(A) The two Pst phosphate ABC transporters in *M. tuberculosis* are diagramed. Components of the transporters that represent aggravating or alleviating interactions with *secA2* are colored with blue representing alleviating interactions and red representing aggravating interactions. (B) Reduced phosphate import in the *secA2* mutant, due to reduced export of the solute binding protein PhoS1, may induce the RegX3 regulon which is known to be stimulated by low phosphate conditions. Increased RegX3 induction leads to increased levels of the RegX3 regulated Esx5 which is proposed to increase outer membrane permeability that mediates increased nutrient uptake. RegX3 also induced *pstA1* which feeds back and negatively regulated *regX3*.

Table 4.1 Significant genetic interactions with *secA2*

Genes listed possess Tn insertions that resulted in more than a 2-fold difference in survival in the *secA2* mutant background as compared to the H37Rv background and have an adjusted p-value < 0.05. Aggravating interactions (reduced survival in *secA2* mutant background) are shaded red while alleviating interactions (increased survival in *secA2* mutant background) are shaded blue.

Gene	Name	Description	Functional Category	TA sites	log2 (secA2/H37Rv)	p-value	Adjusted p-value	Transmembrane domain	Sec signal sequence	Tat signal sequence
Aggravating Interactions										
Rv0929	pstC2	phosphate ABC transporter integral membrane component	Cell Wall and Cell Processes	17	-4.8	1.0E-05	1.0E-05	X		
Rv1565c	-	hypothetical protein	Cell Wall and Cell Processes	46	-4.71	1.0E-05	1.0E-05	X		
Rv3680	-	possible anion transporter ATPase	Cell Wall and Cell Processes	20	-3.5	1.0E-05	1.0E-05			
Rv1009	rpfB	resuscitation-promoting factor	Cell Wall and Cell Processes	12	-3.47	1.0E-05	1.0E-05	X	X	
Rv1836c	-	hypothetical protein	Conserved Hypotheticals	43	-3.34	1.0E-05	1.0E-05	X		
Rv1085c	-	acyl-CoA synthetase	Virulence, Detoxification, Adaptation	11	-3.25	1.0E-05	1.0E-05	X		
Rv0928	pstS3	phosphate binding lipoprotein	Cell Wall and Cell Processes	22	-3.23	1.0E-05	1.0E-05		X	
Rv0177	Mam1C	Mce associated protein	Conserved Hypotheticals	12	-3.22	1.0E-04	0.01	X		
Rv1622c	cydB	integral membrane cytochrome D ubiquinol oxidase	Intermediary Metabolism and Respiration	22	-3.07	2.0E-04	0.02	X		
Rv3679	-	possible anion transporter ATPase	Cell Wall and Cell Processes	15	-2.98	1.0E-05	1.0E-05			
Rv2782c	pepR	possible zinc protease	Intermediary Metabolism and Respiration	13	-2.89	1.0E-05	1.0E-05			
Rv2316	uspA	sugar ABC transporter integral membrane component	Cell Wall and Cell Processes	13	-2.83	7.0E-04	0.04	X		X
Rv0475	hbhA	heparin binding hemagglutinin	Cell Wall and Cell Processes	9	-2.77	5.0E-04	0.03			
Rv0930	pstA1	phosphate ABC transporter integral membrane component	Cell Wall and Cell Processes	17	-2.71	1.0E-05	1.0E-05	X		
Rv2583c	relA	GTP pyrophosphokinase	Intermediary Metabolism and Respiration	36	-2.66	8.0E-04	0.05			
Rv1421	-	hypothetical protein	Conserved Hypotheticals	20	-2.6	2.0E-04	0.02			
Rv1013	pks16	acyl-CoA synthetase	Lipid Metabolism	21	-2.53	1.0E-05	1.0E-05			
Rv3086	adhD	zinc type alcohol dehydrogenase	Intermediary Metabolism and Respiration	11	-2.48	1.0E-05	1.0E-05			
Rv2190c	ripC	hypothetical protein	Virulence, Detoxification, Adaptation	20	-2.48	1.0E-05	1.0E-05	X	X	
Rv0642c	mmaA4	methoxy mycolic acid synthase	Lipid Metabolism	18	-2.45	3.0E-04	0.02			
Rv0820	phoT	phosphate ABC transporter ATPase	Cell Wall and Cell Processes	12	-2.4	1.0E-05	1.0E-05			
Rv3134c	-	hypothetical protein	Conserved Hypotheticals	9	-2.19	2.0E-04	0.02			
Rv3526	kshA	oxidoreductase	Intermediary Metabolism and Respiration	22	-1.83	4.0E-04	0.03			

Rv2707	-	conserved transmembrane alanine and leucine rich protein	Conserved Hypotheticals	28	-1.75	1.0E-05	1.0E-05	X		
Rv2476c	gdh	NAD dependent glutamate dehydrogenase	Intermediary Metabolism and Respiration	64	-1.54	1.0E-04	0.01			
Rv1623c	cydA	integral membrane cytochrome D ubiquinol oxidase	Intermediary Metabolism and Respiration	23	-1.4	6.0E-04	0.04	Y		
Rv2696c	-	conserved hypothetical alanine, glycine, and valine rich protein	Conserved Hypotheticals	10	-1.18	1.0E-05	1.0E-05			
Alleviating Interactions										
Rv3078	hab	hydroxylaminobenzene mutase	Intermediary Metabolism and Respiration	6	6.61	1.0E-05	1.0E-05	X		
Rv3108	-	hypothetical protein	Conserved Hypotheticals	7	6.35	1.0E-05	1.0E-05			X
Rv3516	echA19	enoyl-CoA hydratase	Lipid Metabolism	7	4.42	2.0E-04	1.9E-02			
Rv1845c	Blar	hypothetical protein	Cell Wall and Cell Processes	14	4.32	1.0E-05	1.0E-05	X	X	
Rv1798	EccA5	hypothetical protein	Cell Wall and Cell Processes	30	4.22	1.0E-05	1.0E-05			
Rv2328	PE23	PE family protein	PE/PPE	12	3.6	1.0E-04	1.2E-02			
Rv1691	-	hypothetical protein	Conserved Hypotheticals	11	3.13	1.0E-04	1.2E-02			
Rv3311	satS	hypothetical protein	Conserved Hypotheticals	16	3.08	1.0E-05	1.0E-05			
Rv3717	-	hypothetical protein	Conserved Hypotheticals	12	2.98	1.0E-05	1.0E-05		X	
Rv0012	-	conserved membrane protein	Cell Wall and Cell Processes	16	2.94	1.0E-05	1.0E-05	X		
Rv0933	pstB	phosphate ABC transporter ATPase	Cell Wall and Cell Processes	12	2.92	3.0E-04	2.3E-02			
Rv3518c	cyp142	cytochrome p450 monooxygenase	Intermediary Metabolism and Respiration	13	2.87	3.0E-04	2.3E-02			
Rv1506c	-	hypothetical protein	Conserved Hypotheticals	20	2.87	3.0E-04	2.3E-02			
Rv3577	-	hypothetical protein	Conserved Hypotheticals	14	2.87	2.0E-04	1.9E-02			
Rv0353	hspR	Heat shock protein transcriptional repressor	Virulence, Detoxification, Adaptation	6	2.83	4.0E-04	2.9E-02			
Rv0124	PE_PGRS2	PE-PGRS family protein	PE/PPE	13	2.82	2.0E-04	1.9E-02		X	
Rv2409c	-	hypothetical protein	Conserved Hypotheticals	20	2.77	1.0E-05	1.0E-05			
Rv1458c	-	antibiotic ABC transporter ATPase	Cell Wall and Cell Processes	14	2.49	1.0E-05	1.0E-05			
Rv3450c	EccB4	conserved membrane protein	Cell Wall and Cell Processes	15	2.47	4.0E-04	2.9E-02	X		
Rv3696c	glpK	glycerol kinase	Intermediary Metabolism and Respiration	29	2.31	1.0E-05	1.0E-05			
Rv2237	-	hypothetical protein	Conserved Hypotheticals	17	2.3	3.0E-04	2.3E-02			
Rv1607	chaA	ionic transporter integral membrane protein	Cell Wall and Cell Processes	10	2.11	7.0E-04	4.4E-02	X		
Rv3274c	fadE25	acyl-CoA dehydrogenase	Lipid Metabolism	19	2.01	2.0E-04	1.9E-02			
Rv0936	pstA2	phosphate ABC transporter integral membrane component	Cell Wall and Cell Processes	20	1.97	3.0E-04	2.3E-02	X		
Rv2226	-	hypothetical protein	Conserved Hypotheticals	25	1.95	7.0E-04	4.4E-02			
Rv3720	-	fatty acid synthase	Lipid Metabolism	32	1.85	1.0E-05	1.0E-05			

Rv2051c	ppm1	Polyprenol-monophosphomannose synthase	Cell Wall and Cell Processes	33	1.84	1.0E-04	1.2E-02	X		
Rv0362	mgtE	Mg ²⁺ transporter transmembrane protein	Cell Wall and Cell Processes	16	1.71	3.0E-04	2.3E-02	X		
Rv0874c	-	hypothetical protein	Conserved Hypotheticals	9	1.67	3.0E-04	2.3E-02			
Rv2222c	glnA2	glutamine synthase	Intermediary Metabolism and Respiration	20	1.55	1.0E-05	1.0E-05			
Rv1884c	rpfC	resuscitation-promoting factor	Cell Wall and Cell Processes	6	1.52	7.0E-04	4.4E-02		X	
Rv0488	-	conserved integral membrane protein	Cell Wall and Cell Processes	9	1.51	1.0E-04	1.2E-02	X		
Rv0007	-	conserved membrane protein	Cell Wall and Cell Processes	10	1.35	7.0E-04	4.4E-02	X		
Rv3310	SapM	acid phosphatase	Cell Wall and Cell Processes	17	1.28	3.0E-04	2.3E-02	X	X	
Rv3136	PPE51	PPE family protein	PE/PPE	21	1.14	5.0E-04	3.4E-02			

Table 4.2 Potential SecA2 substrates

Presented in this table are alleviating interactions that are predicted to encode for an exported protein (ie have a predicted Sec or Tat signal sequence) thus have the potential to be exported by the SecA2 pathway (p-value<0.05).

Gene	Name	Description	Functional Category	TA sites	log2 (secA2/H37Rv)	p-value	Adjusted p-value	Sec signal sequence	Tat signal sequence
Rv3108	-	hypothetical protein	Conserved Hypotheticals	7	6.35	1.0E-05	1.0E-05		X
Rv1845c	-	hypothetical protein	Cell Wall and Cell Processes	14	4.32	1.0E-05	1.0E-05	X	
Rv3717	-	hypothetical protein	Conserved Hypotheticals	12	2.98	1.0E-05	1.0E-05	X	
Rv0124	PE_PGRS2	PE-PGRS family protein	PE/PPE	13	2.82	2.0E-04	0.02	X	
Rv3310	SapM	acid phosphatase	Cell Wall and Cell Processes	17	1.28	3.0E-04	0.02	X	
Rv1884c	rpfC	resuscitation promoting factor	Cell Wall and Cell Processes	6	1.52	7.0E-04	0.04	X	
Rv0455c	-	hypothetical protein	Conserved Hypotheticals	11	2.68	1.2E-03	0.06	X	
Rv0179c	lprO	possible lipoprotein	Cell Wall and Cell Processes	22	1.34	1.4E-03	0.06	X	
Rv0125	pepA	possible serine protease	Intermediary Metabolism and Respiration	10	2.4	4.2E-03	0.13	X	X
Rv3803c	fbpD	secreted MPT51/MPB51	Lipid Metabolism	16	1.13	4.8E-03	0.14	X	
Rv1076	lipU	possible lipase	Intermediary Metabolism and Respiration	21	1.47	5.3E-03	0.14		X
Rv0875c	-	possible conserved exported protein	Cell Wall and Cell Processes	12	1.59	6.0E-03	0.14	X	
Rv0403c	mmpS1	possible conserved membrane protein	Cell Wall and Cell Processes	7	1.53	6.7E-03	0.15	X	
Rv3034c	-	possible transferase	Intermediary Metabolism and Respiration	13	2.96	7.2E-03	0.15	X	
Rv0862c	-	hypothetical protein	Conserved Hypotheticals	29	1.66	8.6E-03	0.17		X
Rv2518c	lppS	possible lipoprotein	Cell Wall and Cell Processes	21	3.73	0.01	0.21	X	
Rv2403c	lppR	possible lipoprotein	Cell Wall and Cell Processes	7	2.98	0.01	0.21	X	
Rv1040c	PE8	PE family protein	PE/PPE	8	1.52	0.01	0.22	X	
Rv0747	PE_PGRS10	PE-PGRS family protein	PE/PPE	16	1.6	0.02	0.25	X	
Rv3576	lppH	possible lipoprotein	Cell Wall and Cell Processes	13	1.57	0.03	0.31	X	
Rv3810	pirG	exported repetitive protein precursor	Cell Wall and Cell Processes	13	3.45	0.03	0.31	X	
Rv3593	lppF	possible lipoprotein	Cell Wall and Cell Processes	19	2.39	0.04	0.34	X	
Rv3555c	-	hypothetical protein	Conserved Hypotheticals	12	1.98	0.04	0.35		X
Rv0578c	PE_PGRS7	PE-PGRS family protein	PE/PPE	27	1.41	0.04	0.35	X	
Rv0265c	-	iron transport lipoprotein	Cell Wall and Cell Processes	9	2.02	0.05	0.36		X
Rv0846c	MmcO	possible oxidase	Intermediary Metabolism and Respiration	31	1.18	0.05	0.37	X	X
Rv1075c	-	conserved exported protein	Cell Wall and Cell Processes	18	1.04	0.05	0.37	X	X

Table 4.3 Clusters of genetic interactions with *secA2*

Genetic interactions were grouped into clusters by predicted function. Genetic interactions included in this analysis represent mutations that resulted in more than a 2-fold difference in survival in the *secA2* mutant background as compared to the H37Rv and an adjusted p-value < 0.1. Alleviating interactions are shaded blue while aggravating are shaded red.

Gene	Name	Description	Functional Category	TA sites	log2 (secA2/H37Rv)	p-value	Adjusted p-value	Transmembrane domain	Sec signal sequence	Tat signal sequence
Esx Secretion										
Rv1798	EccA5	hypothetical protein	Cell Wall and Cell Processes	30	4.22	1.0E-05	1.0E-05			
Rv3450c	EccB4	conserved membrane protein	Conserved Hypotheticals	15	2.47	4.0E-04	2.9E-02	X		
Rv3879c	EspK	Hypothetical alanine and proline rich protein	Cell Wall and Cell Processes	38	0.85	4.0E-04	0.03			
Rv1387	PPE20	PPE family protein	Conserved Hypotheticals	26	-0.82	2.5E-03	0.09			
Phagosome Maturation Arrest										
Rv3310	SapM	acid phosphatase	Lipid Metabolism	17	1.28	3.0E-04	0.02	X	X	
Rv1506c	-	hypothetical protein	Conserved Hypotheticals	20	2.87	3.0E-04	0.02			
Rv3879c	EspK	Hypothetical alanine and proline rich protein	Cell Wall and Cell Processes	38	0.85	4.0E-04	0.03			
Rv2506	-	Transcriptional regulatory protein	Regulatory Proteins	9	2.57	1.3E-03	0.06			
Stress Related Hits										
Rv1845c	BlaR	hypothetical protein	Conserved Hypotheticals	14	4.32	1.0E-05	1.0E-05	X	X	
Rv0353	HspR	Heat shock protein transcriptional repressor	Cell Wall and Cell Processes	6	2.83	4.0E-04	0.03			
Rv1884c	rpfC	resuscitation-promoting factor	Cell Wall and Cell Processes	6	1.52	7.0E-04	0.04		X	
Rv0516c	OprA	hypothetical protein	Conserved Hypotheticals	9	2.14	1.3E-03	0.06			
Rv2034	-	ArsR-type repressor protein	Regulatory Proteins	3	1.91	1.4E-03	0.06			
Rv2583c	relA	GTP pyrophosphokinase	Intermediary Metabolism and Respiration	36	-2.66	8.0E-04	0.05			
Rv1009	rpfB	resuscitation-promoting factor	Cell Wall and Cell Processes	12	-3.47	1.0E-05	1.0E-05	X	X	
Rv3134c	-	hypothetical protein	Conserved Hypotheticals	9	-2.19	2.0E-04	0.02			
Copper										
Rv0190	RicR	hypothetical protein	Conserved Hypotheticals	3	2.46	2.0E-03	0.08			
Rv2199c	-	Conserved integral membrane protein	Cell Wall and Cell Processes	8	1.86	2.1E-03	0.08	Y		
Rv0850	-	putative transposase	Insertion Seqs and Phage	9	-3.33	9.0E-04	0.05			
Rv3851	-	conserved membrane protein	Conserved Hypotheticals	2	-7.68	1.2E-03	0.06	Y	Y	
Cholesterol										
Rv3516	echA19	enoyl-CoA hydratase	Conserved Hypotheticals	7	4.42	2.0E-04	0.02			
Rv3518c	cyp142	cytochrome p450 monooxygenase	Cell Wall and Cell Processes	13	2.87	3.0E-04	0.02			
Rv3274c	fadE25	acyl-CoA dehydrogenase	Virulence, Detoxification, Adaptation	19	2.01	2.0E-04	0.02			
Rv3526	kshA	oxidoreductase	Virulence, Detoxification, Adaptation	22	-1.83	4.0E-04	0.03			
Rv2476c	gdh	NAD dependent glutamate dehydrogenase	Cell Wall and Cell Processes	64	-1.54	1.0E-04	0.01			

Peptidoglycan										
Rv3717	-	hypothetical protein	Conserved Hypotheticals	12	2.98	1.0E-05	1.0E-05		X	
Rv2222c	glnA2	glutamine synthase	Conserved Hypotheticals	20	1.55	1.0E-05	1.0E-05			
Rv2199c	-	Conserved membrane protein	Cell Wall and Cell Processes	8	1.86	2.1E-03	0.08	x		
Rv1566c	-	Possible inv protein	Virulence, Detoxification, Adaptation	10	-2.61	5.0E-03	0.14	X	X	X
Rv2190c	ripC	hypothetical protein	Conserved Hypotheticals	20	-2.48	1.0E-05	1.0E-05	X	X	
Rv2316	uspA	sugar ABC transporter integral membrane component	Cell Wall and Cell Processes	13	-2.83	7.0E-04	0.04	X		X
Transporters										
Rv0933	pstB	phosphate ABC transporter ATPase	Intermediary Metabolism and Respiration	12	2.92	3.0E-04	0.02			
Rv0936	pstA2	phosphate ABC transporter integral membrane component	Cell Wall and Cell Processes	20	1.97	3.0E-04	0.02	X		
Rv1458c	-	antibiotic ABC transporter ATPase	Intermediary Metabolism and Respiration	14	2.49	1.0E-05	1.0E-05			
Rv1607	chaA	ionic transporter integral membrane protein	Cell Wall and Cell Processes	10	2.11	7.0E-04	0.04	X		
Rv0362	mgtE	Mg2+ transporter transmembrane protein	Cell Wall and Cell Processes	16	1.71	3.0E-04	0.02	X		
Rv0488	-	conserved integral membrane protein	Conserved Hypotheticals	9	1.51	1.0E-04	0.01	X		
Rv0929	pstC2	phosphate ABC transporter integral membrane component	Cell Wall and Cell Processes	17	-4.8	1.0E-05	1.0E-05	X		
Rv0928	pstS3	phosphate binding lipoprotein	Lipid Metabolism	22	-3.23	1.0E-05	1.0E-05		X	
Rv0930	pstA1	phosphate ABC transporter integral membrane component	Cell Wall and Cell Processes	17	-2.71	1.0E-05	1.0E-05	X		
Rv0820	phoT	phosphate ABC transporter ATPase	Virulence, Detoxification, Adaptation	12	-2.4	1.0E-05	1.0E-05			
Rv3680	-	possible anion transporter ATPase	Cell Wall and Cell Processes	20	-3.5	1.0E-05	1.0E-05			
Rv3679	-	possible anion transporter ATPase	Virulence, Detoxification, Adaptation	15	-2.98	1.0E-05	1.0E-05			
Rv0177	Mam1C	Mce associated protein	Conserved Hypotheticals	12	-3.22	1.0E-04	1.0E-02	X		
Rv2316	uspA	sugar ABC transporter integral membrane component	Cell Wall and Cell Processes	13	-2.83	7.0E-04	0.04	X		X
Rv2937	drbB	Daunorubicin-DIM- ABC transporter integral membrane component	Cell Wall and Cell Processes	23	-1.53	1.0E-03	0.05	X		
Rv0876c	-	Conserved transmembrane protein	Cell Wall and Cell Processes	26	-1.89	1.8E-03	0.08	X		

Mtb lipids										
Rv1506c	-	hypothetical protein	Conserved Hypotheticals	20	2.87	3.0E-04	0.02			
Rv2051c	ppm1	Polyprenol-monophosphomannose synthase	Cell Wall and Cell Processes	33	1.84	1.0E-04	0.01	X		
Rv3696c	glpK	glycerol kinase	Intermediary Metabolism and Respiration	29	2.31	1.0E-05	1.0E-05			
Rv1604	impA	PROBABLE INOSITOL-MONOPHOSPHATASE IMPA (IMP)	Cell Wall and Cell Processes	13	3.23	1.2E-03	0.06			
Rv1565c	-	hypothetical protein	Cell Wall and Cell Processes	46	-4.71	1.0E-05	1.0E-05	X		
Rv0642c	mmaA4	methoxy mycolic acid synthase	Cell Wall and Cell Processes	18	-2.45	3.0E-04	0.02			
Rv2937	drbB	Daunorubicin-DIM- ABC transporter integral membrane component	Cell Wall and Cell Processes	23	-1.53	1.0E-03	0.05	X		
Rv2252	-	diacylglycerol kinase	Lipid Metabolism	17	-3.33	1.2E-03	0.06			
Rv2956	-	hypothetical protein	Conserved Hypotheticals	18	-3.62	1.3E-03	0.06			
Rv3779	-	Conserved transmembrane protein	Cell Wall and Cell Processes	47	-1.82	2.5E-03	0.09	X		

Table 4.4 Primers used in this study

Primer name	Sequence
Adapter 1.1	TAC CAC GAC CA-NH2
Adapter 2.1	ATG ATG GCC GGT GGA TTT GTG NNA NNA NNNTGG TCG TGG TAT
Sol-mar	'AATGATACGGCGACCACCGAGATCTACACTCTTTCCCTACACGACGCTCTTCCGATCTCGGGGACTTATCAGCCAACC
Sol-mar 1b	'AATGATACGGCGACCACCGAGATCTACACTCTTTCCCTACACGACGCTCTTCCGATCTTCCGGGACTTATCAGCCAACC
sol-mar 4b	AATGATACGGCGACCACCGAGATCTACACTCTTTCCCTACACGACGCTCTTCCGATCTGATACGGGGACTTATCAGCCAACC
sol-mar 5b	AATGATACGGCGACCACCGAGATCTACACTCTTTCCCTACACGACGCTCTTCCGATCTATCTACGGGGACTTATCAGCCAACC
Sol-AP1-tagged-57	CAAGCAGAAGACGGCATAACGAGATAAG TAG AGGTGACTGGAGTTCAGACGTGTGCTCTTCCGATCTATGATGGCCGGTGGATTTGTG
Sol-AP1-tagged-100	CAAGCAGAAGACGGCATAACGAGATACA CGA TCGTGACTGGAGTTCAGACGTGTGCTCTTCCGATCTATGATGGCCGGTGGATTTGTG
Sol-AP1-tagged-473	CAAGCAGAAGACGGCATAACGAGATCGC GCG GTGTGACTGGAGTTCAGACGTGTGCTCTTCCGATCTATGATGGCCGGTGGATTTGTG
Sol-AP1-tagged-373	CAAGCAGAAGACGGCATAACGAGATCAT GAT CGGTGACTGGAGTTCAGACGTGTGCTCTTCCGATCTATGATGGCCGGTGGATTTGTG
Sol-AP1-tagged-598	CAAGCAGAAGACGGCATAACGAGATGAG ATC TTGTGACTGGAGTTCAGACGTGTGCTCTTCCGATCTATGATGGCCGGTGGATTTGTG
Sol-AP1-tagged-651	CAAGCAGAAGACGGCATAACGAGATGCC GAT GTGTGACTGGAGTTCAGACGTGTGCTCTTCCGATCTATGATGGCCGGTGGATTTGTG

REFERENCES

1. World Health Organization. Global tuberculosis report 2016. World Health Organization; 2016.
2. Awuh JA, Flo TH. Molecular basis of mycobacterial survival in macrophages. *Cell Mol Life Sci*. Springer International Publishing; 2017 May;74(9):1625–48.
3. Hilbi H, Haas A. Secretive bacterial pathogens and the secretory pathway. *Traffic*. 2012 Sep;13(9):1187–97.
4. Ligon LS, Hayden JD, Braunstein M. The ins and outs of *Mycobacterium tuberculosis* protein export. *Tuberculosis (Edinb)*. 2012 Mar;92(2):121–32.
5. Braunstein M, Brown AM, Kurtz S, Jacobs WR. Two nonredundant SecA homologues function in mycobacteria. *J Bacteriol*. 2001 Dec;183(24):6979–90.
6. Braunstein M, Espinosa BJ, Chan J, Belisle JT, Jacobs WR. SecA2 functions in the secretion of superoxide dismutase A and in the virulence of *Mycobacterium tuberculosis*. *Mol Microbiol*. 2003 Apr;48(2):453–64.
7. Kurtz S, McKinnon KP, Runge MS, Ting JP-Y, Braunstein M. The SecA2 secretion factor of *Mycobacterium tuberculosis* promotes growth in macrophages and inhibits the host immune response. *Infect Immun*. 2006 Dec;74(12):6855–64.
8. Sullivan JT, Young EF, McCann JR, Braunstein M. The *Mycobacterium tuberculosis* SecA2 system subverts phagosome maturation to promote growth in macrophages. *Infect Immun*. 2012 Mar;80(3):996–1006.
9. Feltcher ME, Gunawardena HP, Zulauf KE, Malik S, Griffin JE, Sasseti CM, et al. Label-free Quantitative Proteomics Reveals a Role for the *Mycobacterium tuberculosis* SecA2 Pathway in Exporting Solute Binding Proteins and Mce Transporters to the Cell Wall. *Mol Cell Proteomics*. 2015 Jun;14(6):1501–16.
10. Srinivasan L, Ahlbrand S, Briken V. Interaction of *Mycobacterium tuberculosis* with host cell death pathways. *Cold Spring Harb Perspect Med*. 2014 Jun 26;4(8):a022459–9.
11. Portal-Celhay C, Tufariello JM, Srivastava S, Zahra A, Klevorn T, Grace PS, et al. *Mycobacterium tuberculosis* EsxH inhibits ESCRT-dependent CD4(+) T-cell activation. *Nat Microbiol*. Nature Publishing Group; 2016 Dec 5;2(2):16232.
12. Wolff KA, la Peña de AH, Nguyen HT, Pham TH, Amzel LM, Gabelli SB, et al. A

- redox regulatory system critical for mycobacterial survival in macrophages and biofilm development. Boshoff HI, editor. *PLoS Pathog.* 2015 Apr;11(4):e1004839.
13. Subbian S, Mehta PK, Cirillo SLG, Bermudez LE, Cirillo JD. A *Mycobacterium marinum* mel2 Mutant Is Defective for Growth in Macrophages That Produce Reactive Oxygen and Reactive Nitrogen Species. *Infect Immun.* 2006 Dec 20;75(1):127–34.
 14. Nambi S, Long JE, Mishra BB, Baker R, Murphy KC, Olive AJ, et al. The Oxidative Stress Network of *Mycobacterium tuberculosis* Reveals Coordination between Radical Detoxification Systems. *Cell Host & Microbe.* 2015 Jun 10;17(6):829–37.
 15. Ligon LS, Rigel NW, Romanchuk A, Jones CD, Braunstein M. Suppressor analysis reveals a role for SecY in the SecA2-dependent protein export pathway of *Mycobacteria*. *J Bacteriol.* 2013 Oct;195(19):4456–65.
 16. DeJesus MA, Gerrick ER, Xu W, Park SW, Long JE, Boutte CC, et al. Comprehensive Essentiality Analysis of the *Mycobacterium tuberculosis* Genome via Saturating Transposon Mutagenesis. Stallings CL, editor. *MBio.* 2017 Jan 17;8(1):e02133–16.
 17. Orme I, Gonzalez-Juarrero M. Animal models of *M. tuberculosis* Infection. *Curr Protoc Microbiol.* Hoboken, NJ, USA: John Wiley & Sons, Inc; 2007 Nov;Chapter 10:Unit10A.5–10A.5.29.
 18. Sasindran SJ, Torrelles JB. *Mycobacterium Tuberculosis* Infection and Inflammation: what is Beneficial for the Host and for the Bacterium? *Front Microbiol.* Frontiers; 2011;2:2.
 19. Babu M, Arnold R, Bundalovic-Torma C, Gagarinova A, Wong KS, Kumar A, et al. Quantitative genome-wide genetic interaction screens reveal global epistatic relationships of protein complexes in *Escherichia coli*. Sassetti CM, editor. *PLoS Genet.* 2014 Feb;10(2):e1004120.
 20. Griffin JE, Gawronski JD, DeJesus MA, Ioerger TR, Akerley BJ, Sassetti CM. High-resolution phenotypic profiling defines genes essential for mycobacterial growth and cholesterol catabolism. Ramakrishnan L, editor. *PLoS Pathog.* 2011 Sep;7(9):e1002251.
 21. Costanzo M, Baryshnikova A, Bellay J, Kim Y, Spear ED, Sevier CS, et al. The genetic landscape of a cell. *Science.* 2010 Jan 22;327(5964):425–31.
 22. Joshi SM, Pandey AK, Capite N, Fortune SM, Rubin EJ, Sassetti CM. Characterization of mycobacterial virulence genes through genetic interaction

- mapping. *Proc Natl Acad Sci USA*. 2006 Aug 1;103(31):11760–5.
23. DeJesus MA, Ioerger TR. Normalization of transposon-mutant library sequencing datasets to improve identification of conditionally essential genes. *Journal of Bioinformatics and Computational Biology*. World Scientific Publishing Company; 2016 Jun;14(03):1642004.
 24. Perkowski EF, Zulauf KE, Weerakoon D, Hayden JD, Ioerger TR, Oreper D, et al. The EXIT Strategy: an Approach for Identifying Bacterial Proteins Exported during Host Infection. Swanson MS, editor. *MBio*. 2017 Apr 25;8(2):e00333–17.
 25. Lew JM, Kapopoulou A, Jones LM, Cole ST. TubercuList--10 years after. *Tuberculosis (Edinb)*. 2011 Jan;91(1):1–7.
 26. Zhang YJ, Reddy MC, Ioerger TR, Rothchild AC, Dartois V, Schuster BM, et al. Tryptophan biosynthesis protects mycobacteria from CD4 T-cell-mediated killing. *Cell*. 2013 Dec 5;155(6):1296–308.
 27. D'Andrea LD, Regan L. TPR proteins: the versatile helix. *Trends Biochem Sci*. 2003 Dec;28(12):655–62.
 28. Lamb JR, Tugendreich S, Hieter P. Tetratrico peptide repeat interactions: to TPR or not to TPR? *Trends Biochem Sci*. 1995 Jul;20(7):257–9.
 29. Job V, Mattei P-J, Lemaire D, Attree I, Dessen A. Structural basis of chaperone recognition of type III secretion system minor translocator proteins. *J Biol Chem*. 2010 Jul 23;285(30):23224–32.
 30. Kruh NA, Trout J, Izzo A, Prenni J, Dobos KM. Portrait of a pathogen: the *Mycobacterium tuberculosis* proteome in vivo. Aziz RK, editor. *PLoS ONE*. 2010 Nov 11;5(11):e13938.
 31. Davis JK, Paoli GC, He Z, Nadeau LJ, Somerville CC, Spain JC. Sequence analysis and initial characterization of two isozymes of hydroxylaminobenzene mutase from *Pseudomonas pseudoalcaligenes* JS45. *Appl Environ Microbiol*. American Society for Microbiology (ASM); 2000 Jul;66(7):2965–71.
 32. Mikels AJ, Nusse R. Wnts as ligands: processing, secretion and reception. *Oncogene*. Nature Publishing Group; 2006 Dec 4;25(57):7461–8.
 33. Vergne I, Chua J, Lee H-H, Lucas M, Belisle J, Deretic V. Mechanism of phagolysosome biogenesis block by viable *Mycobacterium tuberculosis*. *Proc Natl Acad Sci USA*. 2005 Mar 15;102(11):4033–8.

34. McDonough JA, McCann JR, Tekippe EM, Silverman JS, Rigel NW, Braunstein M. Identification of functional Tat signal sequences in *Mycobacterium tuberculosis* proteins. *J Bacteriol.* 2008 Oct;190(19):6428–38.
35. Petersen TN, Brunak S, Heijne von G, Nielsen H. SignalP 4.0: discriminating signal peptides from transmembrane regions. *Nat Methods.* 2011 Sep 29;8(10):785–6.
36. Feltcher ME, Gibbons HS, Ligon LS, Braunstein M. Protein export by the mycobacterial SecA2 system is determined by the preprotein mature domain. *J Bacteriol.* 2013 Feb;195(4):672–81.
37. Stewart GR, Patel J, Robertson BD, Rae A, Young DB. Mycobacterial mutants with defective control of phagosomal acidification. *PLoS Pathog. Public Library of Science;* 2005 Nov;1(3):269–78.
38. Pethe K, Swenson DL, Alonso S, Anderson J, Wang C, Russell DG. Isolation of *Mycobacterium tuberculosis* mutants defective in the arrest of phagosome maturation. *Proc Natl Acad Sci USA.* 2004 Sep 14;101(37):13642–7.
39. Brodin P, Poquet Y, Levillain F, Peguillet I, Larrouy-Maumus G, Gilleron M, et al. High content phenotypic cell-based visual screen identifies *Mycobacterium tuberculosis* acyltrehalose-containing glycolipids involved in phagosome remodeling. Deretic V, editor. *PLoS Pathog.* 2010 Sep 9;6(9):e1001100.
40. Puri RV, Reddy PV, Tyagi AK. Secreted acid phosphatase (SapM) of *Mycobacterium tuberculosis* is indispensable for arresting phagosomal maturation and growth of the pathogen in guinea pig tissues. Neyrolles O, editor. *PLoS ONE. Public Library of Science;* 2013;8(7):e70514.
41. Balhana RJC, Swanston SN, Coade S, Withers M, Sikder MH, Stoker NG, et al. bkaR is a TetR-type repressor that controls an operon associated with branched-chain keto-acid metabolism in *Mycobacteria*. *FEMS Microbiol Lett.* 2013 Aug;345(2):132–40.
42. Senaratne RH, Sidders B, Sequeira P, Saunders G, Dunphy K, Marjanovic O, et al. *Mycobacterium tuberculosis* strains disrupted in mce3 and mce4 operons are attenuated in mice. *J Med Microbiol. Microbiology Society;* 2008 Feb;57(Pt 2):164–70.
43. Pandey AK, Sasseti CM. Mycobacterial persistence requires the utilization of host cholesterol. *Proc Natl Acad Sci USA.* 2008 Mar 18;105(11):4376–80.
44. Rana AK, Singh A, Gurcha SS, Cox LR, Bhatt A, Besra GS. Ppm1-encoded polyprenyl monophosphomannose synthase activity is essential for lipoglycan

- synthesis and survival in mycobacteria. Tyagi AK, editor. PLoS ONE. 2012;7(10):e48211.
45. Jackson M. The mycobacterial cell envelope-lipids. Cold Spring Harb Perspect Med. 2014 Aug 7;4(10):a021105–5.
 46. Domenech P, Reed MB. Rapid and spontaneous loss of phthiocerol dimycocerosate (PDIM) from *Mycobacterium tuberculosis* grown in vitro: implications for virulence studies. *Microbiology (Reading, Engl)*. Microbiology Society; 2009 Oct 30;155(11):3532–43.
 47. Quigley J, Hughitt VK, Velikovskiy CA, Mariuzza RA, El-Sayed NM, Briken V. The Cell Wall Lipid PDIM Contributes to Phagosomal Escape and Host Cell Exit of *Mycobacterium tuberculosis*. Kaufmann SHE, editor. *MBio*. 2017 Mar 7;8(2):e00148–17.
 48. Prigozhin DM, Mavrici D, Huizar JP, Vansell HJ, Alber T. Structural and biochemical analyses of *Mycobacterium tuberculosis* N-acetylmuramyl-L-alanine amidase Rv3717 point to a role in peptidoglycan fragment recycling. *J Biol Chem*. 2013 Nov 1;288(44):31549–55.
 49. Sassetti CM, Rubin EJ. Genetic requirements for mycobacterial survival during infection. *Proc Natl Acad Sci USA*. 2003 Oct 28;100(22):12989–94.
 50. Harth G, Masleša-Galić S, Tullius MV, Horwitz MA. All four *Mycobacterium tuberculosis* *glnA* genes encode glutamine synthetase activities but only GlnA1 is abundantly expressed and essential for bacterial homeostasis. *Mol Microbiol*. Blackwell Science Ltd; 2005 Oct 10;58(4):1157–72.
 51. Böth D, Steiner EM, Izumi A, Schneider G, Schnell R. RipD (Rv1566c) from *Mycobacterium tuberculosis*: adaptation of an NlpC/p60 domain to a non-catalytic peptidoglycan-binding function. *Biochem J*. Portland Press Limited; 2014 Jan 1;457(1):33–41.
 52. Mavrici D, Marakalala MJ, Holton JM, Prigozhin DM, Gee CL, Zhang YJ, et al. *Mycobacterium tuberculosis* FtsX extracellular domain activates the peptidoglycan hydrolase, RipC. *Proc Natl Acad Sci USA*. 2014 Jun 3;111(22):8037–42.
 53. Lenz LL, Mohammadi S, Geissler A, Portnoy DA. SecA2-dependent secretion of autolytic enzymes promotes *Listeria monocytogenes* pathogenesis. *Proc Natl Acad Sci USA*. 2003 Oct 14;100(21):12432–7.
 54. Davis KM, Weiser JN. Modifications to the peptidoglycan backbone help bacteria to

- establish infection. *Infect Immun.* 2011 Feb;79(2):562–70.
55. Martinac B, Saimi Y, Kung C. Ion Channels in Microbes. *Physiological Reviews.* 2008 Oct 1;88(4):1449–90.
 56. Peirs P, Lefèvre P, Boarbi S, Wang X-M, Denis O, Braibant M, et al. *Mycobacterium tuberculosis* with disruption in genes encoding the phosphate binding proteins PstS1 and PstS2 is deficient in phosphate uptake and demonstrates reduced in vivo virulence. *Infect Immun.* 2005 Mar;73(3):1898–902.
 57. Braibant M, Lefèvre P, de Wit L, Peirs P, Ooms J, Huygen K, et al. A *Mycobacterium tuberculosis* gene cluster encoding proteins of a phosphate transporter homologous to the *Escherichia coli* Pst system. *Gene.* 1996 Oct 17;176(1-2):171–6.
 58. Elliott SR, Tischler AD. Phosphate starvation: a novel signal that triggers ESX-5 secretion in *Mycobacterium tuberculosis*. *Mol Microbiol.* 2016 May;100(3):510–26.
 59. Tischler AD, Leistikow RL, Kirksey MA, Voskuil MI, McKinney JD. *Mycobacterium tuberculosis* requires phosphate-responsive gene regulation to resist host immunity. *Infect Immun. American Society for Microbiology;* 2013 Jan;81(1):317–28.
 60. Rifat D, Bishai WR, Karakousis PC. Phosphate depletion: a novel trigger for *Mycobacterium tuberculosis* persistence. *J Infect Dis.* 2009 Oct 1;200(7):1126–35.
 61. Schnappinger D, Ehrt S, Voskuil MI, Liu Y, Mangan JA, Monahan IM, et al. Transcriptional Adaptation of *Mycobacterium tuberculosis* within Macrophages: Insights into the Phagosomal Environment. *The Journal of Experimental Medicine.* 2003 Sep 1;198(5):693–704.
 62. Voskuil MI, Schnappinger D, Visconti KC, Harrell MI, Dolganov GM, Sherman DR, et al. Inhibition of respiration by nitric oxide induces a *Mycobacterium tuberculosis* dormancy program. *The Journal of Experimental Medicine.* 2003 Sep 1;198(5):705–13.
 63. Hatzios SK, Baer CE, Rustad TR, Siegrist MS, Pang JM, Ortega C, et al. Osmosensory signaling in *Mycobacterium tuberculosis* mediated by a eukaryotic-like Ser/Thr protein kinase. *Proc Natl Acad Sci USA.* 2013 Dec 24;110(52):E5069–77.
 64. Sala C, Haouz A, Saul FA, Miras I, Rosenkrands I, Alzari PM, et al. Genome-wide regulon and crystal structure of Blal (Rv1846c) from *Mycobacterium tuberculosis*. *Mol Microbiol. Blackwell Publishing Ltd;* 2009 Mar;71(5):1102–16.
 65. Stewart GR, Snewin VA, Walzl G, Hussell T, Tormay P, O'Gaora P, et al.

- Overexpression of heat-shock proteins reduces survival of *Mycobacterium tuberculosis* in the chronic phase of infection. *Nat Med*. 2001 Jun;7(6):732–7.
66. Weiss LA, Stallings CL. Essential roles for *Mycobacterium tuberculosis* Rel beyond the production of (p)ppGpp. *J Bacteriol*. 2013 Dec;195(24):5629–38.
 67. Primm TP, Andersen SJ, Mizrahi V, Avarbock D, Rubin H, Barry CE. The stringent response of *Mycobacterium tuberculosis* is required for long-term survival. *J Bacteriol*. American Society for Microbiology (ASM); 2000 Sep;182(17):4889–98.
 68. Darwin KH. *Mycobacterium tuberculosis* and Copper: A Newly Appreciated Defense against an Old Foe? *J Biol Chem*. 2015 Jul 31;290(31):18962–6.
 69. Festa RA, Jones MB, Butler-Wu S, Sinsimer D, Gerads R, Bishai WR, et al. A novel copper-responsive regulon in *Mycobacterium tuberculosis*. *Mol Microbiol*. Blackwell Publishing Ltd; 2011 Jan;79(1):133–48.
 70. Shi X, Festa RA, Ioerger TR, Butler-Wu S, Sacchettini JC, Darwin KH, et al. The copper-responsive RicR regulon contributes to *Mycobacterium tuberculosis* virulence. *MBio*. 2014 Feb 18;5(1):e00876–13–e00876–13.
 71. Rowland JL, Niederweis M. A multicopper oxidase is required for copper resistance in *Mycobacterium tuberculosis*. *J Bacteriol*. 2013 Aug;195(16):3724–33.
 72. Gröschel MI, Sayes F, Simeone R, Majlessi L, Brosch R. ESX secretion systems: mycobacterial evolution to counter host immunity. *Nature Reviews Microbiology*. 2016 Sep 26;14(11):677–91.
 73. Delogu G, Sali M, Fadda G. The biology of mycobacterium tuberculosis infection. *Mediterr J Hematol Infect Dis*. 2013 Nov 16;5(1):e2013070.
 74. Sassetti CM, Boyd DH, Rubin EJ. Comprehensive identification of conditionally essential genes in mycobacteria. *Proc Natl Acad Sci USA*. 2001 Oct 23;98(22):12712–7.
 75. McCann JR, McDonough JA, Pavelka MS, Braunstein M. Beta-lactamase can function as a reporter of bacterial protein export during *Mycobacterium tuberculosis* infection of host cells. *Microbiology (Reading, Engl)*. 2007 Oct;153(Pt 10):3350–9.
 76. Long JE, DeJesus M, Ward D, Baker RE, Ioerger T, Sassetti CM. Identifying essential genes in *Mycobacterium tuberculosis* by global phenotypic profiling. *Methods Mol Biol*. New York, NY: Springer New York; 2015;1279(Chapter 6):79–95.

77. DeJesus MA, Ambadipudi C, Baker R, Sasseti C, Ioerger TR. TRANSIT--A Software Tool for Himar1 TnSeq Analysis. Gardner PP, editor. PLoS Comput Biol. Public Library of Science; 2015 Oct;11(10):e1004401.
78. Perkowski EF, Miller BK, McCann JR, Sullivan JT, Malik S, Allen IC, et al. An orphaned Mce-associated membrane protein of Mycobacterium tuberculosis is a virulence factor that stabilizes Mce transporters. Mol Microbiol. 2015 Dec 29.

CHAPTER 5

Discussion

Mycobacterium tuberculosis, the causative agent of the disease tuberculosis, is responsible for causing approximately 1.8 million deaths each year (1). Currently one-third of the world population is infected with *M. tuberculosis*. In addition to this high burden of disease, the spread of drug resistant strains of *M. tuberculosis* and the lack of an efficacious vaccine creates a serious global health emergency (2). Therefore, a better understanding of the mechanisms of *M. tuberculosis* pathogenesis is urgently required.

In order to promote disease, *M. tuberculosis* exports proteins outside of the bacterial cell into the host environment where the proteins can interfere with host defense mechanisms, such as phagosome maturation (3). The SecA2 pathway is one system *M. tuberculosis* utilizes to export such proteins. Unlike the SecA1 ATPase, which is responsible for the bulk of housekeeping export and is essential for bacterial viability, SecA2 is a non-essential specialized SecA ATPase required for exporting a relatively small subset of proteins (4). The SecA2 pathway, although not essential for growth of *M. tuberculosis* in vitro, is required for virulence of *M. tuberculosis* in both murine and macrophage models of infection (5,6).

The requirement for SecA2 during infection suggests that SecA2 and its exported effectors play important roles in *M. tuberculosis* pathogenesis.

Previously it was shown that the SecA2 pathway is required for virulence of *M. tuberculosis*; however, the proteins exported by SecA2 that contribute to pathogenesis have remained largely unknown (6). The work presented in this dissertation improves our understanding of the functions of the SecA2 pathway in virulence by identifying proteins that depend on SecA2 for export, characterizing the functions of two proteins exported by SecA2 in phagosome maturation arrest, and identifying previously unknown functions of the SecA2 pathway during murine infection. This work revealed several themes in SecA2 protein export discussed below.

SecA2 and phagosome maturation arrest

Typically, once taken up into macrophages, the host delivers microbes to phagosomes that subsequently mature, acidify, and fuse with a lysosome resulting in the killing and degradation of the microbe. In contrast, *M. tuberculosis* arrests this process and is then able to replicate in phagosomes that do not mature or acidify (7,8). Although the ability of *M. tuberculosis* to arrest phagosome maturation and replicate in macrophages is critical for virulence, much remains unknown about this basic aspect of pathogenesis (9). It was previously shown that the SecA2 pathway is required for phagosome maturation arrest and consequently growth of *M. tuberculosis* in macrophages, indicating proteins exported by the SecA2 pathway play essential roles in this process (9).

SecA2 export of SapM and PknG contributes to phagosome maturation arrest

Work presented in this dissertation shows that SecA2 exports two effectors of phagosome maturation arrest: SapM and PknG. Through an approach of adding back export of SapM and/or PknG to the *secA2* mutant, we demonstrated that SecA2 export of both effectors contributes to phagosome maturation arrest and growth of *M. tuberculosis* in macrophages. Through these experiments, we also increased our understanding of the functions of these individual effectors in phagosome maturation arrest. Our studies revealed roles for SapM phosphatase activity in inhibition of EEA1, Rab5-Rab7 exchange and acidification. We additionally demonstrated a role for PknG in inhibition of Rab5-Rab7 exchange and acidification, but there was no effect on EEA1. As a host target of PknG remains unknown, the identification of phagosome maturation steps inhibited by PknG could lead to the later identification of a host target.

SapM is predicted to function in phagosome maturation arrest by dephosphorylating PI3P on phagosomal membranes, and data presented in this dissertation supports this model (10). As PI3P is localized on the cytoplasmic face of the phagosome, it is presumed that SapM would need to cross the phagosomal membrane into the macrophage cytosol in order to function (11). Using immunofluorescence with anti-SapM antibodies (provided by Vojo Deretic) we investigated the location of SapM during *M. tuberculosis* infection of macrophages. In macrophages infected with H37Rv or a strain of H37Rv with increased SapM secretion (pJTS130), SapM was seen expanding beyond the phagosome into the macrophage cytosol as infection progresses. This represents the first evidence of SapM localization to the host cytosol. Although export of SapM from the bacterial cell is dependent on SecA2, escape of SapM from the *M. tuberculosis* phagosome was not dependent on the

SecA2 pathway as evidenced by localization of SapM in the host cytosol of *secA2* mutant infected macrophages (Figure 5.1).

The mechanism(s) for *M. tuberculosis* proteins important for pathogenesis escaping the phagosome and reaching the host cytosol remains unknown. The Esx1 export pathway secretes the ESAT-6 protein, which permeabilizes the phagosomal membrane and allows cytoplasmic access to at least some *M. tuberculosis* molecules (12). Consequently, Esx1 is a candidate pathway for enabling SapM transit from the phagosomal lumen to the host cytoplasm. By localizing SapM in macrophages infected with a *M. tuberculosis* mutant strain lacking the Esx1 export system (*eccDI*) we tested the possibility of SapM cytosolic access depending upon Esx1. Macrophages infected with the *eccDI* mutant revealed SapM delivery to the cytoplasm at comparable levels as H37Rv. Thus, Esx1 does not appear to be responsible for SapM localization to the host cytoplasm. We also constructed a *secA2/eccDI* double mutant and saw a similar result as with macrophages infected with the *secA2* mutant. This result further confirms that SapM accesses the cytosol but that it does so in a manner that is independent of both SecA2 and Esx pathways indicating there must be an alternative mechanism releasing *M. tuberculosis* proteins from the phagosome and further study is required.

Although we primarily see PknG localized in the cell wall and bacterial cytoplasm, PknG has been reported to be fully secreted and has even been detected in the macrophage cytosol (13-15). Like SapM, although PknG has been identified in the host cytosol the specific mechanism of phagosomal escape remains unknown. The specific functions and targets of PknG in phagosome maturation arrest by *M. tuberculosis* are not as clear as SapM. Unlike SapM, in addition to a role in phagosome maturation arrest, PknG also has

physiological functions in the cytoplasm of *M. tuberculosis*. For example, PknG phosphorylates GarA which de-represses the TCA cycle (16,17). PknG also phosphorylates the mycobacterial ribosomal protein L13 leading to redox homeostasis and thus protection from oxidative stresses (18). The function of PknG in redox homeostasis has been suggested to contribute to the role of PknG in phagosome maturation arrest (18). However, the cytoplasmic functions of PknG are insufficient to explain the defect of the *secA2* mutant in phagosome maturation arrest as the *secA2* mutant accumulates unexported protein in the cytoplasm (15). Furthermore, the *secA2* mutant does not exhibit a redox homeostasis defect, as assessed by sensitivity to redox stress. Overexpression of PknG did not increase resistance of the *secA2* mutant to redox stress. Taken together these findings indicate that that PknG has additional, exported, functions in the host. As PknG is similar to eukaryotic serine/threonine kinases it is not surprising that PknG has targets within the host. Our data suggest a role for PknG in inhibition of Rab5-Rab7 exchange as well as a function in the inhibition of phagosome acidification independent of the assembly of V-ATPase on phagosomes. The specific host target(s) of PknG are unknown but our data suggest that PknG targets a Rab5-Rab7 exchange factor or a signaling pathway upstream. PknG has been shown to lead to the degradation of the host protein PKC α ; however, the implications of this on *M. tuberculosis* phagosome maturation arrest remain to be investigated (19).

SecA2 inhibits phagosomal acidification through multiple mechanisms

The ability of *M. tuberculosis* to exclude V-ATPase from the phagosome is generally assumed to account for the lack of acidification of *M. tuberculosis* phagosomes (20). Somewhat surprisingly, our studies demonstrate that SapM and PknG inhibit acidification without blocking recruitment of the V-ATPase. Restoration of SapM and/or PknG export to

the *secA2* mutant partially rescued the acidification defect of the *secA2* mutant but had no affect recruitment of V-ATPase to the phagosome. Thus, this result indicates the existence of additional mechanism(s) for *M. tuberculosis* to prevent phagosome acidification that were not previously appreciated. One potential explanation for how *M. tuberculosis* affects phagosome acidification independent of V-ATPase exclusion is by direct inhibition of the functionality of the V-ATPase pump. Phosphorylation of the ATPase subunit of V-ATPase has been shown to regulate activity of the proton pump; therefore, SapM and/or PknG may alter the phosphorylation state of V-ATPase (21). Another possibility is that *M. tuberculosis* indirectly alters the function of V-ATPase by affecting the counter ion flux that is required for acidification to occur (22). In order for V-ATPase to pump in positively charged hydrogen, either positively charged ions (such as sodium or potassium) need to be exported from the phagosome or negative charged ions need to be imported (such as chloride). Thus, one possibility is that *M. tuberculosis* affects the ability of the host to import/export these ions, or *M. tuberculosis* itself could export or import ions affecting the net charge of the phagosome. Unfortunately, the ion channels used by the host that provide the counter ion gradient in phagosomes are not known, making it difficult to directly investigate the effect, if any, *M. tuberculosis* has on these channels. An indirect way of examining the ion balance of the *M. tuberculosis* phagosome is by examining the transcriptional response of *M. tuberculosis* in phagosomes. *M. tuberculosis* is known to induce a specific set of genes in response to high levels of chloride; thus, by examining the expression levels of these genes it may be possible to assess the ion environment of the *M. tuberculosis* phagosome (23). Finally, in addition to affecting the counter ion gradient, *M. tuberculosis* could potentially affect an H⁺ importer that contributes to the acidification of the phagosome. Phagosomes in

macrophages possess a H⁺ pump called Hv1 (24,25). Unlike V-ATPase, much less is known about the localization and function of Hcv1. It is currently not known if *M. tuberculosis* affects recruitment and/or function of Hcv1 during infection.

SecA2 exports additional effectors of phagosome maturation arrest

In addition to SapM and PknG, SecA2 must export at least one additional effector of phagosome maturation arrest that inhibits Rab5-Rab7 exchange and V-ATPase assembly on the phagosome, as restoration of both SapM and PknG export in the *secA2* mutant did not result in complete rescue of these defects. PtpA, which binds subunit H of V-ATPase and thereby disrupts assembly of the proton pump on phagosomes, is a candidate for this missing SecA2-exported effector (26). PtpA is a phosphatase secreted by *M. tuberculosis* that has been detected in the host cytosol during infection (27). PtpA is a compelling candidate for a missing phagosome maturation arrest effector exported by SecA2. However, our attempts to detect native or overexpressed levels of secreted PtpA in culture supernatants were unsuccessful, which has prevented us from determining if PtpA is a SecA2-exported protein.

Another candidate for a missing SecA2 exported effector of phagosome maturation arrest is LipO. We identified the predicted lipase LipO as a SecA2 dependent exported protein in a mass spectrometry analysis of the *secA2* mutant cell wall (described in Chapter 2). LipO was reduced approximately 7-fold in the cell wall of the *secA2* mutant compared to H37Rv. The SecA2 dependency of LipO was validated by constructing an HA tagged version of LipO and examining export to the *M. tuberculosis* cell wall by Immunoblot (Figure 5.2 A). A *lipO* transposon mutant of *M. tuberculosis* is defective in preventing phagosome acidification suggesting that LipO contributes *M. tuberculosis* phagosome maturation arrest

(28,29). To examine the contribution of SecA2 export of LipO to *M. tuberculosis* phagosome maturation arrest we took the same approach as with SapM and PknG. When export of LipO was increased in the *secA2* mutant, it resulted in a partial rescue in the acidification defect of the mutant but had no effect on EEA1 recruitment to phagosomes (Figure 5.2 B and C). The specific function of LipO in the host and the importance of SecA2 export of LipO remain to be determined.

Genetic interaction studies highlight the role of SecA2 in phagosome maturation arrest

Genetic interaction studies of the *secA2* mutant also highlighted the important role of SecA2 in phagosome maturation arrest. SapM along with three additional genes implicated in phagosome maturation arrest were identified as genetically interacting with *secA2*. For example, transposon mutants in *rv2506* were identified as alleviating interactions with a *secA2* mutation. Rv2506 is a transcriptional repressor, therefore absence of *rv2506* may result in the upregulation of proteins involved in phagosome maturation arrest that have similar functions as SecA2 exported effectors (29,30). The genes regulated by Rv2506 are not currently known. Identification of the Rv2506 regulated genes could lead to further understanding of the SecA2 pathway in phagosome maturation arrest. More importantly, the regulon could reveal novel, SecA2 independent, *M. tuberculosis* effectors of phagosome maturation arrest.

Not only did our studies extend what was known about SecA2 and phagosome maturation arrest pathways, but they also uncovered a previously unknown function for the SecA2 pathway in autophagosome maturation arrest. Autophagy is an innate host response that controls *M. tuberculosis* infection (3). Autophagosomes progress through similar

maturation stages as phagosomes and *M. tuberculosis* is able to arrest the process of autophagosome maturation (31-33). However, much less is understood about the mechanisms of *M. tuberculosis* autophagosome maturation arrest. Our studies demonstrated an unappreciated role for SecA2 in autophagosome maturation arrest as well as roles for the SecA2 exported SapM and PknG in in this process.

SecA2 and transporters

The well-studied SecA2 substrates, the Msmeg1704 and Msmeg1712 lipoproteins of *M. smegmatis*, represent one class of SecA2 dependent substrates, solute binding proteins (SBPs) (34). SBPs are cell wall localized proteins that deliver solutes to permease components of ATP-binding cassette (ABC) transporters for import using energy from ATP hydrolysis. Although there are no direct homologs of Msmeg1704 and Msmeg1712 in *M. tuberculosis*, quantitative mass spectrometry reveals numerous SBPs that are also SecA2 dependent in *M. tuberculosis* (15). In *M. tuberculosis*, nearly all of the SBPs identified in the cell wall fraction (13 out of 15) are present at lower levels in the *secA2* mutant cell wall. All of the *M. tuberculosis* SecA2 dependent SPBs are lipoproteins with predicted signal peptides. Given the possibility of SecA2 substrates being distinguished by a tendency to fold prior to export, it is notable that 4 of the 13 SBPs reduced in the *secA2* mutant of *M. tuberculosis* have predicted or proven signal peptides for the Tat export pathway, which exports folded proteins (35). There are also examples of SBPs with Tat signal peptides in other bacteria, suggesting that cytoplasmic folding is a common property of the SBP family (36,37). The

trend of SBPs being SecA2 dependent may also extend to other SecA2-only systems, as there is some evidence that SecA2 may also export SBPs in *Listeria* (38).

Although most SBPs in *M. tuberculosis* have not been directly studied and their substrates remain unknown, SBPs can import a wide range of solutes (39). Thus, the role of SecA2 in exporting SBPs could be important for nutrient acquisition and affect the ability of *M. tuberculosis* to thrive in the host. In particular, the role of SecA2 in exporting PhoS1, indicates an effect of SecA2 on phosphate import and levels as evidenced by genetic interactions identified with *secA2* (40). The connection between SecA2 and phosphate acquisition should be validated by examining growth of the *secA2* mutant in low phosphate conditions as well as investigating the transcriptional response of the *secA2* mutant to low phosphate.

Interestingly, the genetic interaction study revealed a role for SecA2 that extends beyond ABC transporters. Of the 62 genetic interactions identified for *secA2*, 9 corresponded to components of ABC transporters and 8 corresponded to components of different types of transporters. In addition to ABC transporters, genes encoding for components of ion transporters and efflux pumps were also found to interact with *secA2*. This result suggests that SecA2 may export components of other transporters in addition to ABC transporters. Alternatively, defects in the import of nutrients that result from export defects in solute binding proteins in the *secA2* mutant may affect the transport or nutrient needs of the mycobacterial cell. Further studies are required to distinguish between these two possibilities.

SecA2 and lipid homeostasis

Another class of proteins exported by SecA2 are Mce transporter components. Mce transporters are thought to function similarly to ABC transporters, in that they recognize an extracytoplasmic substrate (in this case a lipid) and import it into the cytoplasm using ATP hydrolysis (41). Mce transporters are composed of about 10 proteins. All of these components are exported proteins that either possess a transmembrane domain or a signal peptide. The Mce proteins are proposed to recognize the lipid substrate and deliver it to a permease and, therefore, are functionally similar to SBPs of ABC transporters (41). Supporting this speculated similarity, there are presumed lipid importing SBPs of Gram negative bacteria that possess Mce-like domains (42). *M. tuberculosis* has four Mce transporters. The best studied Mce transporter is Mce4, which imports cholesterol (43). Because cholesterol catabolism is critical to *M. tuberculosis* pathogenesis, Mce4 has an important role in virulence (43,44). Furthermore, studies in mice suggest that Mce4 is required for *M. tuberculosis* persistence during chronic infection (43). Mce1 is proposed to be a mycolic acid re-importer (45,46). Mce1 is required for optimal growth in macrophages; however, there are conflicting reports concerning the requirement for Mce1 in murine infections (46-51).

Multiple exported components of Mce1 and Mce4 transporters are identified by quantitative mass spectrometry as being SecA2 dependent in *M. tuberculosis* (15). Six components of Mce1 and six components of Mce4 are significantly reduced in the *secA2* mutant cell wall. The impact of SecA2 on multiple Mce components is not a transcriptional effect (as ruled out by qRT-PCR). Rather, these findings are consistent with the *secA2* mutant having a defect in the export of Mce proteins. Levels of MceG, the presumed ATPase for

Mce transporters, are also reduced in the *secA2* mutant of *M. tuberculosis*. Collectively, these data suggest a link between SecA2 and lipid import in mycobacteria.

Our genetic interaction study also suggests a role for SecA2 export in cholesterol and lipid import/metabolism. We identified 15 genetic interactions associated either with cholesterol or *M. tuberculosis* lipid transport/homeostasis. Although we did not identify Mce4 transporter components in this analysis, we did identify several genes involved in cholesterol use by *M. tuberculosis* as genetic interactions with *secA2*. Furthermore, we showed that SecA2 is required for optimal growth on cholesterol. The fact that no *mce4* genes were identified as genetic interactors with *secA2* may reflect the fact that Mce4 is important for the later persistence stage of infection in the murine model as opposed to the earlier growth in vivo phase of infection that was the focus of our search for genetic interactions. *M. tuberculosis* replicates *in vivo* until an effective T-cell (TH1) cell mediated immune response is established at 21 days post-infection, after which time *M. tuberculosis* persists in the host throughout the remainder of the infection (43,52). The identification of genetic interactions related to cholesterol during the growth in vivo stage of infection may suggest that SecA2 has a second connection to cholesterol in addition to Mce4. Further research is required to fully understand the connection(s) between SecA2 and cholesterol as well as the potential role for SecA2 in the persistent stage of infection.

Genetic interaction studies also revealed connections between SecA2 export and several lipid components of the mycobacterial cell envelope. SecA2 was linked to synthesis, modification, or transport of lipoarabinomannan (LAM), 2,3-diacyltrehaloses (DAT), and phthiocerol dimycocerosates (PDIM). LAM is a lipid in the mycobacterial cell envelope that has multiple functions in virulence including anti-inflammatory, anti-apoptotic, and anti-

phagosome maturation properties (53). DAT lipids have been shown to contribute to the virulence of *M. tuberculosis* by participating in phagosome maturation arrest (54). PDIM is an important virulence factor in the *M. tuberculosis* cell envelope that contributes to many virulence properties including macrophage invasion, masking of immune stimulating PAMPS, resistance to reactive nitrogen intermediates (RNI), phagosomal escape and induction of necrosis (53,55). It is intriguing that SecA2 has similar functions in the pathogenesis of *M. tuberculosis* as these three mycobacterial lipids, and it suggests that SecA2 or SecA2 exported proteins may be involved in the export or modification of these lipid components of the cell envelope. Further research is required to identify the connection between SecA2 and cell envelope lipids.

SecA2 and the Mycobacterial cell wall

The identification of many genes related to lipid transport and homeostasis as genetic interactions with *secA2* suggests that SecA2 may export proteins that alter the mycobacterial cell envelope. One of the largest functional categories representing alleviating and aggravating interactions corresponds to genes that function in *M. tuberculosis* cell wall and cell processes (29% and 52% respectively). As only 19% of the *M. tuberculosis* genome falls into the cell wall and cell processes functional category, this finding further suggests SecA2 contributes to formation/maintenance of the mycobacterial cell wall (56). The large number of genetic interactions involving the mycobacterial cell wall could be due to the fact that several proteins in *M. tuberculosis* depend upon the SecA2 export pathway for export to the

cell wall (15). This result suggests a role for SecA2 in *M. tuberculosis* cell wall maintenance that was not appreciated before.

Furthermore, additional genetic interactions suggest a role of SecA2 in the mycobacterial cell envelope that extends beyond lipids. Genetic interactions indicate that SecA2 may function in peptidoglycan synthesis/maintenance. Genetic interaction studies identified *rv3717* as an alleviating interaction with *secA2*. Consequently, Rv3717 may represent a previously unknown SecA2 substrate. Rv3717 is an amidase that binds peptidoglycan fragments and is predicted to function in peptidoglycan recycling (57). Along with three other genetic interactions involved in peptidoglycan synthesis, this data suggests that the *secA2* mutant may have altered peptidoglycan. Supporting this result, the *secA2* mutant is significantly more sensitive to both lysozyme and carbenicillin which hydrolyze peptidoglycan or inhibit peptidoglycan synthesis respectively. Although this study represents the first indication of mycobacterial amidases being exported by SecA2 in mycobacteria, amidases are among the SecA2 dependent proteins identified in *Listeria monocytogenes* (38).

SecA2 and the *M. tuberculosis* stress response

An unexpected discovery of quantitative mass spectrometry studies of the *M. tuberculosis* *secA2* mutant, is the identification of multiple DosR regulated cytoplasmic proteins as being more abundant in the *secA2* mutant. The DosR regulon consists of 49 genes that are under the control of the DosR/S/T two component system (58). DosR-regulated proteins are induced by a number of stresses associated with infection, including hypoxia and nitric oxide

stress, and it is strongly induced during *M. tuberculosis* infection of macrophages, mice, guinea pigs and humans (58-60).

A transcriptional effect can account for the increase in DosR regulated proteins in the *secA2* mutant. Further, under conditions that induce the DosR regulon, the *secA2* mutant responds quicker and to a much higher degree than wild-type, leading to transiently higher levels of DosR regulated proteins. The earlier induction of the DosR regulon may be due to an increased sensitivity of the *secA2* mutant to DosR- inducing stimuli or due to a basal level of stress in the *secA2* mutant that primes the mutant to respond more quickly to stimuli. Since DosR is known to be induced in macrophages, this increased induction of the DosR regulon in the *secA2* mutant is likely to occur *in vivo* (59). Furthermore, macrophages infected with the *secA2* mutant produce higher levels of reactive nitrogen intermediates, which is a stimulus for induction of the DosR regulon, so this DosR upregulation may be even more pronounced during infection (60). It is possible that increased induction of DosR regulated proteins contributes to the phenotypes of the *secA2* mutant *in vivo*. For example, one DosR regulated protein increased in the *secA2* mutant, Rv0079, induces macrophage production of pro-inflammatory cytokines, including TNF- α , which is a phenotype elicited by the *secA2* mutant in macrophages (61).

Further indications that the *secA2* mutant is innately under stress or could be more prone to stress are evident in genetic interactions with *secA2*. Several of the identified interactions with *secA2* are in stress response pathways. Specifically, we identified three alleviating interactions in genes that encode repressors of stress response pathways. These alleviating interactions may reflect suppression of *secA2* mutant stress-related phenotypes. In the absence of these repressors, the stress response pathways are constitutively active and this

could have the effect of making the *secA2* mutant to more resistant to stressors encountered in the host. One such regulator, OprA, is involved in resistance to osmotic stress indicating that the *secA2* mutant may experience osmotic stress in the host (62). The osmotic stress may be due to function of the SecA2 pathway in exporting ABC transporter components as altered solute import/export may affect the osmotic state of the bacterial cell. The increased stress in the *secA2* mutant as well as the increased induction of DosR could be due to an altered or weakened cell wall (as discussed above) that renders the mutant more sensitive to stress or the localization of the *secA2* mutant to a more stressful environment in the host (i.e.a mature acidic phagosome).

Taken together, the findings presented in this dissertation have significantly improved our understanding of the roles of the SecA2 export pathway in the virulence of *M. tuberculosis*. The different approaches used in this dissertation have built upon each other and reinforced conclusions about the function of SecA2 export in *M. tuberculosis*. There is now a greatly expanded list of known SecA2 exported proteins in *M. tuberculosis* along with additional candidates that await validation. In addition, we identified two specific SecA2 substrates that work together to promote phagosome maturation arrest, which is the first time the combined effect of two effectors has been examined. Prior to this work, it was completely unknown which *M. tuberculosis* effectors were responsible for the role of SecA2 in phagosome maturation arrest. Furthermore, the use of genetic interaction mapping with *secA2* revealed a larger than appreciated effect of SecA2 on transporters, the mycobacterial cell wall, stress response, cholesterol utilization, and copper resistance. This dissertation demonstrates that by identifying proteins exported by SecA2 and understanding their function we can further our understanding of *M. tuberculosis* pathogenesis.

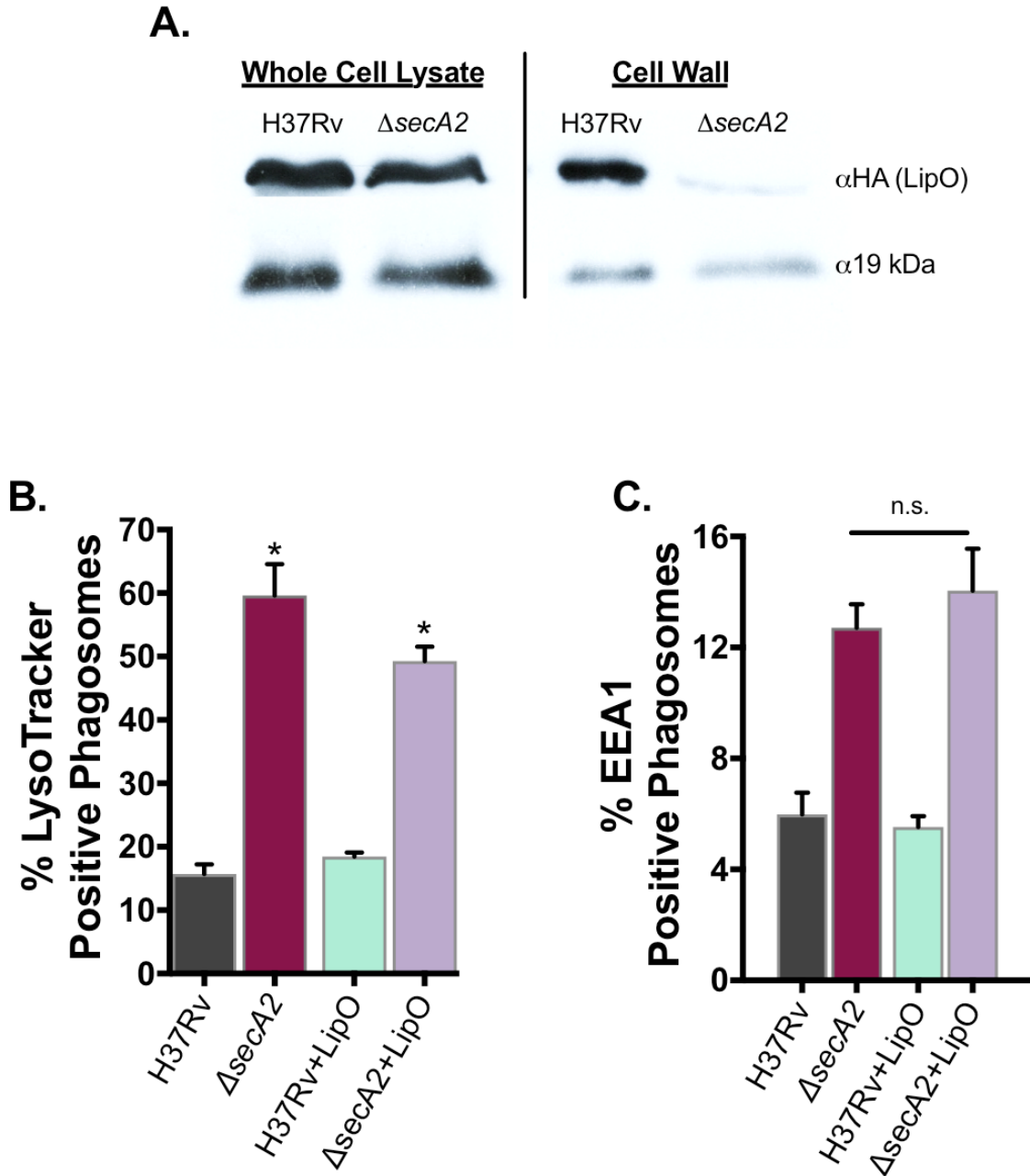


Figure 5.2 SecA2 export of LipO contributes to phagosome maturation arrest

(A) Equal protein from cell lysates or cell wall fractions from the wild-type strain H37Rv and the *secA2* mutant expressing a HA tagged LipO construct were examined for levels of LipO or the SecA2 independent loading control 19kDa by Immunoblot. The percentage of *M. tuberculosis* containing phagosomes that co-localized with LysoTracker (B) or EEA1 (C) at 1hr post infection was determined. * $p < 0.01$ ANOVA Holm-Sidak post Hoc test. Data represents at least two independent experiments.

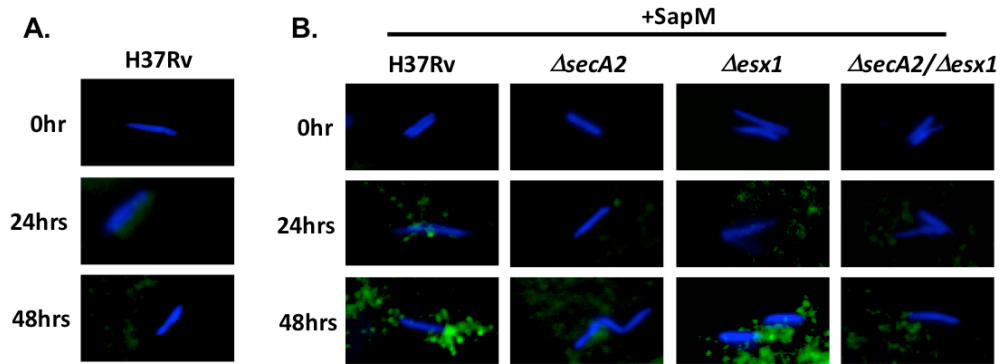


Figure 5.2 SapM is localized to the cytosol of infected macrophages

(A) Murine bone marrow derived macrophages were infected with H37Rv and fixed as specified time-points post infection. Using Immunofluorescence with SapM antibodies, SapM was visualized in the infected cells. (B) Murine bone marrow derived macrophages were infected with strains overexpressing SapM and fixed as specified time-points post infection. Using Immunofluorescence with SapM antibodies, SapM was visualized in the infected cells. Representative images from each timepoint are shown. *M. tuberculosis* was visualized using the native autofluorescence in the CFP channel. SapM was visualized using Texas-Red conjugated secondary antibodies (Santa Cruz).

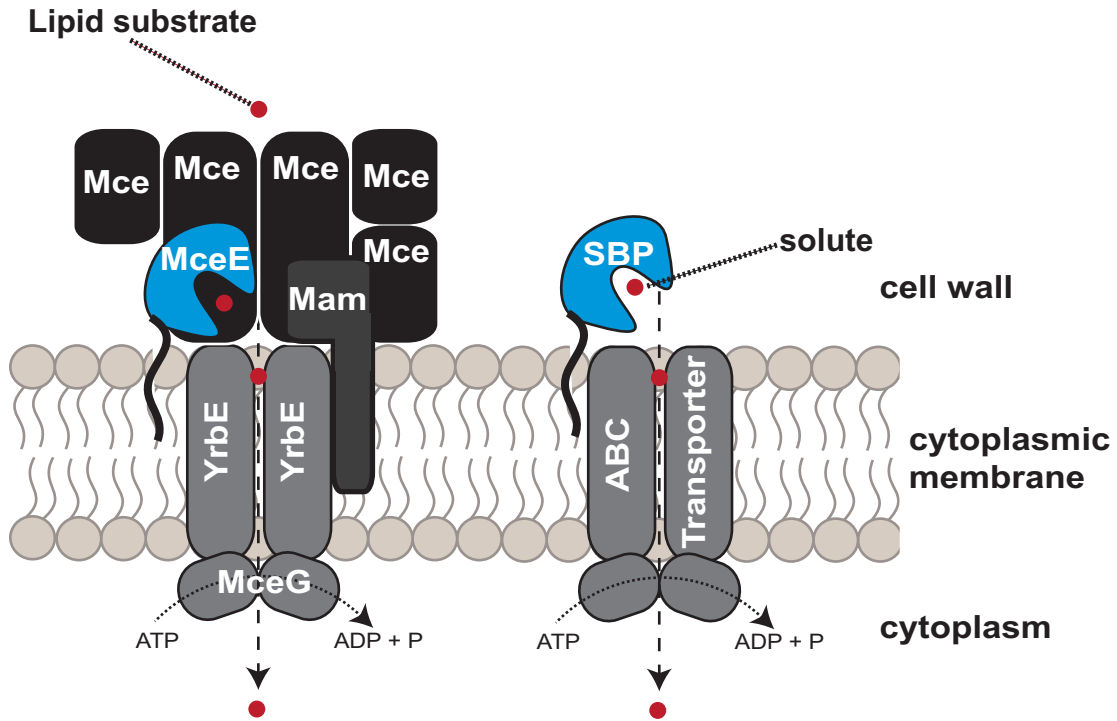


Figure 5.3 Solute binding proteins and Mce proteins are exported by the SecA2 pathway.

Two classes of SecA2 dependent substrates are SBPs and Mce proteins. Both SBPs and Mce proteins are involved in solute acquisition. In the case of SBPs this involves import of a solute through an ABC transporter permease using energy provided by ATP hydrolysis. Mce transporters are thought to function in a similar manner as ABC transporters to import a lipid substrate through a YrbE permease in an ATP-dependent manner. Although the diagram of an Mce transporter is speculative the similarities between these two systems are compelling.

REFERENCES

1. World Health Organization. Global tuberculosis report 2016. World Health Organization; 2016.
2. Smith T, Wolff KA, Nguyen L. Molecular Biology of Drug Resistance in *Mycobacterium tuberculosis*. In: Pathogenesis of *Mycobacterium tuberculosis* and its Interaction with the Host Organism. Berlin, Heidelberg: Springer Berlin Heidelberg; 2012. pp. 53–80. (Current Topics in Microbiology and Immunology; vol. 374).
3. Hussain Bhat K, Mukhopadhyay S. Macrophage takeover and the host-bacilli interplay during tuberculosis. *Future Microbiol. Future Medicine Ltd London, UK*; 2015;10(5):853–72.
4. Braunstein M, Brown AM, Kurtz S, Jacobs WR. Two nonredundant SecA homologues function in mycobacteria. *J Bacteriol.* 2001 Dec;183(24):6979–90.
5. Braunstein M, Espinosa BJ, Chan J, Belisle JT, Jacobs WR. SecA2 functions in the secretion of superoxide dismutase A and in the virulence of *Mycobacterium tuberculosis*. *Mol Microbiol.* 2003 Apr;48(2):453–64.
6. Kurtz S, McKinnon KP, Runge MS, Ting JP-Y, Braunstein M. The SecA2 secretion factor of *Mycobacterium tuberculosis* promotes growth in macrophages and inhibits the host immune response. *Infect Immun.* 2006 Dec;74(12):6855–64.
7. Armstrong JA, Hart PD. Response of cultured macrophages to *Mycobacterium tuberculosis*, with observations on fusion of lysosomes with phagosomes. *The Journal of Experimental Medicine.* The Rockefeller University Press; 1971 Sep 1;134(3 Pt 1):713–40.
8. Awuh JA, Flo TH. Molecular basis of mycobacterial survival in macrophages. *Cell Mol Life Sci.* Springer International Publishing; 2017 May;74(9):1625–48.
9. Sullivan JT, Young EF, McCann JR, Braunstein M. The *Mycobacterium tuberculosis* SecA2 system subverts phagosome maturation to promote growth in macrophages. *Infect Immun.* 2012 Mar;80(3):996–1006.
10. Vergne I, Chua J, Lee H-H, Lucas M, Belisle J, Deretic V. Mechanism of phagolysosome biogenesis block by viable *Mycobacterium tuberculosis*. *Proc Natl Acad Sci USA.* 2005 Mar 15;102(11):4033–8.
11. Jeschke A, Haas A. Deciphering the roles of phosphoinositide lipids in phagolysosome biogenesis. *Commun Integr Biol.* Taylor & Francis; 2016 May;9(3):e1174798.
12. de Jonge MI, Pehau-Arnaudet G, Fretz MM, Romain F, Bottai D, Brodin P, et al. ESAT-6 from *Mycobacterium tuberculosis* Dissociates from Its Putative Chaperone CFP-10 under Acidic Conditions and Exhibits Membrane-Lysing Activity. *J Bacteriol.*

2007 Aug 1;189(16):6028–34.

13. Walburger A, Koul A, Ferrari G, Nguyen L, Prescianotto-Baschong C, Huygen K, et al. Protein kinase G from pathogenic mycobacteria promotes survival within macrophages. *Science*. 2004 Jun 18;304(5678):1800–4.
14. Cowley S, Ko M, Pick N, Chow R, Downing KJ, Gordhan BG, et al. The *Mycobacterium tuberculosis* protein serine/threonine kinase PknG is linked to cellular glutamate/glutamine levels and is important for growth in vivo. *Mol Microbiol*. Blackwell Science Ltd; 2004 Jun;52(6):1691–702.
15. Feltcher ME, Gunawardena HP, Zulauf KE, Malik S, Griffin JE, Sasseti CM, et al. Label-free Quantitative Proteomics Reveals a Role for the *Mycobacterium tuberculosis* SecA2 Pathway in Exporting Solute Binding Proteins and Mce Transporters to the Cell Wall. *Mol Cell Proteomics*. 2015 Jun;14(6):1501–16.
16. Mueller P, Pieters J. Identification of mycobacterial GarA as a substrate of protein kinase G from *M. tuberculosis* using a KESTREL-based proteome wide approach. *J Microbiol Methods*. 2017 May;136:34–9.
17. O'Hare HM, Durán R, Cerveñansky C, Bellinzoni M, Wehenkel AM, Pritsch O, et al. Regulation of glutamate metabolism by protein kinases in mycobacteria. *Mol Microbiol*. Blackwell Publishing Ltd; 2008 Dec;70(6):1408–23.
18. Wolff KA, la Peña de AH, Nguyen HT, Pham TH, Amzel LM, Gabelli SB, et al. A redox regulatory system critical for mycobacterial survival in macrophages and biofilm development. Boshoff HI, editor. *PLoS Pathog*. 2015 Apr;11(4):e1004839.
19. Chaurasiya SK, Srivastava KK. Downregulation of protein kinase C- α enhances intracellular survival of *Mycobacteria*: role of PknG. *BMC Microbiol*. BioMed Central; 2009 Dec 24;9(1):271.
20. Sturgill-Koszycki S, Schlesinger PH, Chakraborty P, Haddix PL, Collins HL, Fok AK, et al. Lack of acidification in *Mycobacterium* phagosomes produced by exclusion of the vesicular proton-ATPase. *Science*. 1994 Feb 4;263(5147):678–81.
21. Alzamora R, Thali RF, Gong F, Smolak C, Li H, Baty CJ, et al. PKA regulates vacuolar H⁺-ATPase localization and activity via direct phosphorylation of the α subunit in kidney cells. *J Biol Chem*. 2010 Aug 6;285(32):24676–85.
22. Soldati T, Neyrolles O. *Mycobacteria* and the intraphagosomal environment: take it with a pinch of salt(s)! *Traffic*. 2012 Aug;13(8):1042–52.
23. Tan S, Sukumar N, Abramovitch RB, Parish T, Russell DG. *Mycobacterium tuberculosis* responds to chloride and pH as synergistic cues to the immune status of its host cell. Bishai WR, editor. *PLoS Pathog*. 2013;9(4):e1003282.
24. Chemaly El A, Nunes P, Jimaja W, Castelbou C, Demaurex N. Hv1 proton channels

differentially regulate the pH of neutrophil and macrophage phagosomes by sustaining the production of phagosomal ROS that inhibit the delivery of vacuolar ATPases. *Journal of Leukocyte Biology*. Society for Leukocyte Biology; 2014 May;95(5):827–39.

25. Ramsey IS, Ruchti E, Kaczmarek JS, Clapham DE. Hv1 proton channels are required for high-level NADPH oxidase-dependent superoxide production during the phagocyte respiratory burst. *Proc Natl Acad Sci USA*. 2009 May 5;106(18):7642–7.
26. Wong D, Bach H, Sun J, Hmama Z, Av-Gay Y. Mycobacterium tuberculosis protein tyrosine phosphatase (PtpA) excludes host vacuolar-H⁺-ATPase to inhibit phagosome acidification. *Proc Natl Acad Sci USA*. 2011 Nov 29;108(48):19371–6.
27. Bach H, Papavinasasundaram KG, Wong D, Hmama Z, Av-Gay Y. Mycobacterium tuberculosis Virulence Is Mediated by PtpA Dephosphorylation of Human Vacuolar Protein Sorting 33B. *Cell Host & Microbe*. 2008 May;3(5):316–22.
28. Pethe K, Swenson DL, Alonso S, Anderson J, Wang C, Russell DG. Isolation of Mycobacterium tuberculosis mutants defective in the arrest of phagosome maturation. *Proc Natl Acad Sci USA*. 2004 Sep 14;101(37):13642–7.
29. Stewart GR, Patel J, Robertson BD, Rae A, Young DB. Mycobacterial mutants with defective control of phagosomal acidification. *PLoS Pathog*. Public Library of Science; 2005 Nov;1(3):269–78.
30. Balhana RJC, Swanston SN, Coade S, Withers M, Sikder MH, Stoker NG, et al. bkaR is a TetR-type repressor that controls an operon associated with branched-chain keto-acid metabolism in Mycobacteria. *FEMS Microbiol Lett*. 2013 Aug;345(2):132–40.
31. Chandra P, Kumar D. Selective autophagy gets more selective: Uncoupling of autophagy flux and xenophagy flux in Mycobacterium tuberculosis-infected macrophages. *Autophagy*. Taylor & Francis; 2016;12(3):608–9.
32. Chandra P, Ghanwat S, Matta SK, Yadav SS, Mehta M, Siddiqui Z, et al. Mycobacterium tuberculosis Inhibits RAB7 Recruitment to Selectively Modulate Autophagy Flux in Macrophages. *Sci Rep*. Nature Publishing Group; 2015 Nov 6;5(1):16320.
33. Romagnoli A, Etna MP, Giacomini E, Pardini M, Remoli ME, Corazzari M, et al. ESX-1 dependent impairment of autophagic flux by Mycobacterium tuberculosis in human dendritic cells. *Autophagy*. Taylor & Francis; 2012 Sep;8(9):1357–70.
34. Gibbons HS, Wolschendorf F, Abshire M, Niederweis M, Braunstein M. Identification of two Mycobacterium smegmatis lipoproteins exported by a SecA2-dependent pathway. *J Bacteriol*. 2007 Jul;189(14):5090–100.
35. Feltcher ME, Gibbons HS, Ligon LS, Braunstein M. Protein export by the mycobacterial SecA2 system is determined by the preprotein mature domain. *J*

- Bacteriol. 2013 Feb;195(4):672–81.
36. Chater KF, Biró S, Lee KJ, Palmer T, Schrempf H. The complex extracellular biology of *Streptomyces*. *FEMS Microbiol Rev*. 2010 Mar;34(2):171–98.
 37. Shruthi H, Babu MM, Sankaran K. TAT-pathway-dependent lipoproteins as a niche-based adaptation in prokaryotes. *J Mol Evol*. Springer-Verlag; 2010 Apr;70(4):359–70.
 38. Lenz LL, Mohammadi S, Geissler A, Portnoy DA. SecA2-dependent secretion of autolytic enzymes promotes *Listeria monocytogenes* pathogenesis. *Proc Natl Acad Sci USA*. 2003 Oct 14;100(21):12432–7.
 39. Braibant M, Gilot P, Content J. The ATP binding cassette (ABC) transport systems of *Mycobacterium tuberculosis*. *FEMS Microbiol Rev*. 2000 Oct;24(4):449–67.
 40. Peirs P, Lefèvre P, Boarbi S, Wang X-M, Denis O, Braibant M, et al. *Mycobacterium tuberculosis* with disruption in genes encoding the phosphate binding proteins PstS1 and PstS2 is deficient in phosphate uptake and demonstrates reduced in vivo virulence. *Infect Immun*. 2005 Mar;73(3):1898–902.
 41. Casali N, Riley LW. A phylogenomic analysis of the Actinomycetales mce operons. *BMC Genomics*. BioMed Central; 2007 Feb 26;8(1):60.
 42. Malinverni JC, Silhavy TJ. An ABC transport system that maintains lipid asymmetry in the gram-negative outer membrane. *Proc Natl Acad Sci USA*. 2009 May 12;106(19):8009–14.
 43. Pandey AK, Sasseti CM. Mycobacterial persistence requires the utilization of host cholesterol. *Proc Natl Acad Sci USA*. 2008 Mar 18;105(11):4376–80.
 44. Senaratne RH, Sidders B, Sequeira P, Saunders G, Dunphy K, Marjanovic O, et al. *Mycobacterium tuberculosis* strains disrupted in mce3 and mce4 operons are attenuated in mice. *J Med Microbiol*. Microbiology Society; 2008 Feb;57(Pt 2):164–70.
 45. Cantrell SA, Leavell MD, Marjanovic O, Iavarone AT, Leary JA, Riley LW. Free mycolic acid accumulation in the cell wall of the mce1 operon mutant strain of *Mycobacterium tuberculosis*. *J Microbiol*. 4 ed. 2013 Oct;51(5):619–26.
 46. Forrellad MA, McNeil M, Santangelo M de LP, Blanco FC, García E, Klepp LI, et al. Role of the Mce1 transporter in the lipid homeostasis of *Mycobacterium tuberculosis*. *Tuberculosis (Edinb)*. 2014 Mar;94(2):170–7.
 47. Rengarajan J, Bloom BR, Rubin EJ. Genome-wide requirements for *Mycobacterium tuberculosis* adaptation and survival in macrophages. *Proc Natl Acad Sci USA*. 2005 Jun 7;102(23):8327–32.

48. McCann JR, McDonough JA, Sullivan JT, Feltcher ME, Braunstein M. Genome-wide identification of *Mycobacterium tuberculosis* exported proteins with roles in intracellular growth. *J Bacteriol.* 2011 Feb;193(4):854–61.
49. Shimono N, Morici L, Casali N, Cantrell S, Sidders B, Ehrt S, et al. Hypervirulent mutant of *Mycobacterium tuberculosis* resulting from disruption of the *mce1* operon. *Proc Natl Acad Sci USA.* 2003 Dec 23;100(26):15918–23.
50. Joshi SM, Pandey AK, Capite N, Fortune SM, Rubin EJ, Sassetti CM. Characterization of mycobacterial virulence genes through genetic interaction mapping. *Proc Natl Acad Sci USA.* 2006 Aug 1;103(31):11760–5.
51. Gioffré A, Infante E, Aguilar D, Santangelo M de LP, Klepp L, Amadio A, et al. Mutation in *mce* operons attenuates *Mycobacterium tuberculosis* virulence. *Microbes Infect.* 2005 Mar;7(3):325–34.
52. Delogu G, Sali M, Fadda G. The biology of mycobacterium tuberculosis infection. *Mediterr J Hematol Infect Dis.* 2013 Nov 16;5(1):e2013070.
53. Jackson M. The mycobacterial cell envelope-lipids. *Cold Spring Harb Perspect Med.* 2014 Aug 7;4(10):a021105–5.
54. Brodin P, Poquet Y, Levillain F, Peguillet I, Larrouy-Maumus G, Gilleron M, et al. High content phenotypic cell-based visual screen identifies *Mycobacterium tuberculosis* acyltrehalose-containing glycolipids involved in phagosome remodeling. Deretic V, editor. *PLoS Pathog.* 2010 Sep 9;6(9):e1001100.
55. Quigley J, Hughitt VK, Velikovskiy CA, Mariuzza RA, El-Sayed NM, Briken V. The Cell Wall Lipid PDIM Contributes to Phagosomal Escape and Host Cell Exit of *Mycobacterium tuberculosis*. Kaufmann SHE, editor. *MBio.* 2017 Mar 7;8(2):e00148–17.
56. Lew JM, Kapopoulou A, Jones LM, Cole ST. *TubercuList--10 years after.* *Tuberculosis (Edinb).* 2011 Jan;91(1):1–7.
57. Prigozhin DM, Mavrici D, Huizar JP, Vansell HJ, Alber T. Structural and biochemical analyses of *Mycobacterium tuberculosis* N-acetylmuramyl-L-alanine amidase Rv3717 point to a role in peptidoglycan fragment recycling. *J Biol Chem.* 2013 Nov 1;288(44):31549–55.
58. Boon C, Dick T. How *Mycobacterium tuberculosis* goes to sleep: the dormancy survival regulator *DosR* a decade later. *Future Microbiol.* Future Medicine Ltd London, UK; 2012 Apr;7(4):513–8.
59. Schnappinger D, Ehrt S, Voskuil MI, Liu Y, Mangan JA, Monahan IM, et al. Transcriptional Adaptation of *Mycobacterium tuberculosis* within Macrophages: Insights into the Phagosomal Environment. *The Journal of Experimental Medicine.* 2003 Sep 1;198(5):693–704.

60. Voskuil MI, Schnappinger D, Visconti KC, Harrell MI, Dolganov GM, Sherman DR, et al. Inhibition of respiration by nitric oxide induces a *Mycobacterium tuberculosis* dormancy program. *The Journal of Experimental Medicine*. 2003 Sep 1;198(5):705–13.
61. Kumar A, Lewin A, Rani PS, Qureshi IA, Devi S, Majid M, et al. Dormancy Associated Translation Inhibitor (DATIN/Rv0079) of *Mycobacterium tuberculosis* interacts with TLR2 and induces proinflammatory cytokine expression. *Cytokine*. 2013 Oct;64(1):258–64.
62. Hatzios SK, Baer CE, Rustad TR, Siegrist MS, Pang JM, Ortega C, et al. Osmosensory signaling in *Mycobacterium tuberculosis* mediated by a eukaryotic-like Ser/Thr protein kinase. *Proc Natl Acad Sci USA*. 2013 Dec 24;110(52):E5069–77.